12th AIVC Conference

Air Movement and Ventilation Control Within Buildings

(held at Château Laurier, Ottawa, Canada
24-27 September 1991)

Proceedings

Volume 2

Co-Sponsors:

IEA Energy Conservation in Buildings and Community Systems
Annex 18 'Demand Controlled Ventilating Systems'
Annex 20 'Air Flow Patterns within Buildings'

CONTENTS (i)

Volume 2

Preface

International Energy Agency

The International Energy Agency (IEA) was established in 1974 within the framework of the Organisation for Economic Co-operation and Development (OECD) to implement an International Energy Programme. A basic aim of the IEA is to foster co-operation among the twenty-one IEA Participating Countries to increase energy security through energy conservation, development of alternative energy sources and energy research development and demonstration (RD&D). This is achieved in part through a programme of collaborative RD&D consisting of forty-two Implementing Agreements, containing a total of over eighty separate energy RD&D projects. This publication forms one element of this programme.

Energy Conservation in Buildings and Community Systems

The IEA sponsors research and development in a number of areas related to energy. In one of these areas, energy conservation in buildings, the IEA is sponsoring various exercises to predict more accurately the energy use of buildings, including comparison of existing computer programs, building monitoring, comparison of calculation methods, as well as air quality and studies of occupancy. Seventeen countries have elected to participate in this area and have designated contracting parties to the Implementing Agreement covering collaborative research in this area. The designation by governments of a number of private organisations, as well as universities and government laboratories, as contracting parties, has provided a broader range of expertise to tackle the projects in the different technology areas than would have been the case if participation was restricted to governments. The importance of associating industry with government sponsored energy research and development is recognized in the IEA, and every effort is made to encourage this trend.

The Executive Committee

Overall control of the programme is maintained by an Executive Committee, which not only monitors existing projects but identifies new areas where collaborative effort may be beneficial. The Executive Committee ensures that all projects fit into a pre-determined strategy, without unnecessary overlap or duplication but with effective liaison and communication. The Executive Committee has initiated the following projects to date (completed projects are identified by *):

I Load Energy Determination of Buildings*
II Ekistics and Advanced Community Energy Systems*
III Energy Conservation in Residential Buildings*

IV Glasgow Commercial Building Monitoring*
V Air Infiltration and Ventilation Centre
VI Energy Systems and Design of Communities*
VII Local Government Energy Planning*
VIII Inhabitant Behaviour with Regard to Ventilation*
IX Minimum Ventilation Rates*
X Building HVAC Systems Simulation*
XI Energy Auditing*
XII Windows and Fenestration*
XIII Energy Management in Hospitals*
XIV Condensation*
XV Energy Efficiency in Schools
XVI BEMS - 1: Energy Management Procedures
XVII BEMS - 2: Evaluation and Emulation Techniques
XVIII Demand Controlled Ventilating Systems
XIX Low Slope Roof Systems
XX Air Flow Patterns within Buildings
XXI Thermal Modelling
XXII Energy Efficient Communities
XXIII Multizone Air Flow Modelling

Annex V Air Infiltration and Ventilation Centre

The IEA Executive Committee (Building and Community Systems) has highlighted areas where the level of knowledge is unsatisfactory and there was unanimous aggreement that infiltration was the area about which least was known. An infiltration group was formed drawing experts from most progressive countries, their long term aim to encourage joint international research and increase the world pool of knowledge on infiltration and ventilation. Much valuable but sporadic and uncoordinated research was already taking place and after some initial groundwork the experts group recommended to their executive the formation of an Air Infiltration and Ventilation Centre. This recommendation was accepted and proposals for its establishment were invited internationally.

The aims of the Centre are the standardisation of techniques, the validation of models, the catalogue and transfer of information, and the encouragement of research. It is intended to be a review body for current world research, to ensure full dissemination of this research and based on a knowledge of work already done to give direction and firm basis for future research in the Participating Countries.

The Participants in this task are Belgium, Canada, Denmark, Germany, Finland, Italy, Netherlands, New Zealand, Norway, Sweden, Switzerland, United Kingdom and the United States of America.

AIR MOVEMENT & VENTILATION CONTROL WITHIN BUILDINGS
12th AIVC Conference, Ottawa, Canada
24-27 September, 1991

POSTER 1

SIMULATION OF A MULTIPLE-NOZZLE DIFFUSER

(IEA Annex 20, Subtask 1, Research Item 1.20)

Qingyan Chen* and Alfred Moser

Swiss Federal Institute of Technology Zurich
Energy Systems Laboratory
ETH-Zentrum, CH-8092 Zurich, Switzerland

---

* Present address:
TNO Institute of Applied Physics (TPD)
P. O. Box 155, 2600 AD Delft, The Netherlands

SYNOPSIS

The air diffusion in a room is dominated by the diffuser type and the air supply parameters of the diffuser. The design of a diffuser used in practice is often complex. Reliable information from simulations can be useful in improving diffuser design. And the correct airflow pattern computed can help us to understand the flow phenomenon in order to obtain a comfortable indoor environment. Accurate flow information around the diffuser is therefore required.

A "HESCO"-type diffuser was selected as an example for the validation exercise in the IEA Annex 20 project (Air flow pattern within buildings). It consists of 84 small round nozzles that are arranged in four rows in an area of 0.71 m x 0.17 m. With the same effective area, the diffuser is simulated by 1, 12, and 84 simple rectangular slots and by the momentum method. In the momentum method, the supply air momentum is set to be that of the 84 small round nozzles. The simulation of the diffuser is incorporated in the airflow computation in a room. The three dimensional flow is computed by a flow program with a low-Reynolds-number k-ε model of turbulence.

Corresponding measurements from other researchers are used for comparison. It may be concluded that the momentum method and the method which uses 84 simple rectangular slots predict air velocity and temperature distributions in the room similar to those from the experiments. The computing cost with the 84 slots method is extremely high. Hence, the momentum method is suggested to be used to simulate a complex diffuser in practice.

INTRODUCTION

The air diffusion in a room is dominated by diffuser type and the air supply parameters of the diffuser. The difficulty in analysis of airflow around a jet diffuser is that the geometry configuration of a diffuser used in practice is complex, and the flow is three-dimensional, turbulent, and with a considerably high Reynolds number. It is necessary to acquire accurate flow information around the diffuser and to simulate the diffuser correctly in airflow computations.

There are several methods applicable for simulating a complex diffuser. The inlet box model used by Nielsen *et al* (1979) is one of the earliest models. In principle,

the model can be used for predicting room air motion with any kind of inlet diffuser. But the data used in the inlet box model must be obtained from experiment or a more detailed computation. However, the data needed in the model may not be always available.

Recently, Nielsen (1990) imposed a formula for a jet diffuser based the results from experiment. Lemaire (1990) applied the formula to prescribe velocity profile of a diffuser so that room airflow can be computed. The results are promising. Since the formula varies with the diffuser type, this method requires a large amount of time and effort.

Heikkinen (1990a) simulated a complex diffuser by a so-called basic model. In the basic model, the diffuser is simulated by a rectangular slot with the same effective area as the complex diffuser. The method was used to predict the airflow in a room with a complex diffuser under iso-thermal condition. It gave a reasonable indication of the airflow pattern in the room although there are discrepancies between the computations and experiment. But the method is not suitable for non-isothermal flow as will be discussed in this paper.

The aim of the paper is to find a suitable tool to simulate the air velocity and temperature distribution in a room with a complex jet diffuser. The tool could be used to improve diffuser design. And the correct airflow pattern computed can give a better understanding of the flow phenomena which may be useful in obtaining a comfortable indoor environment.

SIMULATION OF A MULTIPLE-NOZZLE DIFFUSER

A "HESCO"-type diffuser as shown in Figure 1a was selected as an example for the validation exercise in the IEA Annex 20 project. The diffuser is a modern air terminal device and available on the market. It consists of 84 small round nozzles that are arranged in four rows in an area of 0.71 m x 0.17 m. The flow direction of each nozzle can be adjusted, and a flow which has a complicated three-dimensional structure close to opening with a high entrainment of room air may result.

With the same effective area, the diffuser is simulated by two methods: the simple-rectangular-slot method and the momentum method. As shown in Figures

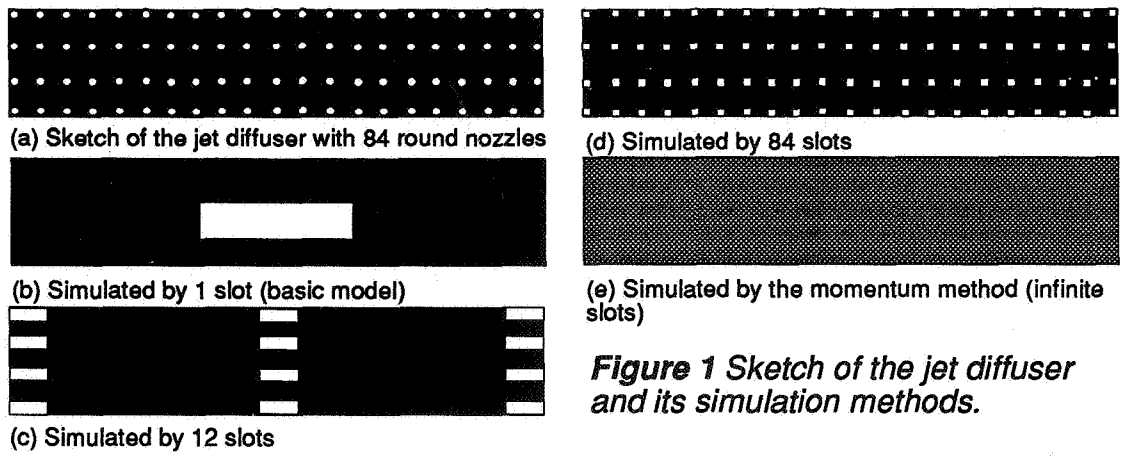

***Figure 1** Sketch of the jet diffuser and its simulation methods.*

1b-d, the 84 round nozzles can be simulated by 1, 12, or 84 rectangular slots, respectively. The total effective area of the 1, 12, or 84 slots is the same as that of the 84 round nozzles. The one slot method is defined as the basic model in the IEA Annex 20 project. In the momentum method, the supply air momentum, mV_{in}, is set to be that of the 84 small round nozzles:

$$m\ V_{in} = m \text{ (volume inflow rate / effective area)} \qquad (1)$$

where m is the mass inflow rate. This method can be regarded as setting infinite nozzles/slots as shown in Figure 1e. In the numerical approach, it is performed by characterizing the flow rate in the inlet with a fraction of the effective area over gross area of the diffuser. The fraction indicates the area of the grid cells within the inlet area available for the supply air. Different diffusers can be simulated by giving different supply momentum and its initial directions, .

In the present study, the low-Reynolds-number k-ε model of turbulence is used (Chen *et al.* 1990) to predict turbulent diffusion in airflow computation. This model has been verified to be more suitable for predicting indoor airflow and heat transfer since the agreement between the computed and measured results is very good. A more detailed description of the model and the comparison between the computed results and experimental data are given by Chen *et al.* (1990) and Borth (1990). The turbulence model was implemented in the airflow program PHOENICS-84 (Chen 1990) that is developed by Rosten and Spalding (1987). The computations involve the solution of three-dimensional equations for the conservation of mass, momentum (u, v, w), energy (H), turbulence energy (k), and the dissipation rate of turbulence energy (ε). The governing equations of the model can be expressed in a standard form:

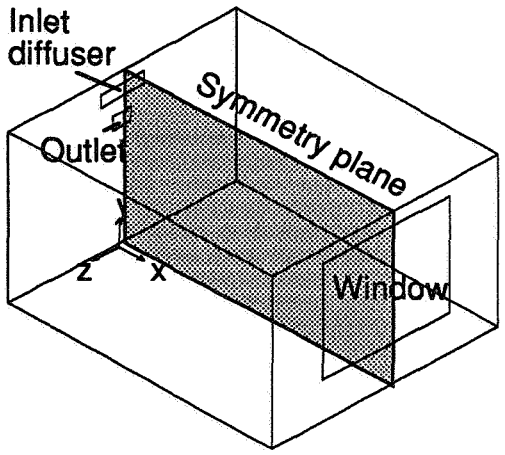

***Figure 2** Sketch of the room with a jet diffuser.*

$$\text{div}\,(\rho \vec{V} \phi - \Gamma_\phi \,\text{grad}\,\phi) = S_\phi \tag{2}$$

where ρ is the air density, $\vec{V}$ is the air velocity vector, Γ_ϕ is the diffusive coefficient, S_ϕ is the source term of the general fluid property, and ϕ can be any one of 1, *u, v, w, k,* ε, or *H*. When ϕ = 1, the equation changes into the continuity equation.

RESULTS

For more reliable information, the simulation of the HESCO diffuser is incorporated in the airflow computation in a room as shown in Figure 2. The room is 4.2 m long, 3.6 m wide, and 2.5 m high with the diffuser placed in the rear wall near the ceiling. Since the room is symmetrical in plane z = 0, the computations are carried out for half of the room. The front wall has a hot window surface for modeling a summer cooling situation. The window size is 2.0 m in width and 1.6 m in height with a surface temperature of 30°C and the rest enclosure surfaces 20°C. All 84 nozzles are adjusted with an angle 40° upwards. The actual inlet area (effective area) is 0.008 m^2. The air change rate of the room is 3 ach which corresponds to a mass inflow of 0.0315 m^3/s. This implies that the mean velocity of the supply air is 3.94 m/s. The turbulence intensity of the supply air is estimated to be 10%. The supply air temperature specified by IEA Annex 20 is 15.0°C. An outlet is placed below the inlet with a

dimension of 0.3 m in width and 0.2 m in height. Corresponding measurements, which were carried out in different IEA Annex 20 participating countries (Fossdal 1990; and Heikkinen 1990), are used for comparison.

The same grid distribution (22 x 34 x 34) was used for all the computations for half of the room to eliminate the error caused by grid diffusion. In the one-slot method (basic model), the slot was simulated by 7 x 4 cells. Each slot has 4 x 2 cells in the 12-slot method. However, only one cell is used for each slot in the 84-slot method because of the huge computing cost. The round nozzles are simulated by rectangular ones as shown in Figures 1b, 1c, and 1d. More than five hours of CPU time is used for each computation in a CRAY X/MP super computer. The sum of the absolute mass residuals of each cell is about 10% of the mass inflow and the continuity error between the inlet and outlet is 0.5% of the mass inflow.

The computational results are illustrated in Figures 3 to 6. Figures 3a, 4a, 5a, and 6a are the velocity vectors in plane z =0.0 m (the symmetrical plane); Figures 3b, 4b, 5b, and 6b the velocity vectors in plane x = 4.10 m (near the window); Figures 3c, 4c, 5c, and 6c the velocity vectors in plane y = 2.425 m (near the ceiling via the inlet); Figures 3d, 4d, 5d, and 6d the velocity vectors in plane y = 0.10 m (near the floor); and Figures 3e, 4e, 5e, and 6e and 3f, 4f, 5f, and 6f the velocity scalar and air temperature in the symmetrical plane respectively. The results predicted by the one-slot and 12-slot methods are quite different from those by the 84-slot and momentum methods. The later two methods give similar results.

The computed results have been compared with the experiments carried out by Fossdal (1990), and Heikkinen (1990). Although the experiments are conducted on the same specification by IEA Annex 20, there are differences between the measurements as shown in Figures 7 and 8. The comparisons are only indicated for the symmetrical plane because it is the most important plane. We have noted that there is an asymmetry in the experiments but the asymmetry is not significant. The comparison for the velocity profiles concludes that the 84-slot and momentum methods are in reasonable agreement with the measurements. In general, the computed air temperature is about 1 K lower than the measured (Figure 8). There are differences in the thermal and flow boundary conditions as given in Table 1.

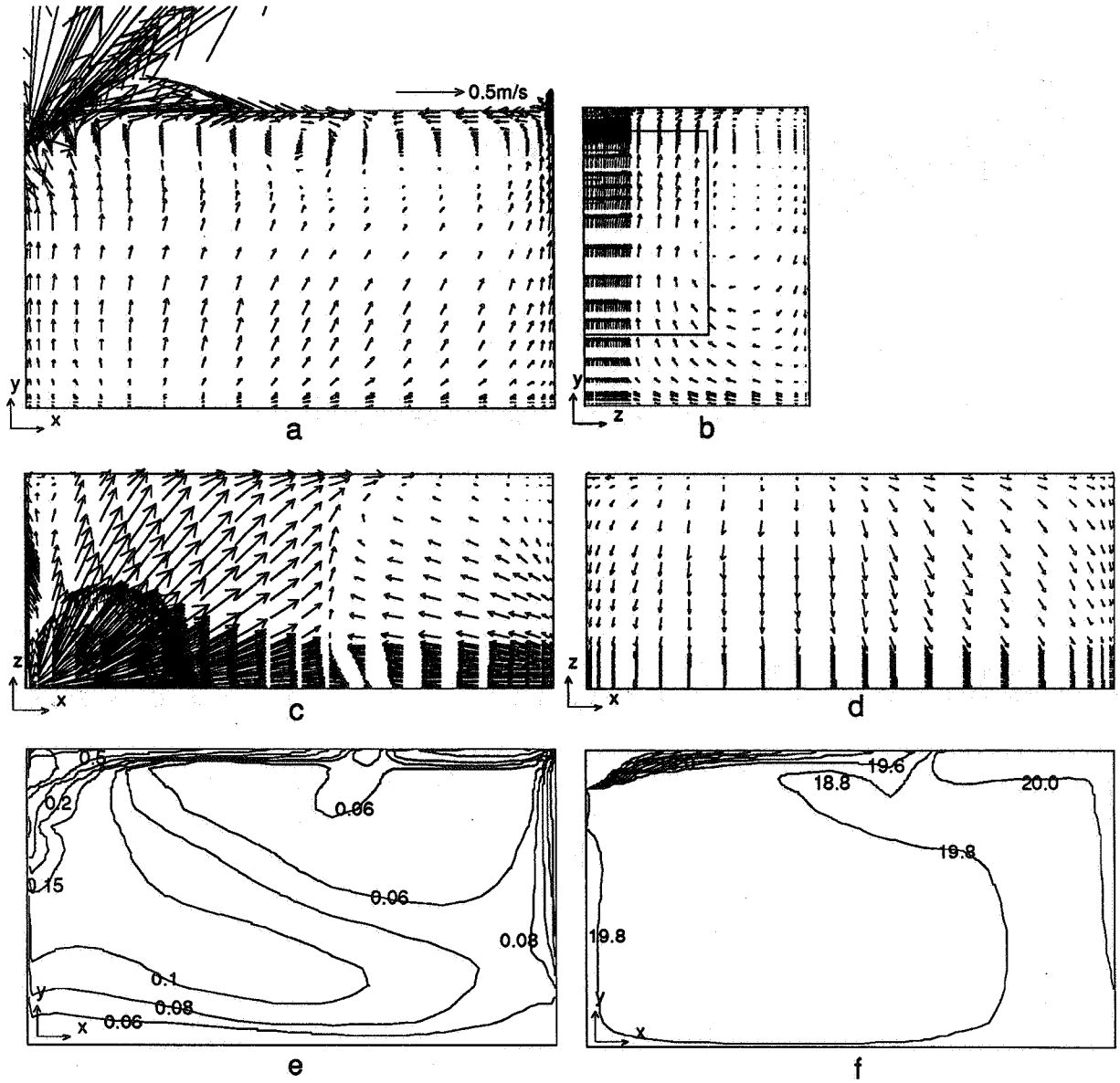

Figure 3 *Velocity and temperature distributions simulated by the one-slot method. (a) velocity vectors in plane z = 0.0 m (symmetrical plane); (b) velocity vectors in plane x = 4.10 m; (c) velocity vectors in plane y = 2.425 m; (d) velocity vectors in plane y = 0.10 m; (e) velocity scalar in plane z = 0.0 m; (f) temperature in plane z = 0.0 m (°C).*

Higher surface temperatures in the experiments will result in a higher temperature of room air. However, the heat exchange between the window surface and room air, which is computed by the low-Reynolds-number model, may be a little bit smaller since the grids used in the boundary are not sufficient. This will give a lower temperature of room air. Figure 7 shows that the temperature profiles by the 84-slot and momentum methods are very similar to

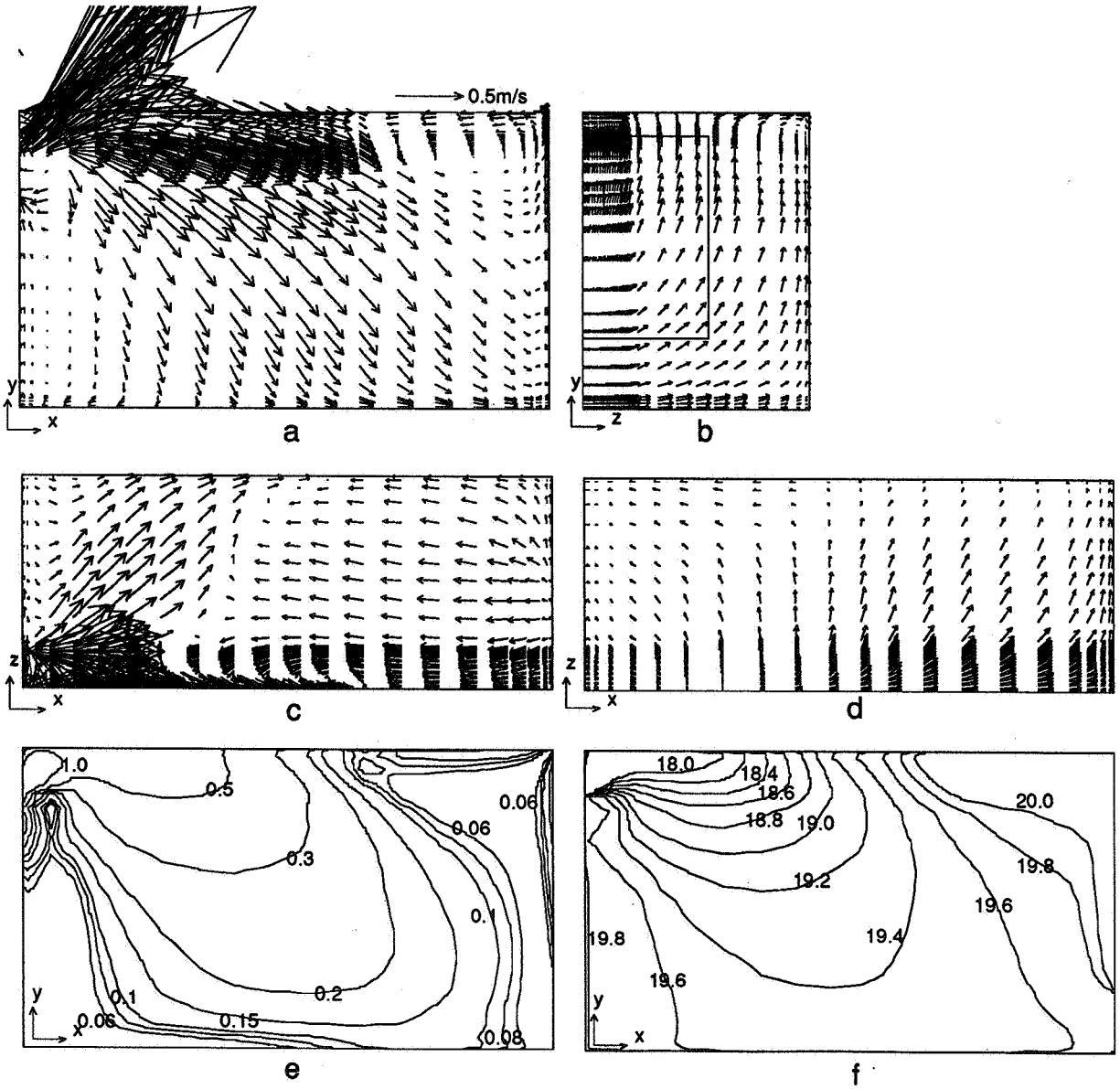

Figure 4 *Velocity and temperature distributions simulated by the 12-slot method. (a) velocity vectors in plane z = 0.0 m (symmetrical plane); (b) velocity vectors in plane x = 4.10 m; (c) velocity vectors in plane y = 2.425 m; (d) velocity vectors in plane y = 0.10 m; (e) velocity scalar in plane z = 0.0 m; (f) temperature in plane z = 0.0 m (°C).*

those measured regardless the average temperature of room air.

The simulated velocity distrbution by the one-slot method (Figures 3a and 3c) shows that the jet deflects from the ceiling in the mid-length of the room. The simulation by the 12-slot method presents similar results. This implies that the air

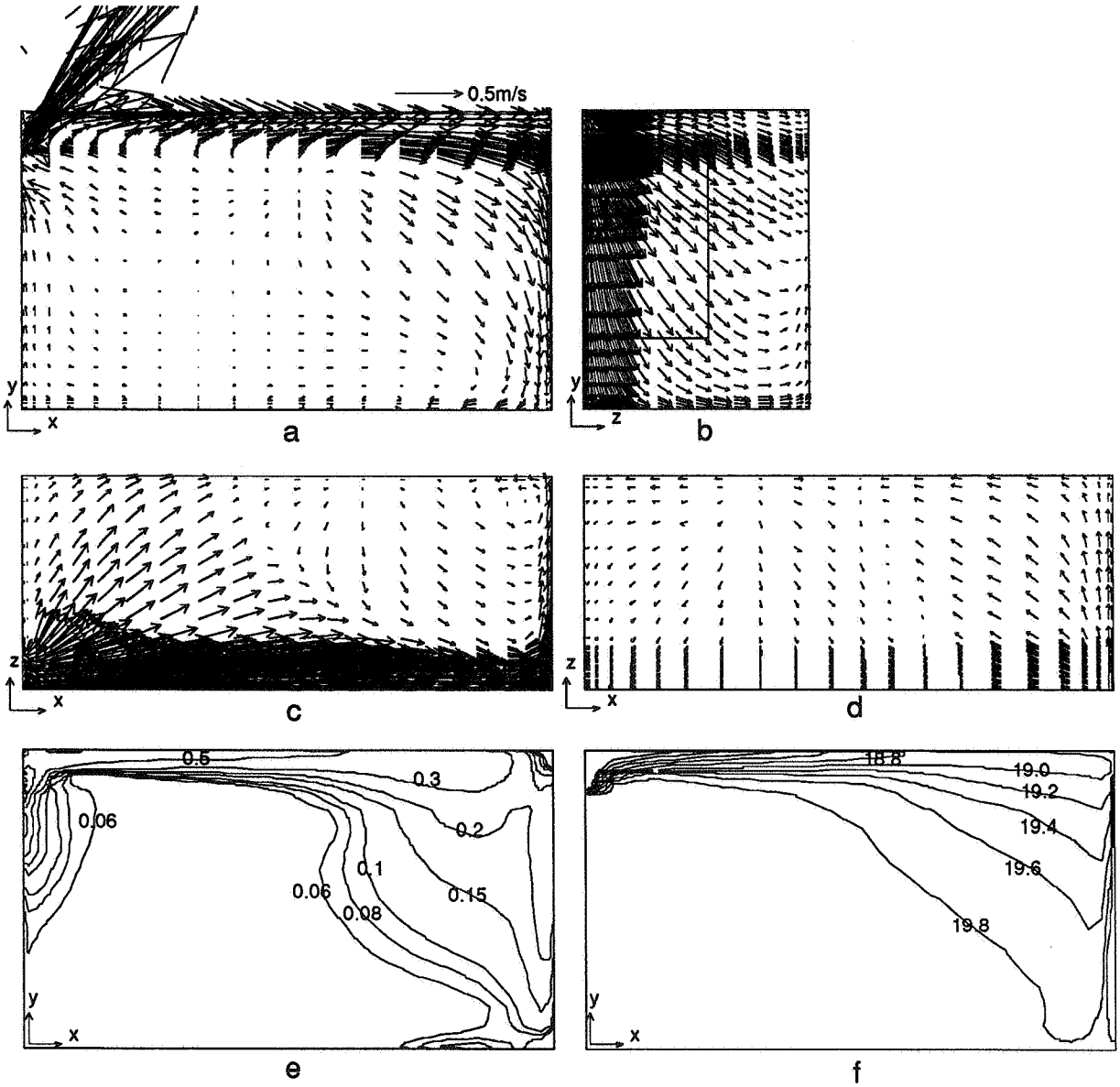

Figure 5 *Velocity and temperature distributions simulated by the 84-slot method. (a) velocity vectors in plane z = 0.0 m (symmetrical plane); (b) velocity vectors in plane x = 4.10 m; (c) velocity vectors in plane y = 2.425 m; (d) velocity vectors in plane y = 0.10 m; (e) velocity scalar in plane z = 0.0 m; (f) temperature in plane z = 0.0 m (°C).*

velocity decay from the jet is too fast by comparing the corresponding experimental data as shown in Figure 7. It is difficult to identify which computation, by the 84-slot method or by the momentum method, is in better agreement with the measurements because there are some differences in the two sets of experimental data.

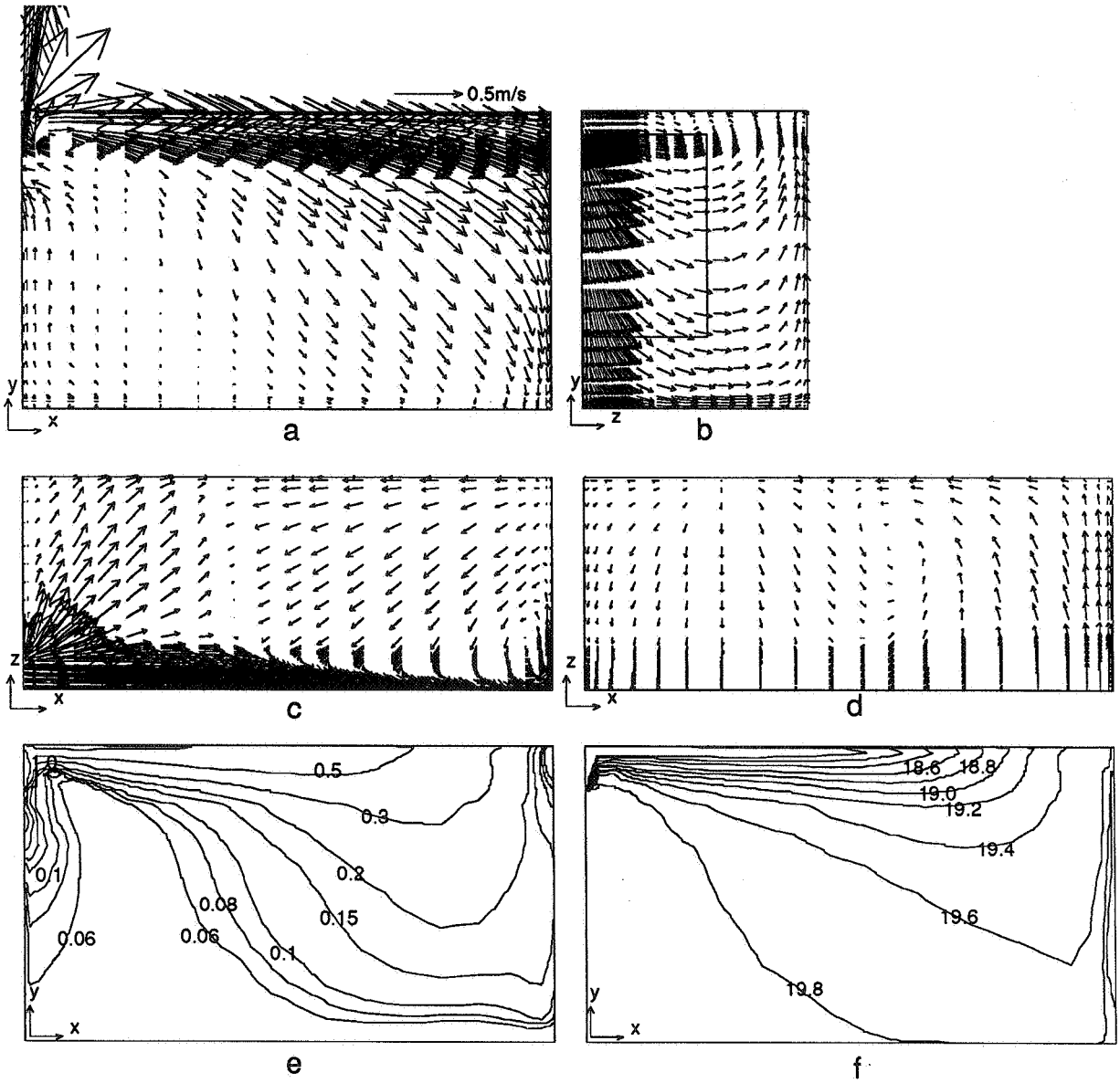

Figure 6 *Velocity and temperature distributions simulated by the momentum method. (a) velocity vectors in plane z = 0.0 m (symmetrical plane); (b) velocity vectors in plane x = 4.10 m; (c) velocity vectors in plane y = 2.425 m; (d) velocity vectors in plane y = 0.10 m; (e) velocity scalar in plane z = 0.0 m; (f) temperature in plane z = 0.0 m (°C).*

The computing cost with such a fine grid is too high to be used at present in practical applications. It is found that the inlet simulated by 28 slots gives very close results to those by 84 slots. If less slots are used, the grid employed for simulating the inlet can be reduced. As a result, computing cost will be lower considerably. The momentum method could be the most economical one among

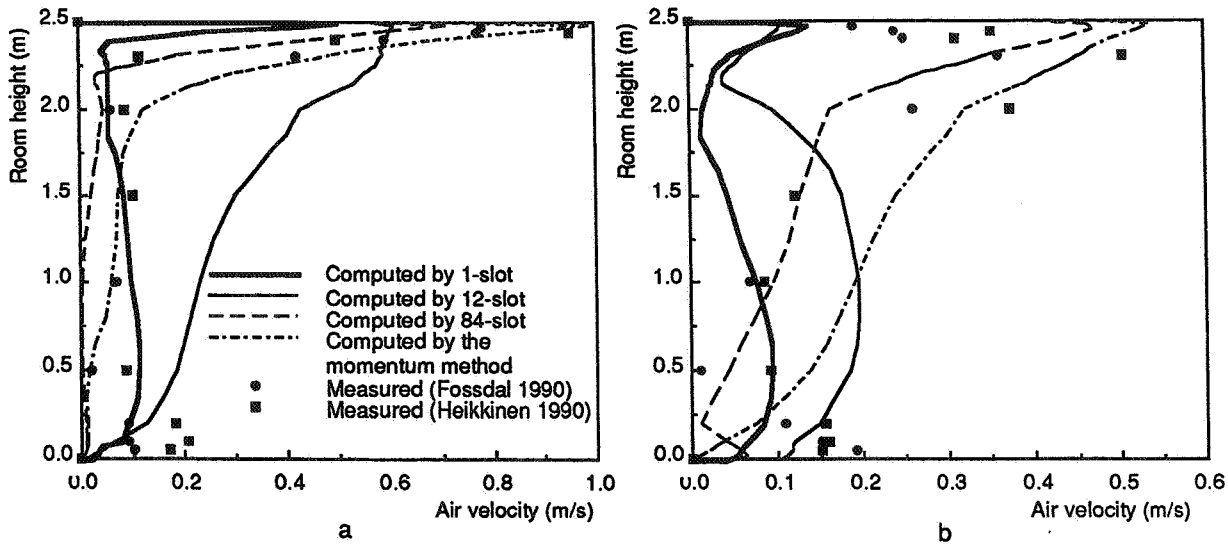

Figure 7 Comparison between the computations and measurements on velocity in z = 0.0 m plane. (a) at x = 1.4 m section and (b) at x = 3.0 m section.

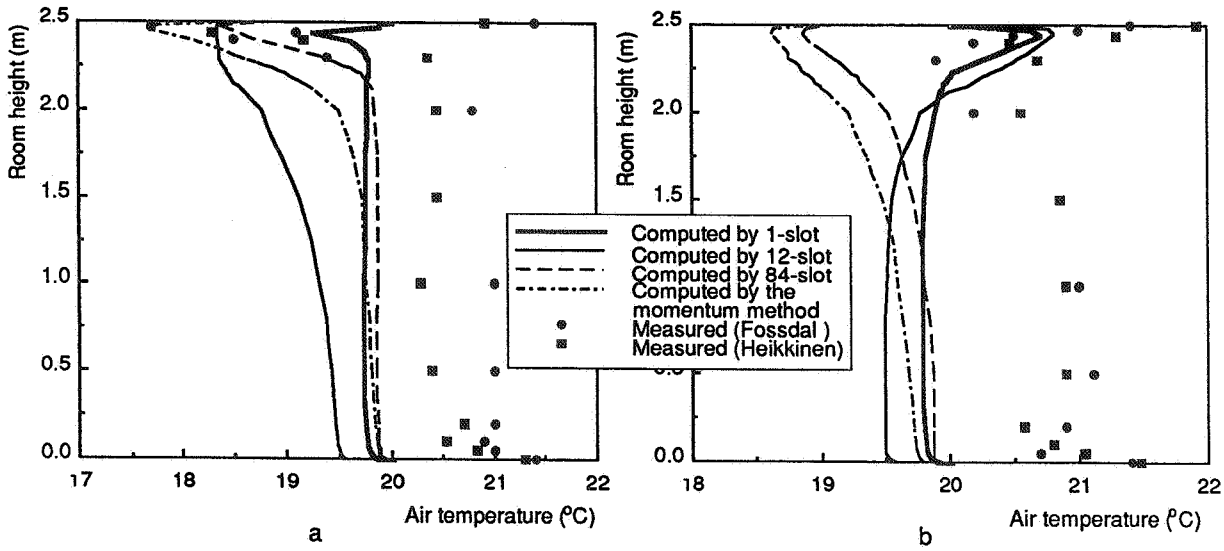

Figure 8 Comparison between the computations and measurements on air temperature in z = 0.0 m plane. (a) at x = 1.4 m section and (b) at x = 3.0 m section.

those method because only a few grids are required for describing an inlet. Another computation by the momentum method is done with a grid distribution of 22 x 29 x 15. The results are nearly the same as those by 22 x 34 x 34. Hence,the momentum method is recommended to be used to simulate a complex diffuser in practice.

Table 1 Boundary conditions in the experiments and computations.

Case	Inflow ach	T_{inlet} °C	T_{window} °C	$T_{surface}$ °C	T_{outlet} °C
Fossdal	3.0	14.0	30.3	21.4	20.8
Heikkinen	3.0	14.94	29.87	21.26	20.72
1 slot	3.0	15.0	30.0	20.0	19.70
12 slots	3.0	15.0	30.0	20.0	19.87
84 slots	3.0	15.0	30.0	20.0	20.08
Momentum	3.0	15.0	30.0	20.0	20.04

CONCLUSION

A number of approximated methods have been used to simulate a high-momentum jet diffuser with 84 round nozzles. Corresponding measurements from other researchers are used for comparison. The momentum method and the method using 84 simple rectangular slots predict air velocity and temperature distributions in the room similar to those from the experiments. The computing cost with the 84 slots method is extremely high. Hence, the momentum method is suggested to be used to simulate a complex diffuser in practice.

ACKNOWLEDGEMENTS

This investigation was financially supported by the Swiss Federal Office of Energy (BEW).

REFERENCES

Borth, J. 1990.
"Numerical simulation of air flows in rooms"
European Research Community on Flow Turbulence and Combustion Bulletin, Vol. 5, pp. 9-14.

Chen, Q. 1990.
"Construction of a low Reynolds number k-ε model"

The PHOENICS Journal of Computational Fluid Dynamics and Its Applications, Vol. 3, No. 3, pp. 288-329.

Chen, Q.; Moser, A.; and Huber, A. 1990.
"Prediction of buoyant, turbulent flow by a low-Reynolds-number k-ε model"
ASHRAE Transactions, Vol. 96, Part 1, pp. 564-573.

Fossdal, S. 1990.
"Measurement of Testcase E (Mixed Convection, Summer Cooling)"
Preliminary Report of International Energy Agency Annex 20.

Heikkinen, J. 1990.
"Measurements of Case B2, B3, E2 and E3"
Working Report of International Energy Agency Annex 20.

Heikkinen, J. 1990a.
"Modelling of the air inlet device"
Working Report of International Energy Agency Annex 20.

Lemaire, A.D. 1990.
"Simulation of test case b"
Presented in the 6th IEA Annex 20 Expert Meeting, Nice, France.

Nielsen, P.V.; Restivo, A.; and Whitelaw, J.H. 1979.
"Buoyancy-affected flows in ventilated rooms"
Numerical Heat Transfer, Vol. 2, pp. 115-127.

Nielsen, P.V. 1990.
"Selection of air terminal device"
Working Report of International Energy Agency Annex 20

Rosten, H.I. and Spalding, D.B. 1987.
"The PHOENICS Reference Manual (Version 1.4)"
Report No. TR200, CHAM Ltd., London.

AIR MOVEMENT & VENTILATION CONTROL WITHIN BUILDINGS
12th AIVC Conference, Ottawa, Canada
24-27 September, 1991

POSTER 2

A New Handbook on Measurement Techniques Related to Airflow Patterns Within Buildings

Claude-Alain Roulet
LESO-PB
Solar Energy and Building Physics Research Laboratory
Ecole Polytechnique Fédérale,
Lausanne, Switzerland

Luk Vandaele
BBRI-WTCB-CSTC
Belgian Building Research Institute,
Limelette, Belgium.

Synopsis

A new handbook, describing in details the measurement techniques which could be used to better understand the infiltration and ventilation in buildings is presented. This handbook results from the cooperation between Annex 20 and Annex 5 of the IEA ECB program. It presents the techniques for detecting and measuring as well the air leakages as the air flows in buildings and in ventilation systems. Methods related to ventilation efficiency and effectiveness, like the measurement of the age of air, are also described.

Introduction

Improving comfort and indoor air quality as well as minimizing the pollution and energy consumption are of growing importance in many countries. For that purpose, the use of theoretical models and simulation computer codes is useful. Planning rules are also published to increase the quality of the construction and the performances of the ventilation systems.

The reality however does not always follows theoretical models, nor is the actual work always a perfect execution of the proposed design. This results sometime in uncomfortable or even sick buildings (too leaky or too tight envelope, too much contaminants), in dysfunction of the HVAC system (too much or not enough air, shortcuts, spreading of contaminants) or high energy consumption. On the other hand, some theoretical models or computer programs do not follow the reality, that is do not reproduce it in a satisfactory way.

In order to assess the reality, to control the building and ventilation system performances and to evaluate models and computer programs, measurements are of great help, if not unavoidable. Such measurement techniques are described in the literature, but, except the AIVC Measurement Guide[1], no comprehensive review, describing the many techniques in much detail, was available.

As a result of a close collaboration between the Annex 20, subtask 2 contributors and the AIVC, a technical handbook was prepared, based on the AIVC Measurement Guide, but greatly extended to take into account the latest developments in measurement methods related to ventilation[2]. It is concerned with the measurement of those parameters which are important in gaining an understanding of air infiltration and ventilation.

A short history

From the early beginning of the IEA-ECB Annex 20 "Airflow Patterns Within Buildings", it was decided, within the subtask 2 "Multizone Air Flows" to contribute to the development of new measurement techniques, adapted to the study of air flow patterns in multizone buildings. As usual in such international programs, it was intended to publish a report describing the methods developed in the frame of the Annex 20. These methods would be enhanced pressurization tests and multizone tracer measurement techniques.

Since the AIVC was interested in picking some information from this report to complete its Measurement Guide, it was proposed that the Annex 20 report would be several packs of sheets which could be inserted in the AIVC Guide. For that purpose, information was gathered as well from the literature (using AIRBASE) as from every Annex 20, subtask 2 participant. On that base, two reports, one on enhanced pressurization test methods and the other on multizone tracer measurement techniques, were drafted. Looking at these drafts, two facts were clearly seen:

a) because of the particular structure of the AIVC guide, it would be difficult to integrate these drafts into the Guide, and,

b) it might be interesting to extend the description as well to the techniques related to the age of air and to ventilation efficiency and effectiveness, as to measurement methods which could be applied to ventilation systems.

Therefore, the authors agreed with the Head of AIVC to make together a completely new edition of the AIVC Measurement Guide. Texts, figures and informations coming from the Guide were merged with the draft Annex 20 reports. This new, combined draft was completed with two more parts concerning measurement techniques related to indoor air quality and to ventilation systems and submitted to the Annex 20 participants and to the Steering Group of the AIVC.

At that time, it appeared that this new draft, if useful for the scientists going to make measurements in the field, might be too complex and too detailed for non specialists, or, in other words, that the new draft was not for the same public as the AIVC Guide. It was therefore decided in the Steering Group of Annex 5 that the new draft will be published as a new Technical Note and that the AIVC Guide will remain, with some additions prepared by the AIVC.

Content of the Handbook

This handbook is hence the result of a strong collaboration between the Annex 20, subtask 2 and the Annex 5. The latest developments in measurement methods related to ventilation were described by Annex 20 participants and large portions of the Measurement Techniques Guide first published in 1988 by the AIVC and describing the techniques already known at that time were reviewed and integrated, in order to make this handbook as comprehensive as possible.

The complete book is 286 pages thick, the relative importance or the various parts can be seen in Table 1. Its content is summarized below.

Table 1: Number of pages, figures and tables in the various parts.

Part	Pages	Figures	Tables
I	18	4	11
II	74	42	11
III	92	28	6
IV	24	3	5
V	18	7	0
Appendices	56	23	15
Index	4	0	0
Total	286	107	48

The introduction provides a general overview of infiltration and ventilation in buildings. Ventilation studies are discussed and the aims of the guide outlined.

Part I defines the parameters which are important, presents the reasons why they should be measured and gives a guide to the selection of techniques for particular applications. Summaries of the main techniques available are presented, which are cross referenced with the main body of the guide. This part intends to help answering the question: *"Which measurement technique should I use to get the value I require?"*. This part contains the following chapters:

1. Structure of the Handbook
2. Introduction
3. Selecting a Technique

Part II, **Air Leakage Measurement Methods**, presents the theory and practice of measuring the airtightness of the building envelope and its components as well as of the internal partitions within the building. In general, this part answers the question: *"How could I quantify airtightness of a building as a whole, of particular zones or particular building components and how could I detect or visualize leaks?"*.

One chapter is dealing with the measurement of the two basic physical variables in the representation of air leakage, namely pressure and air flow rate. A large number of currently available techniques and equipments for the actual determination of overall airtightness and components leakages, both qualitatively and quantitatively, are presented, often accompanied by an example from practice. The global structure is:

1. Introduction
2. Principles of the Pressurization Techniques
3. Pressure and Air Flow Measurements
4. Current techniques
5. Treatment of Results
6. Equipment
7. Airtightness Measurement Techniques Standards

Part III, **Air Flow Measurement Methods,** presents the theory and practice of measuring air exchange rates and the related contaminant flow rates, as well in single zone as in multizone buildings. Air exchange between a building and the external environment is examined, as is the air exchange between the various internal spaces of a building. This part is for those which have the following questions: *"I would measure air flow rates within single and multi-zone buildings. Which are the methods? Which instruments could I use? How could I measure and interpret the results?* The answers are found in the chapters listed below:

1. Introduction, Objective of Measurements
2. Basic Equations
3. Principles of Different Methods for Determining Outdoor Air Flow Rates into a Building and Interzonal Air Flow Rates
4. Treatment of Results
5. Components of a Tracer Measurement System
6. Examples of Systems
7. Comparisons of Methods
8. Standards

Part IV, **Measurement Methods Related to Efficiency,** presents some measurement methods which may be useful to qualify the indoor air and the efficiency of the ventilation system. This part however does not describe the techniques for the measurement of contaminant concentrations. It will only help people which wonder *"How old is my fresh air? Where are the dead zones? Does the contaminants stay long in my breathing area?"*. The addressed matters include the following:

1. Introduction
2. Definitions
3. Local Age of Air
4. Planning of Mapping Experiments
5. Room Mean Age of Air and Air Exchange Efficiency
6. Measurement Methods Related to Ventilation Effectiveness

Part V, **Measurements on Ventilation Systems,** describes measurement methods able to qualify a system, namely to measure the flow rates in the ventilation network and to control its tightness. As well the simple measurement of the air flow rate in one duct as techniques allowing to assess all the flows in a ductwork are described. The answered question is here: "How could I control if my (mechanical) ventilation system works as planned?". The following chapters are found in this part:

1. Introduction
2. Measurement of the Air Flow Rate in a Duct
3. Air Flow Rates in a Ventilation Network
4. Efficiency of the Ventilation System
5. Measurement of Air Tightness of a Duct or Network

Appendices are provided either to give informations on general tools or to lighten the main text from informations which may be useful only to specialists. These are:

A 1. Unit Conversion Tables
A 2. Error Analysis
A 3. Identification Methods
A 4. Example of Multizone Pressurization in a Realistic Case
A 5. Strength of the Passive PFT Sources
A 6. Algorithm to Control a Constant Concentration System
A 7. Glossary

An **index** with some 430 entries is located at the end of the book, to help users in looking for the good information.

How to use this handbook?

There are many measurement techniques which could be used to study the air flow patterns within buildings. Remember however that measurements are often time consuming and expensive. They generally require sophisticated instruments which are not always immediately available. For all these reasons, measurements should be carefully planned and performed only when required. Measurement is the answer, but what is the question?.

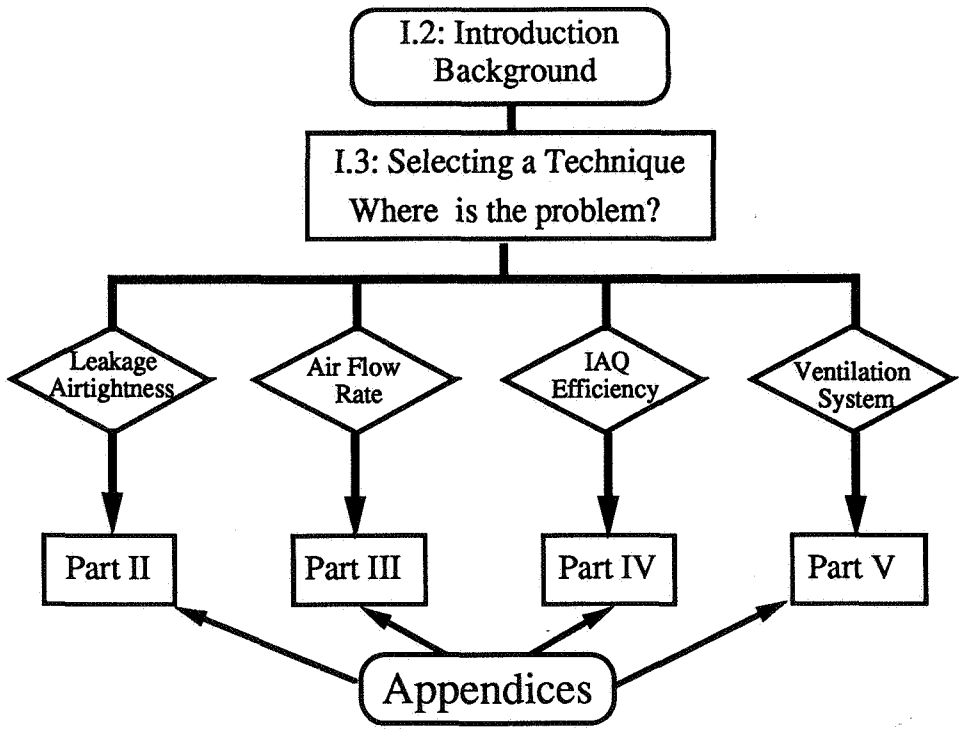

Figure 1: Structure of the Handbook.

To use this handbook (as any measurement technique) efficiently, one should first answer the following basic questions, in the following order:

1) What is the problem to be solved?
2) Which physical data may be useful to solve my problem?
3) Out of these data, which could be simply guessed and which ones should really be measured?
4) Which technique could be used to measure the required data?
5) How should I use that measurement technique?
6) How should I interpret the results to answer my questions?

After, and only after answering these questions, the experiment can be defined, the instruments installed, the measurement performed, the results treated and the problem solved.

The presented handbook only helps answering questions 4) to 6), as it is shown in Figure 1, which represents the structure of the book.

Conclusions

This publication intends to help scientists wanting to make measurements in the field of air infiltration and ventilation in buildings. It should be used as a handbook and can be opened when required at the pages of interest. The index and detailed tables of content may help in finding the proper information.

For some specialists, parts of the handbook will seem too simple, while newcomers may require some basic teaching before reading the details of some interpretation methods. It is impossible to prepare a text which is at the ideal level for any reader, but we nevertheless hope that every reader will find the necessary information.

Acknowledgements

The preparation of the handbook presented here depended on the effort and cooperation of many individuals and organizations. It is mainly based on information received from research workers, who have gained experience developing and using specific measurement techniques. Written contributions were received from:

AIVC, Coventry (UK): Peter S. Charlesworth and Martin Liddament.
BBRI Limelette, (Belgium): Peter Wouters and R. Bossicard.
BRE, Garston (UK): Roger Stephen and Richard Walker.
Brookhaven National Laboratory (USA): Russell Dietz.
Brüel & Kjaer, Naerum (DK): Bjørn Kvisgaard.
CBS, Concordia University, Montreal (Canada): Fariborz Haghighat.
CEES Princeton University (USA): David Harrje.
EMPA, Dübendorf (Switzerland): Viktor Dorer.
LBL, Berkeley, Cal (USA): Max Sherman and Mark Modera.
LESO-EPFL, Lausanne (Switzerland): R. Compagnon and J.-M. Fürbringer.
LNE, Trappes (France): Pascal Launey.
NIST, Gaithersburg MD (USA): J. Axley, A. Persily and R. Grot.
Politecnico di Torino, (Italy): R. Borchielini and M. Cali.
SIB, Gävle, (Sweden): Mats Sandberg and Hans Stymne
UMIST, Manchester (UK): Roger Edwards.
Willan Building Services, (UK): Chris Irwin.

In addition valuable advice and assistance concerning the content of this publication was gratefully received from the AIVC and from those who attended the Annex 20 working meetings.

The authors would like to thank particularly David Harrje (Coupeville, WA. USA), Martin Liddament (AIVC), Richard Walker and Roger Stephens (BRE, UK) for their assistance in proof reading the handbook.

References

1] **Charlesworth, P. S.:** Air Exchange Rate and Airtightness Measurement Techniques - An Application Guide. *Air Infiltration and Ventilation Centre (AIVC), Warwick (UK), 1988, AIRBASE #3292.*

2] **Roulet, C.-A. and Vandaele, L:** Airflow Patterns Within Buildings, Measurement Techniques. *Technical Note, Air Infiltration and Ventilation Centre (AIVC), Warwick (UK), 1991*

AIR MOVEMENT & VENTILATION CONTROL WITHIN BUILDINGS
12th AIVC Conference, Ottawa, Canada
24-27 September, 1991

POSTER 3

Stochastic model of inhabitant behavior in regard to ventilation

C.-A. Roulet, P. Cretton, R. Fritsch and J.-L. Scartezzini

Laboratoire d'Energie Solaire et de Physique du Bâtiment
Ecole Polytechnique Fédérale de Lausanne
CH - 1015 Lausanne

Synopsis

Airflow rates are directly affected by the amount of open area and consequently by the inhabitant behavior with respect to window opening. In this paper, a stochastic model using Markov chains, developed at the LESO to generate time series of single-window opening angle is modified to generate multiple window openings. It is based on data measured by the TNO Delft on 80 identical, 16 openings dwellings located at Schiedam (NL). The model is then validated by a comparison of the real and generated data. The use of this model within building air infiltration design programmes should improve significantly the likelihood of the latter.

1. Introduction

1.1. Importance of the Inhabitant

The importance of airflow rates on heating cost and the elimination of pollutants within buildings is a fact and already many softwares are available to simulate them[1]. However, it must be pointed out that all these programmes run with unoccupied buildings, even though airflow rates are closely related to the amount of open area and therefore to the inhabitant behavior concerning window opening. For instance, measurements conducted in 25 Danish buildings shows that in average the increase in the airflow rate due to occupancy is more than 100%[2].

In order to improve future programmes a model simulating window opening during the winter has been developed and was presented elsewhere[3]. This model was based on measured data from four offices of the three storey's LESO experimental office building[4]. Using a method similar described by Fewkes & Ferris[5], the model generates time series of window opening angles with the same statistics (i.e. average opening angle, time correlation, temperature dependance, etc...) as the measured openings for the heating period.

1.2 Driving variables

From the work of IEA-ECB annex 8[2] (and since the 7th AIVC conference), it is well known that the inhabitant behavior concerning the openings depends on several variables. Some of these may drive the opening and closing, some others only one of this action (e.g. the occurrence of rain may enhance the probability of closing the windows). These driving variables are listed in Table 1

Table 1: Possible driving variables for window opening and closing[3].

External variables	Internal variables	"Human" parameters
Outdoor temperature Solar radiation Wind velocity Rain Noise Odors and pollutants	Indoor temperature Odors Contaminants Moisture	Time of the day Type of day Type of building Habits etc.

Several intercorrelations between the openings and some of these variables were examined. It was found that the most significant one is the outdoor temperature[3]. Only this variable is taken into account in the present work. This has moreover the advantage of linking the model to a data which is generally available all around the World in each meteorological station.

The indoor temperature was considered, but not retained as driving variable, the reason being that it is difficult to handle in multiroom infiltration programmes which are seldom combined with a thermal calculation code.

1.3 Basic principles of the model

A simple way of introducing inhabitant behavior in a computer code is to record the windows and doors openings in a dwelling, at a convenient time interval and during a statistically significant time period. These recorded data could then be introduced as input schedule in the computer code, which receives that way exact information on the inhabitant behavior of the monitored dwelling. However, this method presents several inconveniences:

1) The recorded data are valid only together with the meteorological data synchronously recorded on the same site. It is therefore not possible to translate the recorded information to other buildings under other climates.
2) Only the measured inhabitant is represented that way. Other behaviors could however be introduced by performing other measurements and storing other sets of data.
3) The many recorded data use much memory space. The basic data used within the framework of this paper filled fifteen 1.44 Megabyte disks, that is about 20 Megabyte for 80 dwellings.

The purpose of the model is to generate window opening sequences which are similar to the measured ones, but with a very small amount of input data. These input data are obtained by statistical treatment of measured data. The opening sequence is reconstructed by random generation according to some rules resulting from that statistical treatment.

The simplest generation is to close and open the windows following an independant stochastic process, according to frequency and opening time distributions. However, this method does not provide realistic sequences, since it is well known that the opening time depends on the outdoor temperature[2] and it was shown[3] that the opening angle of a window is autocorrelated, which means that the state at a given time depends on the preceding states.

The next step in complexity is the Markov chain, in which the state at one time step depends only on the preceding state. Markovian processes present a non-zero autocorrelation function, but a differential autocorrelation function† which is zero, except at the origin. The Markov chain has proven to be a suitable model for simulating window opening angles[3].

2. Data Used For The Model

The model developed here is based on measurements recorded every 10 minutes in 80 dwellings of a 10-floor building located at Schiedam (Netherlands)[6,7,8]. All the dwellings are similar (Figure 1) and there are 14 dwellings per floor. Each dwelling has 14 windows and two doors, located on both facades as shown on Figure 1.

Measurements of the window opening (using switches) were taken at very short time intervals (20 seconds). In order to discretize the time scale as required by the Markov chain, a time step of 10 minutes was adopted as a compromize, large enough to limit the number of data, and not too short in order not to loose too much accuracy. The opening time during these intervals was calculated for every window. When that opening time was larger than 5 minutes, the window was considered open during 10 minutes, and considered as closed if the open time was less than 5 minutes.

Each dwelling having 14 windows and 2 doors, the status of these was recorded as two bytes of 8 bits, that is 2 ASCII characters. Meteorological variables such as outdoor temperature, wind speed, solar radiation and rain as well as inside air temperature and inlet and outlet heating water temperatures were also recorded.

---

† The differential autocorrelation function is the autocorrelation function of the difference between two successive states.

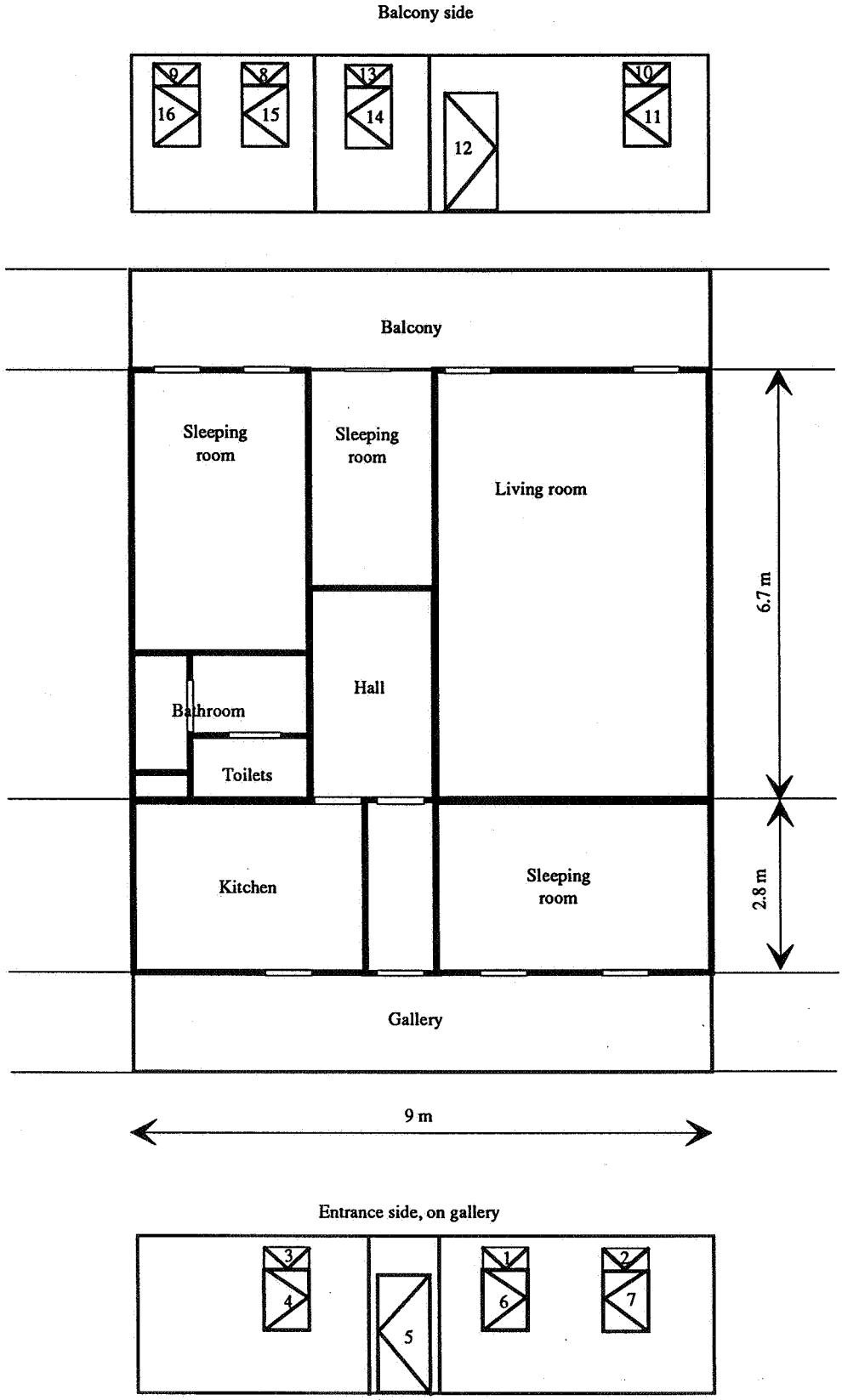

Figure 1: Floor plan of a dwelling and position of windows and doors in the facades and the corresponding numbers[6]

The measurements used for that study were taken during 118 days from winter to summer. These were taken out of longer files, using the following criteria:

- both meteorological data and window openings should be available at each time step,
- there should not be more than 20 minutes between two measurements, i.e. not more than one missing measurement. If one measurement was missing, the preceding data were taken without change.
- series of data with less than 100 measurements (that is shorter than 16.7 hours) were eliminated.

This resulted in a file of 17 043 measurements at 10 minutes interval, which is a pack of several smaller files. The transition between two files (i.e. during apparent time intervals larger than 10 minutes) were not taken into account in the analysis. The final number of valid transitions is then 16 976.

3. Setting up the Model

3.1 Existing model

The existing model[3] was developed to generate time series of window opening angles, which was divided into 6 classes: [0-1[(closed), [1-15[, [15-35[, [35-60[, [60-90[, [90-120] degree. Moreover, it was based on measurements performed in offices with a single openable window. The effect of the outdoor temperature was taken into account by dividing the domain of that variable into 4 classes: [-273-0[, [0-8[, [8-16[, [16-∞[°C. and four series of data were generated and used for each of these four temperature classes.

3.2 Reasons for modifications

The Schiedam measurements are window and door openings (that is either 0 for closed or 1 for open) and one dwelling has 14 windows and two doors, whose opening probabilities are likely to be correlated. The existing model should therefore be modified first to provide time series of openings instead of angles, but also to take account of the many windows in a dwelling.

The difference between the opening angle and the opening indicated by a switch is a trivial but important change: the 6 classes of opening angle of the preceding model are replaced by only two: closed or open. Since the air flow rates through a window depends on the opening angle[9], it is an important issue and maybe a dramatic approximation. However, there are, at our knowledge, no available data providing the opening angle for many windows in dwellings and this model should be based on existing measured data.

3.3 Which user should be simulated?

It is well known[2] that the inhabitant behaviors differ much from each other, and these differences give the basic reason to take them into account in the simulations. Since the measurements were performed on 80 dwellings, there is a large choice of behaviors. Whose of these should be chosen? Which criteria could be used for that choice?

The criteria could be the total opening time of all the windows and doors, the total number of changes or some more complex criterion such as the extra air change rate induced by the behavior. The latter is too complex to be handled and the total opening time was taken as criteria, since it is more related to air flow rates than the number of opening.

One can choose an "average" inhabitant, a "closer", or an "opener". Note that the definition of the "average" dwelling is not obvious. First of all, none of the 80 dwellings has opening times close to the general average for each window. Therefore, it makes no sense to generate an artificial average user by averaging the data over the 80 dwellings. It is proposed here to choose one user which is close to the general average.

This could be the one with the average opening time, μ, closest to the general average (the average being taken as well on time as on the windows), or the one which is the closest for each window and door, that is the one which has the smallest standard deviation, σ, to the average for each opening, summed over the 16 windows and doors.

Some figures are given in Table 2, which shows the dramatic differences between the dwellings. In this Table, μ is the average of the corresponding line and σ is the standard deviation between the corresponding line and the global average. Note that the database used to make that table and hence choose the interesting users is slightly smaller than the complete database used for the rest of the work.

Table 2: Relative windows (and doors) opening times, in ‰, for some selected dwellings.

Side	Gallery side							Balcony side										
Type of room	Bedroom				Kitch.		Door	Living			Bed		Large bedroom					
Opening No:	1	2	6	7	3	4	5	10	11	12	13	14	8	9	15	16	m	s
Global average	156	90	24	19	137	14	6	45	13	20	142	77	257	89	167	36	81	
Average users (see text above):																		
smallest s	135	0	2	0	107	1	1	7	0	1	143	12	303	0	15	0	45	58
closest m	18	4	6	0	145	2	2	0	0	6	320	18	607	99	134	0	85	113
"Closed" user	168	0	7	0	47	10	1	0	0	3	39	10	12	0	4	0	19	93
"Open" user	108	340	0	0	684	0	1	333	1	30	764	938	616	330	11	53	263	345

3.4 How take account of several windows?

The proper way allowing one to take account of the presence of 16 windows in a dwelling is not so obvious, since there are several possibilities. The model based on Markov chains reproduces **transitions** between **states**. The variable(s) representing the state should therefore be first defined.

Having 16 openings, a basic state of these could be represented by a 16-bit word, each bit representing one opening, and be 0 when the window is closed and 1 when open. There are theoretically 2^{16} (about 65 000) such states, hence $2^{16}\times2^{16}$ possible transitions whose probabilities could be represented in a square matrix with more than 4 billion numbers for each temperature class. Most of the elements of this matrix are zero and will not be stored but, nevertheless, this solution is neither practical nor possible. In particular, there are not enough available data (only about 17 000 transitions) to calculate the transition probabilities.

At the other end of the spectrum, each window could be considered as independent, with two states. In this case, the window and door openings of the dwelling would be modelled by 16 transition matrices, 2×2, that is 64 transition probabilities for each temperature class. This model can obviously not reproduce any intercorrelation between the opening sequence of different windows

Any intermediate model could be chosen between these extremes. As a first approximation, the simplest model is developed and tested below.

4. Independent windows model

The 16 windows and doors are assumed to be independent from each other and are treated separately. The state variables are the state of each window or door, e.g. 0 for closed and 1 for open. There are hence four transition probabilities (0 to 0, 0 to 1, 1 to 0 and 1 to 1) for each window and each temperature class.

4.1 Treatment of the data

To fill-up these 16 × 4 matrices (16 for each temperature class), the measured data were treated the following way:

1) A building is chosen and a file is generated from the big basic data file. This file contains, for the 17 000 time steps of 10 minutes, the meteorological data and the 16 window (or doors) openings of the chosen building.

Then, at each time step t_n and for each window or door:

2) the outdoor temperature is examined and the corresponding class noted,

3) the type of transition from the preceding state to the present one is determined and the corresponding element in the transition matrix for that window and that temperature class is incremented by 1. The elements are arranged as shown below:

Closed to Closed	Closed to Open
Open to Closed	Open to Open

4) When the complete file is treated that way, the elements of the transition matrices are divided by the sum of their lines or by 1, whichever is larger. This gives the 16×4 matrices of transition probabilities, for each window and each temperature class. Their elements are the transition probabilities to pass from the initial state to the next state. Since the windows are moved at time intervals which are generally much more than 10 minutes, these matrices are mainly diagonal.

If a line does not contain any transition, the window is either always closed or always open. The corresponding transition matrices are then arificially modified as shown below:

Always closed $\begin{pmatrix} 1 & 0 \\ 1 & 0 \end{pmatrix}$ Always open $\begin{pmatrix} 0 & 1 \\ 0 & 1 \end{pmatrix}$

This slight change ensures first that the sums of the lines are equal to one, as should be the sum of transition probabilities, and secondly that the correponding window will be put in its permanent state at the first time step, even if the starting state does not correspond to the reality.

4.2 Results

The four dwellings presenting an interesting average opening time as shown in Table 2 were treated that way. The 16 976 valid measurements were distributed between the temperature classes the following way:

Temperature class	[- 273, 0[	[0, 8[	[8, 16[	[16, + ∞[
Number of measurements	2743	7495	4241	2497

The Markov transition matrices are given in appendix 1, and can be used in computer codes as described in Section 4.2 below.

Some interesting statistical data are shown in appendix 2. Note that, for all the four chosen dwellings, the window 7 is always closed and the entrance door (5) has a high probability of closing when open. Each dwelling has at least two windows which are always closed. The generous opener (dwelling 41) has three windows which are open more than 95% of the time and his windows 2 and 14 are always open.

4.3 Generation of opening sequences

The technique used to reproduce synthetic data of window opening angle refers to the inverse function method[10]. This method is commonly used with stochastic processes and therefore will just be presented roughly here.

The inverse function method allows the generation of time series of a stochastic process given its distribution function. The only requirement is to dispose of a random number generator with a uniform probability density function between 0 and 1. The generated numbers, going from 0 to 1, are compared to the distribution function as shown on figure 2: for every number given by the generator, there corresponds only one state. In our case, the distribution functions have only two steps and are deduced from the lines of the Markov matrices.

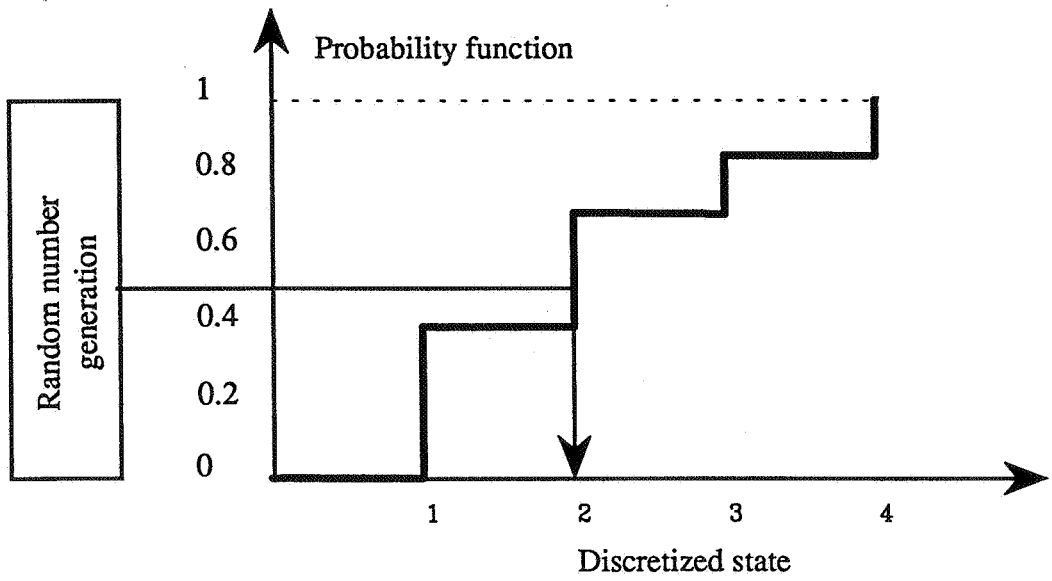

Figure 2: Generating a new state according a distribution function.

The following reconstruction procedure should be used for that model[3]:

1) At time t_0, a starting pattern of open windows is chosen arbitrarily.
2) The value of the outdoor temperature is examined, and the corresponding temperature class T ([- 273, 0[, [0, 8[, [8, 16[, [16, + ∞[ ) is noted. Choose the 16 transition matrices, $\underline{\underline{P}}_{j,T}$ (j = 1-16), corresponding to that class.
3) The line of the transition matrix corresponding to the state of the window j, contains the transition probabilities $P(S_0, S_1)$ to have the window in state S_1, at time t_1, knowing its preceding state S_0. Build the from that line of the matrix: the probability to become (or stay) closed is given in the first column and the probability to become either closed or open is 1..
4) The new state is generated at random according the distribution function, using the inverse function method.
5) Repeat the procedure from step 2 for the next time steps.

To take account of the very low night activity, the openings could be left unchanged from midnight to 7 AM. This was however not done in this work.

5. Evaluation of the Model

5.1 Comments on the evaluation procedure

It should first be stated here that a good evaluation procedure is to compare the air flow rates measured in a dwelling with the corresponding air flow rates obtained by a computer code using the presented model with its Markov matrices based on measurements in the same dwelling. Another, simpler possibility could be to compare computer code results for the same dwelling, obtained on one hand with measured opening schedules and on the other hand with opening schedules generated by the present model. These methods could however not be used within the present work, by lack of time to adapt an existing multizone infiltration code. This adaptation would require not only the present model but also a routine calculating air flow rates through large openings. This could be performed within the Annex 23 of the IEA-ECB research program.

A first estimate of the performances of this model can however be obtained by comparison of major characteristics of the generated data with reality. The compared characteristic are opening duration, frequency of changes, relation with the outdoor temperature and inter correlations between openings.

For that purpose, 6 opening schedules were reconstructed using the procedure described in Section 4.3 and the Markov matrices corresponding to the dwelling 43, whose total opening time was the closest to the global average. A different seed for the random generator was used for each schedule, but the real first state (i.e. the real status of the 16 openings at the first measurement) was always used as starting state. The reason is, that, when starting from a non realistic state (e.g. all windows closed), the Markov process takes some time to reach a realistic behavior. That way, even the first simulated days could be compared to the real data.

From these six rebuilt schedules, some statistics were calculated and compared with the same statistics extracted from the measured schedule. These comparisons are presented below.

5.2 Average duration of the openings

Table A 3.1 in Appendix 3 presents the number of 10 minutes time intervals during which the windows and doors are open, as well for the 6 calculated behaviors as for the measured one. It can immediately be seen that the average synthetic behavior is close to the measured behavior, except maybe for the window 13, in which a relative difference of more than 30 % is observed. χ^2 test, however, is not passed, even with a low probability.

The dispersion between the various rebuilt schedules varies with the opening. Large variations are seen in openings 1, 2, 4, 10, and 13 again. These openings are characterized by being seldom changed but changed anyway. In other words, they have many transitions from closed to closed and open to open, but very few (less than 5) transitions from open to closed or closed to open. In particular, window 13 started open and was closed once during the measurements.

In this case, the accuracy of the off-diagonal transition probabilities is poor (since based on a few transitions) and the re-calculated behavior is therefore not very accurate. This limit does not come from the model itself, but from the relatively small number of measurements on which the model is based. A good reproducibility of the total open time is obtained when the number of off-diagonal transitions is either 0 (always closed or open windows) or larger than 10.

This leads us to a first limitation: **The complexity of the model should be adapted to the available data.** In particular, it has no meaning to prepare detailed Markov matrices with many possibilities of transitions, if some of the transitions are poorly represented in the available data.

5.3 Number of transitions

Table A 3.2 in Appendix 3 presents the number of transitions from one state to the other. Here again, there is a good agreement between calculated and experimental data, the largest dispersions being for windows having few changes of state. This small discrepancy also comes from the reason evoked above. In this case, χ^2 test is passed, with a probability of 97.5 %.

Markov transition matrices were also rebuilt from the calculated data. They were found very similar, when not identical, to the Markov matrices built from the measured data. However, for particular windows like window 13, one rebuilt matrix (for temperature class 3) was purely diagonal, which looks strange, like if the window was closed and open, but without transition. In fact, the only transition was done in another temperature class and such a matrix tells that, for that temperature class, this window remains in the state it was when entering the temperature class.

5.4 Histogram of opening times

Figure 3 shows, always for dwelling 43, histograms of opening times, that is the number of windows open during less than 1 hour, between 1 and 2 hours, etc.... up to open more than 16 hours. The front histogram represents the experimental data, the next 6 ones are the 6 re-calculated data and the last one, in the back, is the average of these. This picture shows a good agreement between these data, except for the large opening times, where the algorithm overestimates the number of windows remaining open during more than 16 hours. Therefore, the χ^2 test is passed only with a probability of 10%.

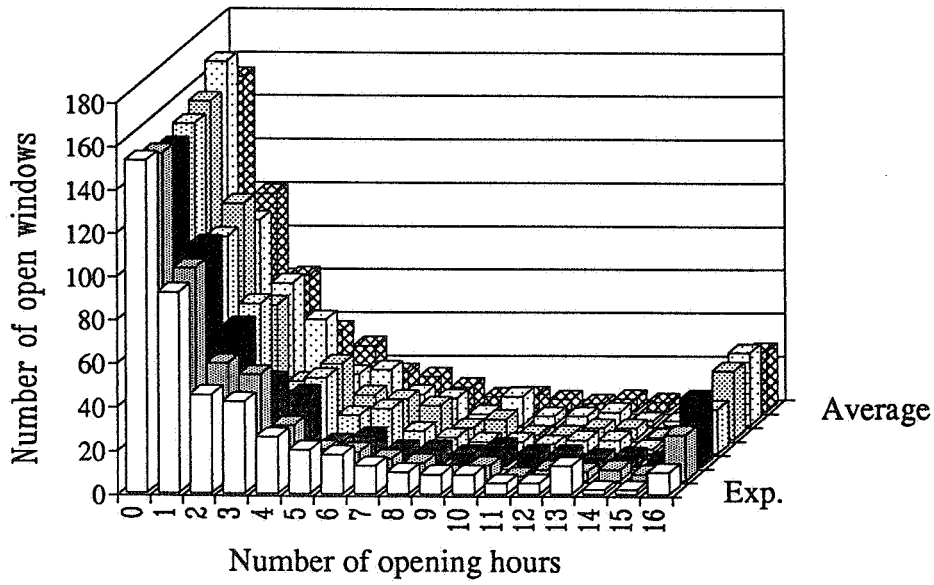

Figure 3: Histograms of opening times for dwelling 43. The experimented data are in front and re-calculated data are in back. The last histogram in the back is the average of re-calculated data.

5.5 Temperature dependance

Probability density function for the number of open windows in dwelling 43 and as a function of the outdoor temperature are presented on Figures 4 and 5, respectively for the experimental data and for one rebuilt set of data. Both figures show that the number of open windows increases with the outdoor temperature, and that general tendency is hence reproduced by the model.

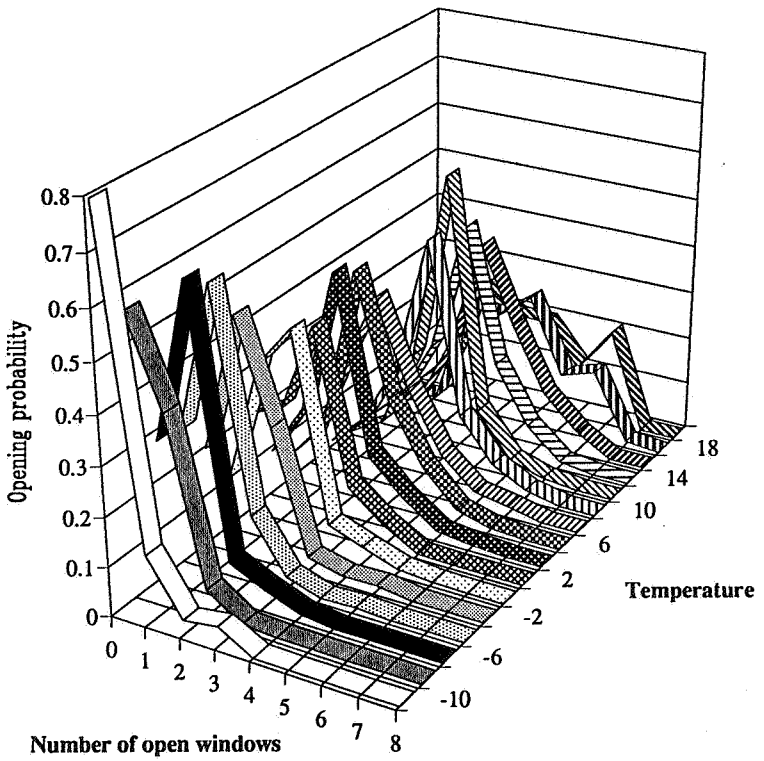

Figure 4: Probability density function for the number of open windows in dwelling 43 and as a function of the outdoor temperature.

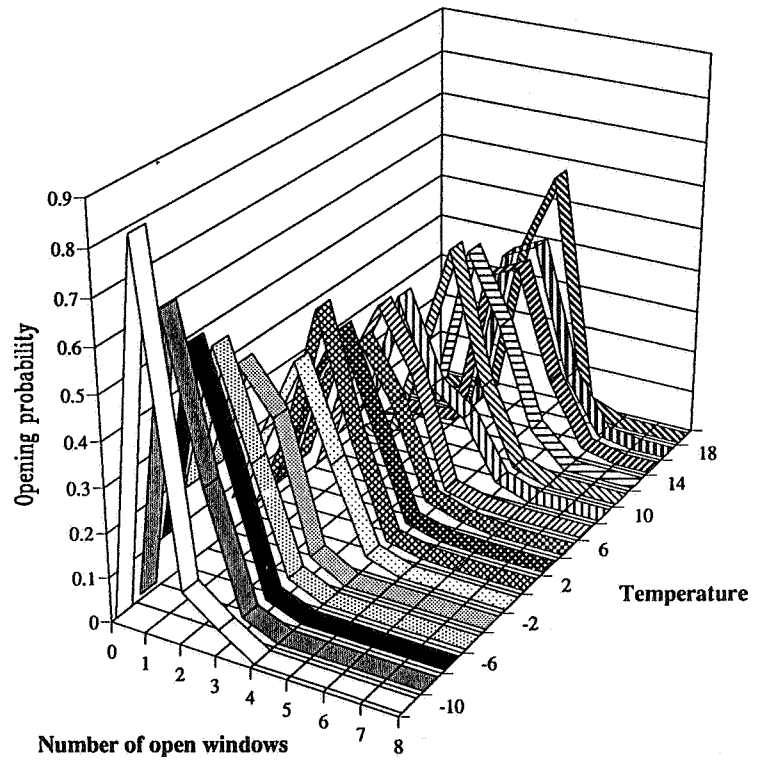

Figure 5: Probability density function for the number of open windows and as a function of the outdoor temperature for the data rebuilt using the model, based on measurements on dwelling 43.

However, large differences can be seen at very low and at high temperatures. At low temperatures (less than -6 °C), the algorithms underpredicts the probability to have all the windows closed and, therefore, overpredicts the probability to have one (or more) window open. At high temperatures (more than 12 °C), the model results in a probability density function which is narrower than the measured one. This summer phenomenon was already mentionned by Fritsch et Al.[3] who have restricted therefore the validity of their model to the heating season.

The small number of samples could also be a cause of that discrepancy. In the 2 degree wide classes which were used for these Figures, the 17000 measurements were inhomogeneously distributed: more than 500 measurements per degree class from -4 up to 8 °C, and 300 or less above 16 and below -6 °C.

5.6 Correlations and variances

The next stage was the comparison of the inter-correlations calculated from the synthetic and real time series of window openings. These cross correlation between the 16 windows and doors themselves and between these and the outdoor temperature and the number of open windows are shown on Tables A3.3 and A3.4 in Appendix 3, for the measured and re-calculated data respectively. These tables are symmetric, and on their diagonals are the variances of each opening.

The variances are very similar and, linking that result with the conclusions from Sections 5.2 to 5.4, one can say that the model reproduces the window openings with the same average opening time, the same average frequency of changes and the same variance. The slight exception is window 13, which moves only once during the measurement period used.

The cross correlations do not give, as one could expect, good results. First of all, there are correlations or anti-correlations between some windows which cannot be neglected, as is shown in Table A2.3. For example, there are some correlation (about 0.3 or more) between the following windows:

1 and 2: fanlights of the gallery-side bedroom,
8 and 9: fanlights of a balcony-side bedroom,
12,14 and 15: the balcony-side door and two bedroom windows located on the same facade.

The reason for the first four is quite obvious: these windows are open at the same time, either when going to bed or when waking up. Note that windows 1 and 2 are seldom open when windows 8 and 9 are open 60 to 80% of the time.

Windows 12, 14 and 15 are the most manipulated but the average opening time is relatively low: from 5% for the door 12 up to 34 % for window 14. It seems that they are open every day during a few hours to ventilate the dwelling.

There are also some anti-correlations, for example between the fanlight 8 and the window 15 located just under it. Window 13 also presents anti-correlations with several other windows, but, as already seen, one cannot have much confidence on the results implying the window 13.

The general conclusion of that is that **there are some correlations (positive and negative), which may not be the same for every user, but which cannot be neglected.** Therefore, the model presented here cannot be perfect, since it is based on independent windows.

This model, however, reproduces some correlations, as it is shown on Table A2.4. For example, openings 12, 14 and 15 as well as fanlights 8 and 9 are also slightly correlated in the reconstructed schedule, but with a lower correlation coefficient. On the other hand, the correlation between windows 1 and 2 disappears completely. These correlations remain because of the deterministic temperature dependance, and does not result from the model

itself.

5.7 Time schedule

The daily time schedule can be reproduced only approximatively by this model, since it can only be introduced in a very rough way: by blocking the opening in their actual state during sleeping hours. In fact, no attempt was made in this direction for the present work, and the comparisons were made between the real time series and a series recalculated without any time-related constraint. Taking account of the real time schedule may give a more realistic result without making the model too complicated.

6. Conclusions

A stochastic model, allowing one to re-calculate the window opening for dwellings was developed from an existing model[3] and based on measurements taken in a large multi-family building located in the Netherlands[6,7,8]. This simple model requires only 16 numbers per opening, that is one 2 by 2 matrix for each temperature class and each opening. Since the sum of the lines of these matrices is one, even only half of these numbers should be really stored, that is a total of 515 numbers for 16 windows and 4 temperature classes

This model is simple. It assumes that the different windows of a dwelling are independent and refers to a basic stochastic process: Markov chains. The outside temperature acts as a driving variable for windows opening or closing. The required data are given for four different types of inhabitants, and allow therefore to simulate the effect of various behaviors on the ventilation in dwellings.

A simplified evaluation procedure was conducted on the generated series. The major statistic characteristics were compared and found to be similar, except for the openings with very few changes.

Two opposite limitations were found: on one hand, the model should be simple enough in order to be elaborated from a limited number of experiments. On the other hand, it could be improved to take account of the interactions between openings. An improvement which will not require more measured data is under study.

Nevertheless, this model could be implemented in the multizone air infiltration simulation programs. Together with a model calculating the air flow rates through large openings, it will allow to take account of different inhabitant behaviors and to predict their effects on ventilation.

Acknowledgements

The authors will gratefully thank Hans Phaff (TNO, Delft, NL) for having provided the data measured at the Schiedam building.

This work, performed within the IEA-ECB, Annex 20 research program, is financed by the Swiss Federal Office of Energy (OFEN/BEW, Bern).

References

1. **M. Liddament:** Air Infiltration Calculation Techniques - An Applications Guide. *AIVC, 1986*
2. **C. Dubrul:** Inhabitant behavior with respect to ventilation - A summary report of IEA Annex VIII. *Technical note AIVC 23 (1988).*
3. **R. Fritsch, A. Kohler, M. Nygård-Ferguson and J.-L. Scartezzini:** Stochastic model of users behavior in regard to ventilation. *Buildings and Environment 25, pp 173-181, 1990*
4. **D. T. Harrje and J. Piggins:** Reporting Guidelines for the Measurement of Airflows and Related Factors in Buildings. *Technical Note AIVC No 32, 1991.* A detailed description of the LESO building is given pp 103-145.
5. **A. Fewkes and S.A. Ferris,** The recycling of domestic waste. A study of the factors influencing the storage capacity and the simulation of the usage patterns, *Building and Environment, Vol. 17 N°3 (1982).*
6. **W. F. de Gids, J. C. Phaff, J. E. F. van Dongen and L. L. M. van Schijndel:** Bewonersgedrag en Ventilatie. *Interim Rapport C 581, July 1985, IMG TNO, Delft (NL)*
7. **J. C. Phaff:** Effect of Instructions to Inhabitants on their Behavior. *Supplement to Proceedings of the 7th AIVC Conference, Stratford-upon-Avon, 1986, pp 55-66.*
8. **J. E. F. van Dongen:** Inhabitants Behavior with Respect to Ventilation. *Supplement to Proceedings of the 7th AIVC Conference, Stratford-upon-Avon, 1986, pp 67-90.*
9. **P.R. Warren**: Ventilation through openings on one wall only, *p. 189. Energy Conservation in Heating, Cooling and Ventilating Building. Hemisphere Publ. Corp. Washington (1978).*
10. **M.S. Bartlett**: An introduction to stochastic processes: Methods and applications, *Cambridge University Press, Cambridge, UK (1979).*

This work will be described in more details in an IEA-ECB Annex 20 report, which will be available by the authors and by the end of 1991.

Appendix 1
Markov matrices of transition probabilities

Table A1.1: Dwelling No 1: Least square deviation to the global average.

Window Number	Temperature class [°C] [-273-0]		]0-8]		]8-16]		]16-∞[	
1	0.9921	0.0079	0.9911	0.0089	0.9885	0.0115	0.984	0.016
	0.0275	0.9725	0.032	0.968	0.0183	0.9817	0.0018	0.9982
2	1	0	1	0	1	0	1	0
	1	0	1	0	1	0	1	0
3	0.989	0.011	0.9861	0.0139	0.9842	0.0158	0.9713	0.0287
	0.0865	0.9135	0.1123	0.8877	0.0424	0.9576	0.0129	0.9871
4	1	0	0.9999	0.0001	0.9998	0.0002	0.9933	0.0067
	1	0	1	0	0.2308	0.7692	0.1538	0.8462
5	1	0	0.9997	0.0003	0.9986	0.0014	0.9909	0.0091
	1	0	1	0	0.4	0.6	0.2637	0.7363
6	0.9996	0.0004	0.9991	0.0009	0.9993	0.0007	0.997	0.003
	1	0	0.0968	0.9032	0.25	0.75	0.0376	0.9624
7	1	0	1	0	1	0	1	0
	1	0	1	0	1	0	1	0
8	0.9926	0.0074	0.9904	0.0096	0.9855	0.0145	0.9773	0.0227
	0.0818	0.9182	0.0102	0.9898	0.0043	0.9957	0.0004	0.9996
9	1	0	1	0	1	0	1	0
	1	0	1	0	1	0	1	0
10	0.9993	0.0007	0.9985	0.0015	0.9966	0.0034	0.9934	0.0066
	0.3333	0.6667	0.1831	0.8169	0.0079	0.9921	0.008	0.992
11	1	0	1	0	0.9973	0.0027	0.9953	0.0047
	1	0	1	0	0.0578	0.9422	0.0896	0.9104
12	1	0	0.9973	0.0027	0.9926	0.0074	0.9634	0.0366
	1	0	0.3333	0.6667	0.1965	0.8035	0.071	0.929
13	0.9989	0.0011	0.9963	0.0037	0.9944	0.0056	0.9981	0.0019
	0.125	0.875	0.0368	0.9632	0.01	0.99	0.0086	0.9914
14	0.9996	0.0004	0.9995	0.0005	0.9953	0.0047	0.9901	0.0099
	1	0	0.0781	0.9219	0.0305	0.9695	0.0148	0.9852
15	0.9996	0.0004	0.9982	0.0018	0.9935	0.0065	0.9756	0.0244
	0.1429	0.8571	0.0522	0.9478	0.0439	0.9561	0.0147	0.9853
16	1	0	1	0	1	0	1	0
	1	0	1	0	1	0	1	0

Table A1.2: Markov matrices of transition probabilities. Dwelling No 2 (Closed User)

Window Number	Temperature class [°C] [-273-0]		]0-8]		]8-16]		]16-∞[	
1	0.9984	0.0016	0.9974	0.0026	0.9942	0.0058	0.9941	0.0059
	0.0139	0.9861	0.0087	0.9913	0.0041	0.9959	0.0054	0.9946
2	1	0	1	0	0.998	0.002	1	0
	1	0	0.0036	0.9964	0.0004	0.9996	0.0004	0.9996
3	0.9989	0.0011	0.9974	0.0026	0.995	0.005	0.9877	0.0123
	0.0254	0.9746	0.0191	0.9809	0.0196	0.9804	0.0354	0.9646
4	0.9996	0.0004	0.9988	0.0012	0.9956	0.0044	0.9947	0.0053
	1	0	0.2326	0.7674	0.1667	0.8333	0.2245	0.7755
5	0.9989	0.0011	0.9991	0.0009	0.9986	0.0014	0.9968	0.0032
	1	0	0.2	0.8	0.5	0.5	0.36	0.64
6	0.9972	0.0028	0.9986	0.0014	0.9988	0.0012	0.9987	0.0013
	0.0272	0.9728	0.0179	0.9821	0.0281	0.9719	0.013	0.987
7	1	0	1	0	1	0	1	0
	1	0	1	0	1	0	1	0
8	0.9992	0.0008	0.9988	0.0012	0.9997	0.0003	0.9983	0.0017
	0.0254	0.9746	0.0125	0.9875	0.0022	0.9978	0.0008	0.9992
9	1	0	1	0	0.9998	0.0002	1	0
	1	0	0.004	0.996	0	1	1	0
10	0.9996	0.0004	1	0	1	0	1	0
	1	0	1	0	1	0	1	0
11	1	0	1	0	1	0	1	0
	1	0	1	0	1	0	1	0
12	1	0	0.9973	0.0027	0.9921	0.0079	0.9762	0.0238
	1	0	0.2564	0.7436	0.0779	0.9221	0.0139	0.9861
13	0.9996	0.0004	0.9997	0.0003	1	0	0.9985	0.0015
	0.1429	0.8571	0.0161	0.9839	0	1	0.0006	0.9994
14	0.9993	0.0007	0.9979	0.0021	0.9947	0.0053	0.9937	0.0063
	0.1429	0.8571	0.0442	0.9558	0.0232	0.9768	0.0105	0.9895
15	1	0	0.9984	0.0016	0.9959	0.0041	0.9944	0.0056
	0.3333	0.6667	0.0254	0.9746	0.0405	0.9595	0.0293	0.9707
16	1	0	0.9999	0.0001	1	0	0.9982	0.0018
	1	0	0.0023	0.9977	0.0426	0.9574	0.0004	0.9996

Table A1.3: Markov matrices of transition probabilities. Dwelling No 41 (Open User).

Window Number	Temperature class [°C] [-273-0]	]0-8]	]8-16]	]16-∞[
1	1 0 0.0278 0.9722	1 0 0 1	0.997 0.003 0.0004 0.9996	1 0 0.0043 0.9957
2	0 1 0 1	0.6667 0.3333 0.0001 0.9999	0 1 0 1	0 1 0 1
3	0.9736 0.0264 0.0016 0.9984	0.9789 0.0211 0.0153 0.9847	0.9768 0.0232 0.0144 0.9856	0.9629 0.0371 0.0042 0.9958
4	0.9996 0.0004 1 0	0.9999 0.0001 1 0	1 0 1 0	0.9971 0.0029 0.1321 0.8679
5	1 0 1 0	0.9993 0.0007 0.3846 0.6154	0.9993 0.0007 0.6667 0.3333	0.9976 0.0024 0.875 0.125
6	1 0 1 0	1 0 1 0	0.9998 0.0002 0.1111 0.8889	1 0 1 0
7	1 0 1 0	1 0 1 0	1 0 1 0	1 0 1 0
8	0 1 0 1	0 1 0 1	0 1 0 1	0 1 0 1
9	0.998 0.002 0.0072 0.9928	0.9995 0.0005 0.0006 0.9994	0.9997 0.0003 0.0014 0.9986	1 0 1 0
10	0.9855 0.0145 0.0004 0.9996	0.9961 0.0039 0.0014 0.9986	0.9995 0.0005 0.0022 0.9978	0.9977 0.0023 0.0006 0.9994
11	1 0 1 0	1 0 1 0	1 0 1 0	1 0 1 0
12	0.9985 0.0015 0.0519 0.9481	0.9921 0.0079 0.033 0.967	0.9887 0.0113 0.0099 0.9901	0.9655 0.0345 0.0085 0.9915
13	0.997 0.003 0.0008 0.9992	0.9842 0.0158 0.0007 0.9993	0 1 0 1	0 1 0 1
14	0 1 0 1	0 1 0 1	0 1 0 1	0 1 0 1
15	0.9981 0.0019 0.0005 0.9995	0.9964 0.0036 0.0031 0.9969	0.9927 0.0073 0.0028 0.9972	0.9994 0.0006 0.0023 0.9977
16	0.9992 0.0008 0.0348 0.9652	0.9987 0.0013 0.0073 0.9927	0.9995 0.0005 0.0202 0.9798	1 0 1 0

Table A1.4: Markov matrices of transition probabilities Dwelling No 43: Total average close to the global average.

Window Number	Temperature class [°C] [-273-0]	]0-8]	]8-16]	]16-∞[
Window 1	0.9993 0.0007 0.0435 0.9565	0.9996 0.0004 0.0702 0.9298	0.9995 0.0005 0.0202 0.9798	1 0 1 0
2	0.9996 0.0004 0.037 0.963	0.9999 0.0001 1 0	1 0 1 0	1 0 1 0
3	0.9924 0.0076 0.058 0.942	0.9898 0.0102 0.0624 0.9376	0.9905 0.0095 0.0645 0.9355	0.9859 0.0141 0.041 0.959
4	0.9996 0.0004 0.25 0.75	0.9995 0.0005 0.1739 0.8261	0.9998 0.0002 1 0	0.9992 0.0008 0.25 0.75
5	0.9996 0.0004 1 0	0.9988 0.0012 0.5 0.5	0.9991 0.0009 1 0	0.9984 0.0016 0.5 0.5
6	1 0 1 0	0.9996 0.0004 0.1667 0.8333	0.9991 0.0009 0.1071 0.8929	1 0 0.0714 0.9286
7	1 0 1 0	1 0 1 0	1 0 1 0	1 0 1 0
8	0.9969 0.0031 0.0035 0.9965	0.9939 0.0061 0.0013 0.9987	1 0 0.0003 0.9997	0.9987 0.0013 0 1
9	0.9956 0.0044 0.014 0.986	0.9977 0.0023 0.0016 0.9984	0.9988 0.0012 0.0008 0.9992	0.9987 0.0013 0 1
10	1 0 1 0	0.9999 0.0001 0.0167 0.9833	1 0 1 0	1 0 1 0
11	1 0 1 0	1 0 1 0	1 0 1 0	1 0 1 0
12	0.9996 0.0004 0.3333 0.6667	0.997 0.003 0.225 0.775	0.9934 0.0066 0.1714 0.8286	0.9862 0.0138 0.0537 0.9463
13	1 0 1 0	1 0 0.0013 0.9987	1 0 0.002 0.998	1 0 1 0
14	0.9963 0.0037 0.1842 0.8158	0.9926 0.0074 0.0679 0.9321	0.995 0.005 0.0083 0.9917	0 1 0 1
15	0.99 0.01 0.0772 0.9228	0.9924 0.0076 0.0475 0.9525	0.993 0.007 0.0277 0.9723	0.9888 0.0112 0.01 0.99
16	1 0 1 0	1 0 1 0	1 0 1 0	1 0 1 0

Appendix 2: Statistics.

16976 valid measurement periods of ten minutes, distributed as follows between the classes

Temperature class [°C]			
[-273-0[	[0-8[	[8-16[	[16-Ñ[
2743	7495	4241	2497

Table A2.1: Number of time intervals during which the window, (i = 1 to 16) is open.

Dwelling	1	2	3	4	5	6	7	8	9	10	11	12	13	14	15	16	sum
1 (small σ)	5850	0	3922	105	103	220	0	9302	0	2211	307	1036	2736	1565	2278	0	29635
2 (closed)	5768	5727	2552	201	73	1226	0	2982	325	1	0	1807	3348	1985	1225	764	27984
41 (open)	5148	16973	11766	55	24	8	0	16976	3034	11570	0	5688	16196	16976	9827	859	115100
43 (same μ)	179	28	2532	36	32	60	0	12692	8599	60	0	837	1260	5781	3839	0	35935

Table A2.2: Number of changes from open to closed or vice-versa, for each window or door (i = 1 to 16).

Dwelling	1	2	3	4	5	6	7	8	9	10	11	12	13	14	15	16	sum
1 (small σ)	218	0	388	36	60	36	0	149	0	65	44	223	99	76	136	0	1530
2 (closed)	74	5	120	81	48	50	0	26	2	2	0	162	8	93	78	10	759
41 (open)	11	1	239	18	28	1	0	0	13	25	0	192	15	0	45	25	613
43 (same μ)	14	4	291	16	36	14	0	27	39	2	0	152	1	139	215	0	950

Appendix 3: Comparisons, made on dwelling 43.

Table A3.1: Number of time intervals during which the window, (i = 1 to 16) is open.

Dwelling	1	2	3	4	5	6	7	8	9	10	11	12	13	14	15	16	sum
43 Rebuilt 1	154	1	2516	45	33	35	0	14458	10269	54	0	945	1325	5473	2797	0	38105
43 Rebuilt 2	293	33	2462	37	17	49	0	11766	7095	134	0	624	362	5589	3931	0	32392
43 Rebuilt 3	210	15	2323	16	38	50	0	12381	8029	48	0	689	1519	5240	3507	0	34065
43 Rebuilt 4	103	42	2860	5	21	55	0	9400	8805	1	0	826	1519	5120	3423	0	32180
43 Rebuilt 5	84	17	2785	34	32	22	0	12429	10976	17	0	641	383	5702	2951	0	36073
43 Rebuilt 6	238	80	3013	64	40	31	0	11217	10539	151	0	975	67	5207	3314	0	34936
Average	180	31	2660	35	30	40	0	11941	9286	68	0	783	863	5388	3316	0	34625
43 measured	179	28	2532	36	32	60	0	12692	8599	60	0	837	1260	5781	3839	0	35935

Table A3.2: Number of changes from open to closed or vice-versa, for each window or door (i = 1 to 16).

Dwelling	1	2	3	4	5	6	7	8	9	10	11	12	13	14	15	16	sum
43 Rebuilt 1	12	2	287	12	40	10	0	26	38	4	0	160	1	152	200	0	943
43 Rebuilt 2	18	4	277	14	22	12	0	37	29	4	0	148	1	191	240	0	997
43 Rebuilt 3	25	2	256	10	40	14	0	34	38	2	0	152	1	162	228	0	964
43 Rebuilt 4	16	6	334	8	26	8	0	25	33	2	0	152	1	143	219	0	973
43 Rebuilt 5	9	4	340	16	42	12	0	28	45	2	0	138	1	138	223	0	998
43 Rebuilt 6	20	10	301	28	36	12	0	30	47	4	0	170	1	169	228	0	1056
Average	17	5	299	15	34	11	0	30	38	3	0	153	1	159	223	0	989
43 (same μ)	14	4	291	16	36	14	0	27	39	2	0	152	1	139	215	0	950

Table A3.3: Cross-correlations between windows, dwelling 43, Experimental Data
On the diagonal (bold characters) are the variances of each window opening.

No	1	2	3	4	5	6	7	8	9	10	11	12	13	14	15	16	T_{ext}	Sum
1	**0.01**	0.34	0.12	0.00	0.02	-0.01	0.00	0.03	0.00	-0.01	0.00	0.03	0.05	-0.01	0.07	0.00	-0.01	0.16
2	0.34	**0.00**	0.06	0.00	0.00	0.00	0.00	-0.07	0.00	0.00	0.00	-0.01	-0.01	-0.03	0.02	0.00	-0.06	0.04
3	0.12	0.06	**0.13**	0.03	0.07	0.04	0.00	0.09	0.05	-0.02	0.00	0.16	0.02	0.04	0.11	0.00	0.06	0.41
4	0.00	0.00	0.03	**0.00**	0.00	0.00	0.00	0.01	0.02	0.00	0.00	-0.01	-0.01	-0.01	-0.01	0.00	0.00	0.05
5	0.02	0.00	0.07	0.00	**0.00**	0.00	0.00	0.02	0.01	0.00	0.00	0.04	0.01	0.01	0.04	0.00	0.02	0.09
6	-0.01	0.00	0.04	0.00	0.00	**0.00**	0.00	0.03	0.03	0.00	0.00	0.01	0.04	0.05	0.06	0.00	0.03	0.12
7	0.00	0.00	0.00	0.00	0.00	0.00	**0.00**	0.00	0.00	0.00	0.00	0.00	0.00	0.00	0.00	0.00	0.00	0.00
8	0.03	-0.07	0.09	0.01	0.02	0.03	0.00	**0.19**	0.36	0.03	0.00	0.00	0.16	0.05	-0.11	0.00	0.16	0.50
9	0.00	0.00	0.05	0.02	0.01	0.03	0.00	0.36	**0.25**	0.06	0.00	0.08	-0.29	0.30	-0.02	0.00	0.26	0.57
10	-0.01	0.00	-0.02	0.00	0.00	0.00	0.00	0.03	0.06	**0.00**	0.00	0.02	-0.02	0.01	0.00	0.00	-0.01	0.07
11	0.00	0.00	0.00	0.00	0.00	0.00	0.00	0.00	0.00	0.00	**0.00**	0.00	0.00	0.00	0.00	0.00	0.00	0.00
12	0.03	-0.01	0.16	-0.01	0.04	0.01	0.00	0.00	0.08	0.02	0.00	**0.05**	-0.04	0.28	0.37	0.00	0.34	0.45
13	0.05	-0.01	0.02	-0.01	0.01	0.04	0.00	0.16	-0.29	-0.02	0.00	-0.04	**0.07**	-0.18	0.03	0.00	-0.01	0.09
14	-0.01	-0.03	0.04	-0.01	0.01	0.05	0.00	0.05	0.30	0.01	0.00	0.28	-0.18	**0.22**	0.44	0.00	0.77	0.64
15	0.07	0.02	0.11	-0.01	0.04	0.06	0.00	-0.11	-0.02	0.00	0.00	0.37	0.03	0.44	**0.17**	0.00	0.41	0.53
16	0.00	0.00	0.00	0.00	0.00	0.00	0.00	0.00	0.00	0.00	0.00	0.00	0.00	0.00	0.00	**0.00**	0.00	0.00
T_{ext}	-0.01	-0.06	0.06	0.00	0.02	0.03	0.00	0.16	0.26	-0.01	0.00	0.34	-0.01	0.77	0.41	0.00		0.62
Sum	0.16	0.04	0.41	0.05	0.09	0.12	0.00	0.50	0.57	0.07	0.00	0.45	0.09	0.64	0.53	0.00	0.62	**1.77**

Table A3.4: Cross-correlations, dwelling 43. Rebuilt data

No	1	2	3	4	5	6	7	8	9	10	11	12	13	14	15	16	T_{ext}	Sum
1	**0.02**	-0.01	0.00	-0.01	0.00	-0.01	0.00	-0.01	0.05	-0.01	0.00	-0.03	-0.02	-0.05	0.02	0.00	-0.06	0.00
2	-0.01	**0.00**	-0.02	0.00	0.00	0.00	0.00	-0.02	-0.04	0.00	0.00	-0.01	-0.01	-0.03	0.03	0.00	-0.08	-0.04
3	0.00	-0.02	**0.12**	0.01	0.01	0.02	0.00	0.02	0.02	0.00	0.00	0.00	-0.06	0.07	0.02	0.00	0.07	0.23
4	-0.01	0.00	0.01	**0.00**	0.00	0.00	0.00	0.00	0.02	0.00	0.00	-0.01	-0.01	-0.01	-0.02	0.00	-0.02	0.01
5	0.00	0.00	0.01	0.00	**0.00**	0.00	0.00	-0.01	-0.01	0.00	0.00	-0.01	0.00	0.01	0.01	0.00	0.01	0.02
6	-0.01	0.00	0.02	0.00	0.00	**0.00**	0.00	0.03	-0.03	0.00	0.00	-0.01	-0.01	-0.03	0.03	0.00	-0.01	0.04
7	0.00	0.00	0.00	0.00	0.00	0.00	**0.00**	0.00	0.00	0.00	0.00	0.00	0.00	0.00	0.00	0.00	0.00	0.00
8	-0.01	-0.02	0.02	0.00	-0.01	0.03	0.00	**0.21**	0.15	-0.12	0.00	-0.03	0.10	-0.12	-0.03	0.00	-0.08	0.25
9	0.05	-0.04	0.02	0.02	-0.01	-0.03	0.00	0.15	**0.24**	-0.08	0.00	-0.02	-0.13	0.01	0.04	0.00	0.12	0.30
10	-0.01	0.00	0.00	0.00	0.00	0.00	0.00	-0.12	-0.08	**0.01**	0.00	0.01	-0.01	-0.04	-0.05	0.00	-0.02	-0.02
11	0.00	0.00	0.00	0.00	0.00	0.00	0.00	0.00	0.00	0.00	**0.00**	0.00	0.00	0.00	0.00	0.00	0.00	0.00
12	-0.03	-0.01	0.00	-0.01	-0.01	-0.01	0.00	-0.03	-0.02	0.01	0.00	**0.04**	-0.03	0.19	0.13	0.00	0.22	0.26
13	-0.02	-0.01	-0.06	-0.01	0.00	-0.01	0.00	0.10	-0.13	-0.01	0.00	-0.03	**0.02**	-0.09	-0.08	0.00	-0.02	0.05
14	-0.05	-0.03	0.07	-0.01	0.01	-0.03	0.00	-0.12	0.01	-0.04	0.00	0.19	-0.09	**0.22**	0.27	0.00	0.69	0.56
15	0.02	0.03	0.02	-0.02	0.01	0.03	0.00	-0.03	0.04	-0.05	0.00	0.13	-0.08	0.27	**0.18**	0.00	0.33	0.45
16	0.00	0.00	0.00	0.00	0.00	0.00	0.00	0.00	0.00	0.00	0.00	0.00	0.00	0.00	0.00	**0.00**	0.00	0.00
T_{ext}	-0.06	-0.08	0.07	-0.02	0.01	-0.01	0.00	-0.08	0.12	-0.02	0.00	0.22	-0.02	0.69	0.33	0.00		0.68
Sum	0.00	-0.04	0.23	0.01	0.02	0.04	0.00	0.25	0.30	-0.02	0.00	0.26	0.05	0.56	0.45	0.00	0.68	**3.95**

AIR MOVEMENT & VENTILATION CONTROL WITHIN BUILDINGS

12th AIVC Conference, Ottawa, Canada
24 - 27 September, 1991

POSTER 4

The use of test chambers for characterizing the emissions of volatile organic compounds from indoor building materials

R. Gehrig, M. Affolter and P. Hofer

Swiss Federal Laboratories for Materials Testing EMPA
Section air pollutants, 8600 Dübendorf Switzerland

Synopsis:

Increasing interest is attributed to the problem of the accumulation of organic vapours emitted from indoor building materials due to an effective insulation of buildings with low ventilation rates. A measurement technique for determining emission rates using a 1 m^3 laminar flow test chamber is described. The aim of this activity is to:

- get compound-specific data on the emissions of various indoor building materials,
- provide emission data for the development and verification of models used to predict indoor concentrations and
- determine the effect of environmental variables as temperature, humidity or air velocity on emission rates.

The work of a COST 613 working group leading to a guideline for measurements using test chambers [1] was an important step to internationally harmonize analysis and data evaluation methods.

List of abbreviations

EMPA	Swiss Federal Laboratories for Materials Testing and Research
EPA	US Environmental Protection agency
VOC	Volatile Organic Compounds
GC/MS	Gas chromatography combined with mass spectrometry
GC/FID	Gas chromatography with flame ionization detector
COST 613	European Concerted Action "Indoor Air Quality and its Impact on Man".

1. Introduction

Public interest in indoor air problems has increased considerably during the last years. Due to better insulation of rooms for reasons of energy saving with correspondingly low air change rates in unventilated rooms and the use of a variety of artificial indoor materials there is a certain risk for higher concentrations of indoor air pollutants.

Measurements of indoor air in fact often shows significantly higher concentrations of air pollutants compared to ambient air [2,3,4]. Often the reason for this increased concentrations are building materials [5,6].

Today there is still a lack of knowledge of type and time dependence of VOC emissions from building materials.

2. Measurements in test chambers

The characterisation of emissions from building materials in real rooms is extremely difficult due to the immense number of parameters influencing VOC concentrations (sources like building materials, furnishing, paints, indoor activities; sinks like walls, plants, carpets; fluctuating room temperature and humidity, air change rate etc.). In order to obtain well defined and reproducible information about VOC emissions from a specific building material, measurements in test chambers with exactly controllable conditions are necessary.

With the support of the Swiss Federal Office for Energy the EMPA started a project aiming at the development of a method for the characterisation of VOC emissions from building materials using test chambers.

International harmonisation of measurement methods is highly desirable in order to reach a good comparability of data obtained by different laboratories. An important step towards this goal was the participation in the work of a COST 613 working group leading to a guideline for measurement of emission factors from indoor materials using test chambers [1], a guideline which made use of a preceeding work in the EPA [7].

3. Design of the test chamber

The test chamber used in this project has a volume of 1 m^3. All parts coming into contact with the air to be measured are of stainless steel. Temperature, humidity and air change rate are controlled. The fresh air is carefully purified from VOC to a low ppb-level. An independent control of the wall temperature allows to avoid cold spots in the system, minimizing thus wall absorption effects. With the internal air recirculation system a known laminar air velocity in the test chamber can be maintained and simultaneously the temperature can be controlled. Fig. 1 gives a schematic view of the test chamber design.

4. Sample collection and analysis

Normally air samples are taken at the exhaust of the chamber. An exactly known volume of air (typically 500 ml) is drawn through adsorption tubes filled with Tenax. Immediately after sampling the tubes are tightly sealed and transferred into the analytical laboratory. The analysis is done after thermal desorption by GC/MS technique for compound identification and by GC/FID technique for quantitative analysis of time series. A more detailed description of these procedures can be found in the COST guideline [1].

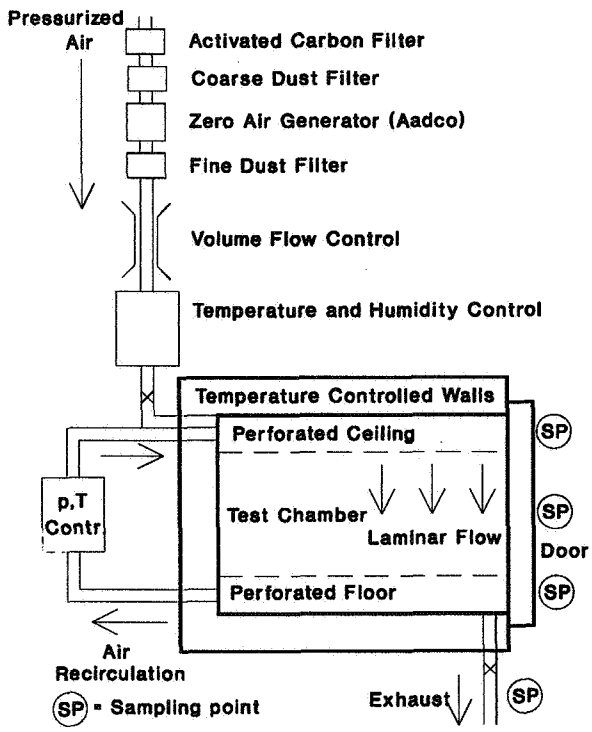

Fig.1: Set-up of test chamber

5. Experimental parameters

The first step in designing an experiment for chamber tests of building materials is to determine the test objectives. For example an architect might be interested in emissions from a variety of materials to be used under a given set of conditions for a specific building. In this case, the experiment would be designed to deal with many materials with one set of environmental conditions. The same may happen, if data for a source emission inventory are to be collected. A manufacturer might want to know the emission characte ristics of a specific product under both normal and extreme conditions. Researchers interested in the interactions among variables would use a more complex design involving ranges of several variables.

Six parameters are generally considered to be critical:

- Temperature (affecting vapour pressures, diffusion coefficients and desorption rates)
- Humidity
- Air exchange rate (defined as mass flow rate of clean air to the chamber divided by the chamber volume)
- Air velocity near the surface of the materials being tested
- Product loading (defined as the ratio of test specimen area to the chamber volume)
- Product age/product history (influencing emission rates very strongly)

For routine testing of indoor materials the following test conditions are recommended:

Temperature:	23^0 C
Relative humidity	45 %
Air exchange rate	0.5 and/or 1 h^{-1}

Concerning product loading and air velocity realistic values should be chosen.

6. Data analysis

The aim of the chamber measurements is to identify the predominant or otherwise interesting components emitted from the investigated materials and to establish quantitative emission rates. These are normally expressed in mass · area^{-1} · time^{-1} (e.g. mg m^{-2} h^{-1}).

6.1. Constant emission rates

For materials with a relatively constant emission rate over the test period the chamber will reach and maintain a constant equilibrium value. The emission factor (ignoring sinks) will then be:

$$E = Qc/A = Nc/L$$

E	=	Emission factor (mg m^{-2} h^{-1})
Q	=	Flow through chamber (m^3 h^{-1})
c	=	Chamber concentration (mg m^{-3})
A	=	Sample area (m^2)
V	=	Chamber volume (m^3)
N	=	Q/V Chamber air exchange rate (h^{-1})
L	=	A/V Chamber loading (m^2 m^{-3})

6.2. Decreasing emission rates

The simplest model (ignoring sinks) assumes that the chamber is an ideally stirred tank reactor and that the change in emission rate can be approximated by a first order decay [7].

$$E = E_0 e^{-kt}$$

leading to:

$$c = L E_0 (e^{-kt} - e^{-Nt})/(N - k)$$

Values of E_0 and k can be obtained from concentration vs. time data series by a non-linear regression.

6.3. General empirical model

The following double-exponential equation for describing the time dependence of VOC concentrations has been successfully used by Colombo et al. [8].

$$c = a(1 - e^{-k_1 t}) - b(1 - e^{-k_2 t})$$

where c and t still denote concentration and time. a and b (mg m^3) are the linear parameters and k_1 and k_2 (h^{-1}) the rate parameters of the equation. This model may equally well fit to data which, starting from zero, increase with time, eventually reaching an asymptotic steady equilibrium value, or to data which pass through a maximum and then decline to zero or to some intermediate equilibrium value.

As an example for this type of data evaluation Figure 2 shows the time dependent concentration of m/p-xylene emitted from kork plates.

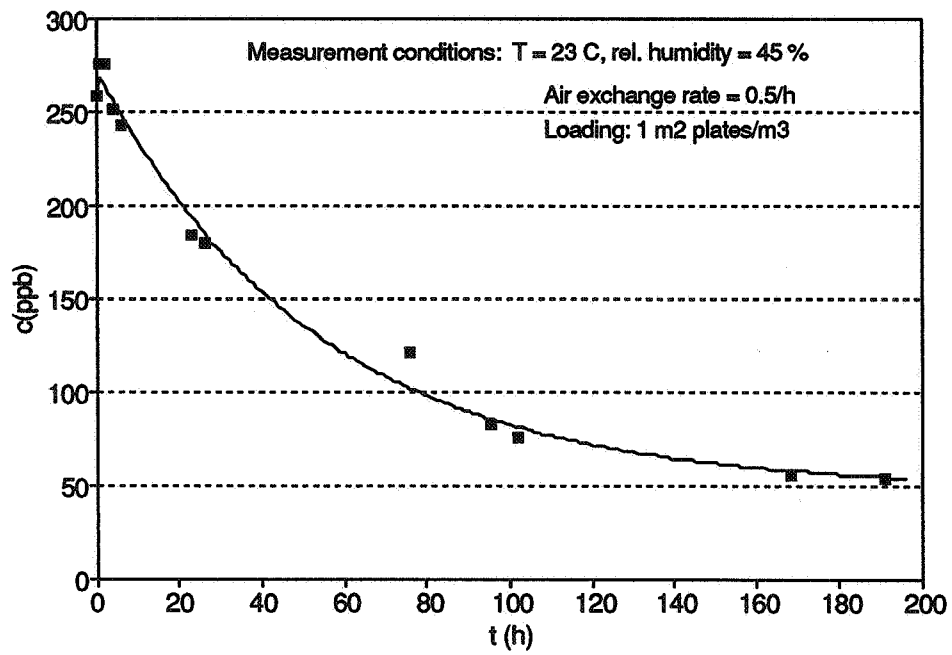

Fig.2: Emissions of m/p-xylene from kork-plates

measured concentrations

calculated concentrations using the best fit of the general empirical model: $c = 273 (1 - e^{-6.14 t}) - 224 (1 - e^{-0.019 t})$

7. Conclusions and recommendations

Emission factors obtained from concentration measurements in test chambers may represent a useful tool for builders, architects or designers of ventilation systems not only to choose the adequate material but also to estimate or model VOC concentrations to be expected in real rooms.

However it is important that laboratories working in this field harmonize their measuring procedures in order to supply comparable and consistent data, which in a later stage could be collected in a data base.

The guideline prepared by the COST 613 working group [1] will hopefully help to reach this goal.

8. Acknowledgements

We gratefully acknowledge the financial supporting by the Swiss Federal Office for Energy for this project.

The authors would like to thank the chairman M. De Bortoli and the members of the COST 613 WG 8 for numerous valuable discussions.

9. References

1. COST Project 613, Report No. 8:
"Guideline for the Characterization of Volatile Organic Compounds Emitted from Indoor Materials and Products Using Small Test Chambers"
Commission of the European Communities, Joint Research Centre Ispra, Institute for the Environment (1991).

2. TICHENOR B.A. and MASON M.A.
"Organic Emissions from Consumer Products and Building Materials to Indoor Environment"
JAPCA 38, 1988, pp 264-268

3. DE.BORTOLI M., KNOEPPEL H., PECCHIO E., PEIL A., ROGORA H., SCHAUENBURG H., SCHLITT H. and VISSERS H.
"Concentrations of selected Organics in Indoor and Outdoor Air in Northern Italy"
Environment International 12, 1986, pp 343-350

4. SEIFERT B., ULLRICH D., MAILHAN W. and NAGEL R.
"Flüchtige organische Verbindungen in der Innenluft"
Bundesgesundheitsblatt 29, 1986, pp 417-424

5. LEBRET E., VAN DE WIEL H.J., BOS H.P., NOIJ D. and BOLEIJ J.S.M.
"Volatile Organic Compounds in Dutch Homes"
Environment International 12, 1986, pp 323-332

6. GIRMAN J.R., HODGSON A.T., NEWTON A.S. and WINKES A.W.
"Emissions of Volatile Organic Compounds from Adhesives with Indoor Applications"
Environment International 12, 1986, pp 317-321

7. TICHENOR B.
"Indoor Air Sources: Using Small Environmental Test Chambers to Characterize Organic Emissions from Indoor Materials and Products"
Report EPA-600/8-89-074 1989

8. COLOMBO A., DE BORTOLI M., PECCHIO E., SCHAUENBERG H., SCHLITT H. and VISSERS H.
"Chamber Testing of organic emission from building and furnishing materials"
Sci. total Envir. 91, 1990, pp 237-249

AIR MOVEMENT AND VENTILATION CONTROL WITHIN BUILDINGS

12th AIVC Conference, Ottawa, Canada
24-27 September, 1991

POSTER 5

VENTILATION FLOW ANALYSIS - FLOW VISUALIZATION AND LDA MEASUREMENTS IN WATER SCALE MODELS, VALIDATION OF NUMERICAL RESULTS

J.R. Fontaine, F. Biolley, R. Rapp, J.C. Sérieys
with technical collaboration of J.C. Cunin

Service Thermique, Ventilation
Institut National de Recherche et de Sécurité
Avenue de Bourgogne, B.P. 27
54501 Vandoeuvre Cédex France

1.1. SYNOPSIS

Within the frame of the IEA Annex 20, laboratory and numerical experiments were conducted in order to study the flow within an isothermal parallepipedic testroom (L x W x H = 4.2 m x 3.6 m x 2.5 m). The air is injected through a complex diffuser (made of 84 nozzles) near the ceiling and is evacuated through a rectangular exit just below the inlet.

While other participants to the Annex 20 made measurements on aeraulic testrooms, we used a hydraulic model scaled to the sixth. The parameters were determined according to a Reynolds similitude. For the experimental approach both Laser Doppler Anemometry and flow visualizations were used. Numerical simulations were carried out using the EOL-3d software developed at INRS.

A comparison between experimental results and numerical predictions is presented. Symmetry, air diffuser modelling and low Reynolds number effects are discussed from both numerical and experimental point of views. The numerical predictions are in good agreement with the experimental results.

1.2. LIST OF SYMBOLS

x, y, z	(m)	:	coordinates
X, Y, Z		:	lines in the occupied zone
L	(m)	:	length of the room or scale model
W	(m)	:	width of the room or scale model
H	(m)	:	height of the room or scale model
y'	(m)	:	y coordinate computed from the ceiling
x_o	(m)	:	virtual origin of the jet
δ	(m)	:	thickness of a wall jet
d	(m)	:	diameter of a nozzle
u, v, w	(m/s)	:	velocity components
u', v', w'	(m/s)	:	fluctuating velocity components
U	(m/s)	:	velocity scale
V	(m/s)	:	mean velocity intensity
V_t	(m/s)	:	mean turbulent velocity
σ	(m/s)	:	velocity standard deviation

u_{rm}	(m/s)	:	maximal radial velocity
u_r	(m/s)	:	radial velocity
U_o	(m/s)	:	velocity in the nozzle
U_x	(m/s)	:	velocity boundary condition at the inlet (box model)
T	(s)	:	time scale
ν	(m^2/s)	:	kinematic viscosity
Q	(m^3/s)	:	flowrate
n, n_a, n_w	(h^{-1})	:	renewal time
$K(\theta)$		:	non dimensional function
h		:	non dimensional function
D		:	constant

2.1. INTRODUCTION

Three dimensional ventilation flows modelling in rooms is a fast expanding subject. One of the goals of IEA Annex 20 was to gather different methods to study well defined testcases in order to provide analysis tools to the conceptors. This paper presents two approaches of flow modelling. The first one is based on numerical simulations and discusses several ways of implementing boundary conditions associated to a complex air diffuser. The second one uses hydraulic simulations and represents the testroom by a water model scaled to the sixth. The parameters are determined according to a Reynolds similitude. This method is flexible and well adapted to flow visualizations. For quantitative analysis, mean and turbulent velocity measurements were performed by Laser Doppler Anemometry.

The visualization of the flow was obtained by injecting fluorescein-dyed water through the inlet and enlightening different vertical and horizontal sections of the testroom with a rotating laser beam.

The different techniques used in this work are first described. An analysis of the flow fields based on LDA measurements, flow visualizations and numerical simulations is then presented. The physical relevance of several assumptions usually used in numerical models is finally discussed with reference to the flow visualization results.

2.2. DESCRIPTION OF THE TESTROOM

The testroom (figure 1) (Heikkinen, 1989) is a L x W x H = 4.2 x 3.6 x 2.5 m^3 parallelepiped. It contains one inlet and one outlet. The air is injected into the room through a complex diffuser. The diffuser consists of 4 rows composed by 21 nozzles (diameter 1.2 10^{-2} m and length 1.5 10^{-2} m). The nozzles are on a 0.71 x 0.17 m^2 rectangle. They are oriented toward the ceiling with an angle $\phi = 40°$. The air exhaust is located below the inlet. It is a simple 0.3 x 0.2 m^2 rectangle.

2.3. THE WATER SCALE MODEL AND THE HYDRAULIC BENCH

The flow is analyzed experimentally by hydraulic simulation. The testroom is represented by an altuglass model scaled to the sixth. The model and the hydraulic bench are sketched on figure 2 and figure 3. The scale model is placed in a 2.25 x 1.75 x 1 m^3 closed experimental tank (1, figure 2). The front face of the tank is in glass and the bottom in altuglass. A pump (2) sucks the water out of the model and transfers it into a 3 m^3 buffer tank (3). A flowmeter (4) monitors the pump flowrate. The air diffuser is modelised by 4 rows of 21 nozzles of diameters 2 10^{-3} m and lengths 1.5 10^{-2} m that will be referred to as nozzles or grid diffuser.

As it is suggested for the testroom, the nozzles are oriented with an angle of 40° with respect to the horizontal plane (1, figure 3). By conservation of mass, water comes from the surroundings of the model (2) and enters through the diffuser. Before entering, the flow is homogenized by a divergent-convergent system (3) equipped with grids. For flow visualization purposes, a dye (fluorescein) can be added (4) and properly mixed with the water sucked into the divergent-convergent zone.

2.4. EXPERIMENTAL SET-UP

We only considered isothermal conditions (T = 15°C ± 2°C).

Similarity

A Reynolds similarity is used :

$$(Re)_a = (U_o d/\nu)_a = (U_o d/\nu)_w = (Re)_w$$

where a is the subscript for air and w for water ;
U_0 is the fluid mean speed in the nozzle of diameter d ;
ν is the kinematic viscosity.

The scaling relations are :

$d_a/d_w = 6$

$\nu_a/\nu_w \approx 15$

length	L_a	=	L_w	*	6
time	T_a	=	T_w	*	2.4
velocity	U_a	=	U_w	*	2.5
flow rate	Q_a	=	Q_w	*	90
renewal time	n_a	=	$n_w/2.4$		

Measurement points

The velocity measurements were performed for the case $n_a = 3h^{-1}$.

a/ The following measurement lines in the comfort zone were considered :
- . line X parallel to the x axis : (y ; z) = (1; 0)
- . line Y parallel to the y axis : (x ; z) = (2.2 ; 0)
- . line Z parallel to the z axis : (x ; y) = (2.2 ; 1)

b/ Some measurement points along the faces of a box surrounding the inlet were added :

$0. \leq x \leq 1.$

$2. \leq y \leq 2.5$

$1.3 \leq z \leq 2.3$

Velocity measurements

The three components of the velocity vectors were measured by Laser Doppler Anemometry.

Longitudinal (u) and vertical components (v) were obtained by measurements through the front face of the experimental tank ; longitudinal (u) and transversal (w) components through the bottom face.

Statistical mean velocities u_m and standard deviations $\sigma = \sqrt{u'^2}$ were computed from (N = 3 072) values of instantaneous velocities.

The computations were done in two steps. First, values of u_m and σ were computed. Then all velocity values u such that $|u - u_m| > 6\,\sigma$ were eliminated and new values of u_m and σ were computed with the remaining data. The amplitude of the mean velocity and turbulent velocity were given by :

$$V = (u_m^2 + v_m^2 + w_m^2)^{1/2}$$

$$V_t = (u'^2 + v'^2 + w'^2)^{1/2}$$

Flow visualization

The flow field can be traced by introducing a dye through the inlet (see section 2.3). Laser tomography is used for visualization : a laser beam reflected by a rotating mirror illuminates a section of the flow. The laser light is absorbed and re-emitted by the fluorescein particles. This produces a picture of the flow which can be recorded by photography and video.

The following tests were performed :

Configuration bg
- room and diffuser as described in section 2.2
- $n_a = 1.5\ h^{-1}$ (bg1) ; $n_a = 3\ h^{-1}$ (bg2) ; $n_a = 6\ h^{-1}$ (bg3)

Configuration bs
- room as described in section 2.2
- air diffuser replaced by a slot (0.71 x 0.016 m^2)
- $n_a = 3\ h^{-1}$

Configuration bb
- room as described in section 2.2
- air diffuser replaced by a basic rectangle (0.18 x 0.062 m^2)
- $n_a = 3\ h^{-1}$

Configuration bs and bb were visualized because some participants to Annex 20 had done some numerical simulations of the room by replacing the real diffuser by a slot or a basic rectangle of equivalent areas.

2.5. NUMERICAL MODEL

Numerical simulations were carried out with the EOL-3d software which is being developed at INRS. EOL has been specially devised to deal with ventilation flows ; in particular it contains several tools to analyze the results with an industrial hygienist point of view. Given a particular configuration, the user easily enters its geometry and the associated boundary conditions. The software helps to find the appropriate grid and to compute the flow. It offers the possibility of computing local ages of air, local purging flowrates, time evolution of local pollutant concentrations after a sudden contaminant release, local (or global) ventilation efficiencies. The two-dimensional version of the software (EOL-2d) working for both isothermal and non-isothermal flows is available. EOL-3d is still under development.

Mathematical model

The core of EOL is largely inspired by the works of the Imperial College group (Gosman et al, 1976) and of the University of Karlsruhe (Demuren et al, 1987). It solves the usual transport equations for momentum, mass, temperature, pollutant concentration... Because of turbulence, only ensemble average quantities are considered. Eddy viscosity is computed using a k-ε model (Launder et al, 1974). The partial differential equations are transformed into finite differences equations in implicit and conservative form using the hybrid scheme. The SIMPLEC algorithm is used to satisfy continuity.

Modelisation of the air diffuser

The main difficulty of the problem lies in the boundary condition associated to the air diffuser. It is out of the scope of most numerical methods to modelise 84 jets located on a small surface (0.71 x 0.17 m^2) of a room. Indeed the required grids would be too large to be handled by the present computers.

We used the box model method (Nielsen, 1989) which offers the advantage of being general and in principle applicable to any air diffuser.

$z = 0$ being a symmetry plane of the configuration, the computations can be restricted to a half box. Nevertheless asymmetric solutions may be observed both numerically and experimentally. This fact will be discussed further.

The box model

The boundary condition associated to the air diffuser is replaced by boundary conditions on two vertical faces of a fictive (half) box surrounding the inlet and bounded by the ceiling. The planes are 0.2 m high. One face is located at a distance of 1.0 m from the diffuser wall ; the other face is parallel to the symmetry plane and distant of 0.5 m from it. On each face, only u_x and u_z are imposed; u_z is computed. A boundary condition $u = U_x$ is kept at the inlet considered as a rectangle of dimensions 0.71 x 0.17 m^2. U_x is such that $n_a = 3\ h^{-1}$. The boundary condition along the box can be considered as an added constraint for the flow field. Similar ideas were used by Lemaire et al (1990).

The components u_x and u_z along the box can be obtained from measurements or from scaling laws. We shall only present results for the second case. Indeed the results obtained from experimental data were not very satisfactory. This was due to the fact that in our hydraulic bench it was very difficult to get reliable results very close to the ceiling. The altuglass ceiling produced important light reflections which disturbed the LDA measurements.

Scaling laws were determined by Skovgaard et al. (1990). The flow under the ceiling is the combination of a three-dimensional wall jet and a radial jet. An oblique impinging jet generates a wall jet with different velocity decays in different directions θ (see figure 4).

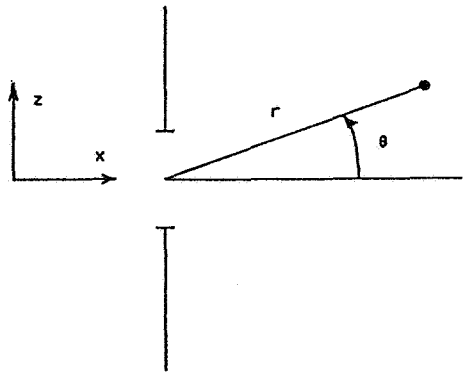

Figure 4 : Definition of coordinates

$$u_{rm}/U_o = K(\theta) / (r + x_o)$$

with u_{rm} : maximal radial velocity
U_o : inlet air velocity
x_o : virtual origin
$K(\theta)$: angular function

x_o and $K(\theta)$ are obtained from experiments. u_{rm} being known, the vertical velocity profile close to the ceiling is obtained from wall jet laws :

$$u_r(y') / u_{rm} = h(y'/\delta)$$

$$\delta = D(x_o + r)$$

h : universal function
δ : boundary layer thickness
$u_r(y')$: radial velocity at a distance y' from the ceiling (y' = H - y)
D : experimental constant

Numerical tests

Three numerical simulations will be discussed.

Simulation S1

Computation for half a room z > 0
$n_a = 3\ h^{-1}$
Boundary condition : box model
Grid : 32 x 36 x 26
Distances between the last grid points and the wall are all .05 m except for the ceiling where it is .02 m

Simulation S2

Computation for the full room
$n_a = 3\ h^{-1}$
Boundary condition : box model (full box)
Grid : 27 x 36 x 33

Simulation S3

Computation for the full room

$n_a = 3\ h^{-1}$

Boundary condition : basic model

Grid : 27 x 36 x 33

In the basic model the real diffuser is replaced by a rectangle (0.18 x 0.062 m^2). The velocity distribution is uniform U_0 is oriented toward the ceiling with an angle $\phi = 40°$. This corresponds to the experimental configuration bb.

S1 has been kept for quantitative comparisons with experiment.

S2 and S3 have been considered to analyze symmetry problems and for comparison with flow visualization experiments.

2.6. RESULTS FOR TEST bg2

Qualitative description of the experiment (flow visualization)

The injected fluid forms a highly turbulent tridimensional jet impinging with an angle on the ceiling (see figures 18 and 20). The jet widens as it flows along the ceiling to the downstream and lateral walls. When it reaches the downstream wall, the fluid spreads out to the sides and the bottom. In short, the jet wraps the testroom.

At the lateral walls near the downstream wall and the ceiling, two streams counteract each other : the one coming from the ceiling in the direction of the main jet and the one bound to the return of the fluid that reached the downstream wall (see figures 20 and 25). Two vertical columns are created in the corners opposite to the diffuser.

Other local features can be observed. First, a small transversal vortex is created in the triangle defined by the jet, the diffuser wall and the ceiling. The vortex rotates in the opposite direction to the main flow circulation and spreads out along the corner. Second, the bottom corners of the diffuser wall present a circulation also opposite to the main flow circulation.

The horizontal sections show that the jet is highly turbulent on the ceiling (see figure 20) but not as much on the bottom (see figure 22).

Quantitative results

The numerical results used in this section are issued from the box model (case S1). The scheme converged after 1 785 iterations and 33 hours of CPU time. The experimental results correspond to the case bg2 : 84 nozzles diffuser and $n_a = 3\ h^{-1}$.

Figures 5 and 6 are experimental and numerical tridimensional flow fields respectively. They both show the highest velocities near all but the lateral walls, due to the jet which flows along the walls. Figure 6 is in good agreement with the qualitative description. For example, the columns created by the two currents that counteract each other on the upper corners opposite to the diffuser exist as well in the numerical simulation. However, the small vortex region found experimentally above the jet is not represented numerically due to the choice of the grid or/and the fictive box method.

Figure 7 is a plot of the experimental (dashed line) and numerical (solid line) mean and turbulent velocities on the X, Y and Z lines representative of the comfort zone. In the comfort zone (zone which is at 0.6 m from the vertical walls and up to 1.8 m above the floor), the mean velocities are always less than 0.15 m/s on the X and Z lines. Numerically, the mean velocities can be slightly higher (0.22 m/s) near the floor on line Y.

Predicted and measured data exhibit high turbulent velocities near the ceiling (line Y) as it could be expected from the flow visualizations.

2.7. EXPERIMENTAL STUDY OF SEVERAL SIMPLIFICATIONS INTRODUCED IN THE NUMERICAL SIMULATIONS

In this section, flow visualization will be used as a tool to understand the physical relevance of some simplifications introduced by numericians the perform simulations of complex flow fields. Three phenomena will be studied :

1/ The symmetry hypothesis.

2/ The diffuser modelling.

3/ The high Reynolds number hypothesis.

The symmetry hypothesis

$z = 0$ is a symmetry plane for all configurations considered in this paper. Indeed both geometry and boundary conditions are the same on both sides of that plane. Therefore, the flow is expected to be symmetric. This explains the fact that most numerical simulations were carried out in half a room (to save computer time).

Both numerical simulations and flow visualizations were conducted for the full room fitted with the real diffuser and with the basic diffuser (rectangle) ; numerical grids were chosen symmetrical with respect to the plane $z = 0$

Surprisingly enough the results of simulations S2 and S3 are non-symmetrical. Looking at successive horizontal cuts of the flows starting from the ceiling we see that the asymmetry is increasing (figures 14-16 and 15-17). Configurations bb leads to a flow much more asymmetric than configuration bg. This is confirmed by flow visualizations (figures 20-22 and 21-23). We would like to stress the fact that both numerical solutions are fully converged results. This might be explained by the fact that the solutions to the flow equations are non unique and that the resolution algorithms have picked one of the two non symmetrical solutions. Imposing a symmetry condition to the flow at $z = 0$ presumably leads to an averaging process.

The diffuser modelling

Looking through the numerical results of simulations S2 and S3 we see that in horizontal planes close to the ceiling the flow fields are quite different (figures 14 and 15). For case S2 the air diffuses more in the direction perpendicular to the inlet than in transverse directions. For case S3, we observe the opposite phenomenon. This is confirmed by flow visualizations (figures 20 and 21). This means that the box model is a better approximation of the real diffuser than the basic model.

Looking in a horizontal plane located just above the inlet ($y \approx 2.3$ m), we observe from the LDA measurements that the flow induced by the jet enters the lateral faces of the fictive box (figure 13). Even though we have introduced boundary conditions with the fluid flowing out of the box for $y \geq 2.32$ m, we see from figure 12 that the flow computed on the plane just below ($y = 2.28$ m) exhibits fluid motion toward the interior of the box. However, the large velocity measured at the center of the front face of the box was not reproduced by the

numerical simulation. These observations illustrate that the choice of the fictive box to impose boundary condition is quite tricky.

Flow visualizations were also been carried out for the three diffusers (see figures 18, 19 and 24) in vertical planes. The following facts were observed :

1/ The inertia of the jet created by the slot inlet (figure 24) is less than for the two other cases. The jet is inclined to stick much faster to the ceiling and is more influenced by the vortex circulation trapped between the jet, the ceiling and the diffuser wall.

2/ The jet issued from the grid is mainly directed along the x-axis (figure 20) and therefore sticks closer to the ceiling, the downstream vertical wall and the ground (figure 18). For the other jet cases (figures 19 and 24), we observe the opposite phenomenon. The basic jet spreads more in the transversal directions (figure 21) and is thinner on the ceiling in the central plane (figure 19).

Low Reynolds effects

Most computer models use the standard k-ε model of Launder and Spalding (Launder et al, 1974). This model assumes the high Reynolds number hypothesis. This means that viscous effects are negligible compared to fully turbulence effects. In particular, this implies that, after scaling, the flow is Reynolds number independent. In other words this means that the flow field corresponding to $n_a = 3\ h^{-1}$ can be almost obtained from the case $n_a = 1.5\ h^{-1}$ by multiplying all velocities by 2. Experimental investigations of Skovgaard et al. have shown that this hypothesis was not satisfied. In this section, we shall use flow visualizations to point out low Reynolds effects.

One manner to discern the low Reynolds effects is to consider the column created by the two countercurrents at the corners opposite to the diffuser wall. Let us consider the x length L_c of the column as defined by figure 25. We should obtain a constant value for the three flowrates if we were at high Reynolds numbers. Figures 25 through 27 are flow visualizations of the front face for increasing Reynolds numbers. It is made clear that the first flowrate has a lower L_c whereas the two others are similar. If this does not demonstrate that the two higher flowrates are similar, it does show that the first flowrate is definitively different from the two others. We are in presence of a low Reynolds effect.

Remark

The flow visualization pictures and numerical flow field map that correspond to each other are listed below.

Numerical simulation	⇔	Flow visualization
figure 10	⇔	figure 18
figure 11	⇔	figure 19
figure 14	⇔	figure 20
figure 15	⇔	figure 21
figure 16	⇔	figure 22
figure 17	⇔	figure 23

2.8. CONCLUSIONS

In this paper the ventilation of a simple room was investigated by two different methods : numerical simulations and hydraulic simulation. For the hydraulic simulation a model scaled to the sixth was used. The flow was analyzed through LDA measurements and visualization.

Numerical simulations were carried out with the EOL-3d software developed at INRS. The real air diffuser was modelised by using the box model which offers the advantage of being general and applicable to other cases. The comparison between experimental results and numerical predictions is fair and acceptable for industrial purposes.

Hydraulic simulation is well suited to analyze air flow patterns in rooms or premises. It is flexible and well adapted to both LDA measurements and flow visualizations. Indeed it is certainly easier to build scale models than full scale rooms. Moreover performing visualization in a water scale model allows to get a picture of a full plane of the flow at once.

Flow visualization was used as a tool to get some insight into the physics of the flow.
In particular, the influence on the flow of several assumptions such as symmetry, diffuser modelling, high Reynolds number hypothesis, usually used by numericians were pointed out.

REFERENCES

1. DEMUREN , A.O., MAJUMDAR, S. and RODI, W.
   "A computer program for solving three-dimensional elliptic flow equations"
   Institüt für Hydromechanik an der Universität Karlsruhe, 1987, unpublished.

2. GOSMAN, A.D. and IDERIAH, F.
   "A general computer program for two-dimensional turbulent recirculating flows"
   Dept of Mech. Eng., Imperial College, London, 1976.

3. HEIKKINEN, J.
   "Specification of testcase B (forced convection, isothermal)"
   Research Item 1.13, IEA Annex 20, Report.

4. LAUNDER, B.E. and SPALDING, D.B.
   "The numerical computation of turbulent flows"
   Comp. Meth. Appl. Mech. Engr., 3, 269, 1974.

5. LEMAIRE, A.D. and ELKHUIZEN, P.A.
   "Simulation of testcase B (forced convection isothermal)"
   IEA Annex 20, report.

6. NIELSEN, P.V.
   "Simplified Models for Room Air Distribution"
   IEA Annex 20, Report, 1989.

7. SKOVGAARD, M., HYLDGAARD, C.E., and NIELSEN, P.V.
   "High and low Reynolds number measurements in a room with an impinging isothermal jet"
   Roomevent Conference, Oslo, 1990.

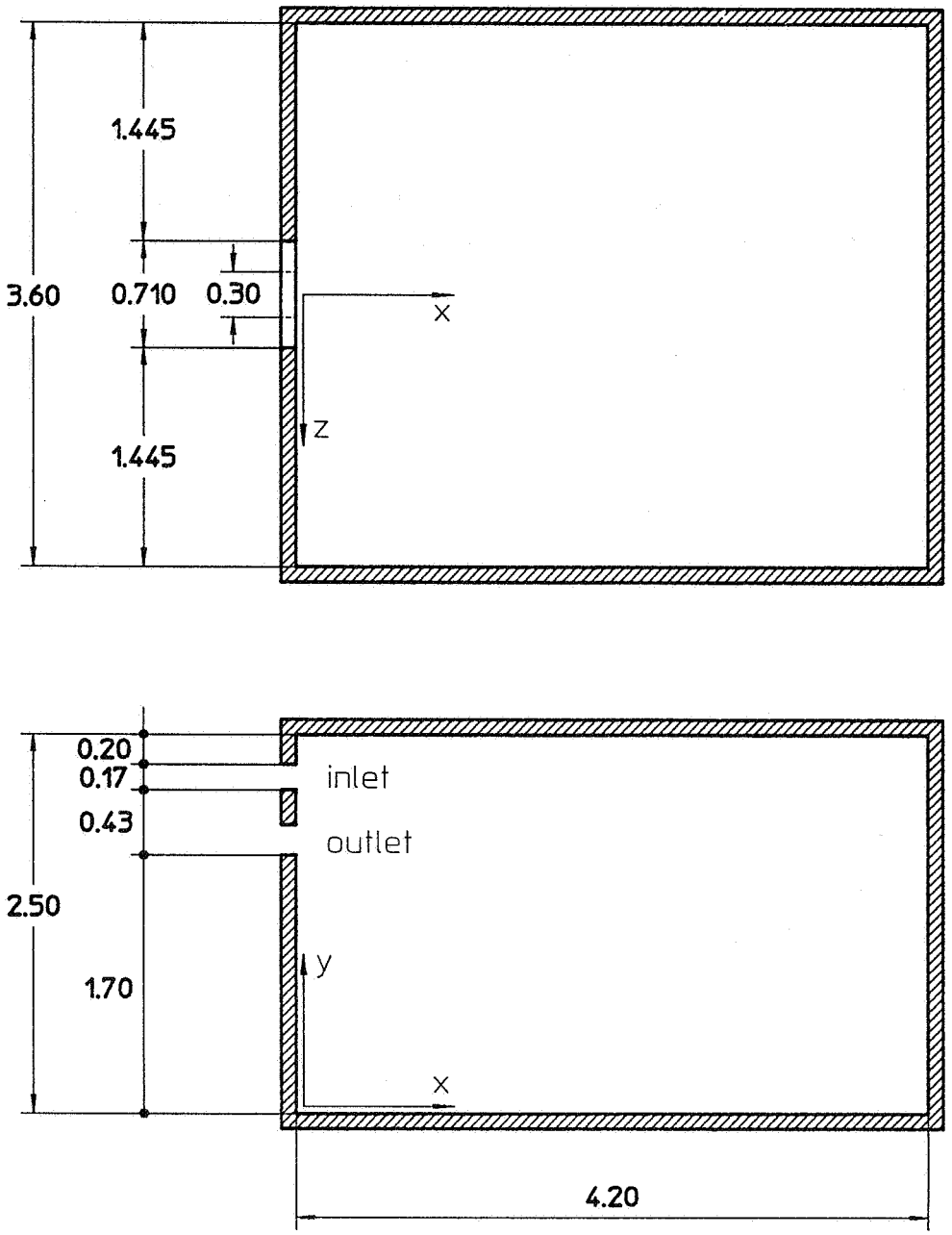

Figure 1 : Testcase b (IEA Annex 20)

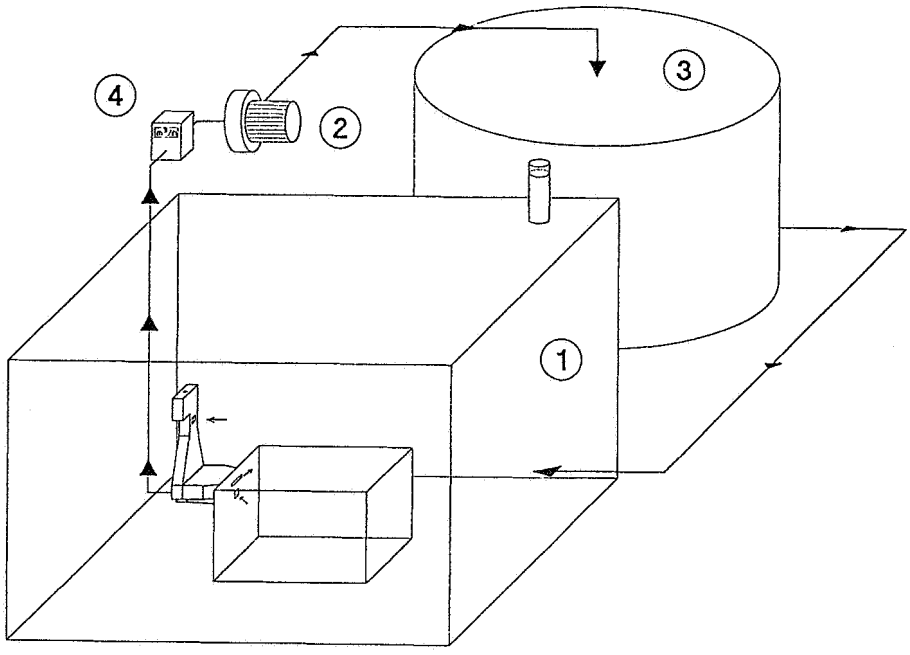

Figure 2 : Sketch of the hydraulic bench

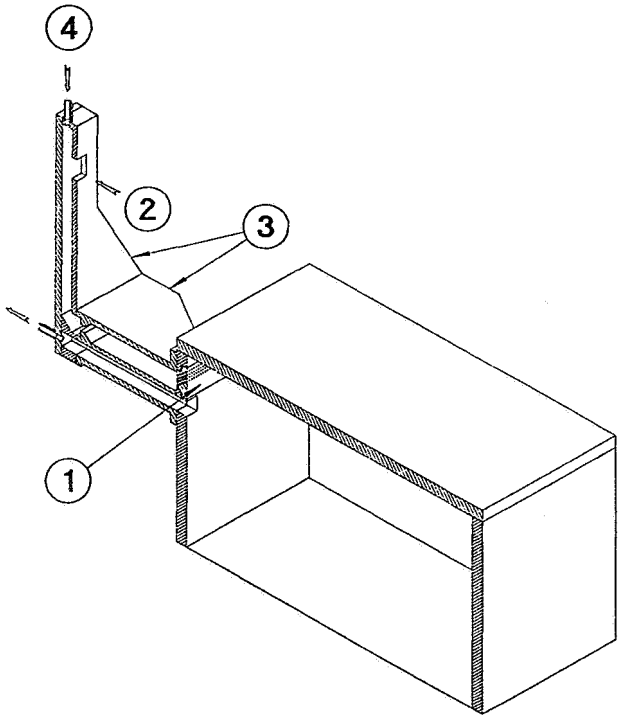

Figure 3 : Testroom model (scale 1/6)

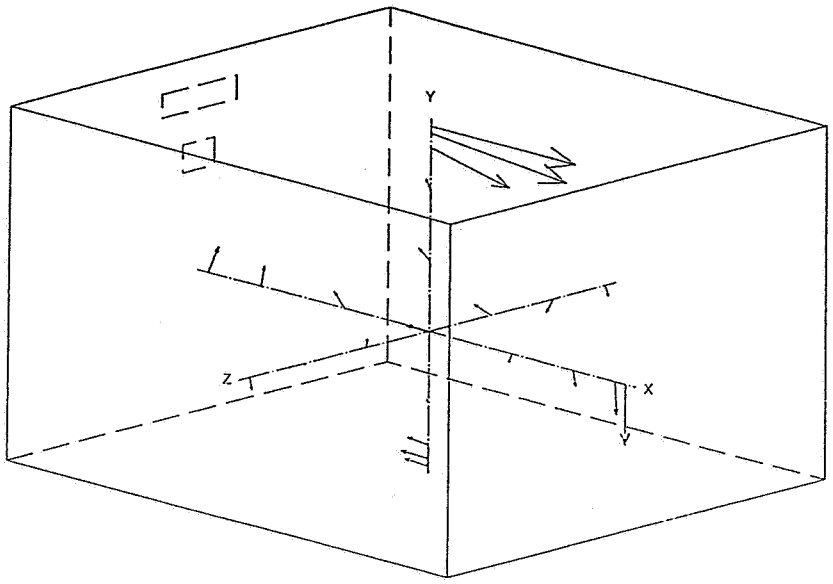

Figure 5 : Three dimensional velocity field obtained from laser anemometry on lines X, Y, Z ($n_a = 3\ h^{-1}$)

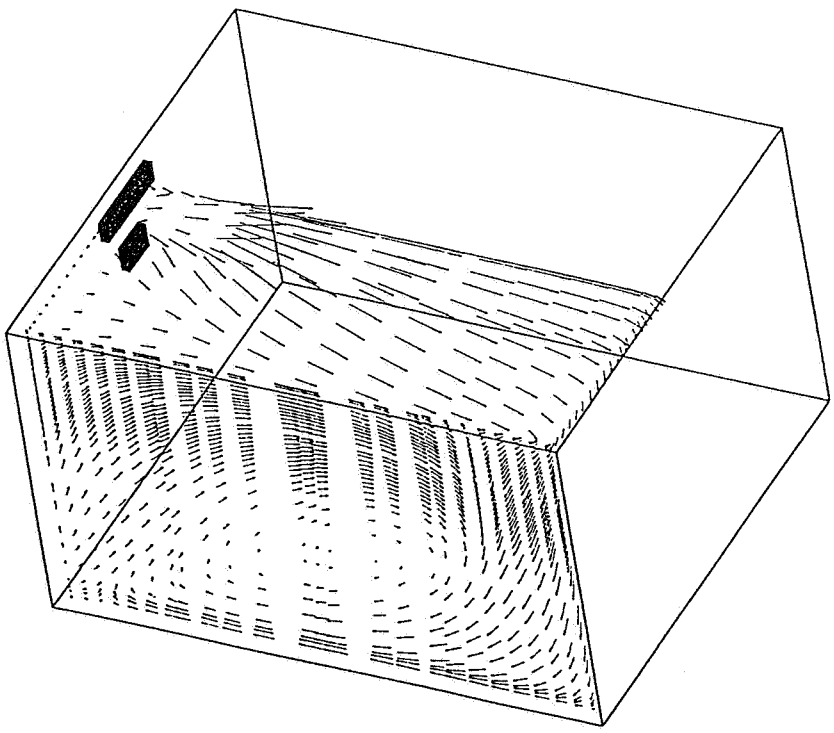

Figure 6 : Three dimensional velocity field obtained from EOL-3d Simulation S1, $n_a = 3\ h^{-1}$

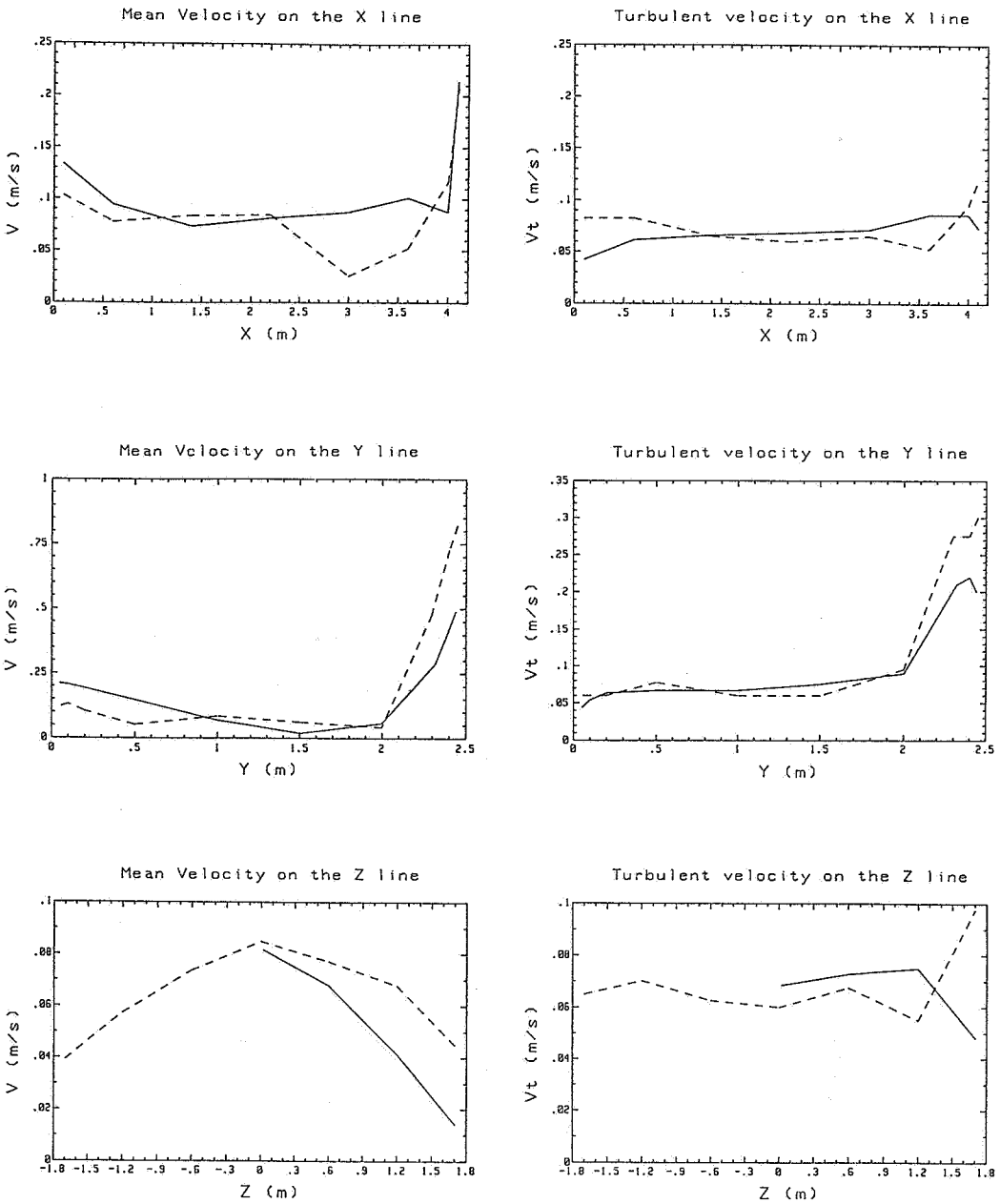

Figure 7 : Mean and turbulent velocities

_____ numerical prediction

---------- experimental measurements transformed into air values according to the relations of section 2.4

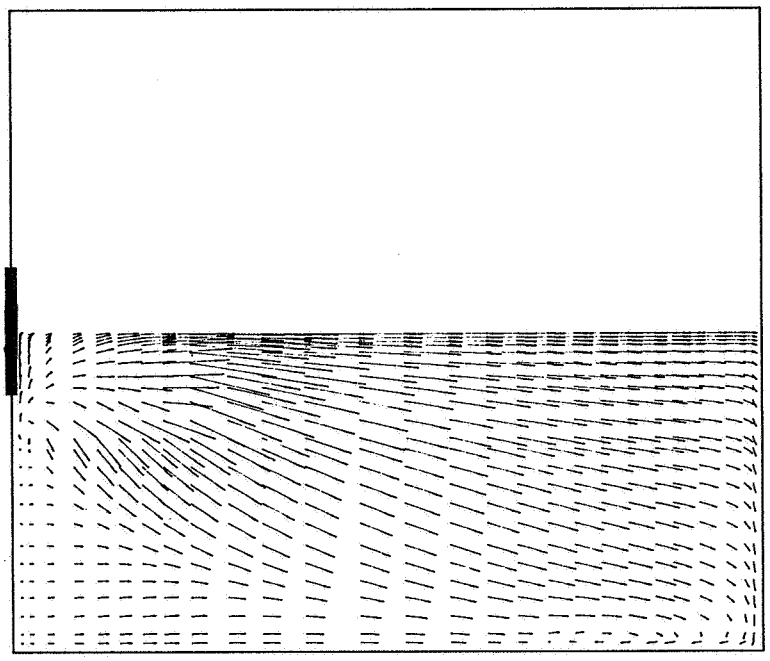

Figure 8 : Horizontal cut of the flow field associated to S1 (y = 2.48 m).
Box model and symmetry assumption ; $n_a = 3\ h^{-1}$

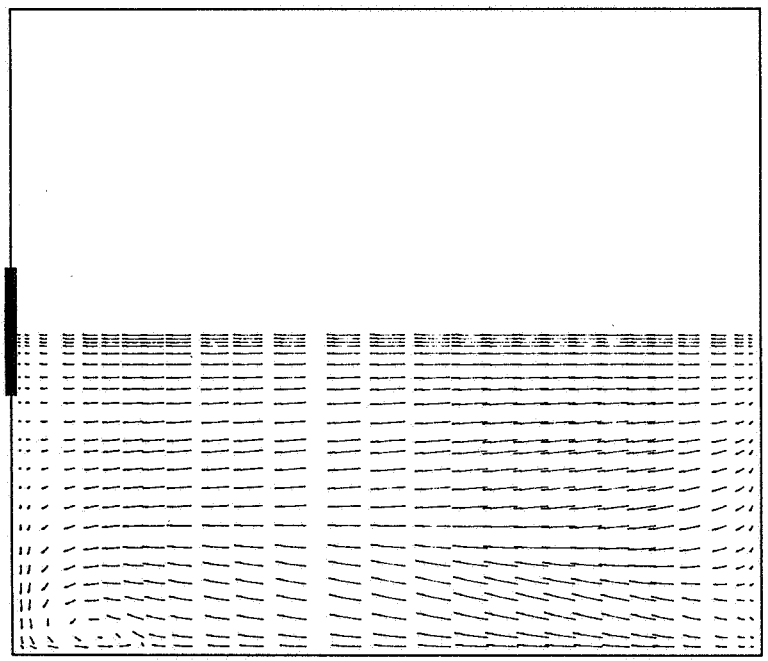

Figure 9 : Horizontal cut of the flow field associated to S1 (y = 0.1 m).
Box model and symmetry assumption ; $n_a = 3\ h^{-1}$

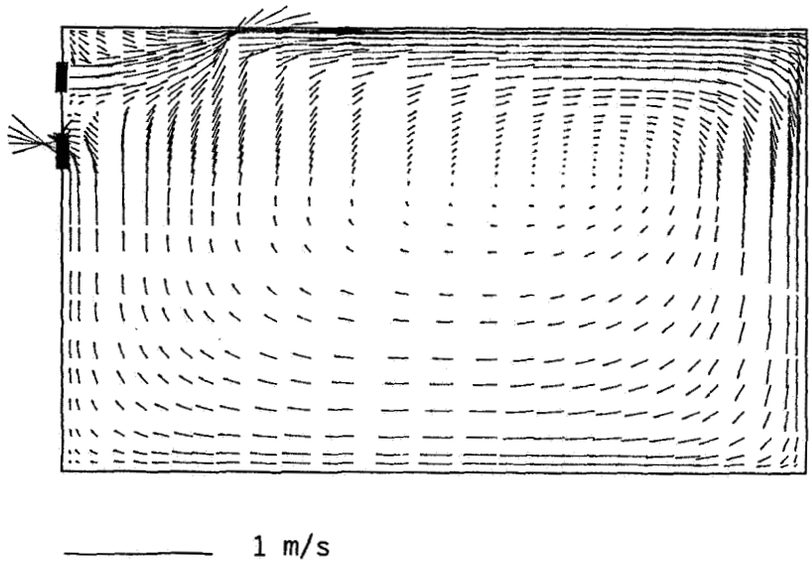

Figure 10 : Vertical cut of the flow field associated to S1 (z = 0.02 m).
Box model and symmetry assumption ; $n_a = 3\ h^{-1}$

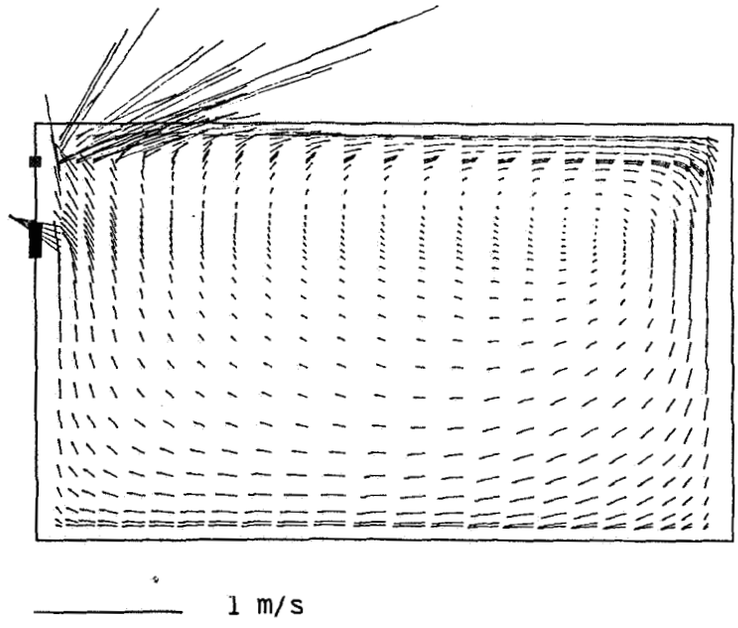

Figure 11 : Vertical cut of the flow field associated to S3 (z = 0.02 m).
Box model, no symmetry assumption ; $n_a = 3\ h^{-1}$

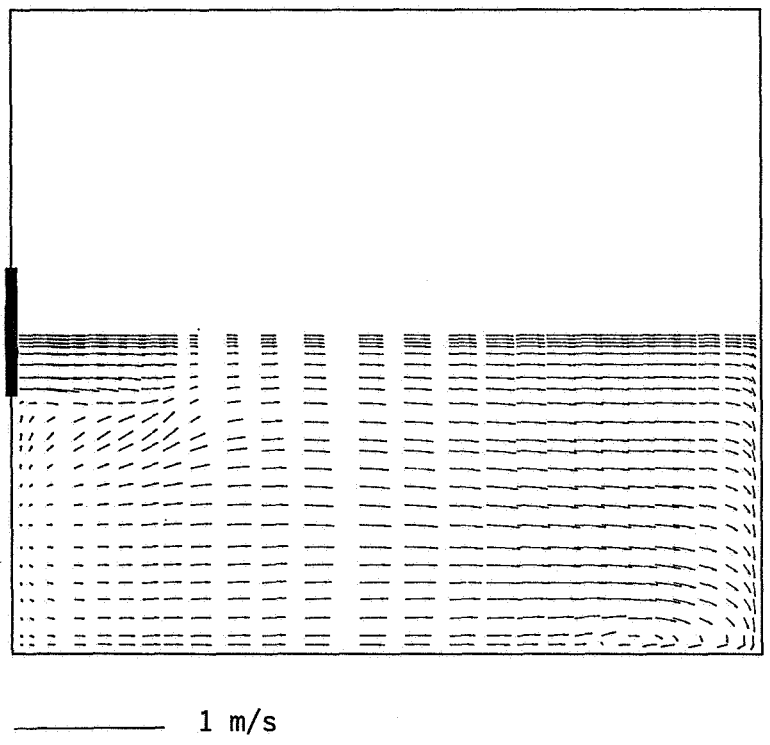

Figure 12 : Horizontal cut of the velocity field associated to S1 (y = 2.28 m).
Box model and symmetry assumption ; $n_a = 3\ h^{-1}$

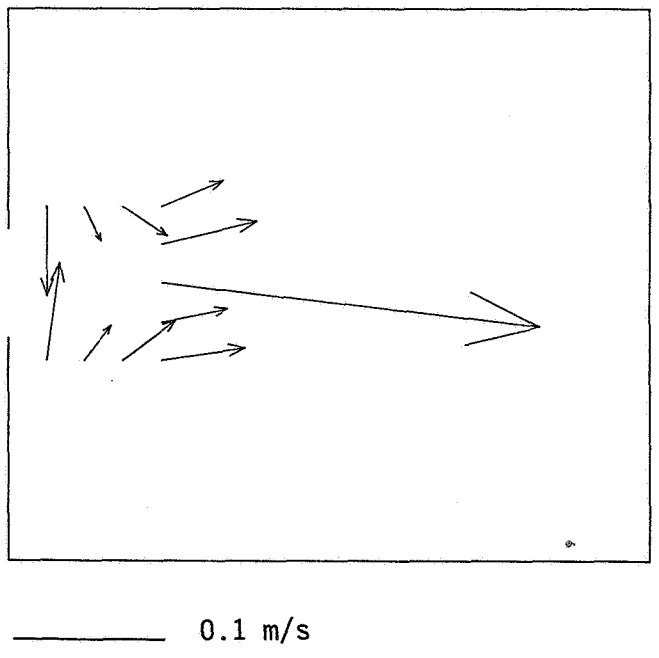

Figure 13 : Horizontal cut of the velocity field associated to bg2
in the vicinity of the air diffuser (y = 2.3 m). LDA measurements for $n_a = 3\ h^{-1}$

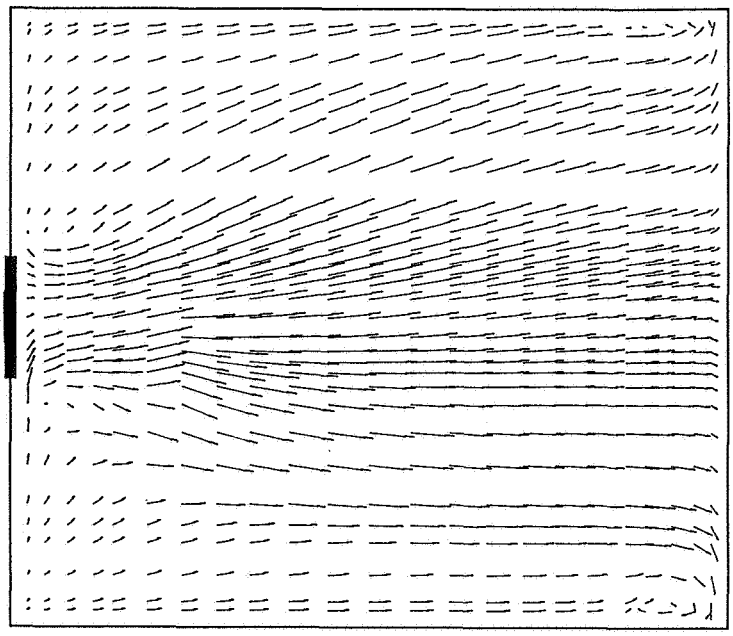

Figure 14 : Horizontal cut of the flow field associated to S2 (y = 2.4 m).
Box model, no symmetry assumption ; $n_a = 3\ h^{-1}$

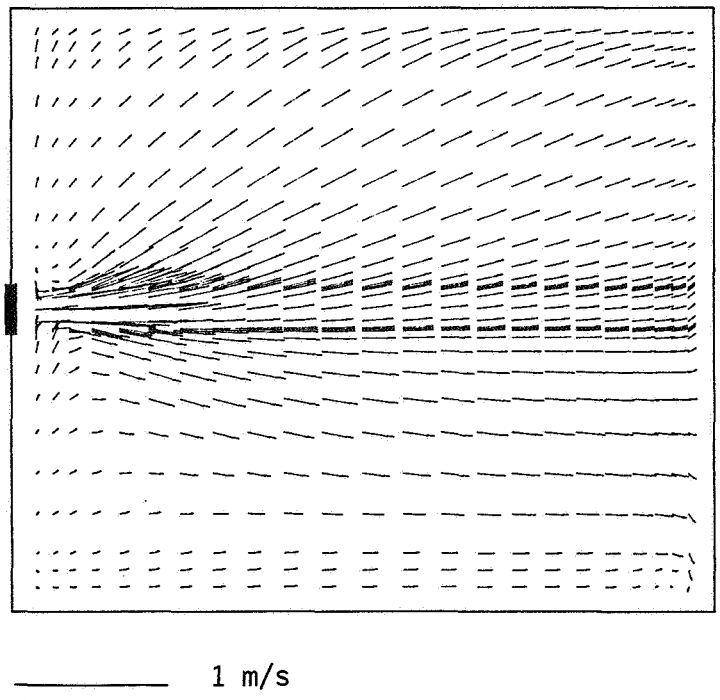

Figure 15 : Horizontal cut of the flow field associated to S3 (y = 2.42 m).
Basic model, no symmetry assumption ; $n_a = 3\ h^{-1}$

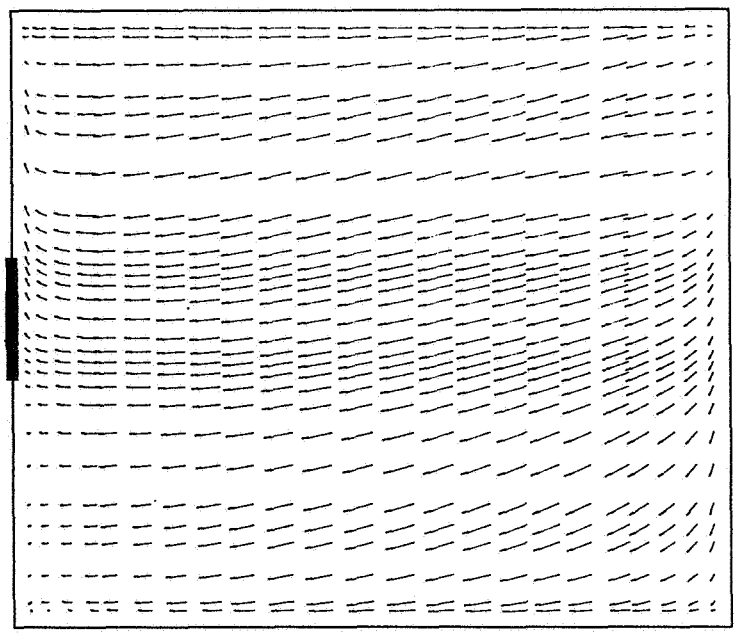

Figure 16 : Horizontal cut of the flow field associated to S3 (y = 0.1 m).
Box model, no symmetry assumption ; $n_a = 3\ h^{-1}$

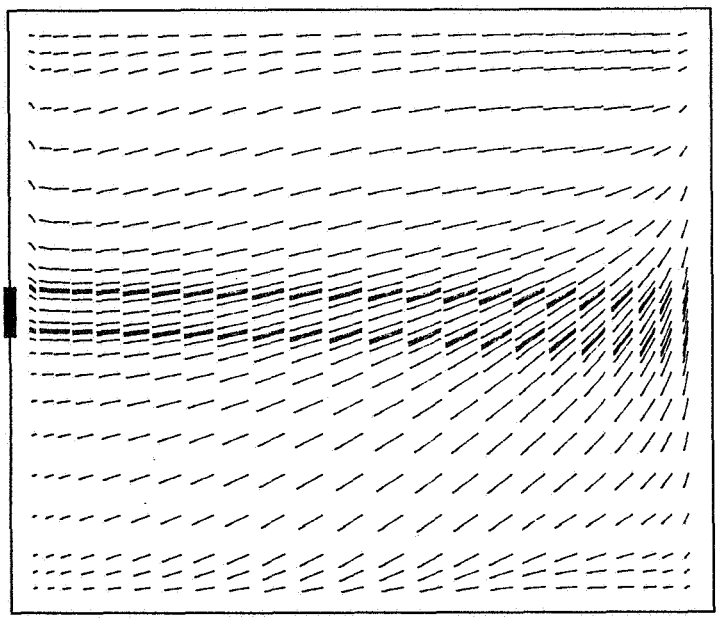

Figure 17 : Horizontal cut of the flow field associated to S3 (y = 0.1 m).
Basic model, no symmetry assumption ; $n_a = 3\ h^{-1}$

Figure 18 : Flow visualization in the central plane (z = 0 m).
Case bg2, nozzles diffuser ; $n_a = 3\ h^{-1}$

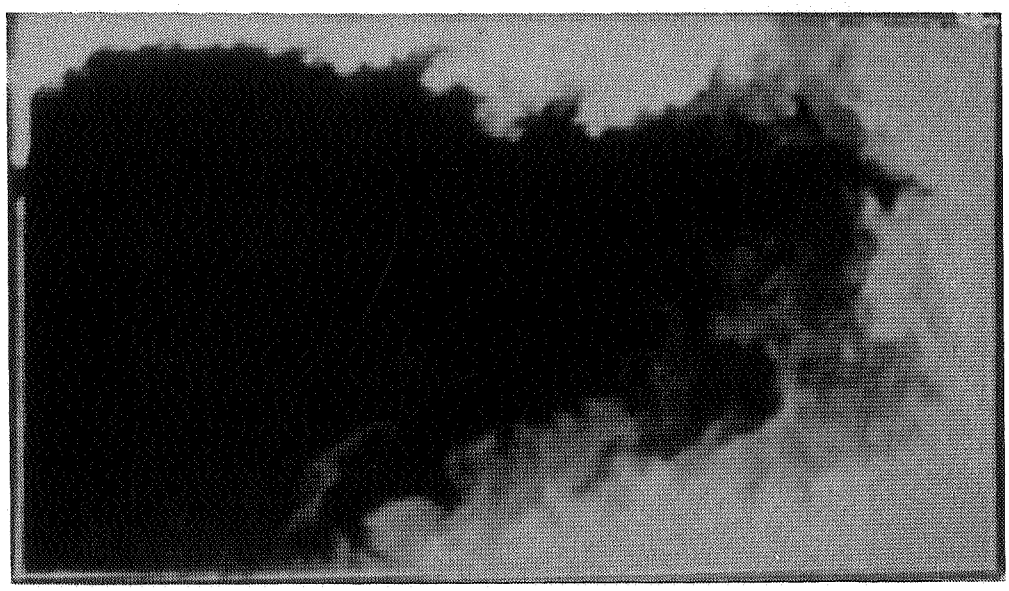

Figure 19 : Flow visualization in the central plane (z = 0 m).
Case bb, basic diffuser ; $n_a = 3\ h^{-1}$

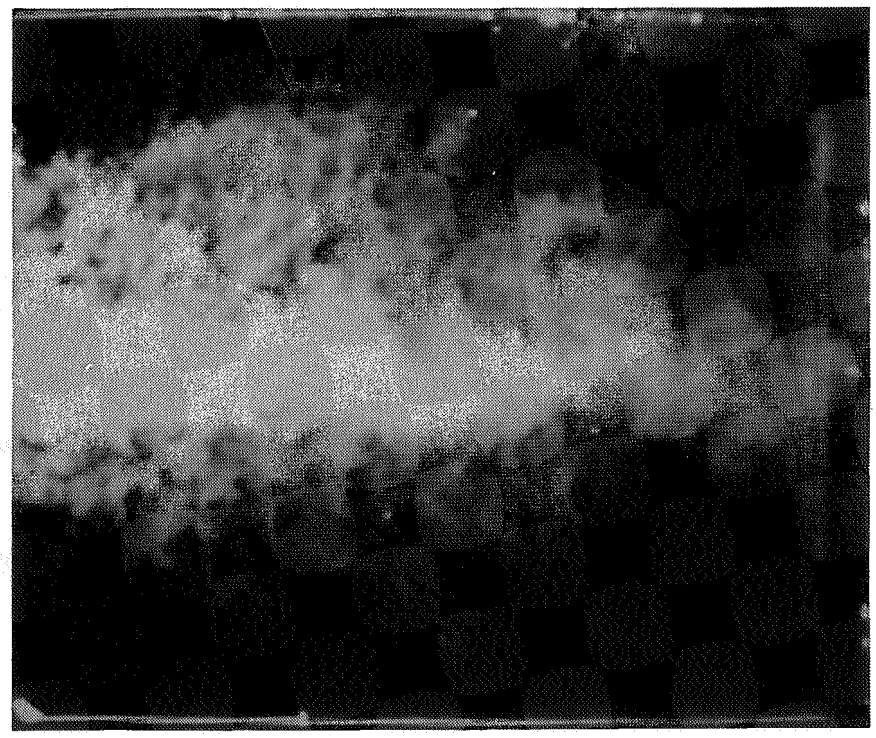

Figure 20 : Flow visualization in a horizontal plane close to the ceiling (y = 2.4 m). Case bg2, nozzles diffuser ; $n_a = 3\ h^{-1}$

Figure 21 : Flow visualization in a horizontal plane close to the ceiling (y = 2.4 m). Case bb, basic diffuser ; $n_a = 3\ h^{-1}$

Figure 22 : Flow visualization in a horizontal plane at the bottom (y = 0.1 m).
Case bg2, nozzles diffuser ; $n_a = 3\ h^{-1}$

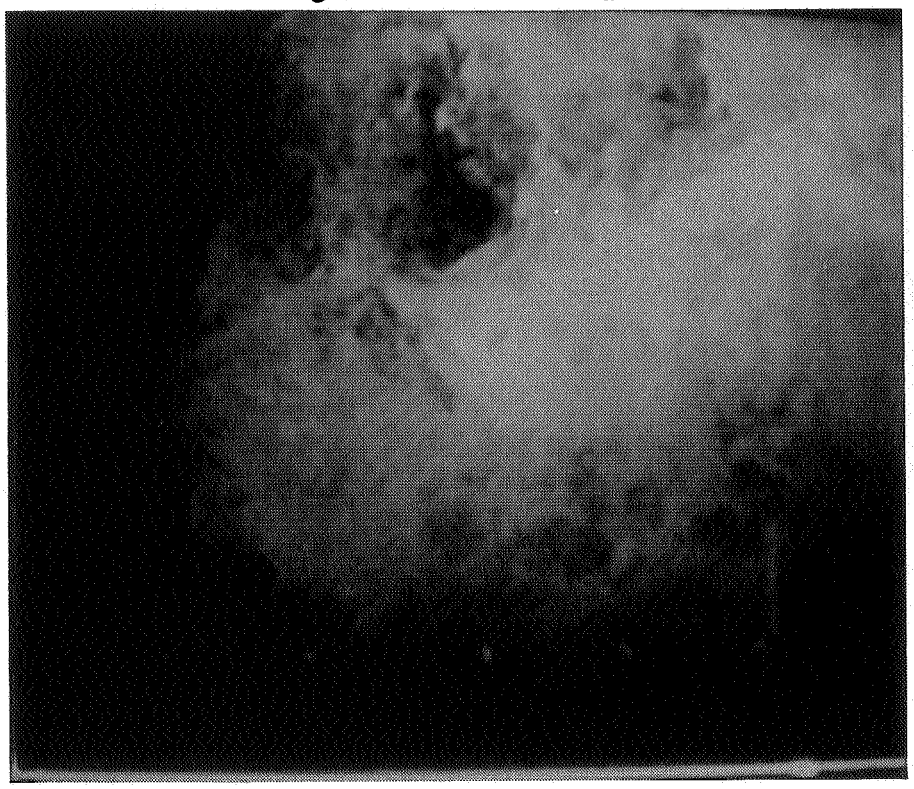

Figure 23 : Flow visualization in a horizontal plane at the bottom (y = 0.1 m).
Case bb, basic diffuser ; $n_a = 3\ h^{-1}$

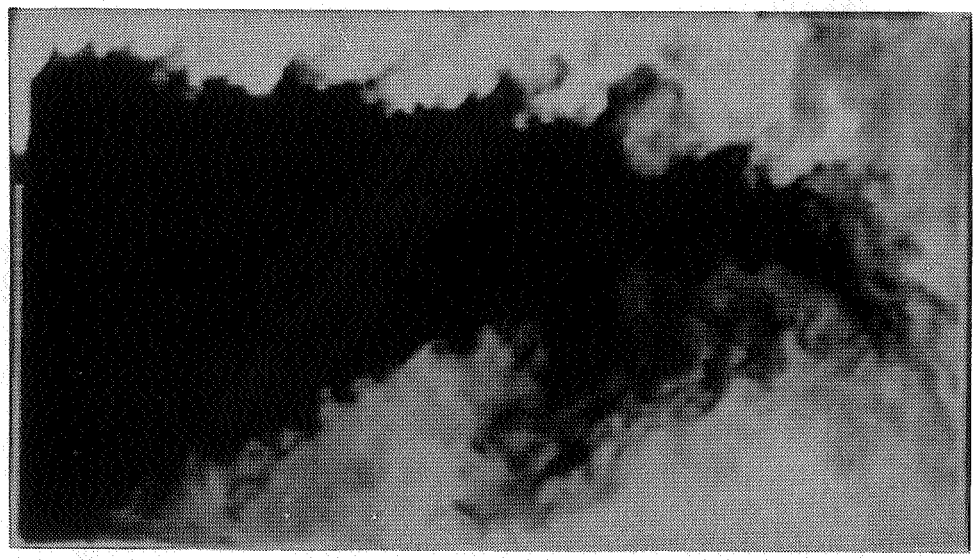

Figure 24 : Flow visualization in the central plane (z = 0 m).
Case bs, slot diffuser ; $n_a = 3\ h^{-1}$

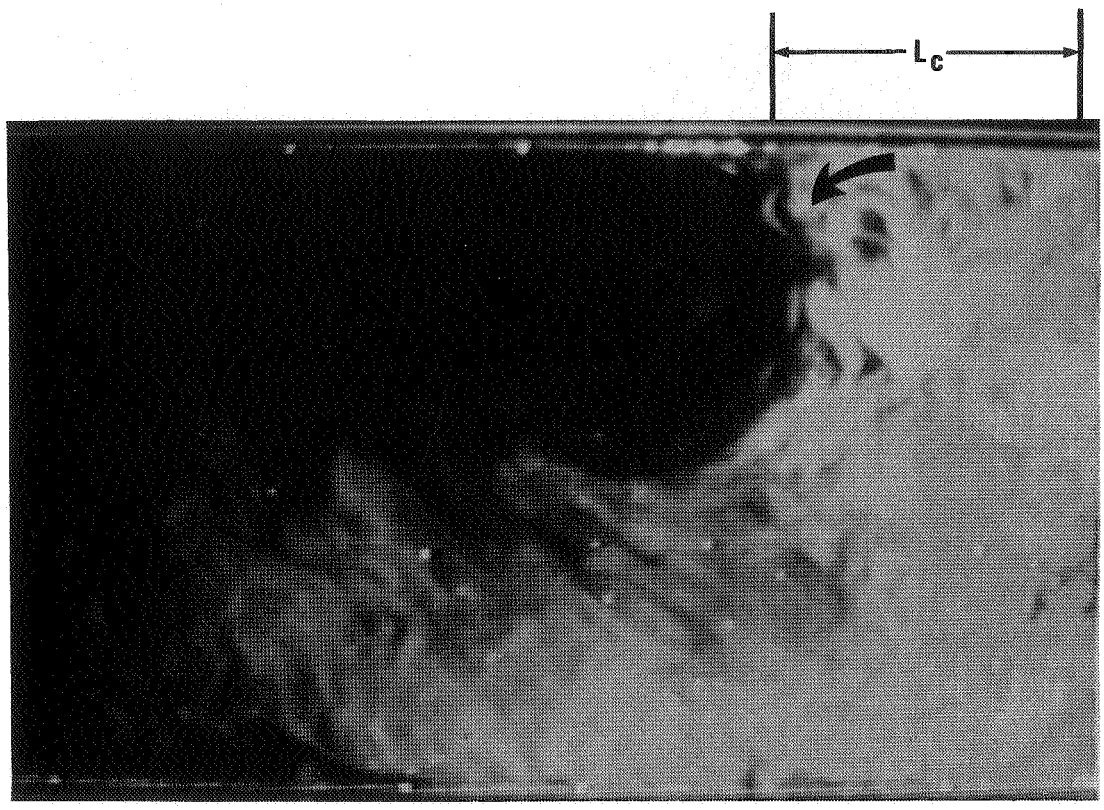

Figure 25 : Flow visualization in the front plane (z = 1.7 m).
Case bg1, nozzles diffuser ; $n_a = 1.5\ h^{-1}$

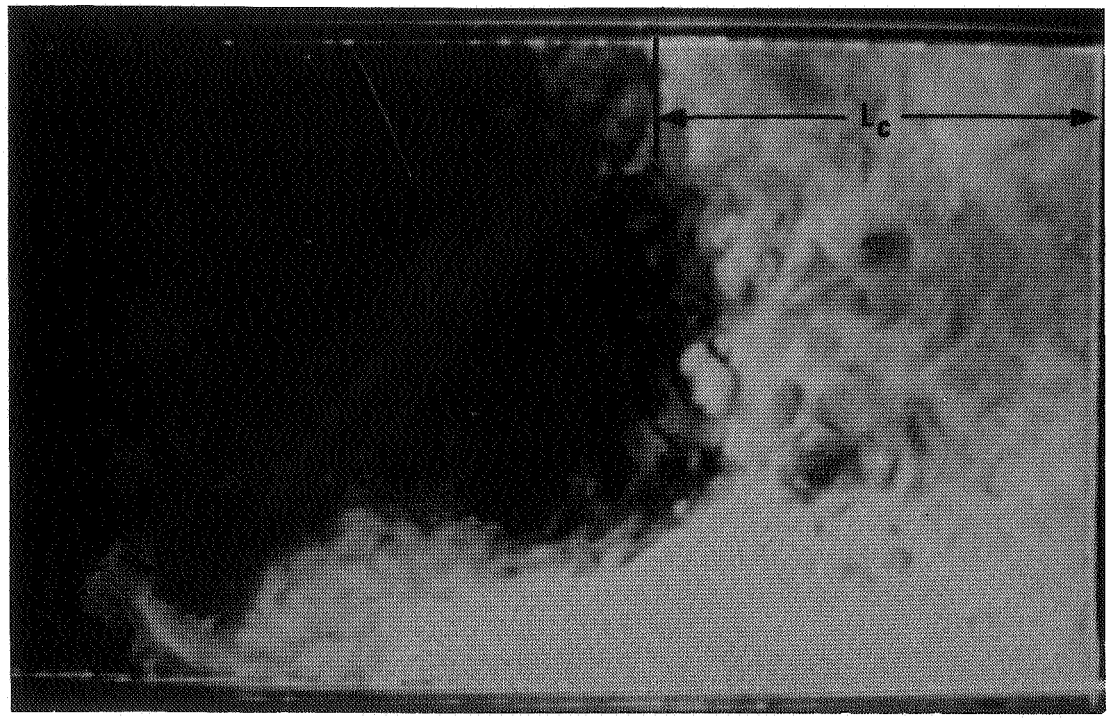

Figure 26 : Flow visualization in the front plane (z = 1.7 m).
Case bg2, nozzles diffuser ; $n_a = 3\ h^{-1}$

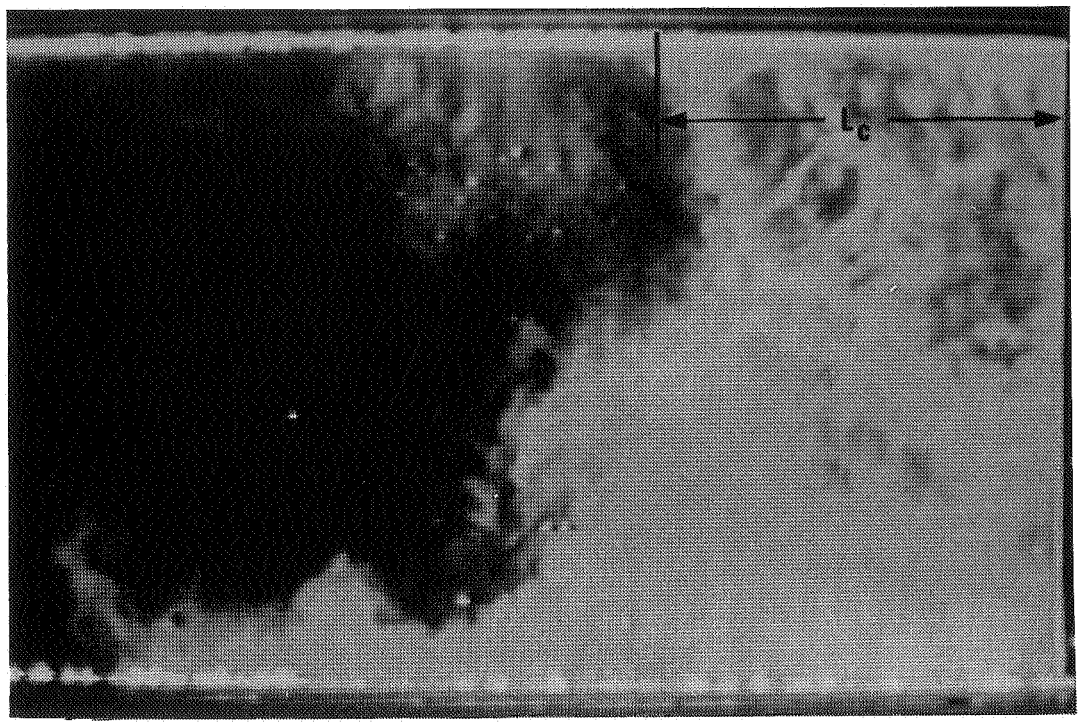

Figure 27 : Flow visualization in the front plane (z = 1.7 m).
Case bg3, nozzles diffuser ; $n_a = 6\ h^{-1}$

AIR MOVEMENT & VENTILATION CONTROL WITHIN BUILDINGS

12th AIVC Conference, Ottawa, Canada
24-27 September, 1991

POSTER 6

SCALING OF AIR FLOW PATTERNS IN ROOM VENTILATION

(Annex 20, Subtask 1, Research Item 1.23)

ALFRED MOSER

Swiss Federal Institute of Technology, ETH,
Energy Systems Laboratory, Energietechnik ML,
ETH-Zentrum, CH-8092 Zurich,
Switzerland

SYNOPSIS

Is it possible to translate a computed flow field to a design case with different physical dimension? - This and related questions must be answered when the results of the "air flow pattern atlas", as proposed in the IEA Annex 20, should be applied to actual ventilation systems.

Looking up a case in the atlas and transforming results to an actual application is like interpolating in a table. If geometries are similar, scaling laws may be applied. The interpolation problem also arises when numerical or experimental data from literature must be translated to a case at hand. Scaling rules show whether and how measurements on scale models may be translated to full-scale.

The poster identifies dominant physical parameters of jet- and buoyancy-driven air flows in rooms. It lists non-dimensional parameters that are important for the air flow and those that are not. The difficulty of running scale-model tests for natural convection in large spaces is analyzed.

LIST OF SYMBOLS

Most symbols are explained in the text. The physical constants used in calculations are given below for air at 20 °C:

Gravitational constant,	g	=	10	m/s^2
Density of air,	ρ	=	1.2	kg/m^3

Coefficient of thermal expansion; for perfect gas equal to $1/T$, where T is a mean absolute temperature,

	β	=	1/300	$°K^{-1}$

Specific heat at constant pressure,

	c_p	=	1000	J/kg°K
Kinematic viscosity of air,	ν	=	1.5E-5	m^2/s
Thermal conductivity.	k	=	0.025	W/m°K

1. Introduction

The goal of the Research Item 1.23, a subtask-1 project of Annex 20, was to develop a concept for a design tool that allows the engineer to assess air flow pattern, comfort, and indoor air quality without running an expensive flow field simulation code. This was accomplished by pre-calculating many flow patterns in typical rooms for selected values of the relevant parameters to cover a wide range of conceivable design applications. The air flow patterns are stored in a data base and documented in a catalogue called the "Atlas", [1]-[4].

Of course, it would be nice if the pre-calculated cases could be "stretched" to an actual design case with the same geometric proportions. The usefulness of the "Atlas" would greatly be enhanced. This technique is successfully employed in many fields of engineering, such as aero- and thermodynamics [5].

The task of making laboratory experiments of air flows in large spaces also requires knowledge of scaling laws. The relevant parameters and problems related to scaling of air movement in atria and other large enclosures was discussed by Whittle [6].

In this paper, some principles of dimensional analysis and theory of modelling are reviewed and applications to room air flow are demonstrated. Studies by Heikkinen [7] and Chen et al. [8] suggest that the supply air jet of Annex-20 benchmark tests is characterized mainly by its mass flow and momentum. Therefore, these quantities have been used in the definitions of non-dimensional parameters [9], [10]. It is concluded that exact scaling with mixed and free convection is possible only to a limited extent.

2. Characteristic parameters of room air flow

The result of a numerical flow field computation carried out for a specific room may not only be applied to the original case but can be converted to other cases that are *similar* to the original. This technique is routinely used in calculations of the flow field around airfoils, for instance. The computation, that was done once, provides drag and lift coefficients. The actual lift force in physical units may be obtained for any size airfoil by simple multiplications, provided the non-dimensional parameters, such as Reynolds and Mach numbers are the same and the two profiles are geometrically similar.

For scaling to be valid, the original room geometry and air flow must be physically similar to the target situation. But this requires:

(1) Geometric similarity (e.g., rooms have the same height-to-length ratio, etc.), and

(2) the relevant characteristic dimensionless parameters must have the same numerical values (e.g., the same Archimedes number).

Before discussing scaling, some technical terms will be defined [2].

Geometry is the complete geometric description of the solid envelope around the room air, expressed in physical units. Normally this is given as a large number, N, of points that describe the room inner surface including obstructions and furniture,
x_i , y_i , z_i , $\quad i = 1, \ldots N$

Size, H is a typical dimension of the room, for instance the room height, in physical units.

Shape, S is the non-dimensional geometry of the room, it is defined by the points

$$X_i = x_i/H \ , \quad Y_i = y_i/H \ , \quad Z_i = z_i/H, \qquad i = 1, \ldots N$$

Location is a particular position within the flow field, e.g., the specific point where a velocity was measured. It is given in physical units or dimensionless:

$$\text{loc} = (x \ , \ y \ , \ z) \quad \text{or}$$
$$\text{LOC} = (X \ , \ Y \ , \ Z) = (x/H \ , \ y/H \ , \ z/H)$$

Characteristic constant
is a parameter in physical units which has only one (constant) value throughout the experiment and is known before calculations. It is typical of the relevant physics of the problem. Examples: Inlet air velocity, v_o , viscosity, ν , also *size*, H.

Parameter P is a non-dimensional group of characteristic constants, and hence an input quantity. A particular experiment may depend on several parameters, P_j, $j = 1, \ldots J$. Examples:
$Re = v_o H/\nu$, Ra, Ar, etc.

Variable Q is a non-dimensional group of output variables:

$$Q_k = Q_k(LOC), \qquad k = 1, \ldots K$$

$$= \text{function}(S, P_1, P_2, \ldots P_J, LOC)$$

Examples: Nu, v/v_o at a given location, etc.

A computation will probably still be done in physical units to reduce the risk of making input errors. The results may be converted to dimensionless form and stored in arrays of the form

$$Q_k(S, P_1, P_2, \ldots P_J, LOC), \quad k = 1, \ldots K$$

where LOC refers to the grid points of the computational mesh.

3. Air flow pattern with a supply air jet and a heat source

Some of the cases used within Annex 20, Subtask 1, to evaluate numerical methods, and many of the "Atlas" sample office rooms [3], dealt with air flow patterns that were driven by air jets from a supply diffuser and some had internal heat sources such as radiators or personal computers. In this section, the relevant characteristic constants are listed, and a corresponding set of non-dimensional parameters is proposed.

The numerical exercises with a supply air diffuser "HESCO", that blows the fresh air through many small directional nozzles, have shown that the inlet should be characterized by the total mass flow and momentum of the combined air jet [7], [8]. With these complex inlet devices, it is difficult to measure the effective inlet area. Therefore, the inlet cross-sectional area does not appear as characteristic constant.

The supply mass flow, m, and jet momentum, f, are:

$$m = \int \rho \, v \, dA \tag{1}$$

$$f = \int \rho \, v^2 \, dA \tag{2}$$

Where v is the local velocity component normal to dA, and the integral is taken over the cross section of the diffuser. With these two characteristic constants, the nominal inlet velocity and effective cross section are defined by

$$v_o = f / m \quad (3)$$

$$A = m / \rho v_o \quad (4)$$

The list of characteristic constants may include the following:

m mass flow of air supply, eq.(1),

f momentum (or thrust) of air supply jet, eq.(2),

H *Size* of geometry, i.e., height of room,

ΔT temperature difference between supply and exhaust air, in steady state, This temperature increase characterizes the combined effect of all internal heat sources that release energy into the room air. No separate parameter for heat input is required.

g gravitational constant,

ρ density,

β coefficient of thermal expansion; for perfect gas equal to 1/T , where T is a mean absolute temperature,

c_p specific heat at constant pressure,

ν kinematic viscosity of air,

k thermal conductivity.

Do these 10 characteristic constants, together with the *shape* of the room, completely define the case? It is the experience and judgement of the engineer to know which parameters influence the physics of an air flow situation and which are not so important. So far, nothing has been said about radiation, which mainly transfers energy between surfaces but may also feed the air itself through infra-red absorption by the gas mixture

(mainly by water-vapor or CO_2). Another factor not mentioned is the turbulence intensity of the supply air.

Assuming that the dominant parameters have been identified, dimensional analysis tells us that the number of independent *parameters* is = (number of physical constants) - (number of basic units). With *length, time, mass,* and *temperature* as basic units, we should find 10 - 4 = 6 non-dimensional parameters.

There are many ways to define a set of parameters, however certain groups are in standard use. Six parameters are proposed below [10]. Some may look unfamiliar, but they are still required to define the situation completely. Of course, other combination may be constructed depending on user preferences.

Reynolds number $\quad Re = (f/m)\ H\ /\ \nu = v_o\ H\ /\ \nu$

Archimedes number $\quad Ar = \beta\ \Delta T\ g\ H\ m^2\ /\ f^2$

$= \beta\ \Delta T\ g\ H\ /\ v_o^2$, with v_o of eq.(3)

Prandtl number $\quad Pr = \rho\ c_p\ \nu\ /\ k$

Size-of-inlet parameter

$P_4 = m^2\ /\ (\rho\ f\ H^2) = A\ /\ H^2$ with A of eq.(4)

Temperature-ratio parameter

$P_5 = \beta\ \Delta T = \Delta T\ /\ T$

Thermal-to-potential-energy parameter

$P_6 = c_p\ \Delta T\ /\ g\ H$

These $J = 6$ non-dimensional parameters, together with a description of the *shape* (non-dimensional geometry) of the room, and its details, should uniquely characterize the boundary conditions of the flow under investigation. Other parameters may be constructed, but they will always be combinations of the six above, as for example

$$P_5^2\ /\ Ar\ P_6 = v_o^2\ /\ c_p\ T\ .$$

This last combination is proportional to the square of a Mach number.

It may surprise that the air change rate (*ach*) does not appear. It is not a characteristic parameter because it has dimension of reciprocal time; two air flow patterns may be similar even if the corresponding air change rates are different.

It turns out that only the first four parameters have any significance for room air flow. P_5 and P_6, and the Mach number as well, are unimportant. The complete set of six parameters has been listed for formal reasons.

The size-of-inlet parameter, P_4, would be given by the proportions of room and air diffuser geometries if the effective inlet cross section, A of eq.(4), is always proportional to the geometric inlet area. P_4 is needed to determine each of f and m and not only their ratio, $f/m = v_o$. The effective area, A, which is not in the set of characteristic constants, may be computed from f and m, eq.(4). It is assumed that P_4 will not change much between geometrically similar rooms.

In conclusion then, it can be stated that for practical purposes, two forced-ventilation non-isothermal air flow patterns are similar if Re, Ar, P_4, and Pr are the same. To satisfy these four definition equations, a total of 10 variables are available. But six of these are physical constants and are known as soon as the medium (air) and ambient conditions are given. That means that only the quantities m, f, H, and ΔT are free to solve the system of four equations. A closer look shows that none of these variables appears in the Prandtl number, i.e., Pr is already nailed down by the physical constant. And we end up with four variables for three equations.

In this example, one of the four may be arbitrarily chosen, - for instance the *size* (H) of the room, - and the others are then fixed by the similarity requirement.

4. Air flow pattern with free convection

The approach of analysis is the same here as in the previous section. But it is understood that for free or natural convection no air is blown into the room. Therefore, the parameters related to the air supply device disappear from the list of characteristic constants:

H *Size* of geometry, i.e., height of room,

ΔT temperature difference between typical hot and cold surfaces,

g gravitational constant,

ρ density,

β coefficient of thermal expansion (= 1/T),

c_p specific heat at constant pressure,

ν kinematic viscosity of air,

k thermal conductivity.

With these 8 characteristic constants, 4 independent parameters may be formed [10]:

Rayleigh number $\quad Ra = \beta\, c_p\, \Delta T\, g\, H^3\, \rho\, /\, \nu\, k$

Prandtl number $\quad Pr = \rho\, c_p\, \nu\, /\, k$

Temperature-ratio parameter

$$P_5 = \beta\, \Delta T = \Delta T\, /\, T$$

Thermal-to-potential-energy parameter

$$P_6 = c_p\, \Delta T\, /\, g\, H$$

Two free-convection air flow situations are now similar if the geometric configurations (*shape*) are similar and these J = 4 parameters have the same values. Experience tells us that only the first two are important in room air flow. Of the 8 variables appearing in the two definition equations, 6 express physical properties of the medium. Theoretically, the two free variables, H and ΔT, can now be adjusted to obtain the desired values of Ra and Pr. But where are the similar cases when all variables are already committed?

As with mixed convection, only physical constants appear in the Prandtl number. Hence, once the fluid and ambient conditions are selected, Pr is fixed, and may or may not have the desired value. That means, one of H and ΔT may now be arbitrarily chosen, and the other results from imposing the Rayleigh number. Under the assumptions made above, experiments 1 and 2 will be similar if

$$(\Delta T\, H^3)_2 = (\Delta T\, H^3)_1 \qquad (5)$$

5. Limits for scaling air flow patterns in rooms

The aim of this investigation is to find a "cheap" way to transfer information from a pre-calculated air flow pattern to a design situation that is of immediate interest. For instance, the computed air flow pattern with a Rayleigh number of 8.3×10^{10} may be applied to any geometrically similar room with the same Rayleigh number.

Annex-20 test case **d2** has a radiator at 55 °C and a window surface at 5 °C. Taking ΔT equal to the difference of these two temperatures, and H equal to the room height (2.5 m), the Rayleigh number is 8.3×10^{10}, with a Prandtl number of 0.72. Scaling to a room height of H = 3.0 m would require a temperature difference of ΔT = 29 °C (using eq.(5)). This kind of scaling is illustrated in fig. 1. Small changes in H require a large change of ΔT to maintain similarity.

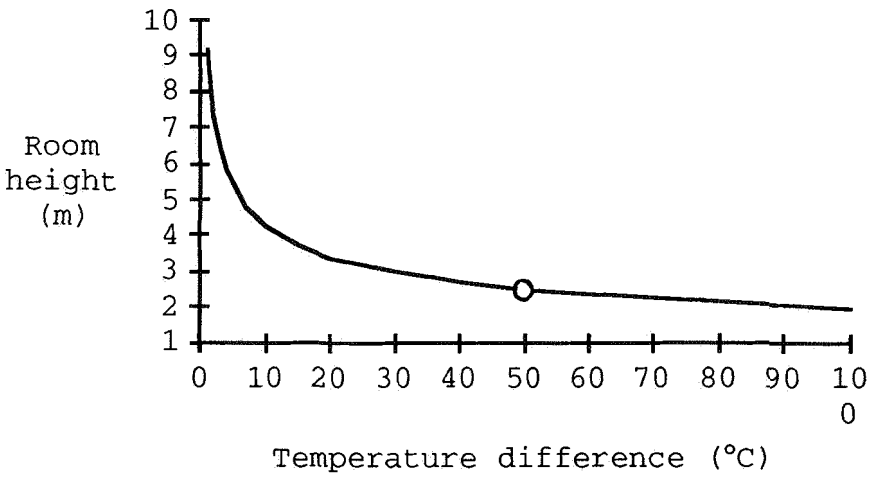

Fig. 1 Combinations of room height, H, and temperature difference, ΔT, that result in a Rayleigh number, Ra = 8.3×10^{10}, assuming the remaining physical parameters are kept constant, eq.(5).

For air flow with forced or mixed convection, two non-dimensional parameters (Re and Ar) plus the *shape* of the geometry must be conserved to maintain similarity, assuming both experiments are conducted in atmospheric air (same Prandtl number) and have the same size-of-inlet parameter, P_4 (Section 3). The free variables are H, v_o, and ΔT. The third parameter, P_4, together with v_o is used to determine m and f.

The possible range of scaling will be illustrated by the Annex-20 test case **e2**, a summer-cooling situation with mixed convection. The following parameters are formed with the room height H = 2.5 m, v_o = 4 m/s, and ΔT = 6 °C:

Test case **e2**:

$$Re = 6.7 \times 10^5$$
$$Ar = 0.031$$
$$P_4 = 0.00128$$

To see how the physical parameters may be varied, v_o is eliminated from Re and Ar to yield

$$Ar\ Re^2 = \beta\ \Delta T\ g\ H^3\ /\ \nu^2 \qquad (6)$$

Again, the product $\Delta T\ H^3$ must be kept constant for fixed Ar and Re, eq.(5). When a pair of values is chosen, v_o follows from the definition of Re, and m and f from P_4.

The limitations to scaling of mixed-convection flows imposed by similarity rules become obvious when the variables H, v_o, and ΔT are combined in one graph, fig. 2.

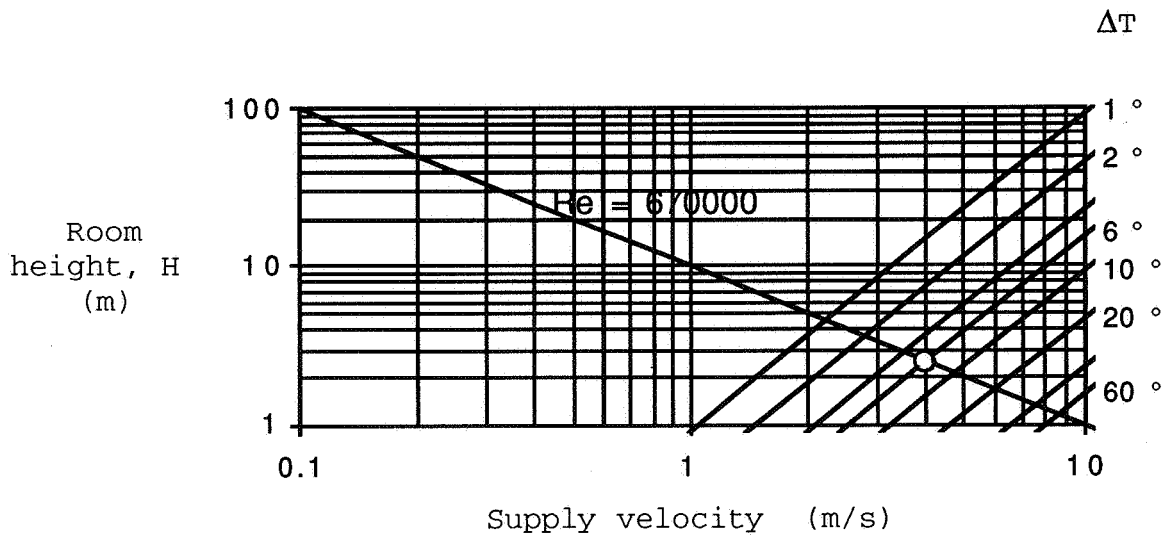

Fig. 2 Mixed convection: Variation of room height, H, supply velocity, v_o, and temperature difference, ΔT, for Re = 6.7 x 10^5 and Ar = 0.031. The array of parallel lines represents constant Ar number at different ΔT.

The Annex-20 test case **e2** is at the intersection of the 6°-line and the Reynolds-number line. If the room height is increased to 4.5 m the supply velocity must be reduced to 2.2 m/s and the temperature difference to about 1 °C. Small relative changes of *size*, H, require a large adjustments of ΔT. This makes scaling difficult.

If the flow is known to be fully turbulent, the condition on Reynolds number may be relaxed, but the $H\text{-}v_o\text{-}\Delta T$ triple should still be on the array of Ar = 0.031 lines (fig.2). This last relationship is also expressed by the definition of the Archimedes number.

6. Scaling of measured or computed results

The results or dependent variables should be expressed as "*Variable* Q_k" of Section 2, i.e., in non-dimensional form. With the set of physical parameters, as introduced in Sections 3 and 4, the Q_k are transformed back into physical quantities.

As shown in the previous section, it is not always possible to reach similarity, even if geometries are similar. If the characteristic parameters P_j do not differ too much, it is suggested [2] to use the same Q_k in both situations. This is often done with heat transfer coefficients, - or with lift and drag coefficients of an airfoil section, - which are assumed to vary little between applications. This procedure is still much better than transferring physical quantities from one case to another.

7. Conclusions

This investigation leads to the following conclusions:

- To scale geometrically similar *free-convection* cases, the product $H^3\ \Delta T$ (height x temperature difference) must be kept constant to conserve Rayleigh number. Thus, scaling up the dimensions of a room is restricted to a narrow range because a slight increase of H requires a large reduction of ΔT.

- To scale geometrically similar *mixed-convection* cases, the product $H^3 \Delta T$ (height x temperature difference) and $v_o H$ (supply velocity x height) must be kept constant to conserve Rayleigh and Reynolds numbers. As in free convection, scaling is also restricted for the same reason.

Hypotheses based on discussions at Annex-20 meetings and on various Annex reports:

- If the flow of two geometrically similar *mixed-convection* cases is fully turbulent it may be admissible to relax Reynolds-number similarity within a small range. Then, the combination $\Delta T \; H \; / \; v_o^2$ must be kept constant to conserve Archimedes number. (Caution, if surface heat transfer is strongly influenced by location of laminar-to-turbulent transition in boundary layers).

- It is hypothesized that measured or computed results of one case may be transferred to a geometrically similar case, even if the non-dimensional parameters do not have exactly the same values. To do this, the *non-dimensional* variables (e.g., Nu, v/v_o, etc.) must be transferred, not the physical ones.

- The supply air jet is characterized by its *mass flow* and *momentum* (thrust). Nominal air velocity, v_o, and effective inlet cross section, A, are derived parameters. A method to measure jet momentum needs still to be developed.

These conclusions are based on using air. Substituting other gases or water for air as test medium may lead to more freedom of scaling.

8. ACKNOWLEDGMENTS

This work was supported by the Swiss Federal Office of Energy, BEW. Valuable advice was given by Dr. Qingyan Chen, now at TNO, Delft, the Netherlands.

9. REFERENCES

1. CHEN Q.
"Simplification principle and data base structure, - a technical note for IEA Annex 20 Research Item 1.23," presented at the 4th Expert Meeting of Annex 20, Lommel, Belgium 1989.

2. MOSER A.
"Interpolation in data base of pre-calculated cases," Technical note on Research Item 1.23, Simplified model with data base of computed flow fields. Annex-20 Working Report, October 1989.

3. CHEN Q., SUTER P., and MOSER A.
"A data base for assessing indoor air flow, air quality, and draft risk," *ASHRAE Transactions*, Vol. 97, Part 2, 1991. (Paper no, 3504 of Indianapolis Annual Meeting, June 1991).

4. CHEN Q., MOSER A., and SUTER P.
"Interpolation theory and influence of boundary conditions on room air diffusion," accepted by *Building and Environment*.

5. HANEL B. and RICHTER E.
"Einführung in die konvektive Wärme- und Stoffübertragung," Reihe Luft und Kältetechnik, Herausg. Günter Heinrich, Verlag Technik GmbH, Berlin, 1990.

6. WHITTLE G.E.
"Air Flow Modelling in Atria," IMechE Seminar 'Atrium Engineering' 26 June 1990.

7. HEIKKINEN J.
"Modelling of a supply air terminal for room air flow simulation," IEA Annex 20, Subtask 1, Research Item 1.24. 12th AIVC Conference, Ottawa, Canada, September 24-27, 1991.

8. CHEN Q. and MOSER A.
"Simulation of a multiple-nozzle diffuser," IEA Annex 20, Subtask 1, Research Item 1.20. 12th AIVC Conference, Ottawa, Canada, September 24-27, 1991.

9. ASHRAE Handbook
"Fundamentals," SI-Edition, 1989.

10. MOSER A.
"Low Reynolds number effects in single-room air flow," Technical note on Research Item 1.1. Annex-20 Working Report, November 1988.

AIR MOVEMENT & VENTILATION CONTROL WITHIN BUILDINGS

12th AIVC Conference, Ottawa, Canada
24-27 September, 1991

POSTER 7

Concentration Distribution in a Ventilated Room under Isothermal Conditions

Per Heiselberg

University of Aalborg
Sohngaardsholmsvej 57, DK-9000 Aalborg, Denmark

Synopsis

The work in this paper contributes to the work in the IEA - Annex 20 "Air Flow Patterns within Buildings" and presents a series of full-scale measurements of the concentration distribution in a room with isothermal mixing ventilation.

Vertical profiles of the concentration in the middle of the room have been measured under different conditions. With the contamination source in the middle of the room the vertical profiles were changed radically with an increase of the air change rate from $n=1.5h^{-1}$ to $n=6h^{-1}$ due to a change in the flow structure in the room. With a constant air change rate the location of the contamination source in the room showed a great influence on the vertical profile. A high velocity around the contamination source resulted in a uniform contaminant distribution in the room, while a low velocity resulted in considerable differences.

Contours of concentration in the centre plane of the room have been measured using different contaminant densities. The densities were low, neutral and high in relation to the density of air. The results showed that the contaminant distribution in the room with the chosen flow conditions depended strongly on the contaminant density, and that the high density case gave the highest concentrations in the occupied zone.

1. Introduction

This paper contributes to the work in the IEA - Annex 20 "Air Flow Patterns within Buildings", subtask 1 "Room Air and Contaminant Flow". One of the objectives of subtask 1 is to acquire experimental data for the evaluation of the performance of air flow models in predicting air velocity, temperature and contaminant distribution.

The approach is to make identical full-scale experiments in identical test rooms with identical inlet devices at different sites. Simultaneous numerical simulations for the measured configurations are carried out. The measured data are compared and a data base establised for the evaluation of the accuracy of the predictions made.

The purpose of this paper is to present the results of a series of full-scale experiments of the contaminant distribution in the IEA - Annex 20 test room. The results can be used for comparison with predictions made by air flow models and to show how the contaminant distribution in a full-scale room looks like under different practical flow conditions. In the experiments the contaminant distribution has been measured under isothermal steady state flow conditions at different air change rates, locations of the contamination source and contaminant densities.

2. Experimental Set-Up

The identical test room for subtask 1 is specified in Lemaire[2]. A sketch of the geometry of the full-scale test room used in these experiments is shown in figure 1. The test room corresponds to the specifications except for the room height of 2.4m (Lemaire[2] specifies 2.5 m).

The inlet device is of the HESCO-type. The diffuser consists of 4 rows with 21 nozzles which can be adjusted to different directions. For these experiments the nozzles have been adjusted to an angle of 40° upwards, see figure 1 and Nielsen[1]. The generated flow pattern is very typical of modern air terminal device design.

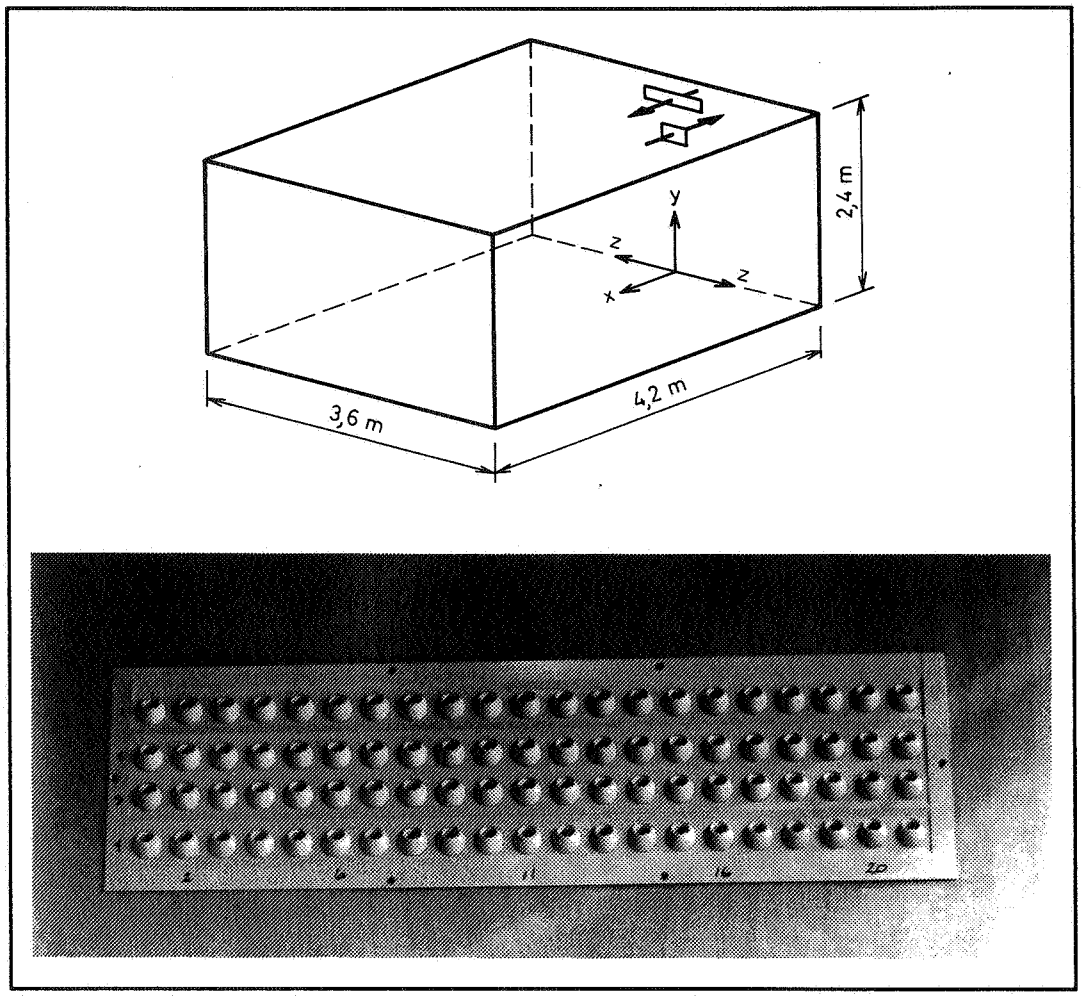

Figur 1. a) Sketch of the geometry of the full-scale test room. b) Close-up of the HESCO inlet device.

The contamination source consists of a ping pong ball (diameter 30mm) with 6 evenly distributed holes with a diameter of 1 mm each. If another location of the source is not stated it is placed approximately in the middle of the test room in the point (x,y,z) = (2.2,1.2,0.0) as specified in Skåret[4]. The tracer gas CO_2 has been used as a contaminant. It has been mixed with the carrier gases N_2 or He in order to give a total contaminant flow rate of 0.025 l/s and different contaminant densities.

The profiles of concentration are based on measurements in 10 points. The points were distributed along a vertical line placed in the centre plane of the test room 2.2 m from the supply opening. The contours of concentration in the centre plane of the test room are based on measurements in 110 points. Figure 2 shows the distribution of the points in the test room. The points are concentrated around the contamination source, where large gradients are expected, at the end wall to see how far the supply air jet penetrates into the room and at the boundary surfaces. The concentrations are measured with a BINOS I.R.-analyzer.

The experiments have taken place under isothermal steady state conditions as specified in Heikkinen[3].

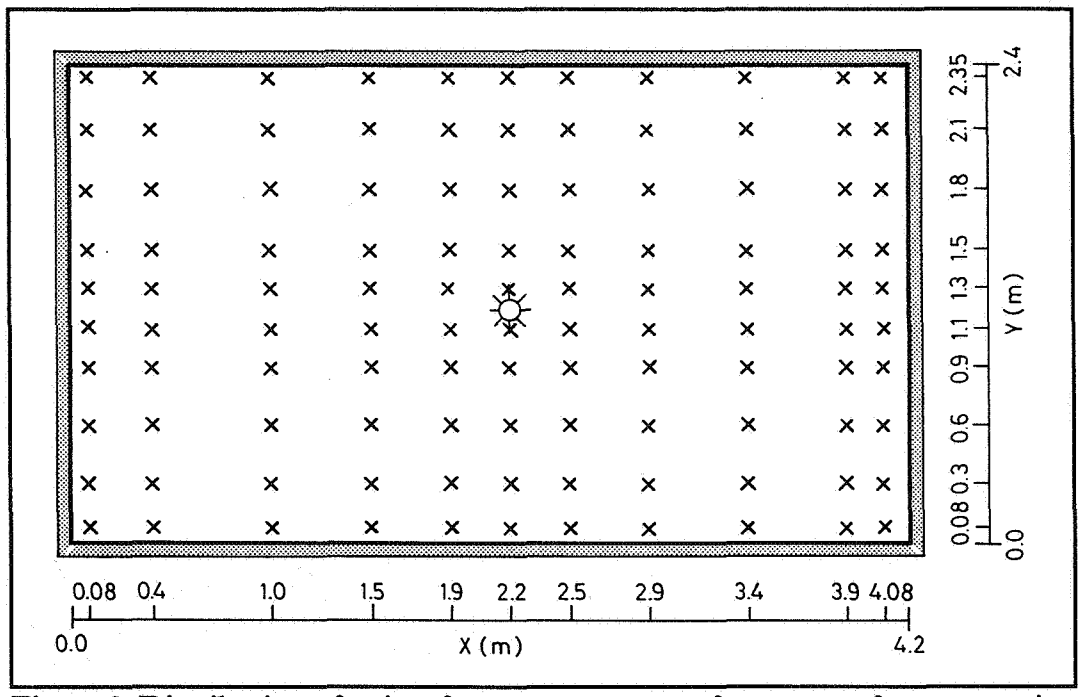

Figure 2. Distribution of points for measurements of contours of concentration in the centre plane of the test room.

3. Profiles of Concentration

Vertical profiles of the concentration in the middle of the test room have been measured for different air change rates and locations of the contamination source. The profiles of concentration are presented as concentration ratios where the reference concentration is the concentration in the exhaust opening.

Figure 3 shows the profiles for three air change rates. The test case with an air change rate of $n=1.5h^{-1}$ represents a small Reynolds number case where low Reynolds number effects are seen in the inlet flow from the diffuser and in the flow structure in the room, see Skovgaard et al.[5] and Skovgaard et al.[6]. The air flow rate is approximately the minimum value required to ventilate an office room. Measurements in Skovgaard et al.[5] show that the throw of the jet is about 4/5 of the room

length and that the maximum velocity in the occupied zone is below 0.1 m/s. The test case with an air change rate of $n=3h^{-1}$ represents the basic case where the air flow rate is about the usual value in office rooms. According to Skovgaard et al.[5] the throw of the jet is approximately room length plus room height and the maximum velocity in the occupied zone is 0.16 m/s, which is the maximum velocity that can be accepted in an office. The test case with an air change rate of $n=6h^{-1}$ represents a high Reynolds number case and it is important for the comparison of the measured and the calculated results. The maximum velocity in the occupied zone is according to Skovgaard et al.[5] about 0.33 m/s.

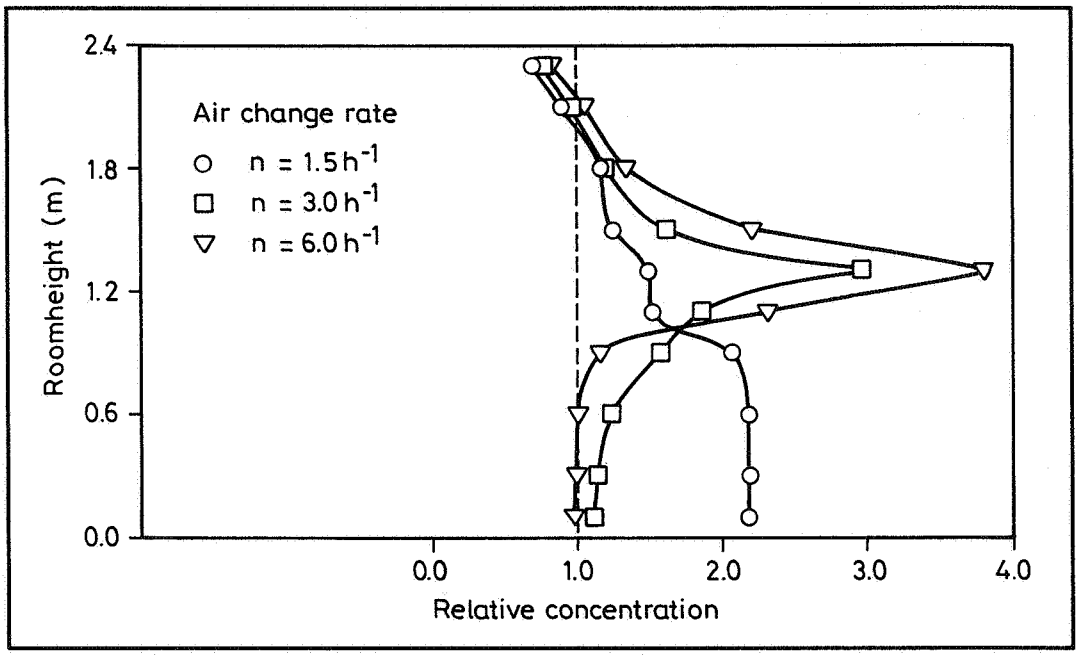

Figure 3. Relative concentration profiles in the middle of the test room for three different air change rates. The contamination source is placed in the middle of the room 1.2 m above the floor. The contaminant density is 1.2 kg/m^3.

The results in figure 3 show in the upper part of the room a concentration distribution in the wall jet created by entrainment of the contaminated room air into the primary air. The concentration distribution is nearly the same for all three air change rates. In the occupied zone the concentration distribution is dependent on the air change rate and it changes radically when the air change rate is changed from $n=1.5h^{-1}$ to $n=3h^{-1}$ due to a change in the flow structure in the room.

At an air change rate of $n=1.5h^{-1}$ the supply air jet only reaches the upper part of the occupied zone and the recirculating flow takes place here. In the lower part of the room there are small velocities and a slow exchange of air and therefore a high level of concentration, see also figure 6.

At an air change rate of $n=3h^{-1}$ the supply air jet reaches the floor in the room and there will be a recirculating flow with large velocities at floor level, see Skovgaard et al.[5]. The contamination source is placed almost in the centre of the recirculating

flow where the velocities and the exchange of air are very small. The level of concentration therefore becomes very high before the contaminant is entrained and discharged with the other air in the room. Model experiments by Oppl[7] and full-scale experiments by Heiselberg et al.[8] show a similar effect when the source is placed in an area with a low velocity.

With an increasing air change rate the contaminant distribution is approximating the distribution at high turbulent flow conditions in the room. This distribution is independent of the air change rate, see Nielsen[9]. The maximum velocity in the occupied zone will, however, be above the acceptable comfort level for office rooms. The contaminant distribution in a room will for practical purposes therefore depend on the supplied air flow rate.

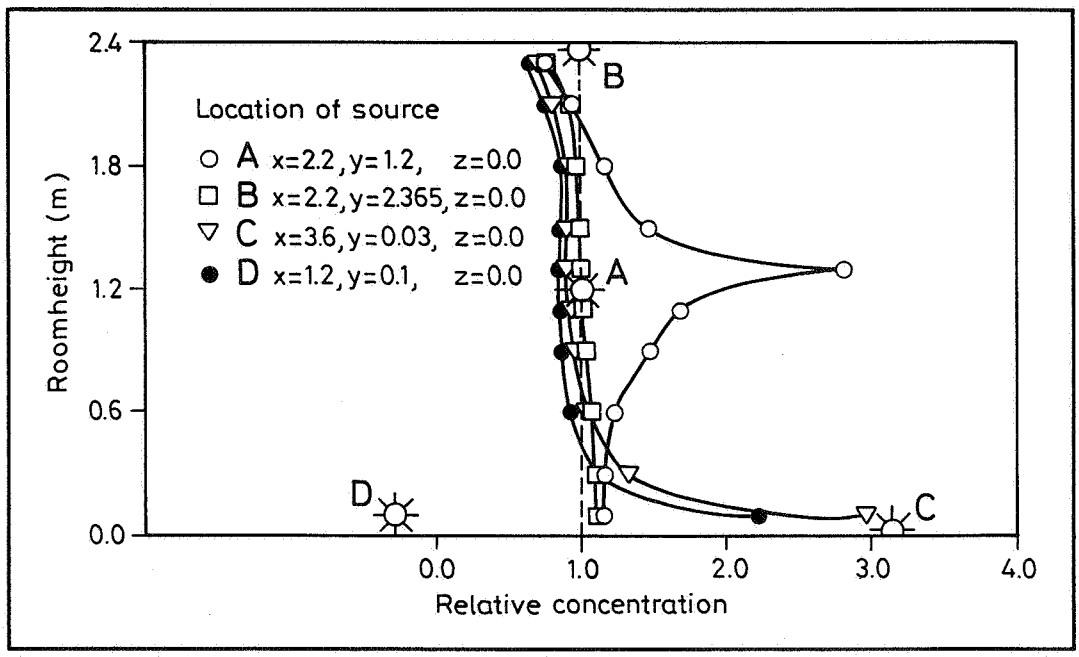

Figure 4. Relative concentration profiles in the middle of the test room for four different locations of the contamination source. The air change rate is $n=3h^{-1}$. The contaminant density is 1.2 kg/m^3.

Figure 4 shows the profiles of concentration for four locations of the contamination source in the room. Location A) is in the middle of the room as specified in Skåret[4]. Here the velocities are very low. Location B) is in the primary jet where the maximum velocity has been measured. Location C) is in the occupied zone where the maximum velocity in the recirculating flow has been measured. Location D) is at floor level where a low velocity has been measured. The velocity measurements are from Skovgaard et al.[5].

The profiles of concentration in the middle of the room depend on the location of the contamination source. A location in the middle of the room where the velocities are very small gives a high level of concentration just around the source because the exchange of air is slow. A location in the primary jet results in a very good mixing of the contaminant and the supply air and gives a quick removal of the contaminant

and a homogeneous contaminant distribution in the whole room. A location of the contamination source at floor level gives a uniform concentration in the upper part of the room and only high concentration in the immediate vicinity of the floor. Corresponding results are found by Oppl[7] and Nielsen[9].

4. Contours of Concentration

Contours of concentration in the centre plane of the test room have been measured for three different contaminant densities. The three test cases with contaminant densities of $s=0.8$ kg/m^3, $s=1.2$ kg/m^3 and $s=1.8$ kg/m^3 represent respectively a case with low density of the contamination source with a tendensy of the contaminant to migrate to the ceiling region, a basic case with neutral density and a case with high density of the contamination source with a tendensy of the contaminant to migrate to the floor region.

The results in the figures 5-7 show that the supply air jet reaches half the way down the opposite end wall and that the recirculating flow takes place in the upper part of the room above the level of the contamination source. The contours of concentration show considerable differences between the three test cases.

Contours of concentration for the high density case in figure 7 show clearly that the contaminant is streaming towards the floor region. Because the supply air jet is not able to flow through the whole room an even stratification of the contaminant arises

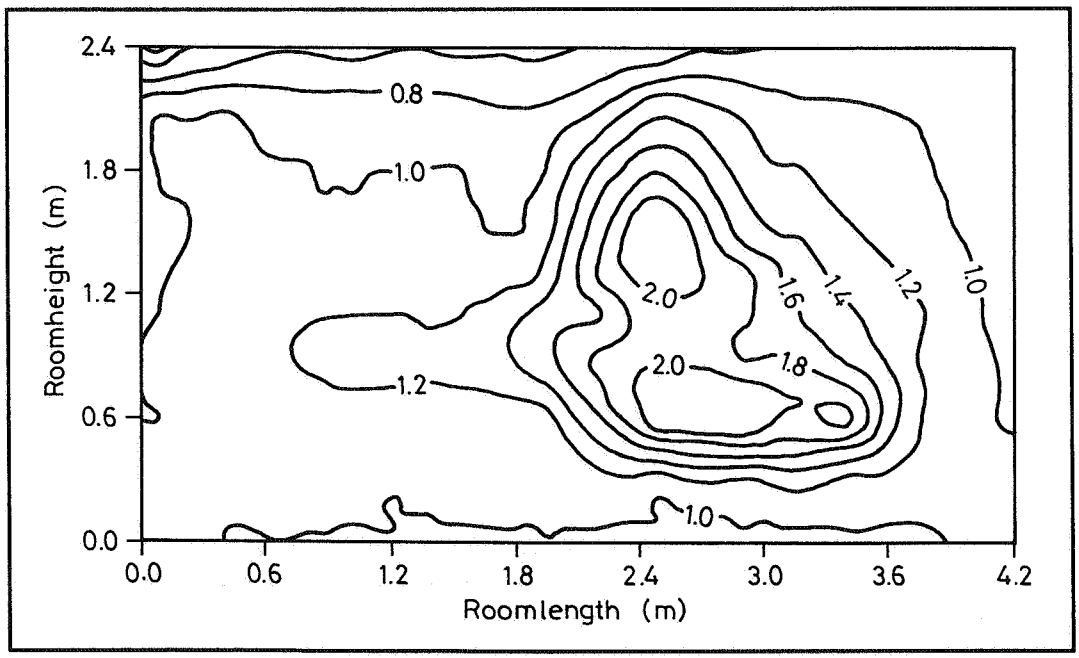

Figure 5. Contours of concentration in the centre plane of the test room. The contamination source is placed in the middle of the room 1.2 m above the floor. The contaminant density is 0.8 kg/m^3.

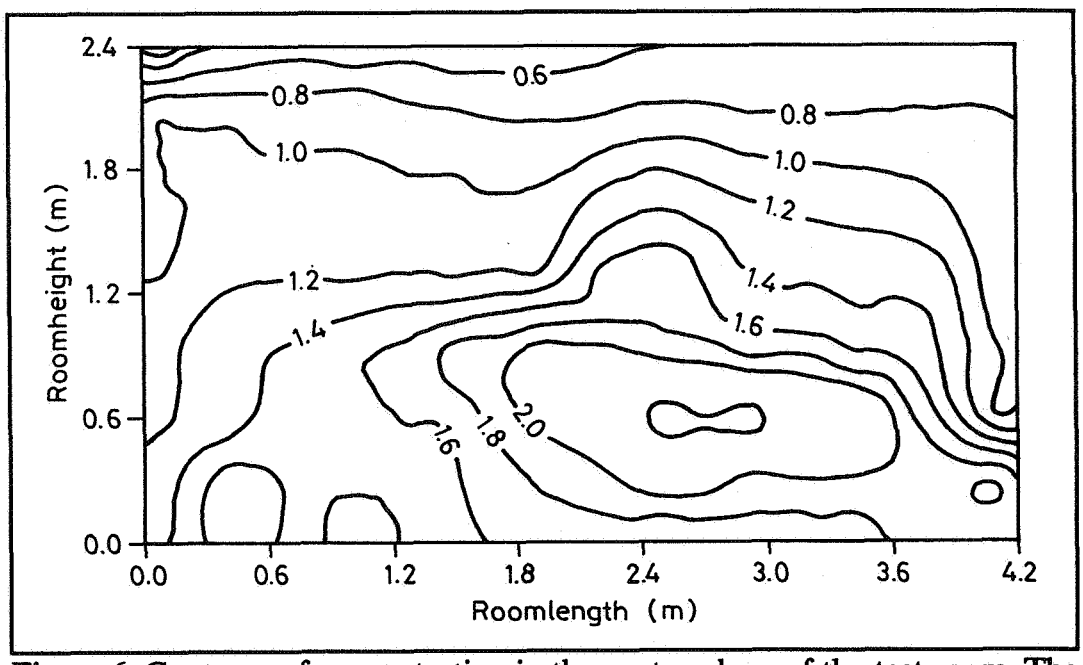

Figure 6. Contours of concentration in the centre plane of the test room. The contamination source is placed in the middle of the room 1.2 m above the floor. The contaminant density is 1.2 kg/m^3.

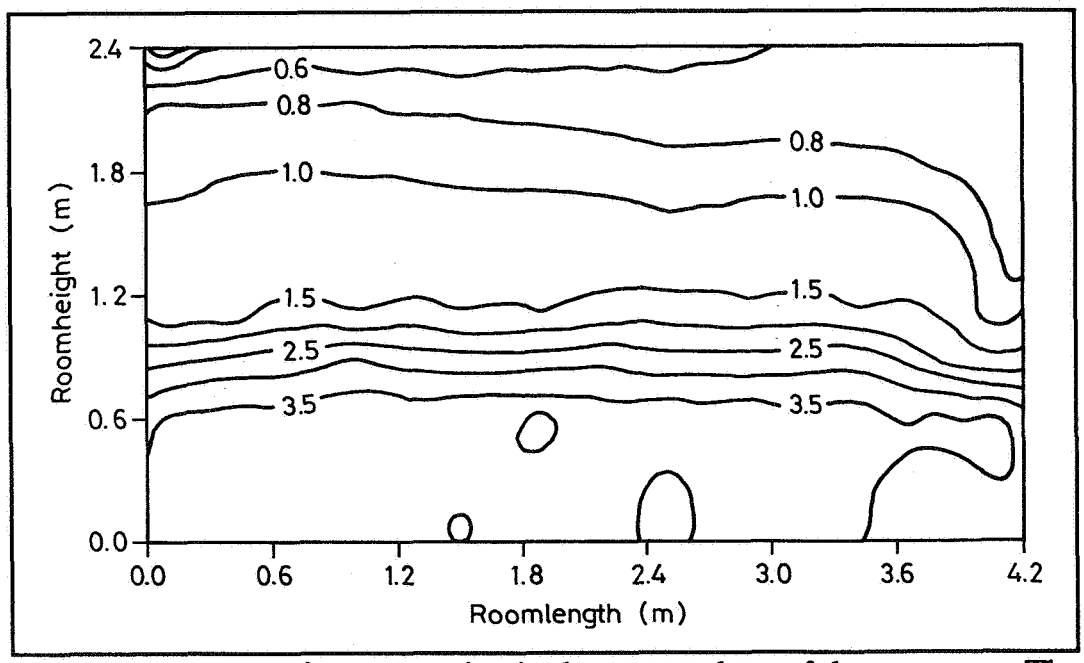

Figure 7. Contours of concentration in the centre plane of the test room. The contamination source is placed in the middle of the room 1.2 m above the floor. The contaminant density is 1.8 kg/m^3.

in the lower part with a large contaminant gradient just below the contamination source and large concentrations near the floor.

Contours of concentration for the neutral density case in figure 6 show that the contaminant distributed to the upper part of the room is mixed with the recirculating room air. The contaminant distributed to the lower part of the room causes a high level of concentration in large areas of the occupied zone because of the low velocities and slow exchange of air in this region of the room.

Contours of concentration for the low density case in figure 5 show high levels of concentration above the contamination source where the contaminant is flowing towards the ceiling and is here entrained by the supply air jet. There are also high levels of concentration below the contamination source.

The considerable differences found between the three test cases will be reduced with an increasing air change rate. The buoyancy effects will decrease and the contaminant distribution will approximate the distribution at high turbulent flow conditions, see experiments by Heiselberg et al.[8], Heiselberg[10] and Murakami et al.[11]

It is not possible from the figures 5-7 to see how the three-dimensional flow conditions in the room are influencing the contaminant distribution in the centre plane.

5. Conclusion

Results of a series of full-scale experiments of the contaminant distribution in the IEA - Annex 20 test room are presented. The results make it possible to evaluate the performance of air flow models in predicting the contaminant distribution in a room for different supply air change rates, locations of the contamination source and contaminant densities.

In rooms ventilated by mixing ventilation, in order to remove contaminants from the occupied zone, the goal for the air distribution system is to achieve an even concentration distribution in the room. This is not always possible, however, but the full-scale experiments have shown that by using as large an air change rate as possible without exceeding the comfort limit for the velocity in the occupied zone, and by making sure that the contamination source is placed in an area of the room with a high velocity the differences can be reduced to a minimum.

The contours of concentration in the centre plane of the room showed at an air change rate of $n=1.5h^{-1}$ considerable differences between the test cases with different contaminant densities. The results showed that it is important for the removal of contaminants in a room that the ventilation system is working in the same direction as the existing buoyancy forces. A contaminant with a high density will flow towards the floor region. With an exhaust placed near the floor the ventilation system will be able to remove the contaminant regardless of the fact that the supply air jet is able to flow through the whole room, and a situation with high

levels of concentration as in figure 7 will be prevented.

The experiments showed that the contaminant distribution in a room will always depend on the location of the contamination source and for practical purposes also on the supplied air flow rate and the contaminant density. High turbulent flow conditions will occur in the room at large air change rates but the velocities in the occupied zone will then be above the acceptable comfort level.

6. References

[1] Nielsen, P.V.
"Selection of air terminal device".
Annex 20 working report R.I.1.2. University of Aalborg, 1988,
ISSN 0902-7513-R8838.

[2] Lemaire, A.D.
"Testrooms, Identical Testrooms".
Annex 20 working report R.I.1.3, May 1989.

[3] Heikkinen, J.
"Specifikation of testcase B (forced convection, isothermal)".
Annex 20 working report R.I.1.13, April 1989.

[4] Skåret, E.
"Specification of testcase F (forced convection, isothermal with contaminants".
Annex 20 working report R.I.1.31, Oct. 1989.

[5] Skovgaard, M., Hyldgaard, C.E. and Nielsen, P.V.
"High and low Reynolds number measurements in a room with an impinging isothermal jet".
Int. Conf. ROOMVENT '90, Oslo 1990.

[6] Skovgaard, M. and Nielsen, P.V.
"Modelling complex inlet geometries in CFD - applied to air flow in ventilated rooms".
12th AIVC Conference, Ottawa Canada, Sept. 1991.

[7] Oppl, L.
"Luftströmung in gelüfteten Raümen".
Öl- und Gasfeuerung, Nr. 9, 1969.

[8] Heiselberg, P. and Nielsen, P.V.
"The contaminant distribution in a ventilated room with different air terminal devices".
Int. Conf. ROOMVENT '87, Stockholm, 1987.

[9] Nielsen, P.V.
"Contaminant distribution in industrial areas with forced ventilation and two-dimensional flow".
IIR-Joint Meeting, Commision E1, Essen, Sept. 1981.

[10] Heiselberg, P.
"Flow conditions in rooms with mixing and displacement ventilation".
(in Danish)
Ph.D.-Thesis, University of Aalborg, Maj 1990, ISSN 0902-7513-R9015.

[11] Murakami, S., Tanaka, T. and Kato, S.
"Numerical Simulation of Air Flow and Gas Diffusion in Room Model - Correspondance between Numerical Simulation and Model Experiments".
4th Int. Symp. on the Use of Computers for Environmental Engineering Related to Buildings, Tokyo, 1983.

AIR MOVEMENT & VENTILATION CONTROL WITHIN BUILDINGS

12th AIVC Conference, Ottawa, Canada
24-27 September, 1991

POSTER 8

Annex 20 SubTask 2.6
Multi-room Ventilation Efficiency

F. Haghighat (Canada)
Dominique Bienfait (France)
Hans Phaff (Netherlands)

Short Summary for the AIVC conference in Ottawa.
This paper belongs to the group of Annex 20 Subtask 2 papers.
A poster presentation is prefered.

Title:

ANNEX 20 Subtask 2.6.
Multiroom Ventilation Efficiency.

Authours: Fariborz Haghighat (Canada)
Dominique Bienfait (France)
Hans Phaff (Netherland)

Summary.

Seen from the AIVC Technotes 21 and 28, Ventilation Efficiency is still a complex concept. Aswell for measurements as for simulations.
Two more or less separate terms are used:

Ventilation Efficiency (=Supply Efficiency)
and
Ventilation Effectiveness (=Contaminant Removal Effectiveness).

In this paper is shown that the Multizone Ventilation Efficiency has a much wider range than Ventilation Efficiency within one room.
In a single room efficiencies can be found for example up to 2 for very good systems. The Multizone Ventilation Efficiency can be for example up to 100 for a good design and system, even if internal doors are used.

Both Ventilation Efficiency terms (Supply - and Removal -) are integrated by looking at the room volume weighted concentrations or concentrations near occupants. This results in a single figure, which does take both phenomenae (Supply - and Removal -) into account. Hereby the complexity of Ventilation Efficiency is greatly reduced. This figure will be called the Ventilation Performance Index (VPI).

A measurement method for VPI is introduced.

A computer code routine is presented that calculates the VPI for multizone airflow models that simulate spread of pollutants.

A procedure is described that uses the VPI to find the optimal ventilation flowrates during the seasons to optimize concentrations and ventilation heatlosses.

All use of indices has limitations. The main limitation on the use of the VPI is the chosen distribution of pollutant sources in the simulated or measured building. A number of examples are given that show the limitations of use for the VPI.

It is expected that the use of the VPI will ease and improve the quality of the analysis of measurement campaigns and series of simulation runs. Building designs can be optimised more thoroughly. Effects of improvements or retrofits on existing buildings can be ranked.

AIR MOVEMENT & VENTILATION CONTROL WITHIN BUILDINGS

12th AIVC Conference, Ottawa, Canada
24-27 September, 1991

POSTER 9

Turbulence Characteristics in Rooms Ventilated with a High Velocity Jet.

M. Sandberg, C.Blomqvist, M.Mattsson

The National Swedish Institute for Building Research
Box 785
S-801 29 Gavle
Sweden

Turbulence characteristics in rooms ventilated with a high velocity jet

M. SANDBERG, C. BLOMQVIST, M. MATTSON
The National Swedish Institute For Building Research
Box 785
S-801 29 GÄVLE
Sweden

Abstract

The measurements reported in this paper were carried out in a mock up of an office room, ventilated by a commercial supply air terminal consisting of 84 nozzles (characteristic dimension $\sqrt{A_s}$ = 0.0975 m). The test room configuration was identical to the one used within the IEA Annex 20 work. Results from isothermal supply is reported. A constant-temperature hot-film anemometer with fast dynamic response was used to record the instantaneous velocities.

The following parameters were recorded

- Mean velocity
- Standard deviation (relative turbulence intensity)
- Turbulent integral length scale and microscale

The turbulent length scale was derived from the autocorrelation function.

The above parameters were recorded at the following locations:

1. At a *fixed* distance from the supply air terminal the *near ceiling velocity* was recorded at different flowrates (Reynolds number). The errors of the velocity readings due to additional heat losses to the the wall were corrected for. By this procedure we obtained the near wall velocity profile (wall function) in a room with normal surface roughness. Both the change in turbulent velocity scale (standard deviation) with distance from the ceiling and the change in turbulent length scale with velocity are reported.

2. At stations *along the perimeter* (ceiling-wall-floor) and at the point where the maximum mean velocity of the wall jet occurred. These measurements provided information regarding the velocity decay in the wall jet and the evolution of the turbulent length scales with distance from the terminal.

1 Introduction

Measurements of turbulence quantities in *free* jets is fairly abundant. One classical example is Wyganski I. & Fiedler H. (1969) and Gutmark E. & Wyganski I. (1976). The first paper is concerned with an axisymmetric jet whereas the last paper reports on a two-dimensional jet. Measurements of wall jets are less abundant, for a review on wall jets see Launder B.E. & Rodi W. (1983).

The more "scientific" orientated measurements of turbulence characteristics have been carried out under specially arranged laboratory situations. Measurements of turbulent quantities in ventilated spaces have been performed by several e.g. Hanzawa et al (1987), Kovanen et al (1987), Sandberg (1987). The main concern in these investigations were the conditions in the occupied space. The analysis of the velocity fluctuations was based on recorded spectral density. The present work is, however, concerned with measurements of the wall jet in an office room. The velocity fluctuations were analyzed by recording the autocorrelation function. All room surfaces had normal surface coating and surface roughness. The jet was issued from a commercial air terminal.

The present investigation was undertaken in order to extend the knowledge of turbulence in a real room situation. In particular the idea was to study the effect of the deflection of the jet that occurs at the corners of the room. Measurements were therefore carried out along the jet trajectory from the inlet to the occupied zone.

2 Test room and experimental procedure

Fig. 1 shows the testroom (WxLxH = 3.6x4.2x2.5 m) and the location of the supply air terminal

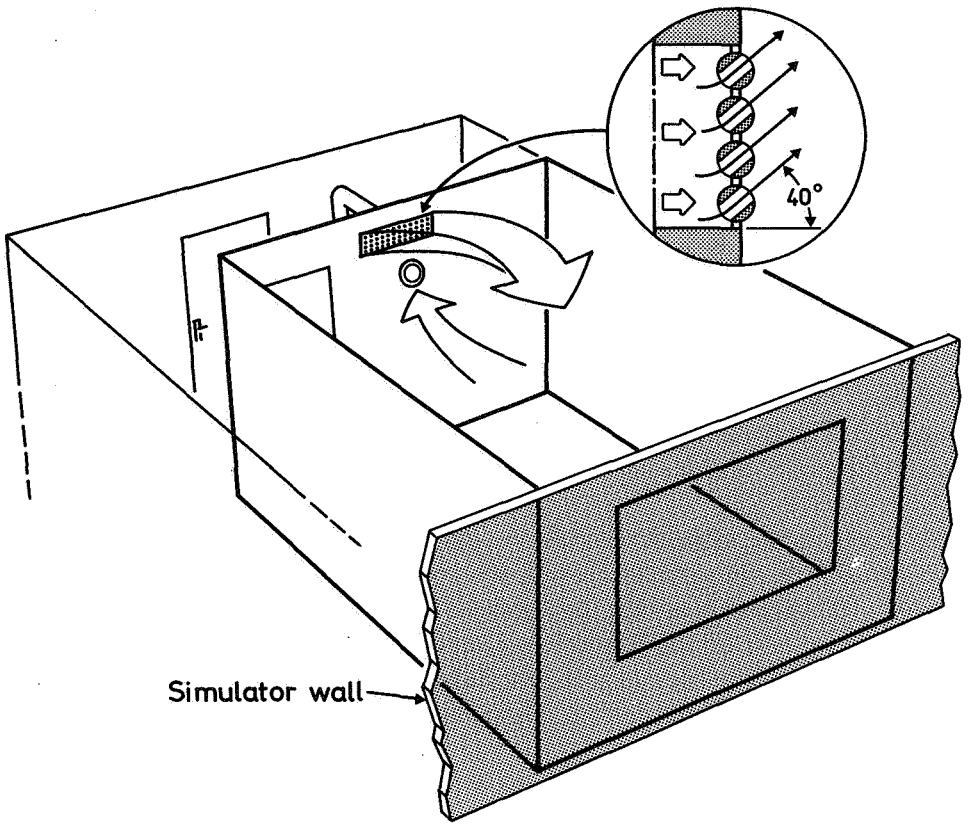

Figure 1 Test room

The supply air terminal consisted of a manifold of 84 small nozzles arranged in four rows and directed *upwards*. The total geometrical opening area A_s of all nozzles amounted to 0.0095 m^2 which gave a characteristic dimension $\sqrt{A_S}$ equal to 0.0975 m.

All velocities were recorded with a temperature compensated bridge (Dantec 56C14) provided with a hot flim probe (Dantec 55R76). The total number of samples collected at each measuring point amounted to 102 400. The sampling rate was 50 or 100 Hz which corresponds to a time of integration of 34 min and 17 min respectively. The signal was filtered at about 40 % of the sampling frequency.

The measurements were carried out in the vertical symmetry plane through the terminal. When the velocities were measured the anemometer was orientated perpendicular to the axis of the flow. All measurements were carried out at isothermal condition.

The experimental conditions are collected in table 1 below.

Table 1 *Listing of experimental parameters*

Flow rate (n) [room volumes/h]	Nominal supply velocity [m/s]	Re_d [1]
1.0	1.11	1 108
1.5	1.66	1 662
2.0	2.21	2 217
3.0	3.32	3 326
4.0	4.42	4 434
5.0	5.53	5 543
6.0	6.63	6 652

Nominal supply velocity is equal to the flow rate divided by the geometrical opening area. The discharge Reynolds number Re_d is based on nominal velocity and the diameter of the nozzle.

We see from the table that the Reynolds number is very low at the lower flow rates. Therefore one can surmise flow in the room to be Reynolds number dependant. Malmström (1974) has show that the spread of a jet to be Reynolds number dependent at those low values on the Reynolds number as one frequently encounters in ventilation engineering. In the literature the minimum Reynolds number for the flow to be Reynolds number independent is reported to lie around $Re_d \approx 10^4$.

Skovgaard et al (1990) recorded the effective area of the same terminal as ours and found the effective area to be Reynolds number dependant. The effective area did not bacome equal to the nominal area until $Re_d \approx 8\,000$.

3 Measurements carried out along the perimeter of the room

Mean velocity and the standard deviation

Fig. 2 shows the mean velocity and standard deviation recorded very close to one of the 84 nozzles of the terminal.

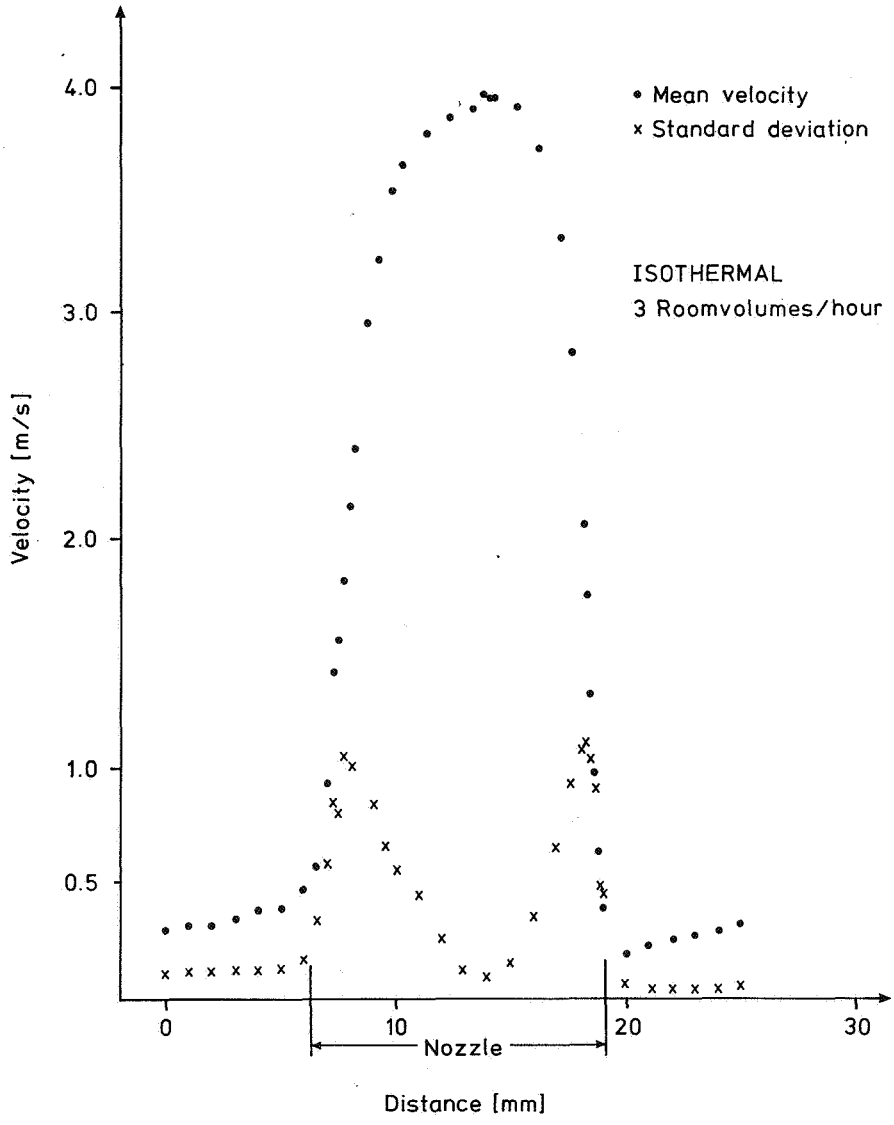

***Figure 2** Mean velocity and standard deviation close to a nozzle (n = 3 roomvol/h)*

The measurements shown in Fig. 2 were carried out in the development region of the jet and the maximum of the turbulence occurs at the center of the mixing region.

Fig. 3 shows the velocities recorded along the perimeter of the room in a vertical plane through the supply.

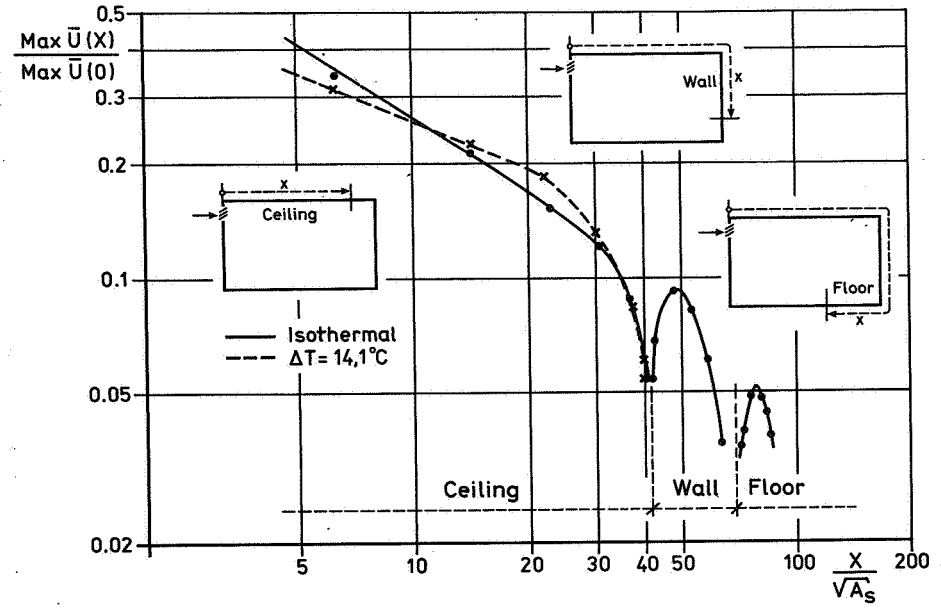

***Figure 3** Maximum mean velocity along the perimeter of the room (n = 3 roomvol/h)*

We see that we have a "short room" so the circulation in the room is set up by a wall jet that follows the perimeter of the room. Fig. 4 shows the maximum velocity in the jet as a function of the distance from the terminal. The data is given in non-dimensional form so the recorded velocity has been divided by the nominal velocity at the inlet and the distance from the outlet has been divided by the square-root of the free opening area.

When the air stream arrives at the opposite wall the velocities in the jet decrease and the thickness of the jet increases. The pressure increases at the wall and the flow is retarded and deflected downwards along the wall. The flow is at first accelerated by the higher pressure and a maximum velocity is attained. After this point the flow decelerates again. We see that the deceleration is now faster than that along the ceiling. At the lower corner the procedure is repeated again and the maximum velocity in the occupied zone is attained at same distance from the wall. The behaviour of the jet can be described as the jet restarting at each corner.

Waschke (1974) studied the effect of deflection of a radial wall jet that was supplied under the ceiling. He showed that the jet along the wall could be considered as a radial jet but now starting from a new virtual origin that did not coincide with the virtual origin of the ceiling jet.

The theory which is valid for flows in infinite or semi-infinite spaces where the ambient is quiescent, predicts that the velocity decay should follow the relation X^{-1}. However, the decay is less rapid and follows approximately the relation $X^{-0.62}$. The deviation from the theory must be due to the fact that the jet is supplied into a finite enclosure. It can be concluded from the measurements that the lateral expansion of the jet is not constrained by the sidewalls. One can surmise that the counterflow set up in the room slows down the decay of the maximum velocity. The jet is therefore expanding into an ambient that is moving. For a so called *weak jet* expanding into an ambient that moves (compound jet) in the same direction as the jet, the theory predicts that the the decay shall follow the relation

$X^{-2/3}$, see Rajartmam N. (1976). This is very close to our result. This may however be a mere coincidence since it is not clear if the theory for compound jets is applicable in this case were the jet itself that sets up the air motion. We can at least conclude that we do not expect theories valid for infinite spaces to be valid in enclosures.

Measurements reported by Skovgaard et al (1990) in the same room configuration and with the same type of terminals show a similar result.

Fig. 4 shows, as a function of flow rate, the maximum mean velocity at two stations. The first point is located under the ceiling 2.2 m from the supply air terminal whereas the second one is located where the maximum mean velocity did occur in the occupied space. The maximum velocity at the floor occurred, at all flow rates, 3.5 m from the backwall which corresponds to 0.7 m from the facade wall.

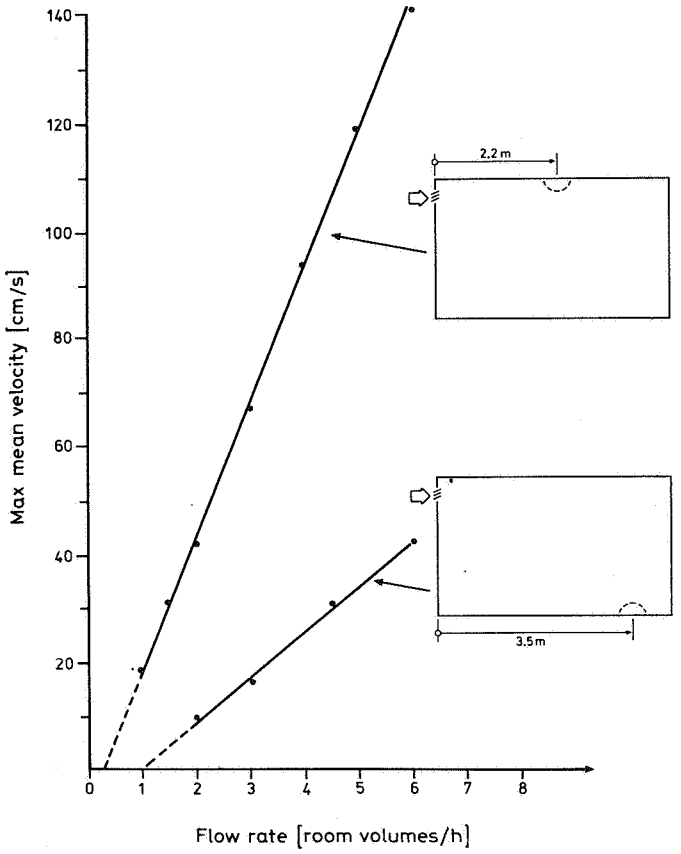

***Figure 4** Maximum mean velocity as a function of flow rate*

By extrapolating the fitted straight lines in Fig. 4 toward lower flow rates we see that they do not pass through the origin. The deviation is larger at the floor-level. This behaviour, that the room velocities at low flow rates are not proportional to the inlet velocities has earlier been documented by Nielsen P V (?).

Autocorrelation measurements and turbulence scales

The correlation of the same velocity component at a fixed point, x_0, is known as the autocorrelation. By definition, the normalized autocorrelation for the velocity fluctuations, u', is given by

$$R_{\Delta t}(x_0,\Delta t) = \frac{\overline{u'(x_0,t)u'(x_0,t+\Delta t)}}{\overline{u'^2}} \qquad (1)$$

Where Δt is the time separation. When the turbulent motion is occurring in a flow with a large mean velocity $\overline{U}$, it is possible for the turbulence to be advected past the point of measurement more rapidly than the pattern of fluctuation is changing. When this is the case the autocorrelation function with time separation Δt can be interpreted as a spatial correlation where separation in distance is equal to (Taylor's transformation):

$$\Delta x = -\overline{U}\Delta t \qquad (2)$$

The above assumption means that the transportation velocity for the turbulence is set approximately equal to the the average velocity, $\overline{U}$. We obtain

$$R_{\Delta x}(x_0,\Delta x) = R_{\Delta t}(x_0,\Delta t) \qquad (3)$$

From the autocorrelation measurements the *integral* scale, Λ_t, is obtained as

$$\Lambda_t = \int_0^\infty R_{\Delta t}(x_0,\Delta t)d(\Delta t) \qquad (4)$$

From our measurements the integral scale was calculated by taking the value on the time axis for which the normalized autocorrelation function had declined to e^{-1}, see Fig. 5. This integral-scale is denoted by Λ_t^e and Λ_x^e (see below).

The Taylor microscale λ_t is defined as:

$$\lambda_t = (2\overline{u'^2}/(\overline{\frac{\partial u'}{\partial t}})^2)^{1/2} \qquad (5)$$

The turbulence scales obtained from the measurements carried out at the same point have then been transformed to turbulence scales for spatial separation by multiplying by the average velocity:

$$\Lambda_x = \overline{U}\Lambda_t \quad \text{and} \quad \lambda_x = \overline{U}\lambda_t \qquad (6)$$

The above transformation can be regarded as purely formal because we can not take for granted that the Taylor hypothesis is strictly applicable to this type of flow since the relative turbulence intensity lies around 20-30 %, which is quite high.

The microscale λ_t has been obtained by fitting the to the parabola

$$1 - R_{\Delta t}(\Delta t) = \left(\frac{\Delta t}{\lambda_t}\right)^2 \tag{7a}$$

to the data close to $\Delta t=0$. This was done by using the equivalent relation

$$\ln(1 - R_{\Delta t}(\Delta t)) = 2\ln\left(\frac{\Delta t}{\lambda_t}\right) \tag{7b}$$

which was plotted in a graph. This method is not very accurate, there are better methods, however it gives the order of magnitude of the microscale.

The autocorrelation function, $R_{\Delta t}$, was recorded at the same point as the data presented in Fig. 3. The next figure shows the autocorrelation function whith a non-dimensional x-axis ($\frac{\Delta x}{x} = \frac{\overline{U}\Delta t}{x}$)

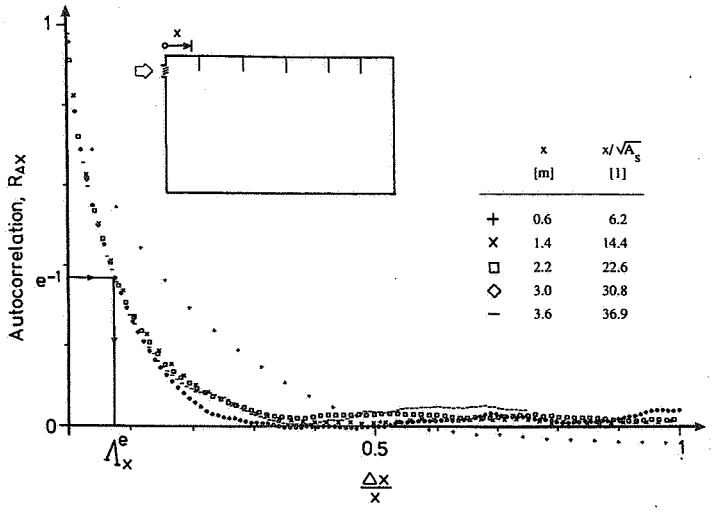

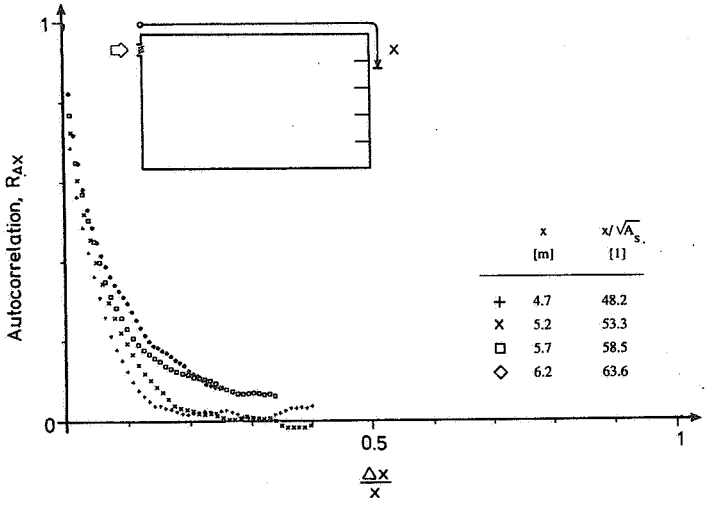

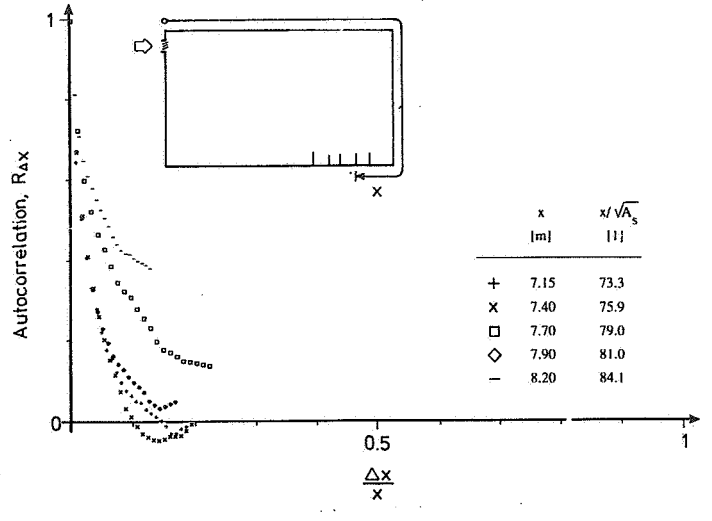

***Figure 5** Autocorrelation function on the jet centre-line. From above*
- *Ceiling*
- *Wall*
- *Floor*

It appears from Fig. 5 that under the ceiling (apart from close to the terminal) the curves collapse on the same line so the structure is self- preserving from ($x/\sqrt{A_s}$=14.4). The integral-scale for the expansion of the jet under the ceiling became, $\Lambda_x^e = 0.076x$. This value is within the range reported by others, see data compiled by Wygnanski & Fiedler (1969).

The autocorrelation functions for the first two measurement points on the wall differ from the function recorded under the ceiling. However, at the following two measuring points on the wall ($x/\sqrt{A_s}$ =58.5 and 63.6) the autocorrelation function does coincide reasonably well with that recorded under the ceiling.

When we come to the measuring points on the floor one can no longer trace any resemblance with the autocorrelation functions recorded further upstream. The behaviour is quite erratic.

The next figure shows the integralscale, Λ_x^e, at the same points as in Fig. 5.

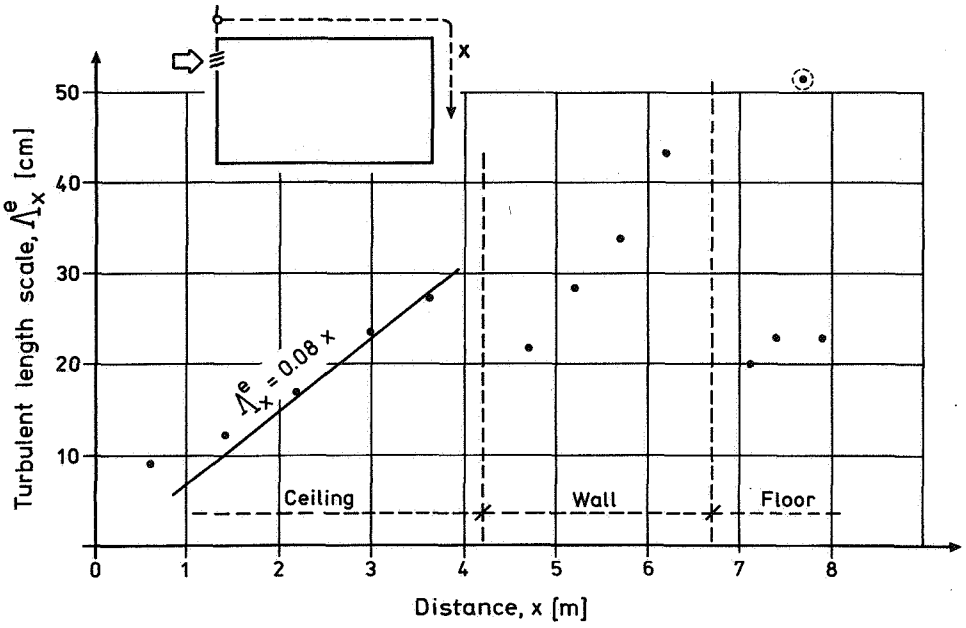

***Figure 6** Integralscale Λ_x^e on the jet centre-line*

Close to the terminal the integralscale is around 10 cm which, as expected, is a value close to the characteristic dimension of the terminal, $\sqrt{A_S}$= 9.8 cm. Also as expected the integralscale first grows linearly with distance from the supply air terminal. After the jet has been deflected at the corner ceiling wall the integral-scale again grows linearly but now "starts" from a lower value. The behaviour is repeated in the next corner. The behaviour of the integralscale along the floor is, however, more erratic.

Table 2 shows the Taylor microscale. The microscale could only be calculated when the velocity had decayed to around 20 cm/s. At higher velocities the sampling frequency, 50 Hz, was too low to resolve the autocorrelation function close to Δt=0.

Table 2 Taylor microscale and ratio between integral and micro scales

X [m]	$X/\sqrt{A_s}$ [1]	λ_x^e [cm]	$\frac{\Lambda_x^e}{\lambda_x^e}$	Location
5.7	58.7	4.7	7.2	Wall
6.2	63.6	5.2	8.3	Wall
7.15	73.3	3.6	5.7	Floor
7.40	75.9	4.1	5.6	Floor
7.70	79.0	5.9	8.9[1]	Floor
7.90	81.0	4.6	5.0	Floor

4 Measurements carried out at a fixed station

All the measurements reported in this subsection was recorded at ceiling level 2.2 m ($x/\sqrt{A_s}$ = 22.6) from the terminal.

Fig. 7 shows the mean velocity, turbulent fluctuation and the turbulent integral scale. The first two quantities have been scaled by the maximum mean velocity (max $\overline{U}$). In Fig. 7 $b_{1/2}$ denotes the half width of the jet.

1. This value is probably too large because the recorded integral-scale is too large, see Fig. 6 (indicated by a dashed circle).

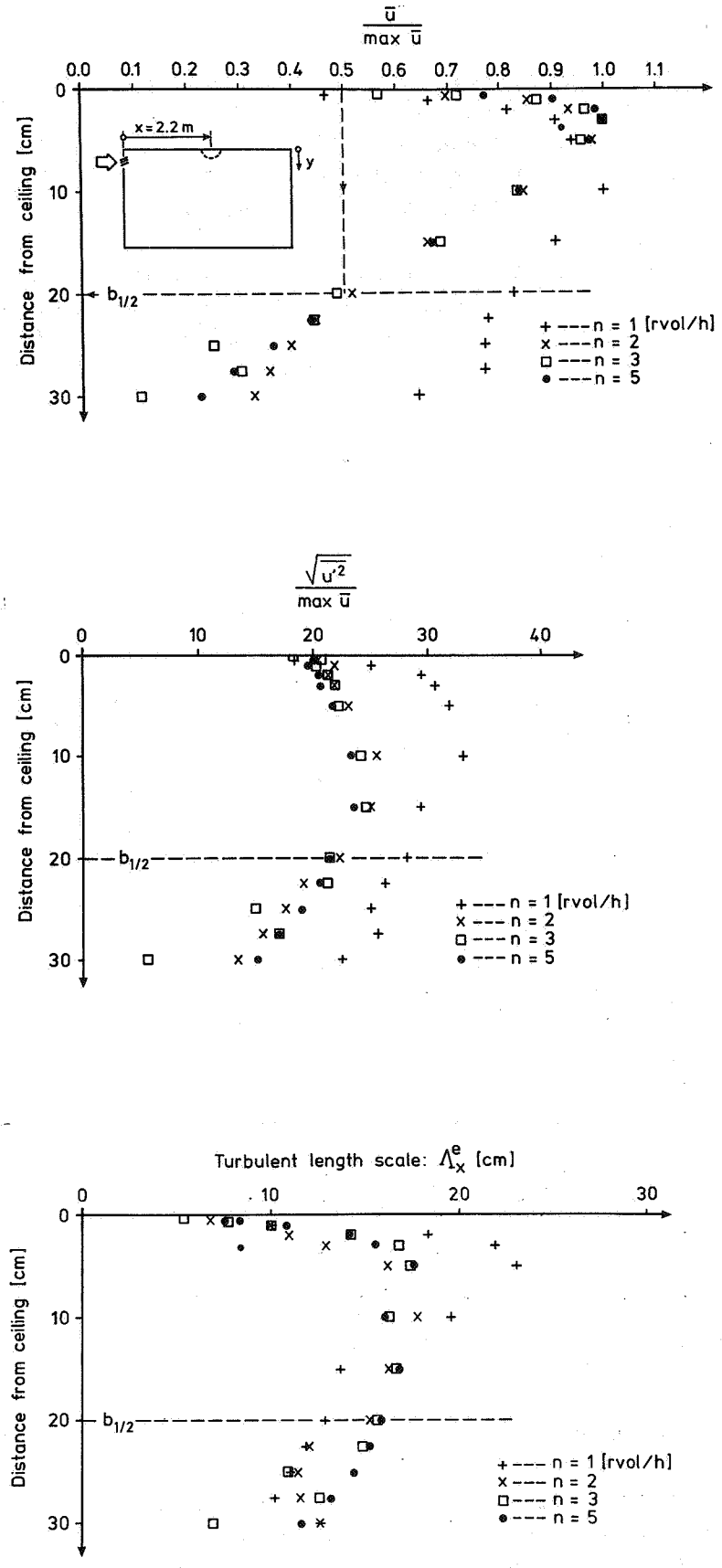

***Figure 7** Recorded distribution of:*

Streamwise mean velocity ($\bar{U}$)
Streamwise turbulent fluctuations ($\sqrt{\overline{u'^2}}$)
Streamwise integral length scale

It appears from Fig. 7 that the mean velocity and the turbulent fluctuations are independent of the flow rate from n = 2 room volumes/h (Re_d = 2 217). The turbulent length scale does not become independent of flow rate until n = 3 roomvolumes/h (Re_d = 3326). In the literature axisymmetric jets are said to be self-similar when $x/\sqrt{A_s} > 40$. The mean velocity fields become self-similar closer to the supply than the turbulent fluctuations that require a longer distance. We are closer than this value and we cannot therefore conclude that the jet behaves in a self-similar manner, although the shape of the distribution does not change with increasing flow rate. Fig. 8 shows the turbulent time scale, λ_t^e, recorded at the point where the maximum mean velocity occurs (around 30 mm under the ceiling).

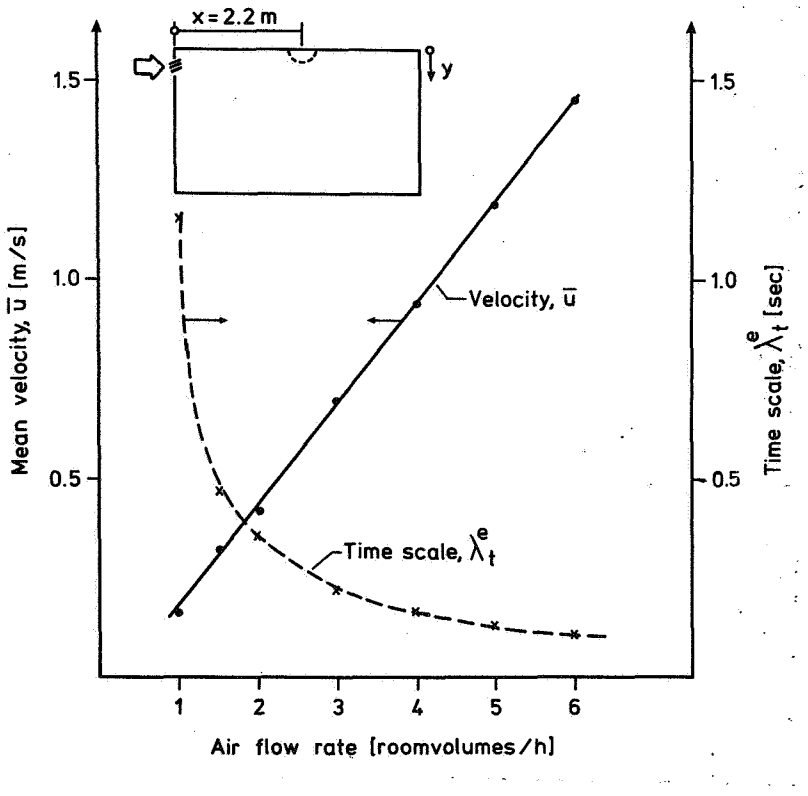

***Figure 8** Turbulent time scale, λ_t^e, as a function of the mean velocity*

As expected the time scale is inversely proportional to the velocity because the integral length scale, $\Lambda_x^e = \overline{U} \cdot \lambda_t^e$, is constant (in this case $\Lambda_x^e \approx 15$ cm)

Near wall measurements

The most important near wall velocity scale is the friction velocity $U_* = \sqrt{\frac{\tau}{\rho}}$. An attempt was made to record the shear stress, τ, at the room surface with a modified Preston Tube. However, this attempt failed because the velocity was too low for the calibration curve of the Preston Tube to be valid. This highlights the common problem when making velocity measurements in ventilated rooms, the velocities are so low that techniques developed within other areas are frequently not applicable.

The problem of recording velocities with hot-wire anemometers near surfaces is well known. Additional heat losses to the wall result in too high velocities. Therefore we used a computational technique described by Bhatia J C et al (1982) for correction of the recorded near surface velocity. The magnitude of the shear stress was obtained from the slope of a graph of velocity versus distance from the surface. The thickness parameter, l, ($l = \nu/U_*$) amounted to: n = 1.5 roomvol/h, l ≈ 0.5 mm: n = 3 roomvol/h, l ≈ 0.3 mm. Fig. 9 shows the near ceiling measurements presented in standard wall coordinates

$$(U^+ = \frac{\overline{U}}{U_*}, Y^+ = \frac{Y}{l})$$

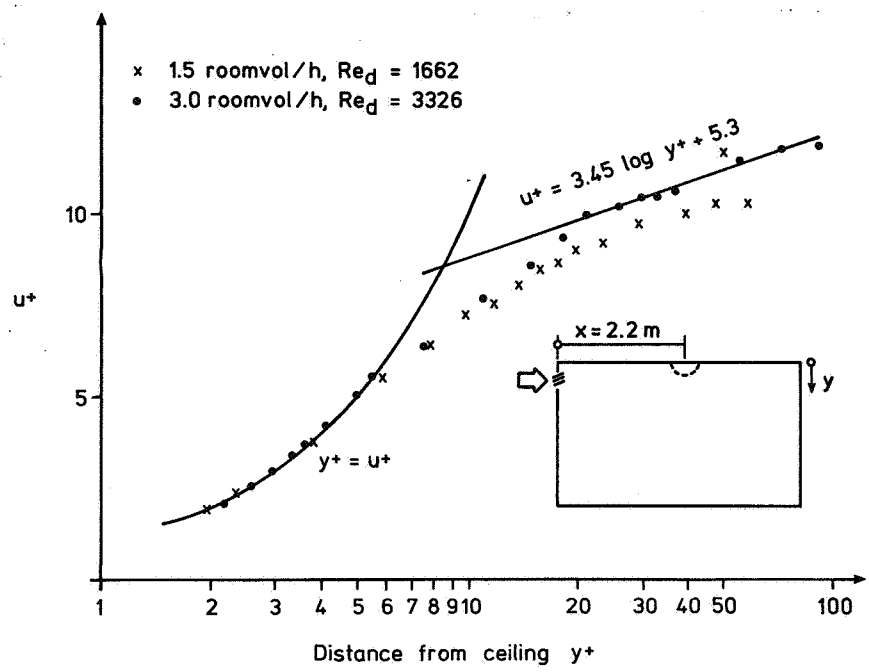

Figure 9 Wall function

It appears in Fig. 9 that the wall function is Reynolds number dependent which shows that the flow is in a transitional region. The coefficient in front of log y^+ was 3.45 in our measurements which is far from the "universally" adopted value of 5.5. This difference may be due to one or combination of the following factors:

- Error in the wall shear stress and subsequently U_*
- The curve fitted over a short region
- Developing flow

Fig. 10 shows the rms-value of the streamwise fluctuations scaled by the friction velocity.

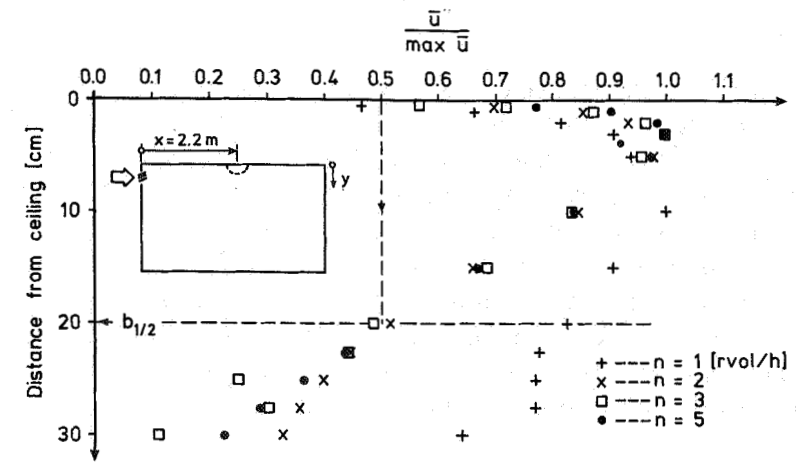

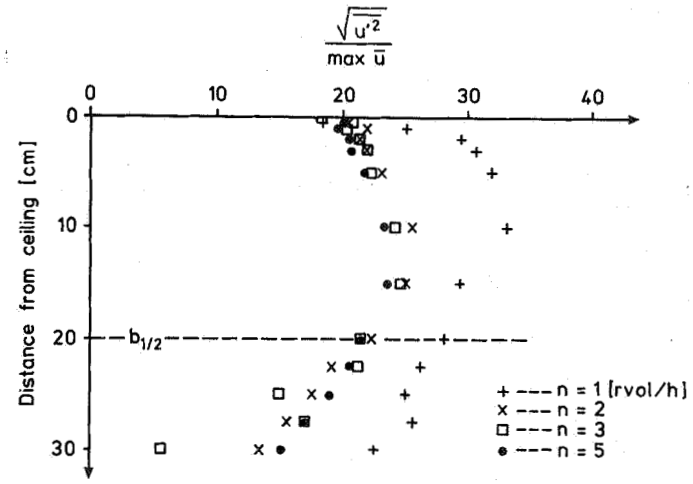

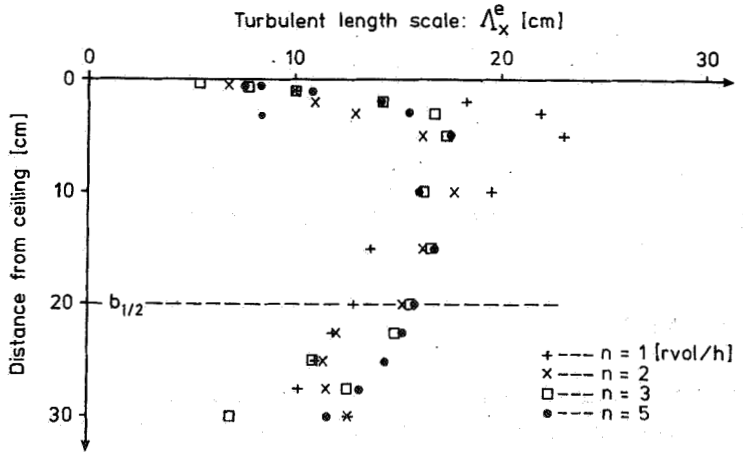

Figure 7 *Recorded distribution of:*

Streamwise mean velocity ($\bar{U}$)
Streamwise turbulent fluctuations ($\sqrt{\overline{u'^2}}$)
Streamwise integral length scale

We see that the relative turbulence intensity at the lower flow rates decreases with increasing flow rates. . This trend is probably a real effect whereas for flow rates higher than 3 roomvolumes per hour the scatter in data reflects uncertainties in the measurements. Finally Fig. 12 shows the turbulent length scale near the wall.

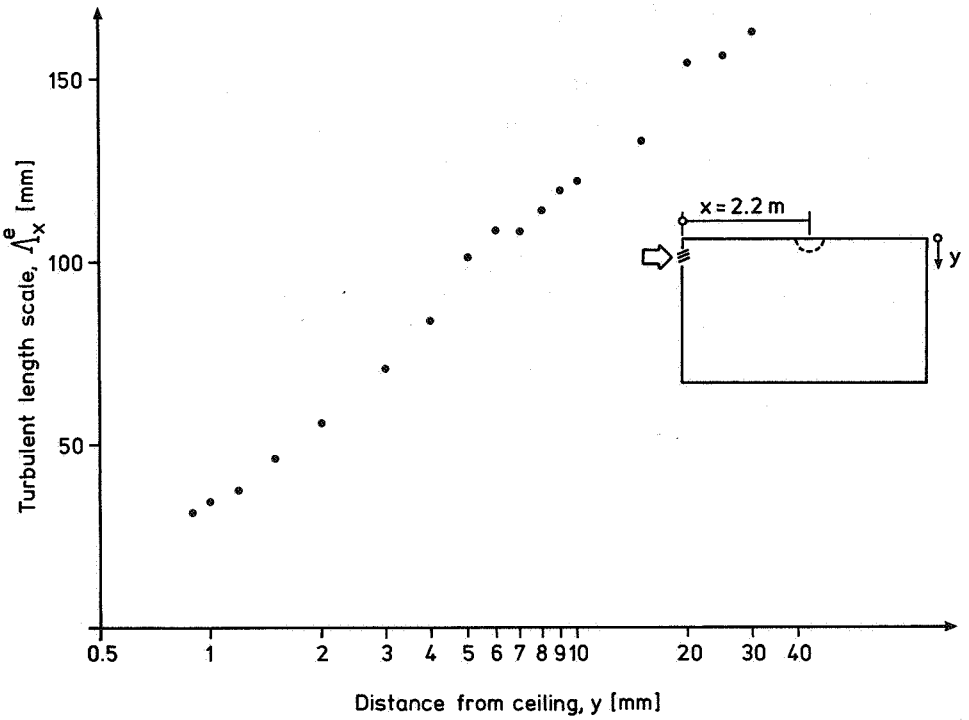

Figure 12 Turbulent length scale (n = 3 roomvolumes/h)

Conclusions

Measurements at a *fixed* station under the ceiling ($x/\sqrt{A_s} = 22.6$), carried out at different flow rates, showed that the streamwise mean velocity and turbulence intensities became independent of the discharge (based on the diameter of the nozzles) Reynolds number (Re_d) for $Re_d > 2\,200$. The corresponding specific flow rate was 2 roomvolumes/hour. The integral length scale became independent of the Reynolds number from $Re_d \approx 3\,300$ (flow rate, 3 roomvolumes/h).

Measurements *near the wall* showed that for $y^+ > 10$ both the mean velocity and the turbulent fluctuations were dependent on the Reynolds number.

Measurements carried out on the jet centre-line (location of max mean velocity) *along the perimeter* of the room (flow rate 3 roomvolumes/h, discharge Reynolds number 3326) showed;

- The *decay of the velocity* in the jet does not coincide with any "classical" formula for a jet in an infinite quiescent ambient

- The *turbulent length scale*, when *close to the terminal*, became equal to the characteristic dimension of the terminal

- Under the ceiling the *turbulent length scale*, Λ^{e}_{ex}, obeys the following relation with the distance, x, from the terminal, $\Lambda^{e}_{x} = 0.076x$

- The *turbulent length scale* became *in the occupied space* approximately twice the characteristic dimensions of the terminal

- The general behaviour of the jet, with regard to the decay of the mean velocity and expansion of the turbulent length scale, along the perimeter of the room can be described as that the jet "restarts" after it has decelerated and been deflected at a corner.

The general conclusions of the findings is that in the case where the jet is supplied into a finite ambient and in particular where the jet is constrained to change direction at room corners has a strong influence on jet behaviour. In order to be of any success at the design stage for assessing the velocities in the occupied space, this room influence must be considered in the testing procedures of supply air terminals.

References

BHATIA, J.C., DURST, F. and JOVANOVIC, J.
"Corrections of hot-wire measurements near wall"
J. Fluid Mech. Vol. **122**, 1982 pp. 411-431

GUTEMARK, E. and WYGNANSKI, I.
"The Planar Turbulent Jet"
J. Fluid Mech., Vol **73**, part 3, 1976, pp. 465 - 495

HANZAWA, H., MELIKOW, A.K. and FANGER, P.O.
"Airflow characteristics in the occupied zone of Ventilated Spaces"
ASHRAE Transactions, Vol **93**, 1987

HINZE, J.O.
"Turbulence, Second Edition"
McGraw - Hill, Inc, 1975

RAJARATNAM, N.
"Turbulent Jets"
Elsevier, 1976

KOVANEN, K., SEPPÄNEN, O., SIRÉN, K. and MAJANEN, A.
"Air velocity, Turbulence Intensity and Fluctuation Frequency in Ventilated Spaces"
Proceedings Roomvent'87, Session 4B, Stockholm, Sweden, 10-12 June 1987

LAUNDER, B.E. and RODI, W.
"The turbulent wall jet - measurements and modelling"
Ann. Rev. Fluid Mech. 1983, Vol **15**, pp 429-459

MALMSTRÖM, T.G.
"Om funktionen hos tilluftsgaller" (In Swedish)
Faibo Grafiska, Stockholm, 1974

SANDBERG, M.
"Velocity Characteristics in Mechanically Ventilated Office rooms"
Proceedings Roomvent-87. Session 2a, 10-12 June, 1987, Stockholm, Sweden

SKOVGAARD, M., HYLDGAARD, P.V, and NIELSEN
"High and Low Reynolds Number Measurements In a Room With An Impinging Isothermal Jet."
Proceedings Roomvent'90, Oslo, Norway, June 13-15, 1990

WASCHKE, G.
"Über die Lüftung mittels isothermer turbulenter radialer Deckenstralen"
Doktor-Ingenieurs Dissertation. Technische Hochschule Aachen, 1974

WYGNANSKI, I. and FIEDLER, H.
"Some measurements in the self-preserving jet"
J. Fluid Mech., Vol **38**, 1969, pp 577-612

AIR MOVEMENT & VENTILATION CONTROL WITHIN BUILDINGS

12th AIVC Conference, Ottawa, Canada
24-27 September, 1991

POSTER 10

SIMULATION OF THERMAL COUPLING BETWEEN A RADIATOR AND A ROOM WITH ZONAL MODELS

ABSTRACT

Zonal models are a promising way to predict air movement in a room with respect to comfort conditions and gradient of temperature, because they require extremely low computer time and may be therefore rather easily included in multizone air movement models.

The main objective of this paper is to study the ability of the zonal models to predict the thermal behaviour of air in case of natural convection coupled with a radiator.

First, we present simplified two zone and five zone models. With the support of the IEA Annex 20 (Air flow pattern within buildings) testcase, we compare the results of the models. Furthermore, a comparison is made with the results of Chen obtained with a Low Reynolds number k-E model.

It appears that five zone model give indoor air temperature profiles consistent with Low Reynolds number k-E model. Concerning the convective heat fluxes, except for the two zone model, the values computed by the models are of the same order of magnitude with lower values for the Low Reynolds k-E number model.

C.INARD[1], D.BUTY[2]

(1):CETHIL, INSA Bât. 307, 20 av.Albert Einstein, F.69621 Villeurbanne
(2):CSTB, 84 av.Jean Jaurès, BP 02, Champs/Marne, F.77421 Marne la Vallée Cedex 2

LIST OF SYMBOLS

Axx :area	(m^2)
Gau :enthalpy flow upper zone-central zone	(W/K)
Gla :enthalpy flow central zone-lower zone	(W/K)
Gpll :enthalpy flow lower zone-air leaving the radiator	(W/K)
Gppl :enthalpy flow air leaving the radiator-plume	(W/K)
Gup :enthalpy flow plume-upper zone	(W/K)
Lra :length of the radiator	(m)
Rxx :thermal resistance	(K/W)
Rxxc :convective thermal resistance	(K/W)
Rxxr :radiative thermal resistance	(K/W)
Txx :surface temperature	(°C)
Tl :mean air temperature of lower zone	(°C)
Tp :mean air temperature of radiator plume	(°C)
Tpl :mean air temperature leaving the radiator	(°C)
Troa :mean air temperature of central zone	(°C)
Tror :room radiant temperature	(°C)
Tu :mean air temperature of upper zone	(°C)
z_0 :virtual origin of radiator plume	(m)

Subscripts:

gl :glazing
wa :vertical walls
ce :ceiling
fl :floor
fa :facade
ra :radiator
tr :trail

1-INTRODUCTION

The present paper deals with different ways to model the thermal behaviour of a heated room with simplified zonal models. With the support of Annex 20 testcase d (natural convection with a radiator) and according to the monozone simulation procedure presented by Lemaire [1], we developed a two zone and a five zone models.

2-SPECIFICATION OF THE TESCASE

Figure 1 shows the thermal network of the testroom with a radiator.

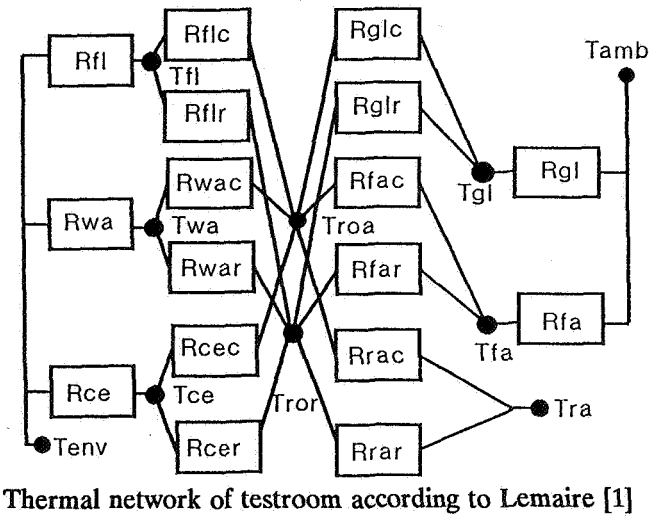

Fig. 1: Thermal network of testroom according to Lemaire [1]

The dimensions of the testroom are 4.2x3.6x2.5 m.
The configuration consists of:

- a window (single glazed) positioned in the front wall (facade) in contact with ambient temperature (Tamb)
- the other walls are in contact with environmental (plenum) temperature (Tenv)
- a radiator (single panel) located below the window in front of the front wall

The dimensions of the window and the radiator are 2.0x1.6m and 2.0x0.3m.
According to Lemaire [1], Table 1 gives the thermal resitances and area of the testroom walls.

	Axx (m^2)	Rxx (K/W)	Rxxc (K/W)	Rxxr (K/W)
Window	3.20	0.0150	0.0887	0.0656
Facade	5.80	0.5225	0.0718	0.0325
Walls	30.00	0.1010	0.0139	0.0063
Ceiling	15.12	0.2004	0.0275	0.0125
Floor	15.12	0.2004	0.0275	0.0125

Table 1: Area and thermal resistances of testroom walls

The radiator convective heat transfer coefficients are calculated using a Nusselt-Rayleigh relation of Kriegel quoted by [1]:

$$Nu = 0.118\ Ra^{1/3}$$

The radiator radiative heat transfer coefficients are computed using simplified Stefan-Boltzmann law for radiation between two surfaces:

$$hrar = \epsilon ra\ \sigma_0\ [(Tra^2 + Tror^2)(Tra + Tror)]$$

with: εra radiator LW emissivity
Furthermore, heat transfer coefficients between the radiator rear face and its backwall are computed assuming that the backwall is adiabatic. For more details see Lemaire [2].

Three cases with different radiator temperatures and ambient temperatures have been considered as can be seen in Table 2.

Case number	Tamb (°C)	Tra (°C)	Rrar (K/W)	Rrac (K/W)
d1	+6.0	46.0	0.2389	0.1424
d2	-0.9	55.0	0.2283	0.1290
d3	-8.0	65.0	0.2170	0.1190

Table 2: Key parameters of the three testcases (Tenv=20°C)

3-THE FIVE ZONE MODEL

3-1-Convective network

The indoor air volume is split into five zones coupled each other with air mass flow rates:
- air leaving the radiator (Tp1)
- thermal plume (Tp)
- upper zone (Tu)
- central zone (Troa)
- lower zone (Tl)

The convective network is shown in figure 2.

Comparing to the thermal network of Fig. 1, we add the trail which represents the opaque wall in contact with the thermal plume.

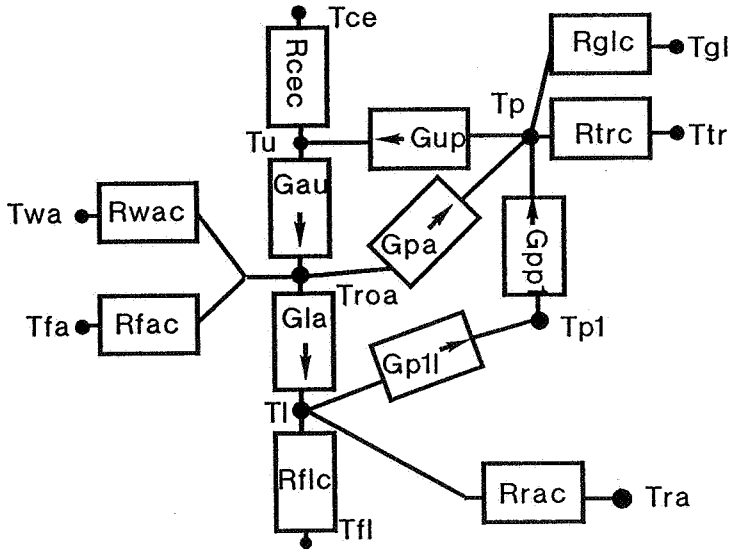

Figure 2: Convective network of testroom with five zones

3-2-Evaluation of enthalpy flows and air temperatures

The convective resistance values are the same than those prescribed in Tables 1 and 2. The trail convective heat transfer coefficient value is the same than the window one (3.52 W/m²K).

From the expression of air mass flow rate in the plume of the radiators [3] and assuming that the radiator is located at 0.1m from the floor, we write:

$$Gpp1 = 9.10^{-3} Cp \left[\left(\frac{Tra-Tl)}{Rrac} \right) / Lra \right]^{1/3} (Hra+0.1-z_0)\, Lra$$

$$Gup = 9.10^{-3} \left[\left(\frac{Tra-Tl}{Rrac} - \frac{Tp-Tgl}{Rglc} - \frac{Tp-Ttr}{Rtrc} \right) / Lra \right]^{1/3} (Height-z_0)\, Lra$$

Then, mass balance equations give:

Gpa = Gup - Gpp1 (1)
Gau = Gup (2)
Gla = Gau - Gpa (3)
Gp1l = Gla (4)

Zone energy balance equations allow us to calculate air temperatures:

Gp1l(Tp1 - Tl) = (Tra - Tl)/Rrac (5)
Gpp1(Tp - Tp1) + Gpa(Tp - Troa) + (Tp - Ttr)/Rtrc + (Tp - Tgl)/Rglc = 0 (6)
Gup(Tu - Tp) + (Tu - Tce)/Rcec = 0 (7)
Gau(Troa - Tu) + (Troa - Twa)/Rwac + (Troa - Tfa)/Rfac = 0 (8)
Gla(Tl - Troa) + (Tl - Tfl)/Rflc = 0 (9)

Because Gpp1 and Gup also depend on Troa and Tp, the calculation must be performed iteratively.

At last, using surface and radiant energy balance we compute surface temperatures and room radiant temperature (Tror).

4-THE TWO ZONE MODEL

In this model, the convective scheme is based on the studies made by A.T.Howarth [4]. The room is divided into two zones, an upper one and a lower one, separated by a neutral plane, accross which the net vertical air mass flow rate is equal to zero.

The main difference with the five zone model is that the plume behaviour is entirely described by only one equation. This equation is a thermal balance for the upper zone, the central zone and the thermal plume of the five zone model. In fact, the two zone model is a simplification of the five zone model.

4-1-Conductive and radiative model

The Howarth's formulation only deals with convective heat fluxes modelling. In order to compare with the model elaborated by Lemaire and with the five zone model, it was necessary to couple this convective formulation with a conductive and a radiative network. For the good homogeneity of this comparison, we choose to adopt the conductive and radiative scheme described by Lemaire.

As in the five zone model, the test chamber is divided into:

- the vertical walls (except the facade)
- the ceiling
- the floor
- the window
- the facade
- the trail

The radiant heat transfers are modelled through heat transfer coefficients calculated with simplified Stefan-Boltzmann law (see Tables 1 and 2).

4-2-Convective model

As a result of the splitting of the room air volume, the unknown temperatures are:

- mean air leaving the radiator (Tp1)
- upper zone mean air temperature (Tu)
- lower zone mean air temperature (Tl)
- average air temperature of the room (Troa)

In order to determine these temperatures, there must be four equations to close the system. The first equation is a balance equation between the convective heat output of the radiator and the convective heat losses at the surfaces.

The heat flow ϕconvwa from the core of the room to the walls and the part of the facade which is not located into the plume is calculated according to the correlation of De Graaf and Van der Held quoted by [5]:

$$\phi convwa = 0.729\ (Twa - Troa)^{1.36} Height^{0.08} \qquad (W/m^2)$$

The heat transfer coefficient at the floor is taken equal to 1 W/m^2K, which is consistent with the correlations presented by many authors. According to Table 1, the window convective heat transfer coefficient is taken equal to 3.52 W/m^2K and for the ceiling we adopt the value 2.40 W/m^2K.

The average air temperature is calculated as a mean value over the height:

$$Troa\ Height = Tl\ zneut + Tu\ (Height - zneut)$$

zneut is the height of the neutral plane. This altitude is calculated assuming the uprising mass flow rate in the plume to be equal to the downward mass flow rate in the boundary cold layers along the wall. The plume mass flow rate is computed by the correlation established by Inard [3] from experiments:

$$Gpp1 = 9.10^{-3} Cp \left[\frac{(Tra-Tl)}{Rrac} / Lra\right]^{1/3} (Hra+0.1-z_0)\, Lra$$

and the mass flow rate mwa in the boundary layers due to natural convection along the walls is expressed in the form [5]:

$$mwa = 0.00145(Troa-Twa)^{0.36}Height^{0.08} \qquad (Kg/ms)$$

The third equation gives the departure temperature of the plume leaving the radiator (eq.5):

$$Gpp1\ (Tp1-Tl) = (Tra-Tl)/Rrac$$

The last equation assumes that the radiator plume is discharged almost immediatly in the upper region. Thus, this zone is in equilibrium at the departing plume temperature modified by heat losses to the glazing, the ceiling and the trail.

We get this equation from five zone model balance equations (eq.1, 6 and 7) and assuming that Tp=Tp1 and Troa=Tu:

$$Gpp1(Tu-Tp1) + \frac{(Tp1-Tgl)}{Rglc} + \frac{(Tu-Tce)}{Rcec} + \frac{(Tp1-Ttr)}{Rtrc} = 0$$

This is the main simplification of the five zone model into a two zone model.

5-RESULTS

5-1-Air temperature profiles

Figure 3 show air temperature profiles computed with the different models. Concerning the two zone and the five zone models, we have arbitrarily located the upper and lower temperatures at 0.10m from the ceiling and the floor, and the central zone temperature at mid height of the cell. Furthermore, we superimposed on these figures the results computed by Chen [6] with a Low Reynolds k-E model.

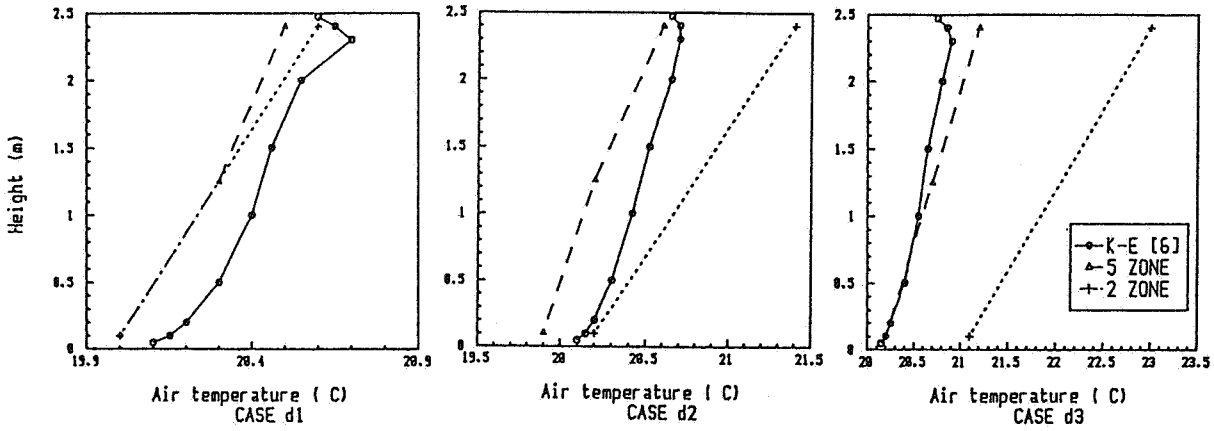

Figure 3: Air temperature profiles

These figures show that air temperature profiles computed with a five zone model and a Low Reynolds k-E number model are very close each other. Concerning the results calculated with the two zone model, we can see that the gap with the others air temperature profiles increase when ambient temperature decrease. In fact, using mean air temperature leaving the radiator instead of plume air temperature for window convective heat flux calculation results in higher values of air temperature leaving the radiator and upper zone air temperature for a given radiator air mass flow.

5-2-Convective heat exchanges

Table 3 shows the convective heat fluxes exchanged between the radiator and the walls of the testroom.

The convective heat fluxes calculated by the five zone model and Chen [6] are of the same order of magnitude though those computed with a Low Reynolds k-E number model are lower with a maximum gap for the radiator convective heat power of 24% (case d3). Note that for Chen's simulation

the boundary conditions are the inside surface temperatures of the walls.

Concerning the results computed with a two zone model and for the same reason raised in section 5-1, we obtain higher convective heat fluxes values.

case d1	two zone model	five zone model	k-E model [6]
window	-209	-120	-108
walls	-63	-63	-48
radiator	272	183	156
case d2	two zone model	five zone model	k-E model [6]
window	-296	-178	-162
walls	-111	-94	-55
radiator	407	272	217
case d3	two zone model	five zone model	k-E model [6]
window	-391	-241	-217
walls	-172	-136	-71
radiator	563	377	288

Table 3: Convective heat fluxes (W)

6-CONCLUSION

We built up two simplified zonal models in order to describe the thermal behaviour of a room heated with a radiator. With the support of the Annex 20 testcase d, we compared the air temperatures and convective heat fluxes calculated. Furthermore, the results are also compared with those computed with a Low Reynolds number k-E model [6].

The simplified five zone model give results consistent with k-E model and the simplified two zone model give higher air temperatures and convective heat fluxes.

REFERENCES

[1] A.D. Lemaire
Specification of testcase d (free convection with radiator)
IEA, Annex 20 work report, 1989, R.I. n°1.15

[2] A.D. Lemaire
Modelling of boundary conditions near the radiator
IEA, Annex 20 work report, 1989, R.I. n°1.12

[3] C. Inard
Contribution à l'étude du couplage thermique entre une source de chaleur et un local
Thèse Doct.: INSA de Lyon, 1988

[4] A.T. Howarth
Temperature distribution and air movements in rooms heated with a convective heat source
PhD Doct.: University of Manchester, 1980

[5] I.L. Balemans
Review of correlations for convection heat transfer from flat surfaces in air
Chaleur et Climats, n°9, 1987

[6] Q. Chen
Simulation of testcase d (free convection with radiator)
IEA, Annex 20 work report, 1990, R.I. n°1.21

AIR MOVEMENT & VENTILATION CONTROL WITHIN BUILDINGS

12th AIVC Conference, Ottawa, Canada
24-27 September, 1991

POSTER 11

PREHEATING AND COOLING OF THE INCOMING AIR OF DWELLINGS USING AN EARTH-LAID PIPE

UNIV.-PROF. H. TRÜMPER, DIPL.-ING. K.-J. ALBERS

Universität Dortmund (FRG)
Fachbereich Bauwesen
Fachgebiet Technische Gebäudeausrüstung
Postfach 50 05 00
August-Schmidt-Straße 6
W-4600 Dortmund 50

Synopsis

The present work is an investigation of ground heat exchangers for the air-conditioning of the supply air to residential buildings. To this end, an analytical approximate solution for the temperature field of the ground in which a ground pipe has been laid is derived. This analytical approximate solution is applicable to a free-lying ground heat exchanger consisting of a single ground pipe. Extensions of this solution enable calculations for ground heat exchangers which are laid around a house, or which consist of several ground pipes connected in parallel.

The analytical approximate solutions form the basis for the derivation of basic principles for the design of ground heat exchangers. The freely-variable parameters which have the greatest influence on the heat output of the ground heat exchanger are the depth of installation and the length of the ground pipe.

As far as the maximisation of the annual heating and cooling yield of the ground heat exchanger is concerned, there exists an optimum installation depth which is determined by the thermal properties of the ground. The length of the ground heat exchanger is determined by the requirement that the air supply temperature at the end of the ground pipe must always exceed 0°C, even when the outdoor air temperature is extremely low. This prevents possible icing-up of the subsequent plate heat exchanger on the exhaust side.

The theoretical investigations are completed by measurements made during one year on a ground heat exchanger installed at a single-family dwelling.

List of symbols

a, a_E	$[m^2/s]$	thermal diffusivity
B_0	[m]	influence breadth
$c_{p,L}$	[kJ/(kg*K)]	specific heat capacity of the air at constant pressure
d_R	[m]	diameter of the ground pipe
k_l	[W/(m*K)]	overall heat transfer coefficient of the ground pipe per unit of length
k_{KW}	$[W/(m^2*K)]$	overall heat transfer coefficient of the cellar wall
$\dot{Q}_{EWT}$	[W]	heating or cooling power of the ground pipe
R_0	[m]	radius of the ground pipe
S_0	[m]	installation depth of the ground pipe
t	[s]	time
t_0	[s]	periodic time
$\dot{V}, \dot{V}_L$	$[m^3/s]$	volume flow of air
x	[m]	course
y	[m]	course
Δz	[m]	unit of length
α	$[W/(m^2*K)]$	convective heat transfer coefficient of the ground pipe
ϑ_A	[°C]	outdoor air temperature
ϑ_E	[°C]	earth temperature
$\vartheta_{E,a}$	[°C]	non-stationary component of the earth temperature

$\vartheta_{E,m}$	[°C]	stationary component of the earth temperature
$\vartheta_{E,O}$	[°C]	temperature at the surface of the earth
$\vartheta_{E,O,m}$	[°C]	stationary component of the temperature at the surface of the earth
$\vartheta_{E,R}$	[°C]	temperature at the surface of the pipe
$\vartheta_{E,R,a}$	[°C]	non-stationary component of the temperature at the surface of the pipe
$\vartheta_{E,R,m}$	[°C]	stationary component of the temperature at the surface of the pipe
ϑ_{Erd}	[°C]	temperature of the earth without ground pipe
$\Delta\vartheta_{Erd}$	[°C]	change of the temperature of the earth without ground pipe
ϑ_{K}	[°C]	temperature of the cellar
ϑ_{L}	[°C]	air temperature
$\vartheta_{L,R,A}$	[°C]	air temperature at the beginning of the ground pipe
$\vartheta_{L,R,E}$	[°C]	air temperature at the end of the ground pipe
ϑ_{m}	[°C]	mean value of the outdoor air temperature
ϑ_{max}	[°C]	maximum value of the outdoor air temperature
ϑ_{W}	[°C]	temperature of the cellar wall
λ_{E}	[W/(m*K)]	thermal conductivity of the earth
ρ_{L}	[kg/m^3]	density of the air

Introduction

In today's low-energy houses, the high degree of thermal insulation has reduced the transmitted heat requirement of buildings to such an extent that the ventilation heat requirement is becoming increasingly significant.

An important step in reducing ventilation heat losses is the installation of mechanical ventilation with heat recovery. The heat recovery unit consists of a plate heat exchanger, an air/air small heat pump or, as described in /1/, a plate heat exchanger followed by an air/air small heat pump.

A further method of reducing ventilation heat losses is the installation of a ground heat exchanger. In winter, the thermal energy stored in the ground is thus employed for pre-heating the outdoor air. This thermal energy is provided entirely by stored solar energy, since in the upper levels of the earth the geothermal heat flux is insignificant. According to Eckert /2/, this can be neglected down to a depth of 100 m. Schick /3/ indicates a value of 1.5 $\mu cal/(cm^2*sec)$ (= 0.063 W/m^2) for the mean specific geothermal heat flux in the upper layers of the earth. Erdösi /4/ gives a value of 0.025 - 0.084 W/m^2 for this heat flux. In contrast, the mean annual value of the average radiation density of sunlight in the western Länder of the Federal Republic of Germany is 114 W/m^2 /5/.

The introduction of a ground heat exchanger improves not only the heat yield but also the operational reliability of the heat-recovery unit described above. In winter, outdoor temperatures significantly lower than 0°C result in icing of the plate heat exchanger on the exhaust side. When a suitably-dimensioned ground heat exchanger is introduced,

the supply air temperature in the plate heat exchanger is never less than 0°C, even when the outdoor air temperature is extremely low. Icing of the plate heat exchanger is thus prevented. Furthermore, the raised supply air temperature results in shortened thaw times in the evaporator of the air/air heat pump.

In summer, the low earth temperature is used for partial cooling of the outdoor air. Since the temperature falls below the dew point at the walls of the ground pipe, condensation results, which partially dries the outdoor air. This process is not to be underestimated from the point of view of comfort, since supply air which is cooler and drier than the outdoor air is subjectively very pleasant in summer. The expressions "partial cooling" and "partial drying" emphasise that the cooling and drying capacities of the ground heat exchanger are smaller than those of conventional air-conditioning equipment, and that it is in no way possible to achieve a defined indoor climate with the aid of the ground heat exchanger alone.

Theoretical Principles

In order to design ground heat exchangers in the simplest possible way, an analytical solution of the ground temperature field for the case of a pipe laid in the ground is derived. Use is made of published partial solutions. Krischer /6/ first made use of the heat-source method and of conformal mapping in order to derive the following equation for the stationary-state ground temperature field of a pipe laid in the ground.

$$\vartheta_E(x,y) = \vartheta_{E,O} - (\vartheta_{E,R} - \vartheta_{E,O}) \cdot \frac{\ln\left(\frac{r_1}{r_2}\right)}{\ln\left(\frac{S_0}{R_0} + \sqrt{\left(\frac{S_0}{R_0}\right)^2 - 1}\right)}$$

$$\text{where: } r_1 = \sqrt{\left(x - \sqrt{S_0^2 - R_0^2}\right)^2 + y^2} \quad ;$$

$$r_2 = \sqrt{\left(x + \sqrt{S_0^2 - R_0^2}\right)^2 + y^2} \qquad (1)$$

The consideration of the monthly mean outdoor temperature reveals that the annual temperature variation, as seen in Fig. 1, is very well represented by a cosine oscillation of the form

$$\vartheta_L = \vartheta_m + (\vartheta_{max} - \vartheta_m) \cdot \cos\left(2\pi \frac{t}{t_0}\right) \qquad (2)$$

For this boundary condition, Grigull and Sandner /7/ made use of the Laplace transformation of the steady state (periodic steady state) to derive a solution for the one-dimensional, non-stationary differential equation for the ground in the absence of the pipe. The assumption of an infinitely large heat interface at the surface of the earth, which is justifiable according to von Cube /8/, results in simplification to

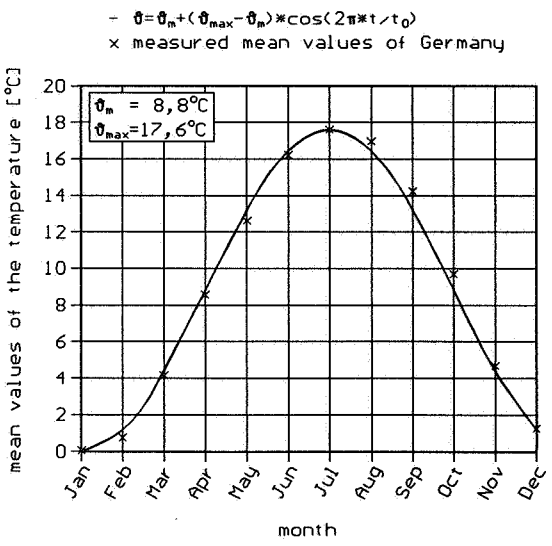

Fig. 1 Course of the outdoor temperature

$$\vartheta_E(x,t) = \vartheta_m + (\vartheta_{max} - \vartheta_m) \cdot e^{-\xi} \cdot \cos(p \cdot t - \xi)$$

$$\text{where:} \quad p = \frac{2\pi}{t_0} \quad ; \quad \xi = x \cdot \sqrt{\frac{\pi}{a \cdot t_0}} \tag{3}$$

Since the differential equation for thermal conduction is a linear, partial differential equation, the superposition principle may be employed. This states that partial solutions of linear, ordinary or partial differential equations may be added.

On the basis of this superposition principle, the following equation is derived in /9/ with the aid of equations 1 and 3 for the non-stationary ground temperature field in the presence of a pipe laid in the ground.

$$\vartheta_E(x,y,t) = \vartheta_{E,O,m} - (\vartheta_{E,R,m} - \vartheta_{E,O,m}) \cdot \frac{\ln\left(\frac{r_1}{r_2}\right)}{\ln\left(\frac{S_0}{R_0} + \sqrt{\left(\frac{S_0}{R_0}\right)^2 - 1}\right)} +$$

$$+ (\vartheta_{max} - \vartheta_m) \cdot e^{-\xi} \cdot \cos(p \cdot t - \xi)$$

$$:= \vartheta_{E,m} + \vartheta_{E,a}$$

$$\text{where: } p = \frac{2\pi}{t_0} \quad ; \quad \xi = x \cdot \sqrt{\frac{\pi}{a \cdot t_0}} \quad ;$$

$$r_1 = \sqrt{\left(x - \sqrt{S_0^2 - R_0^2}\right)^2 + y^2} \quad ;$$

$$r_2 = \sqrt{\left(x + \sqrt{S_0^2 - R_0^2}\right)^2 + y^2} \quad ; \quad \vartheta_{E,O,m} \equiv \vartheta_m \tag{4}$$

The stationary component of the temperature in the ground at the ground pipe $\vartheta_{E,R,m}$ is then

$$\vartheta_{E,R,m} = \frac{k^* \cdot \vartheta_{E,O,m} + \vartheta_{L,R} - \vartheta_{E,R,a}}{k^* + 1}$$

where: $$k^* = 2\pi \frac{\lambda_E}{k_1} \cdot \frac{1}{\ln\left(\frac{S_0}{R_0} + \sqrt{\left(\frac{S_0}{R_0}\right)^2 - 1} \right)} \qquad (5)$$

The thermal balance for a pipe element of length Δz yields the following equation for the air temperature at the end of the pipe element /9/:

$$\vartheta_{L,R,E} = \frac{\rho_L \cdot \dot{V} \cdot c_{p,L} \cdot \vartheta_{L,R,A} + \Delta z \cdot k_1 \cdot \left(\vartheta_{E,R} - \frac{1}{2} \cdot \vartheta_{L,R,A} \right)}{\rho_L \cdot \dot{V} \cdot c_{p,L} + \frac{1}{2} \Delta z \cdot k_1} \qquad (6)$$

The temperature of the earth at the pipe $\vartheta_{E,R}$ is calculated here as follows:

$$\vartheta_{E,R} = \frac{k^* \cdot \vartheta_{Erd,R} + \vartheta_{L,R}}{k^* + 1}$$

where: $$k^* = 2\pi \frac{\lambda_E}{k_1} \cdot \frac{1}{\ln\left(\frac{S_0}{R_0} + \sqrt{\left(\frac{S_0}{R_0}\right)^2 - 1} \right)} \qquad (7)$$

The air temperature which results at the end of a ground pipe of length l is found by (l/Δz)fold application of Equation 6. The sensible heat yield or cooling effect of the ground pipe is given by

$$\dot{Q}_{EWT} = \rho_L \cdot \dot{V} \cdot c_{p,L} \cdot \left(\vartheta_{L,R,E} - \vartheta_{L,R,A} \right) \qquad (8)$$

If, in summer, the temperature in the pipe falls below the dew-point, resulting in the condensation of water-vapour, the total (sensible + latent) cooling output of the ground pipe is given by the difference in enthalpy of the air before and after the ground pipe. The absolute air humidity at the end of the ground pipe is calculated from the water balance of the ground pipe with the aid of the analogy between heat and mass exchange /10/.

The temperatures $\vartheta_{E,R,m}$ (Eqn. 5) and $\vartheta_{E,R}$ (Eqn. 6) have the character of stationary temperatures, even though they are calculated from two non-stationary temperatures. The reason is that, according to the differential equation for the non-stationary temperature field, non-stationary temperatures are a function only of the thermal diffusivity but not of the thermal conductivity. These equations are therefore described as an approximate solution. In the present case, in which monthly mean values of temperature are considered, the temperature changes are small and the time intervals are large, so that the approximate solution is an excellent one.

Fig. 2 shows the earth temperature field which, according to Eqn. 4, results in winter (month: January) at the centre of a 42 m long ground pipe laid at a depth of 3 m. Average values for western Germany of earth parameters and of the course of the outdoor temperature were employed. The volume flow was 140 m^3/h. Inspection of the temperature field near to the ground pipe and consideration of the fact that, according to Ottel /11/,

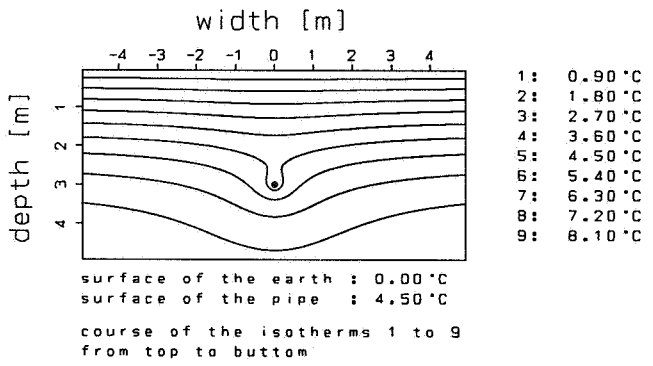

Fig. 2 Earth temperature field

the temperature in the ground at a distance of 2 m from the house is 2-3 K higher than that of the unperturbed ground reveal that the capacities of ground heat exchangers laid around the house are strongly influenced by the house itself.

In order to include the influence of the cellar wall in the analytical approximate solution, the following equation for the temperature increase $\Delta\vartheta_{Erd}$ of the unperturbed ground at a distance y_W from the cellar wall is derived in /9/.

$$\Delta\vartheta_{Erd} = (\vartheta_W - \vartheta_{Erd}) \cdot e^{-\xi_W}$$

$$\text{where: } \xi_W = y_W \cdot \sqrt{\frac{\pi}{a \cdot t_0}} \qquad (9)$$

The temperature at the outer face of the cellar wall ϑ_W is calculated from the 1-dimensional energy balance of the cellar wall, and is:

$$\vartheta_W = \frac{\vartheta_K + k_K^* \cdot \vartheta_{Erd}}{1 + k_K^*}$$

$$\text{where: } k_K^* = \frac{\lambda_E}{k_{KW}} \cdot \sqrt{\frac{\pi}{a \cdot t_0}} \qquad (9a)$$

ϑ_K is here the room temperature of the cellar and k_{KW} is the overall heat transfer coefficient of the cellar wall.

If, in Eqn. 7 for the calculation of the ground temperature at the ground pipe $\vartheta_{E,R}$, the temperature of the unperturbed ground $\vartheta_{Erd,R}$ is replaced by the new 'unperturbed' ground

temperature $\vartheta_{Erd,R,n} = \vartheta_{Erd,R} + \Delta\vartheta_{Erd}$, the influence of the cellar wall is now taken into account.

If, for the ventilation of buildings larger than single-family dwellings, the ground heat exchanger is planned to consist of not one, but of many ground pipes connected in parallel, so-called pipe banks, it must be taken into consideration that the heat output of the individual ground pipes is influenced by their relative positions. In order to determine this influence, /9/ introduces the so-called influence breadth B_0, for which the following relationship is derived. B_0 is here made dimensionless relative to the depth of the ground pipe S_0.

$$B_0^* = \frac{B_0}{S_0} = \frac{2\pi}{\ln\left(S_0^* + \sqrt{S_0^{*2} - 1}\right)}$$

$$\text{where: } S_0^* = \frac{S_0}{R_0} \qquad (10)$$

Eqn. 10 is evaluated graphically in Fig. 3. The ratio of the actual pipe separation to the influence breadth B_0 is a measure of the reduction of the heat and cooling output of the individual pipe in the bank relative to that of the free-lying single ground pipe. This provides a resource with whose aid the analytical approximate solution for the single ground pipe forms the basis for the approximate calculation of the heat

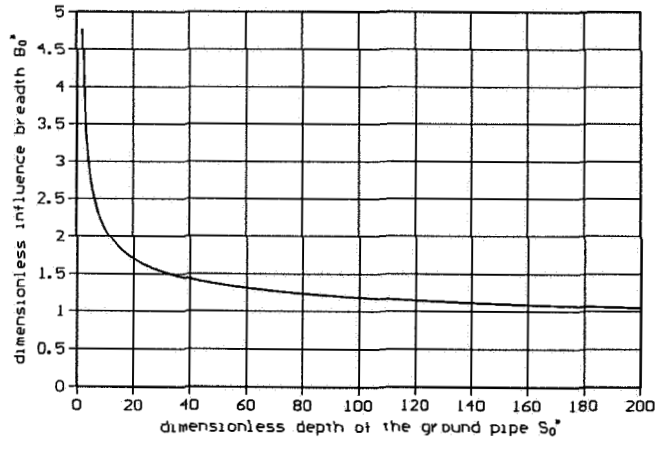

Fig. 3 Course of the dimensionless influence breadth

and cooling output of an entire pipe bank, without the necessity of performing an involved numerical calculation of the ground temperature field.

Experimental results

The ground heat exchanger under investigation was built for a single-family house and is shown schematically in Fig. 4. The ground heat exchanger is 42 m in length and is 125 mm in diameter. The outdoor air is propelled through the ground pipe by means of a tube fan with a measured power requirement of 50 W. The volume flow is 140 m^3/h.

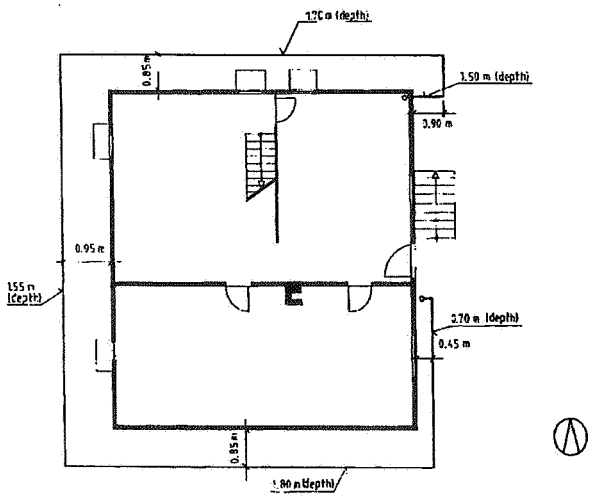

Fig. 4 Scheme of the ground heat exchanger

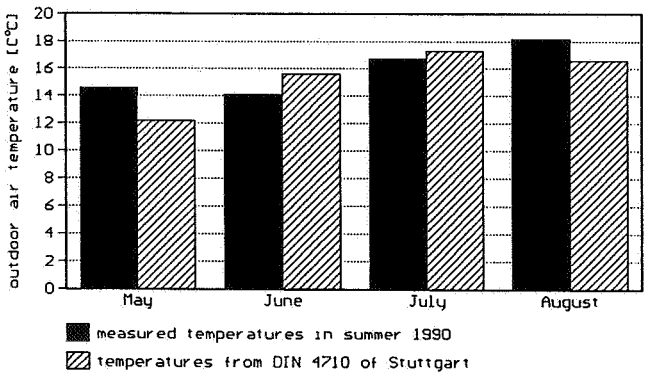

Fig. 5 Outdoor air temperatures

During the summer of 1990 under investigation, the ground heat exchanger provided partially cooled air during the months from May to Oktober. For these months, the experimentally determined monthly mean outdoor air temperatures are plotted in Fig. 5. Since no 20-year mean values exist for the location of the ex-

periment, the 20-year mean values from DIN 4710 /12/ of the air temperature at the location of the meteorological station at Stuttgart are plotted. Even though the 20-year mean values of the air temperature at the location of the ground heat exchanger will differ from those at Stuttgart, it is still possible to make the location independent statement that, in summer 1990, the months May and August were significantly warmer than the long-term mean temperatures.

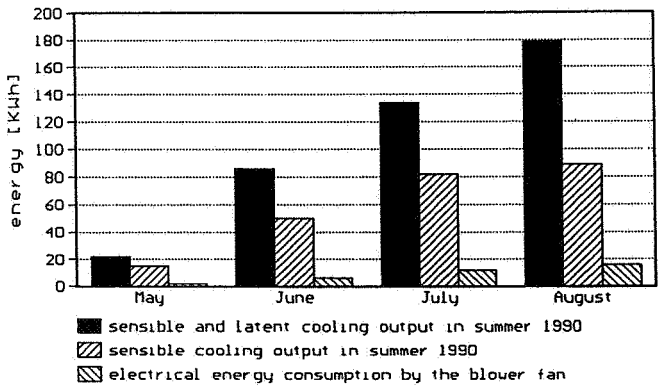

Fig. 6 Cooling output of the ground heat exchanger

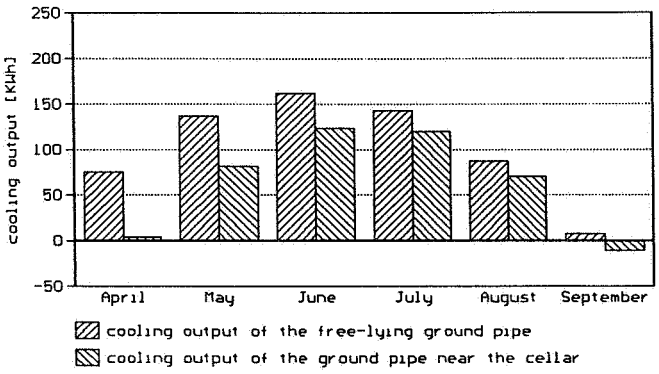

Fig. 7 Cooling output of the ground heat exchanger

Fig. 6 shows the cooling yield achieved in the individual months. A distinction is made here between the sensible and the total (sensible and latent) cooling yield. For the purposes of energetic evaluation, the electrical energy consumed by the blower fan whilst cooling the air is also plotted. During the entire summer of 1990, the ground heat exchanger provided 236 kWh of sensible cooling, or 421 kWh of sensible and latent cooling, whereby 36 kWh of electrical energy had to be supplied. The calculation of a coefficient of performance for the ground heat exchanger analogous to that for a heat-pump cycle yields a value of 6.6 in terms of the sensible cooling yield, and a value of 11.7 in terms of the total (sensible and latent) cooling yield.

Fig. 7 shows the mean cooling yield during the summer months to be expected of the ground heat exchanger under investigation. A negative cooling yield represents a heat yield. Alongside the cooling yield calculated from the analytical approximate solution (left-hand bars), the cooling yield under consideration of the cellar wall according to Eqn. 9 is also indicated (right-hand bars). The influence of the cellar wall upon the cooling yield of the ground heat exchanger becomes apparent in this diagram. Since the cellar wall is warmer than the ground, a nearby ground pipe suffers a significantly reduced cooling yield.

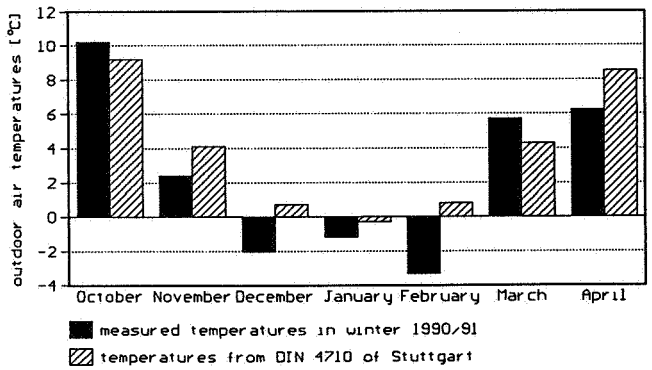

Fig. 8 Outdoor air temperatures

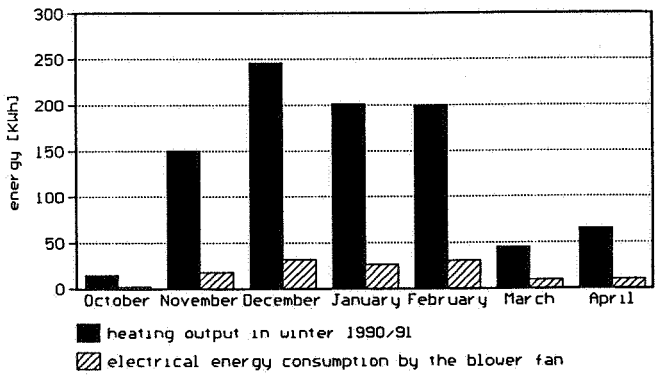

Fig. 9 Heating output of the ground heat exchanger

During the winter of 1990/91 under investigation, the ground heat exchanger provided prewarmed supply air during the months from October to April. Fig. 8 shows the mean monthly values of the outdoor air temperature for these months, alongside the 20-year mean values from DIN 4710 for Stuttgart. This diagram leads to the qualitative conclusion that the months from November to February were significantly colder than the long-term mean temperatures.

The heat yield achieved during the individual months is seen in Fig. 9. The electrical energy expended in

the operation of the blower fan is plotted in addition. During the entire winter 1990/91, the ground heat exchanger provided 923 kWh of heat, for which 127 kWh of electrical energy had to be expended. The ground heat exchanger therefore has a coefficient of performance of 7.3 in terms of the heat yielded.

Fig. 10 shows the mean heat yield to be expected during the winter months. Alongside the heat yield which is calculated from the analytical approximate solution (left-hand bars), the heat yield under consideration of the cellar wall according to Eqn. 9 (right hand bars) is also plotted, analogous to the representation of the summer data. The influence of the cellar wall becomes apparent here: the heat quantity is significantly increased. The excess of heat over that provided by a free-lying ground heat exchanger can not, as described in /9/, be described as a supplementary heat yield, since this heat quantity results from a higher loss of heat from the cellar. The installation of the ground heat exchanger around the house therefore provides no energetic advantages.

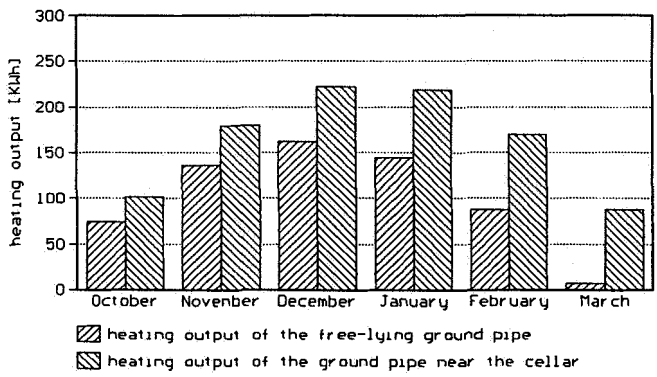

Fig. 10 Heating output of the ground heat exchanger

Design of ground heat exchangers

Many parameters which influence the heat or cooling output of the ground heat exchanger are predetermined by the position, the size and the use of the dwelling for which the

ground heat exchanger is planned. These parameters are the thermal diffusivity and the thermal conductivity of the earth, the course of the outdoor temperature, and the volume of supply air. The only freely variable parameters which significantly influence the heat or cooling output are the depth and the length of the ground heat exchanger.

Figs. 11 and 12 show the mean expected annual heating and cooling yields of the ground heat exchanger investigated as a function of the installation depth, as calculated from the analytical approximate solution. It is apparent from these diagrams that an optimum installation depth exists at which the heating and cooling yields are maximised. This depth is 4.5 m in the present case. The optimum installation depth is dependent upon the thermal properties of the ground, as shown in /9/.

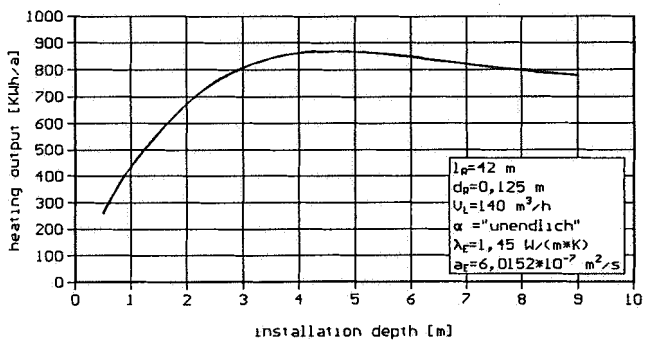

Fig. 11 Heating output of the ground heat exchanger

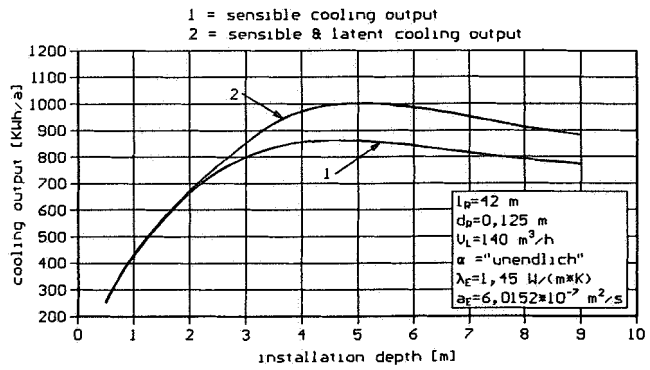

Fig. 12 Cooling output of the ground heat exchanger

The optimum pipe length is determined by the requirement that in winter, even in the case of short-period low-temperature extremes, the supply air temperature behind the ground pipe must always be greater than 0°C. This requirement is of great importance for the operation of the heat-recovery equipment.

Supply air temperatures below 0°C would result in icing of the exhaust air side within the plate heat exchanger of the heat-recovery equipment, which would seriously disrupt the function of the air-conditioning system.

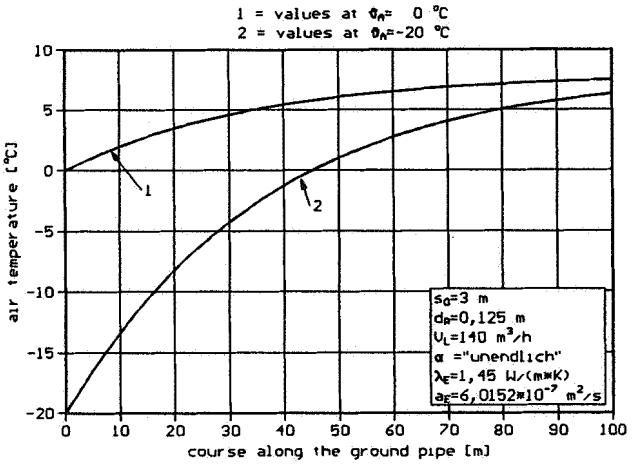

Fig. 13 Course of the air temperature in the pipe

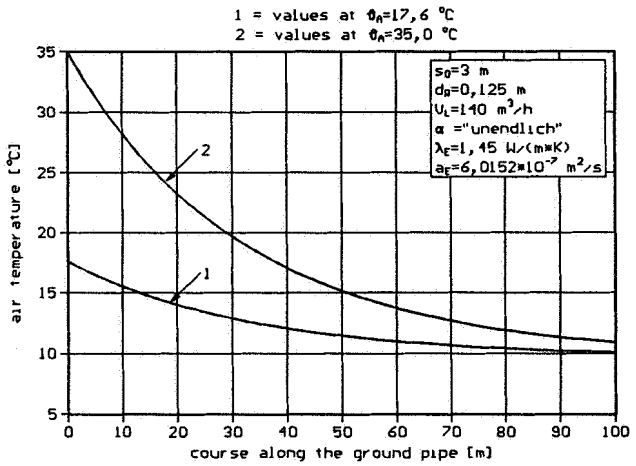

Fig. 14 Course of the air temperature in the pipe

Figs. 13 and 14 show the temperature course along the ground pipe in winter (month: January) and in summer (month: July). In each case, the temperature curve corresponding to the monthly mean value of the outdoor temperature (curve 1), together with the temperature curve resulting from a sudden extreme outdoor temperature (curve 2), are displayed. The extreme values are temperatures which can occur in Germany. Fig. 13 in conjunction with the above mentioned requirement gives the length of the ground heat exchanger under consideration here, laid at a depth of 3 m, to be 45 m.

References

/1/ Trümper, H.; Knoche, K. F.
Mechanische Wohnungslüftung als Grundeinheit
CCI Vol 21 (1987) 8, pp 63-65

/2/ Eckert, E. R. G.
The Ground Used as Energy Source, Energie Sink, or for Energy Storage
Energy Vol 1 (1976) pp 315-323

/3/ Schick, R.; Schneider, G.
Physik des Erdkörpers
Stuttgart, Ferdinand Enke Verlag 1973

/4/ Erdösi, I; Kajtár, L.
Die Änderung des Klimaverhältnisses in unterirdischen Räumen
KI Vol 17 (1989) 6, pp 289-291

/5/ Förster, H.; Hoffmann, E.; Mall, R.
Photovoltaische Stromerzeugung
Fachbericht des Badenwerks 89/1

/6/ Krischer, O.
Das Temperaturfeld in der Umgebung von Rohrleitungen, die in die Erde verlegt sind
Gesundh.-Ing. Vol 59 (1936) 9, pp 537-539

/7/ Grigull, U.; Sandner, H.
Wärmeleitung
Nachdruck der 1. Auflage, Berlin, Heidelberg, Springer Verlag 1986

/8/ Cube v., H. L.
Die Projektierung von erdverlegten Rohrschlangen für Heizwärmepumpen (Erdreich-Wärmequelle)
KI Vol 5 (1977) 6, pp 217-222

/9/ Albers, K.-J.
Untersuchungen zur Auslegung von Erdwärmetauschern für die Konditionierung der Zuluft für Wohngebäude
Dissertation Universität Dortmund 1991

/10/ Renz, U.
Kalorische Apparate
Vorlesungsskript zur gleichnamigen Vorlesung an der RWTH Aachen, Aachen, Lehrstuhl für Wärmeübertragung und Klimatechnik 1987

/11/ Ottel, M.
Die Wärmeverluste des Kellers, Vergleich verschiedener Berechnungsverfahren
Bauphysik Vol 8 (1986) 4, pp 106-110

AIR MOVEMENT & VENTILATION CONTROL WITHIN BUILDINGS

12th AIVC Conference, Ottawa, Canada
24-27 September, 1991

POSTER 12

A New Control Algorithm for the Measurement of Variable Air Change Rates.

R.Rabenstein, F.D. Heidt

Department of Physics
University of Siegen
Adolf-Reichwein-Strasse
D-5900 Siegen
Germany.

ABSTRACT

A new algorithm for the continuous measurement of variable air change rates with tracer gases will be presented. It differs from the constant concentration method by allowing the concentration level to vary according to the air change rate. Also the the mixing process of tracer gas within the room under investigation is considered and limited measurement ranges and injection rates of the tracer gas equipment can be accounted for. The new algorithm has a number of advantages, such as quick response to variations in the air change rate and reduced tracer gas consumption. The development of the control strategy is described and its practical applicability is shown by measurements in a laboratory room.

1 INTRODUCTION

Continuous measurements of time varying air change rates are usually performed by the constant concentration tracer gas method [3]. The basic idea is rather simple, the problem, however, lies in the choice of the control algorithm for the determination of the tracer gas injection rate. Up to now, classical controllers of P-, PI-, PID-type or modifications thereof as well as adaptive control algorithms have been used [2,4,9].

This paper presents a new control algorithm, which incorporates the following points:

1. The target level for the tracer gas concentration is allowed to vary according to the air change rate.
2. The mixing process of the injected tracer gas with the room air is taken into account.
3. The limited range of the tracer gas flow rate controller is considered.

Points 1 and 2 allow a quicker response to changes in the air change rate without causing over- or under-shoots. Furthermore point 1 saves tracer gas by lowering the target level for high air change rates. Point 3 prevents "wind-up" effects in linear controllers [6] as reported e.g. in [4]. This control algorithm will be described in section 2. Section 3 presents measurement results to show its application to the measurement of variable air change rates.

2 DESCRIPTION OF THE CONTROL ALGORITHM

2.1 Determination of Variable Air Change Rates

To determine the time varying air change rate $n(t)$ of a room with volume V and tracer gas injection rate $q(t)$ from the measured tracer gas concentration $c(t)$, we start with the differential form of the tracer gas conservation law for a single zone with constant temperature

$$\dot{c}(t) = - n(t)c(t) + \frac{1}{V}q(t) \tag{1}$$

By integration over a time interval $[t - t_m, t]$ and division by the length t_m, one obtains

$$\frac{\Delta c(t)}{t_m} = -n(t)\ \bar{c}(t) + \frac{1}{V}\ \bar{q}(t) \tag{2}$$

where

$$\begin{aligned} \Delta c(t) &= c(t) - c(t-t_m)\ , \\ \bar{c}(t) &= \frac{1}{t_m}\int_{t-t_m}^{t} c(\tau)d\tau\ , \\ \bar{q}(t) &= \frac{1}{t_m}\int_{t-t_m}^{t} q(\tau)d\tau\ . \end{aligned} \tag{3}$$

It has been assumed, that the air change rate $n(t)$ varies slowly, such that it is approximately constant during the time of integration:

$$\int_{t-t_m}^{t} n(\tau)c(\tau)d\tau \approx n(t)\int_{t-t_m}^{t} c(\tau)d\tau\ . \tag{4}$$

Thus, the slowly varying air change rate can be obtained from (2) as (see also [1,2])

$$n(t) = \frac{\bar{q}(t)}{\bar{c}(t)\ V} - \frac{\Delta c(t)}{\bar{c}(t)}\ \frac{1}{t_m}\ . \tag{5}$$

This relation holds in principle for arbitrary time functions for the tracer gas injection $q(t)$ and concentration $c(t)$. The only assumption for its validity is that the air change rate is constant during the integration time t_m, which may be in the range of a few minutes. The range of the measurement t time is not limited, thus allowing continuous measurements. Two special cases will be briefly mentioned:

- If the tracer gas injection consists of a single pulse completely released within the integration time t_m, then $t_m \cdot \bar{q}(t)$ is the total tracer gas volume. This corresponds to the pulse injection technique [1].

- If the tracer gas injection is controlled such that the concentration remains at the constant level of a prescribed target concentration c_T, then $\bar{c}(t) = c_T = const$, $\Delta c(t) = 0$. One can even omit the integration and obtains the familiar form of the constant concentration technique

$$n(t) = \frac{q(t)}{c_T V} . \tag{6}$$

In general, eqn. (5) could be used for continuous air change rate measurements for (almost) arbitrary values of $q(t)$ and $c(t)$. For practical measurements, however, two restrictions have to be observed:

- The tracer gas injection rate is determined by some kind of flow controller, which can only release gas at a rate between a minimum and maximum value such that $0 \le q_{min} \le q(t) \le q_{max}$.

- Similarly, the measurement device for the tracer gas concentration operates properly only for a given concentration range $0 < c_{min} \le c(t) \le c_{max}$.

This requires that the limited injection rate has to be controlled in such a way, that the concentration remains in the measurement range of the concentration measurement device.

It is important to note, that this control problem differs from the usual constant concentration method. The control of the tracer gas concentration is not a prerequisite for the measurement method, but merely a matter of practical instrumentation considerations. For the constant concentration method, deviations of a few percent of the target concentration are critical. Here, the tracer gas concentration my vary by a factor of 1:10 or more depending on the dynamic range of the concentration measurement device.

There are control algorithms that require an a-priori-knowledge of the air change rate for the determination of the coefficients (e.g. proportional control). Of course, these algorithms are not well suited for air change rate measurements with the constant concentration method. They require additional measures like an integrating term (PI-control) or coefficient adaption. However, these measures tend to slow down the response to changes in the air change rate. With the method suggested by eqn. (5), a dependency of the tracer gas concentration on the air change rate is not a problem, as long as the operating range of the concentration measurement device is not exceeded. It is therefore possible to tune the control algorithm for faster response rather than for minimal deviation from some target concentration. This trade-off will be addressed in the following subsections.

2.2 Mixing Model

The core of the proposed method is a control algorithm for the tracer gas injection rate $q(t)$ to keep the concentration $c(t)$ within the measuring range of the concentration measurement device. This algorithm has to be adapted to the room under investigation. Therefore a mathematical model for the tracer gas injection and exfiltration is required.

The control algorithms described in [2,4,9] consider the room as a black box and use the measured concentration as the only source of information. Depending on the mixing process of the injected tracer gas within the zone, changes in the injection flow rate will lead to concentration changes only after a certain delay time. Consequently, all these algorithms show a rather slow response to variations in the air change rate. After a step-up or step-down of the air change rate, it takes one hour or more until these methods show the new value with acceptable accuracy, as reported in [2,4,9].

The mixing process of tracer gas with a fan has been described by an additional time constant in [10]. It is used, however, only for the characterisation of the controlled system and has not been incorporated into the controller. This model will be elaborated here in more detail to serve as the basis of a control algorithm.

Usually, tracer gas is distributed in the room under investigation by a mixing fan at the location of the tracer gas injection. The resulting time and space dependent concentration field can be described in great simplification by a two-zone-model of a room with volume V according to figure 1. The mixing fan and the injection source are separated by a ficticious zone with volume V_2 from the rest of a room with the volume $V_1 = V - V_2$. Between both zones exists an air flow F_2 which is generated by the mixing fan. The room exchanges air with the exterior at a rate F_1. Zone 1 (room without injection zone) and zone 2 (injection zone) are assumed to be well mixed. Their respective tracer gas concentrations are $c_1(t)$ and $c_2(t)$. The tracer gas balances for both zones (isothermal case) are given by (see [5])

$$\begin{aligned} \dot{c}_1(t) &= -\frac{F_1+F_2}{V_1}\, c_1(t) + \frac{F_2}{V_1}\, c_2(t) \\ \dot{c}_2(t) &= \frac{F_2}{V_2}\, c_1(t) - \frac{F_2}{V_2}\, c_2(t) + \frac{1}{V_2}\, q(t) \,. \end{aligned} \tag{7}$$

The zone of instantaneous mixing of the injected tracer gas is confined to the immediate surroundings of the mixing fan, such that $V_2 \ll V_1$ and $V_1 \approx V$. Then, the relation between infiltration rate F_1 and volume of zone 1 V_1 is approximately given by the air change rate n:

$$\frac{F_1}{V_1} \approx n \tag{8}$$

Under this assumption, the two-zone model given by (7) is related to the one-zone model (1) by

$$\dot{c}_1(t) = -n c_1(t) + \frac{1}{V} q(t) - \frac{V_2}{V} \dot{c}_2(t) \tag{9}$$

This is obtained by rearranging eqns. (7) and (8).

Equations (7) give a state space description of the room under investigation (see [6,7,10,11]). The injection rate $q(t)$ is the input function and $c_1(t)$ and $c_2(t)$ are the state variables. The room concentration $c_1(t)$ is the output function and equal to the first state variable. This state space model will be used for the development of the control algorithm in the next section.

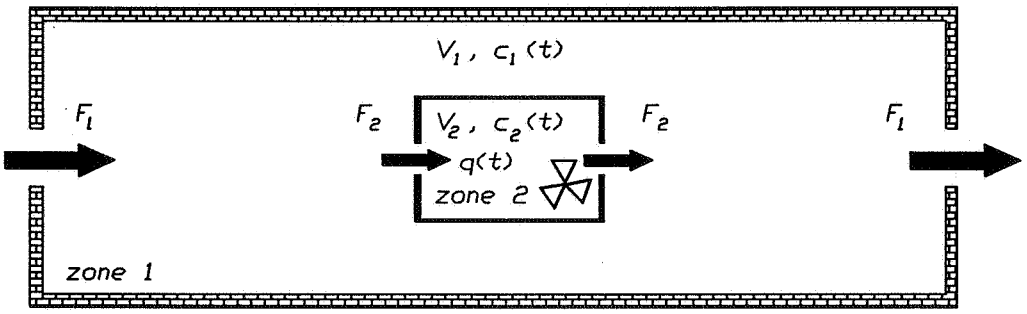

Fig. 1: Two-zone mixing model

2.3 Control Algorithm

A first approach for the control of the tracer gas concentration would be a simple control loop, which computes the injection rate $q(t)$ from the current concentration in the room $c_1(t)$. It has been already discussed that the use of classical control algorithms leads to a slow response, since the influence of the tracer gas injection can only be observed by its retarded effect on the concentration $c_1(t)$.

A faster response could be expected, if not only the room concentration $c_1(t)$ but also the concentration in the injection zone $c_2(t)$ would be used a input to the controller, because an injection acts directly on $c_2(t)$ before $c_1(t)$ is affected. This leads to the concept of state feedback [6,7,10,11], since all state variables are fed into the controller. The problem is that the concentration in the injection zone is not available for real measurements, since the injection zone itself is only a model and not a well defined item.

This problem can be overcome by a state observer [6,7,10,11]. That means here that the two-zone mixing model is included in the control algorithm in order to estimate the non-measureable quantity $c_2(t)$ from the measurable quantities $c_1(t)$ and $q(t)$. This estimate is used for the state feedback. Since the first state variable $c_1(t)$ is known, a reduced-order state observer of first order is sufficient for the estimation of $c_2(t)$. The design of state observation controllers can be found in standard text books on control systems (see e.g. [6,7,10,11]) and will not be outlined here.

Before a concise description of the control algorithm will be given, it is necessary to consider the limited range of the flow control device for the tracer gas injection. While the control algorithm may compute some desired injection rate $q(t)$, the flow controller can only release gas at a rate $q_b(t)$ with limited range, such that

$$q_b(t) = \begin{cases} q_{min} & q(t) < q_{min} \\ q(t) & q_{min} \le q(t) \le q_{max} \\ q_{max} & q_{max} < q(t) \end{cases} \qquad (10)$$

where q_{min} and q_{max} are determined by the type of flow controller. This nonlinearity has to be included into the control algorithm, in order to provide the necessary information on the actual injection rate.

A block diagram of the control algorithm is shown on the left side of figure 2 (dashed box labelled controller). It consists of four components:

- A factor l, which computes the injection rate required to maintain a given target concentration c_T under standard conditions defined in advance. They are based on the two-zone mixing model and include an estimate of the mean air change rate during the measurement. Under- and over-estimation does not effect the accuracy of the measurement but only the tracer gas concentration level that is actually reached.

- A block F_u which computes the partial injection rate $r_u(t)$ from the current injection rate $q_b(t)$ as released by the flow controller.

- A block F_y which computes the partial injection rate $r_y(t)$ from the (smoothed) tracer gas concentration.

- A nonlinear block which computes the tracer gas injection rate as actually released by the flow controller according to (10).

Each of the blocks F_u and F_y simulates a first order differential equation.

2.4 Total System for the Determination of the Air Change Rate

The total system for the determination of the air change rate is shown in figure 2. It consists of the blocks controller, room, smoothing, and evaluation.

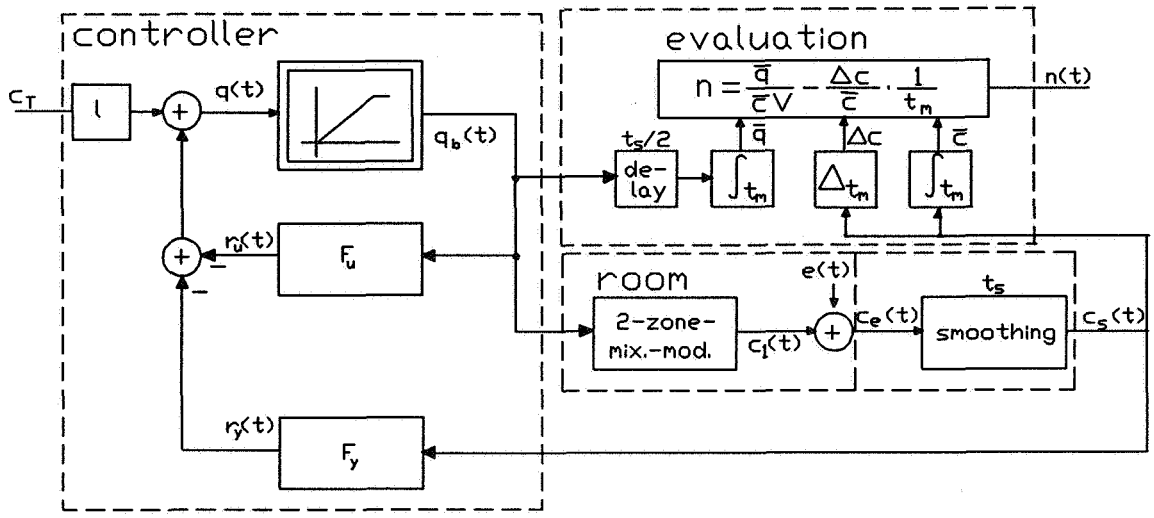

Fig. 2: Total system for the determination of the air change rate

The controller has been described in the previous subsection. The room under investigation responds to the injection rate $q_b(t)$ with the tracer gas concentration $c_e(t)$. Its measurement values can be modelled as the output $c_1(t)$ of the ideal two-zone mixing model and an additive noise signal $e(t)$, which accounts for concentration fluctuations due to incomplete mixing and inhomogeneities in the flow field.

If the control algorithm is to be designed for a fast response to changes in the air change rate, then care has to be taken that short term fluctuations in the measured concentration $c_e(t)$ do not lead to an injection rate $q_b(t)$ with similar fluctuations. To avoid this situation, the measured concentration is smoothed by averaging $c_e(t)$ over a time span t_s. The smoothed concentration $c_s(t)$ is used as input signal to the control algorithm as well as for the determination of the air change rate in the evaluation block.

The evaluation computes the estimate $n(t)$ for the air change rate according to equation (5), where $q_b(t)$ is used for the injection rate. Since smoothing the measured concentration introduces a delay of $t_s/2$, the same delay has to by applied to $q_s(t)$ as well. One may argue, that equation (5) based on the single- zone model (1) is not consistent with a control algorithm based on the two-zone model (7). An evaluation formula based on the two-zone model could be obtained by integrating (9)

over t_m. However, eqn. (9) differs from the single-zone model (1) only by $\dot{c}_2(t)$ scaled by the relation of the injection zone volume to the total volume. Since $V_2/V \ll 1$, this contribution may be neglected and the single-zone model is used instead for the calculation of the air change rate.

It should be noted that the two-zone model appears twice in the total system:

- It is used to describe the influence of the tracer gas injection into the room on the measured concentration. The model parameters depend on the fan size and the air change rate in the room under investigation and may vary with time.

- It has been used for the design of the controller and is contained implicitly in the blocks F_u and F_y. The model parameters were assumed as fixed values.

2.5 Properties of the Controlled System

The properties of the controlled system are analyzed under some simplifying assumptions:

- The tracer gas flow control device operates in the linear range, i.e. $q_b(t) = q(t)$.

- The room under investigation behaves like an ideal two-zone model, such that $e(t) = 0$ and no smoothing is necessary, i.e. $c_s(t) = c_1(t)$.

- The system is in a stationary state. The parameters and the injection rate are constant and any transient terms in the concentration have decayed.

- The flow rate of the mixing fan assumed for the design of the controller equals the flow rate of the mixing fan in the room.

The air change rate assumed for the design of the controller is denoted by n_T, while n_R denotes the actual air change rate in the room under investigation. The measured concentration is $c_R = c_1(t)$.

If the air change rate n_T used for the controller design is equal to the air change rate of the room, then the observer is able to give a correct estimate for the concentration in the injection zone and the measured concentration c_R will be equal to the target concentration c_T.

However, if the air change rate in the room is yet to be determined, then only an estimated value n_T can be used for the design of the controller. The observer based on this value will not produce the correct injection zone concentration, if the actual air change rate n_R differs from n_T. Consequently, also the actual room concentration c_R will differ from the target concentration c_T. It can be shown that the concentration and the air change rate of the model assumptions (c_T, n_T) and of the room (c_R, n_R) are related by

$$\frac{c_R}{c_T} = \frac{n_T+a}{n_R+a} \tag{11}$$

where a is a measure for the DC-gain of the controller. It determines the relation between the concentrations c_R and c_T between the limiting cases:

$$\begin{aligned} a = 0: &\qquad \frac{c_R}{c_T} = \frac{n_T}{n_R} \\ a \to \infty: &\qquad c_R = c_T \end{aligned} \tag{12}$$

For $a=0$ (no control), the relation of the concentrations is inverse to the relation of the air change rates. This corresponds to a constant tracer gas injection. For $a\to\infty$, the measured concentration c_R is equal to the target concentration c_T independent of the air change rate n_R. This is the case of an ideal constant concentration method.

Note, that the DC-gain of the controller determines also the sensitivity to noise in the measured concentration. The noise sensitivity increases with increasing gain. Thus, the controller design is a compromise between sensitvity to noise and deviation from the target concentration. However, the ultimate goal is the determination of the air change rate, where - according to eqn. (5) - a constant concentration is not required. Therefore, the design of the controller may focus on low sensitivity to noise rather than minminal deviation from the target concentration. Choosing a moderate DC-gain will lead to an injection rate $q(t)$ that is little affected by concentration measurement noise and to a concentration level in the room c_R that deviates more or less from the target concentration c_T. A good estimate of the actual air change rate can be expected from these signals (see eqn. (5) and the block "evaluation" in figure 2). The range of possible values for c_R can be adjusted to the measurement range of the tracer gas analyser by selecting proper values for c_T, n_T, and a. A typical value for a is $a = 3 \cdot n_T$.

Inspection of eqn. (11) shows that high air change rates in the room decrease the concentration level and thus the tracer gas consumption for long term measurements. The main advantage of the proposed control configuration becomes apparent in non-stationary situations. It leads to a substantially faster reaction to temporal changes in the air change rate compared to controllers designed for minimal deviation from the target. This will be demonstrated by an example in the next section.

3 MEASUREMENT RESULTS

The system for the determination of the air change rate as depicted in figure 2 has been implemented in one channel of the tracer gas measurement system MULTI-CAT (Multi-channel analysis of tracers) [8]. The result of a measurement in a laboratory room is shown in figure 3. Door and windows were opened and closed during the measurement according to the following schedule:

phase 1	0 - 15 minutes	door and windows closed
phase 2	15 - 40 minutes	door closed, two windows tilted
phase 3	40 - 70 minutes	door open, two windows tilted
phase 4	70 - 100 minutes	door closed, one window tilted

Obviously, the tracer gas concentration is not constant. Instead it reaches a new equilibrium in each phase. This is due to the fact, that the DC-gain of the controller was selected for a high noise supression in the concentration measurement. It can be seen that the injection rate is very smooth, although the concentration curve exhibits quite sizeable short term fluctuations. The air change rate was calculated from the injection and the smoothed concentration by eqn. (5). It varies between ca. 0.5 1/h in phase 1 and up to 14 1/h in phase 3.

The following advantages of this control strategy become apparent from these curves:

- Even with high variations of the air change rate, the variations of the injection rate are rather modest and stay within the linear range of the tracer gas flow control device (here 2 – 100 L/h). Demanding a constant concentration level for all four phases would have led to excessive injection rates (> 100 L/h) in phase 3 or for a reduced concentration level to an injection rate below the minimum value (2 L/h) for phase 1.

- The controller responds quickly to variations of the air change rate. The time series of the air change rate shows, that after each opening or closing of the door or the windows a transition phase of less than 15 minutes is sufficient until a new equilibrium is reached (if it exists at all, see phase 3). Other control strategies, which try to maintain a constant concentration under all circumstances, exhibit a transition phase in the order of one hour and more [2,4,9].

- The concentration level decreases with an increase of the air change rate (see phases 1,2,3). In other words, the exfiltration of tracer gas from the room is under proportional to the

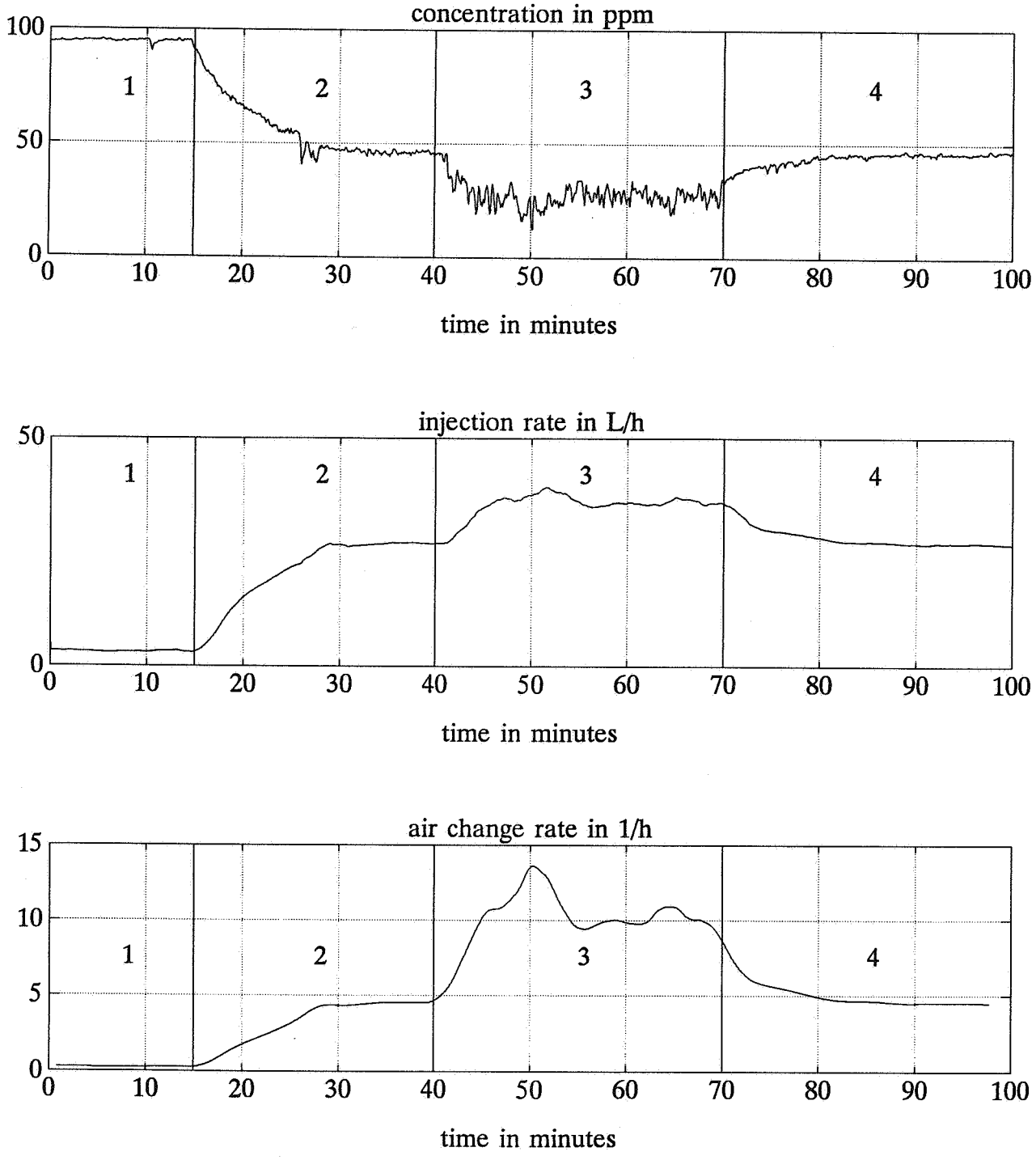

Fig. 3: Measurement of variable air change rate in a laboratory room: measured tracer gas concentration, injection rate, air change rate

exfiltration of air. This leads to a reduced tracer gas consumption for continuous measurements.

CONCLUSION

A new control algorithm for the determination of variable air change rates has been presented. In contrast to the usual constant concentration method, it incorporates the following points:

- The target level for the tracer gas concetration is allowed to vary according to the air change rate.
- The mixing process of the injected tracer gas with the room air is taken into account.
- The limitations of concentration measurement range and tracer gas flow rate are observed.

This approach is rather flexible since the algorithm can be adapted to the measurement conditions on site and to the properties of the tracer gas equipment. The following advantages over existing constant concentration control algorithms have been confirmed by measurements in a laboratory room:

- The variation range of the injection rate can be confined to the flow range of the tracer gas flow control device at hand, even with high variations of the air change rate.

- The controller responds quickly to variations of the air change rate. The response time to a step change of the air change rate is less than 15 minutes.

- The tracer gas consumption for continuous measurements is reduced compared to the constant concentration method.

ACKNOWLEDGEMENT

This work is associated with a research and development project entitled "Weiterentwicklung und Erprobung von Methoden der Luftwechselmessung in Räumen und Gebäuden (further development and application of air exchange measuring methods for rooms and buildings)". The authors gratefully acknowledge the financial support provided by the BMFT (German Ministry for Research and Technology).

LITERATURE

[1] J. Axley, A. Persily: Integral Mass Balances and Pulse Injection Tracer Techniques. Proc. of the 9th AIVC Conference, Gent, Belgium, 1988, Volume 1, pp. 125 - 157

[2] D.L. Bohac: The Use of a Constant Concentration Tracer Gas System to Measure Ventilation in Buildings. PU/CEES Report No. 205, 1986, The Center for Energy and Environmental Studies, Princeton University, USA

[3] P.S. Charlesworth: Air Exchange Rate and Airtightness Measurement Techniques - An Applications Guide. 1988, Air Infiltration and Ventilation Centre, Great Britain

[4] R. Compagnon, A. Kohler, C. Roecker, C.-A. Roulet: Development of an Efficient Control Algorithm for a Multizone Constant Concentration Tracer Gas Air Infiltration Measurement System. Proc. of the 9th AIVC Conference, Gent, Belgium, 1988, Volume 2, pp. 103 - 122

[5] F.D. Heidt, R. Rabenstein, G. Schepers: Comparison of Tracer Gas Methods for Measuring Air Flows in Two Zone Buildings. Proc. of the 11th AIVC Conference, Belgirate, Italy, 1990, Volume 1, pp. 171 - 192

[6] P. Hippe, Ch. Wurmthaler: Zustandsregelung. Springer Verlag, Berlin, Germany, 1985

[7] G.H. Hostetter: Digital Control System Design. Holt, Rinehart and Winston, Inc., New York, USA, 1988

[8] R. Rabenstein, F.D. Heidt: The Man-Machine-Interface for the Air Exchange Measurement System MULTI-CAT. Proc. of the 11th AIVC Conference, Belgirate, Italy, 1990, Volume 1, pp. 131 - 147

[9] M. Sandberg, C. Blomqvist: A Quantitative Estimate of the Accuracy of Tracer Gas Methods for the Determination of the Ventilation Flow Rate in Buildings. Building and Environment, Vol. 20, No. 3, pp. 139-150, 1985

[10] H. Schlitt: Regelungstechnik. Vogel Buchverlag, Würzburg, Germany, 1988

[11] P.K. Sinha: Multivariable Control. Marcel Dekker, Inc., New York, USA, 1984

AIR MOVEMENT & VENTILATION CONTROL WITHIN BUILDINGS

12th AIVC Conference, Ottawa, Canada
24-27 September, 1991

POSTER 13

Advanced Humidity Control Device for the Prevention of Mould

Willigert Raatschen

Dornier GmbH
Postfach 1420, D-7990 Friedrichshafen
Germany

Advanced Humidity Control Device for the Prevention of Mould

Abstract

The knowledge of IEA-Annex 14 'Condensation and Energy' has been applied to develop a new strategy for humidity control in dwellings. The presented control element assures safe prevention from mould growth at a minimum energy consumption.
The advanced humidity control device consists of a surface temperature and an indoor air temperature sensor, from which readings a microcontroller evaluates the appropriate RH setpoint. A humidity sensor then reads the actual RH in the room air and compares it with the momentary setpoint. If the actual RH in the room exceeds the setpoint, a humidity reducing device (a fan, a dehumidifier etc.) can be activated to lower the humidity level in the room. The advanced humidity control device adapts individually to any building's prevailing boundary conditions (insulation quality, thermal bridging, room air temperature, moisture emissions with regard to occupant behaviour) in such a way, that no favourite conditions for the growth of mould occur.

INTRODUCTION

Many buildings in Europe suffer from moisture damages. The reasons are manifold. To develop measures to cure mould growth in buildings, an international project under the leadership of the International Energy Agency (IEA) Annex 14 'Condensation and Energy' was started in 1987. 5 countries (Belgium, Germany, Italy, The Netherlands, and United Kingdom) joined this research project.

Mould problems are a rather widespread reality in these 5 countries, especially in the rented and/or social housing sector. The outdoor climate conditions of these countries are very different. Additionally, there are various other factors, which impact the possibility of mould growth as there is

- the poor quality of the thermal insulation of the building's envelope
- low room air temperature
- high moisture emission rates in the building

In affected buildings often at least 2 of the 3 facts are the reason for having mould growth. In rarer cases only one cause is sufficient to supply favourite conditions for mould growth.

Mould growth usually starts at the thermally weakest spot in a room, in the corner of an outside wall, at the ceiling under a poorly insulated roof, etc, usually there, where severe thermal bridging is.

There is no doubt about, that proper insulation is the best way to prevent mould growth. However, it is not always possible as retrofitting work is often very expensive. Sometimes a building should be pulled down in 2 or 3 years, but till that time the tenants should live in a healthy environment without mould in the house.

Especially in the 5 new German States, the former German Democratic Republic, the building quality is very poor. It is not possible to retrofit all houses at once. Therefore, another technical approach than insulation is needed to reliably prevent mould growth at the lowest consumption of energy possible.

Coping with Mould Growth in the past

Recommendations for occupants with moisture problems in the buildings are manifold:

- they should open windows after showering or cooking
- they should ventilate regularly
- they should keep room temperatures high
- they should reduce vapour emitting activities to a minimum.

Unfortunately, these recommendations are difficult to put into practice. People have - in the interesting range of 40-80% RH - only a very vage perception against relative humidity (RH) in the room air. Therefore, they are not able to correctly react against too high RH-levels in the building. Higher room temperatures result in a higher heating bill; this is often not accepted. To change occupants habits (e.g. drying of clothes inside the apartment, many flower plants, aquarium, etc.) is very difficult and very seldom successful. Reality shows, that any control mechanism, which needs the input of occupants, fails on a long term.

State of the Art Control Strategies

Bathrooms are very often equipped with a simple exhaust fan. There are different devices on the market to activate such a fan to extract moisture.

Manual control: The occupant activates the fan by using an on/off switch

Light-switch control: Mostly applied to bathrooms without windows. If a person enters a bathroom and turns on the light, the fan is also activated by the light switch. If the light is turned off, the fan is also turned off. A more sophisticated way of fan control involves a timer. The fan is activated approx. 2 minutes after the light is switched on and keeps on running for 10-15 minutes after the light is turned-off.

Photo-diode control: For later installation the industry offers a way to save up the wiring between the fan and the light switch. The fan casing is equipped with a photo diode. If the light is turned on, the signal is detected by the photo diode and the fan is controlled in the same manner as with light-switch control.

Interval timer: Another way to keep up with moisture is an interval timer, which activates the fan independently of any activities in the room every hour for 5 minutes. Time intervals can be adjusted.

Hygrostat control: A hygrostat activates the fan, when the RH in the room air is higher than a chosen setpoint.

All control devices on the market should keep moisture damages away from the room but none of these have the potential to really avoid mould growth because they are not linked to the problem. Also the hygrostat control is a pretty poor solution, because the user doesn't know the appropriate setpoint, he has to choose regarding the thermally weakest spot at his wall at his current indoor air temperature conditions. An often recommended setpoint for dwellings is 60-65% RH. This setpoint range is arbitrarily chosen. It will lead to a continously running fan during summer and a too high setpoint during wintertime. Reflecting the following described influencing factors for mould growth this fixed setpoint is not oriented to the problem and therefore neither able to avoid mould nor to safe energy.

Boundary conditions for mould growth

Mould growth depends of

- the relative humidity against the surface
- the surface temperature
- the nutritive quality of the substrate
- and many other minor factors

One goal of IEA-Annex 14 was, to come up with a simple practical approach to state under what conditions mould growth occurs. Mould growth is a very slowly happening process. Short periods of surface condensation will never lead to problems as long as there are periods in between where the surface can dry out again.

Moisture damages are not a question of momentary peak values but of average values of weeks and months.

Advanced Humidity Control

An advanced humidity control strategy must fulfil the following requirements:

- it must be oriented to the problem, i.e. no global solution for a room, the control strategy must be linked to the problem spot of the wall
- it has to take different occupancy patterns into account e.g. low/high room air temperatures, low/high moisture emissions
- it must be independent of the local meteorological conditions
- it should not need any manual adjustments
- it should activate a humidity reducing device in such a way, that the monthly mean RH against the surface is slightly lower than the critical RH, where mould growth may reappear.
- operating just under the critical RH ensures a minimum of energy consumption (e.g. electric energy for a fan, thermal energy for the heating of the ventilated air).

A problem oriented solution has to be adopted to the conditions, where mould growth becomes impossible. Results of IEA-Annex 14 /1/ show that mould germination occurs when the mean water activity against/on a nutrient surface remains higher during a shorter or longer time than a threshold value 'a', a being a function of the mould species, the temperature, the substrate (nutrient), and other things. Using the fact that in steady state, the water activity is nothing other than the RH, the condition for mould germination becomes possible, when $p_s \geq a \cdot p_s^0$, where p_s is the vapour pressure of the room air against the surface and p_s^0 is the saturation pressure of the room air against the surface, which is only a function of the surface temperature ϑ_s.

Mould growth is a very slowly happening process. Unfavourable conditions may prevail throughout longer periods (days, weeks). A first order approximation has been established which says, that the RH against the surface on a monthly base should not be higher than a defined threshold value a, where a is a function of the lowest surface temperature in a room, usually a thermally weak spot in the building envelope.

Description of the Advanced Humidity Control Device

As previously discussed, a problem oriented control strategy has to take the thermally weakest spot of a room into account. Via ventilation or other humidity reducing strategies we have to certify that at this location - on a monthly mean - the RH does not exceed the critical value a.

This is ensured by a controller, Figure 1, which consists of a first temperature sensor to measure the surface

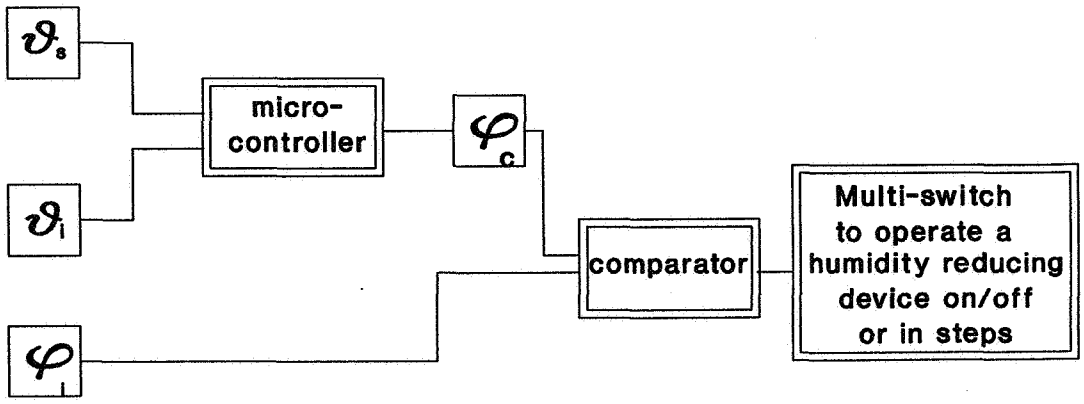

Figure 1: Schematic of control device

temperature ϑ_s at the critical location and a second temperature sensor to measure the room air temperature ϑ_i. From these readings a microcontroller evaluates the appropriate RH setpoint φ_c for the room air. A humidity sensor reads the actual RH φ_i in the room and compares it with the calculated setpoint. If the actual RH exceeds the evaluated setpoint, a first relay is closed. If the room RH still increases, a second relay closes etc. I.e. the control device can operate for example a multi-speed fan.

Field Tests

Field tests have been performed to verify, whether the *a*-value concept holds in practice /2/. As the controller operates due to the momentary values of ϑ_s, ϑ_i, and φ_i, different control algorithms were investigated to operate the fan in such a way, that on a monthly mean the defined threshold value is not exceeded.

In houses with severe moisture problems the system was able to avoid reappearance of mould. During summer the fan run for appox. 10-15 minutes after the end of a shower process. These periods became larger in fall and lasted 6 to 8 hours at minimal fan speed during winter at outdoor temperatures below freezing.

User Behaviour and Acceptance

From the day the humidity controlled system was installed, occupants did never open the bathroom window again. They were highly appreciated by the automatic system which was turned on and off automatically. The mirrors in the bath were free of condensation shortly after showering which increased the quality of living.

In August, when the fan was not installed, the occupants returned to their old habits and ventilated by using the window. It was also appreciated that the extract system prevented the spread of vapour into other rooms of the building.

Limits

The control strategy has no physical limits. If thermal bridging is too severe, i.e. the temperature factor τ which is defined as

$$\tau = \frac{\overline{\vartheta}_s - \overline{\vartheta}_e}{\overline{\vartheta}_1 - \overline{\vartheta}_e}$$

(ϑ_e - exterior temperature; the bars indicate mean values over some days).

is lower than 0.5, it is difficult to avoid mould growth only by ventilation. The air, which is extracted by the fan is supplied to the room partly from outdoors and, usually to a higher proportion, from indoors. As the air of the adjacent rooms has a higher absolute humidity than outdoors, the potential to take up more moisture in the bathroom is reduced. If the setpoint in the bathroom approaches the humidity level of the adjacent rooms the limit is almost reached.

Further Applications

The advanced humidity control device activates one or more switches to operate any device also in more speeds, which has the potential to reduce the humidity level in a room. It can be a fan, which is to be operated in 2 or 3 speeds, it can also be a dehumidifier or a smart window, which is opened and closed automatically or even an electric heating wire attached to the surface to increase the surface temperature.

This advanced humidity control device assures, that the possibility of reappearing mould is at a minimum and the amount of energy used is lowest. It takes the occupant behaviour, which influences the indoor temperature and the vapour emission, directly into account. Furthermore, it is independant of the outdoor climate, as it keeps the humidity reducing device (fan, dehumidifier etc.) running till the threshold criterium is met.

SUMMARY

Based on the knowledge of the biological and physical conditions, under which mould in dwellings germinates and spreads, an *Advanced Humidity Controller* was developed to operate a humidity reducing apparatus (a fan, a dehumidifier etc.) in such a way, that the RH in the room will not exceed a certain threshold value. On one hand mould growth is securely prevented, on the other hand a minimum of energy is used.

Acknowledgements

The work was carried out within the national research and development programme 'Lüftung im Wohnungsbau' (Ventilation in residential buildings) and refers to research grant 0338323C from the Project Management for Biology, Ecology and Energy (BEO) of KFA Jülich GmbH on behalf of the Federal Ministry for Research and Technology (BMFT).

References

/1/ Hens, H.: *Guidelines and Practice*, Vol. 2, report of IEA-Annex 14-'Condensation and Energy', August 1990

/2/ Raatschen, W.: *Advanced Humidity Controlled Ventilation*, a case study of IEA-Annex 18-Demand Controlled Ventilating Systems', Report by DORNIER GmbH, Friedrichshafen, Germany, January 1991

AIR MOVEMENT & VENTILATION CONTROL WITHIN BUILDINGS

12th AIVC Conference, Ottawa, Canada
24-27 September, 1991

POSTER 14

Ventilation and Humidity in Bathrooms

Jan Fransson

The Swedish National Testing and Research Institute
Box 857
S-501 15 BORÅS
Sweden
Tel: +46 33 165000 Fax: +46 33 131979

Synopsis

A laboratory investigation has been made in a modern Swedish bathroom continuously ventilated by an exhaust fan. The tests consisted of measurements of the humidity, temperature and local mean-age after a standard shower. The measurements were mainly made in a non-heated installation.

The maximum relative humidity, in a bathroom , is approximately constant at a given air temperature. This does not seem to be true for the measurement under the bath where the maximum moisture content was found to be constant.

The most accurate measurement was made immediately after the shower. The best results were found by increasing the airflow .The best advantage is the amount of the vapour spread in the room decreases. The increased airflow did not have any effect of the moisture content in the middle of the room and under the bath.

The use of an infrared heater also shows an improved reduction of the moisture content in the middle of the room and extracted moisture. The use of a radiator only showed a reduction of the moisture content in the middle of the room.

One hour after a shower approximately 240 g moisture is extracted and after two hours approximately 340 g moisture is extracted from the bathroom.The extraction of moisture will be much lower during summer when the moisture content in the supply air is high. To reduce the moisture problem in summertime it may be worth considering installing a dehumifier since an increased airflow only will give a small reduction.

List of symbols

Parameters:

q	Air flow (l/s)
t *	Temperature (°C)
RH*	Relative humidity (%)
x*	Moisture content in the air (g/kg)
xa*	Added moisture content, xa* = x*-xin (g/kg)
m	Extracted moisture (g)
m(1)	Extracted moisture during one hour (g)
m(2)	Extracted moisture during two hours (g)
P	Electrical power (W)

Where (*) represents the following locations:

in	Measuring point in the supply air terminal device
out	Measuring point in the exhaust air terminal device
r.1	Measuring point 0.1 m above the floor in the room
r1.1	Measuring point 1.1 m above the floor in the room
r2.0	Measuring point 2.0 m above the floor in the room
b.3	Measuring point 0.3 m above the floor under the bath

1 Introduction

Moisture problems are very common in modern Swedish bathrooms although they are continuously ventilated by an exhaust fan. Condensation on surfaces and high humidity levels are common problems, which may cause rot and mould problems.

The problems usually occur in summertime when the supply air has a very high humidity or in the winter when the wallsurface temperature is low. A high humidity level will also cause discomfort for the user.

When examining moisture problems it is important to know the maximum humidity level is and the time of exposure.

This paper is based on laboratory measurements of a bathroom module. A report is given in [Ref 4].

2 Test procedure

The tests were carried out using a three minute standard shower, 40 °C and 27 l of water [Ref 2], with an airflow rate of 10, 15 and 20 l/s respectively.

The tests were made with three different kinds of heating systems:

- no space heating at all
- a wall mounted electric radiator (R)
- a roof mounted infrared heater (IRH)

As a reference case the 15 l/s airflow with no space heating was chosen according to the Swedish building code.

The tests consisted of measurements of:

- air and surface temperature
- humidity
- local mean-age of the air

2.1 Sampling and preparation

The bathroom made for exhibitions [Ref 1], measures 1.92 x 3.24 x 2.23 m [W x L x H]. Supply air enters the room though the opening between the doorleaf and the doorstep. The air is extracted through an exhaust air terminal device located in the wall over the bath. In order to

simulate the presence of a person, 100 W of heat is generated by an electric heater located in the bathtub. The location of the measuring points is shown in figure 2.1

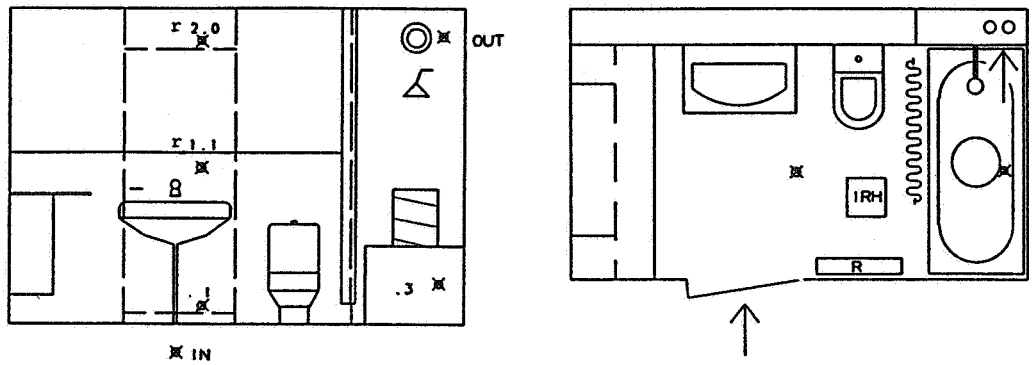

Figure 2.1 Location of measuring points in the bathroom module (See also list of symbols)

Humidity and temperature measurements were made in the supply and exhaust air terminal device, at the height 1.1 m and 0.1 m in the middle of the room and 0.3 m above the floor under the bath. The accuracy of the humidity measurements is better than +/- 5 % RH.

Temperature measurements were made in 8 different points between 0.1 and 2 m above the floor in the room and on the surfaces of the walls and the floor.

Local mean-age of air was measured in the exhaust air terminal device, under the bath and in 6 points between 0.1 m and 2 m above the floor in the room. The measurements were made with nitrous oxide according to [Ref 5] and [Ref 6].

Each test where measured during a period of at least two hours.

3 Results and discussion

3.1 Introduction

The moisture content in the air is a combination of the vapour production from hot water in the shower and evaporation from the wet surfaces. The vapour from the shower is assumed to follow the same slope as the logarithmic concentration-time decay curve of tracergas measurements.The wet surface will then yield a moisture exchange depending on the moisture content in the boundary layer.

The principal humidity curves expressed as relative humidity in the air after a standard shower are shown in figure 3.1.

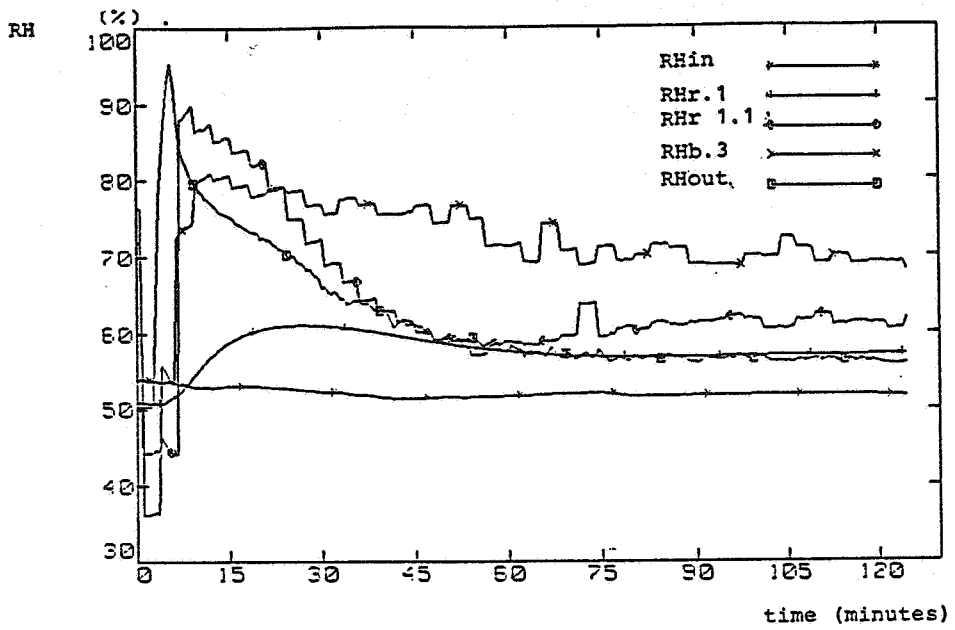

Figure 3.1 Measured humidity transients in a bathroom for the reference case .(15 l/s exhaust airflow ,no space heating)

The maximum humidity is measured in the exhaust air terminal device. The humidity rises to 80 % RH almost immediately and reaches 95-98 % RH when the shower is over. After a couple of minutes the maximum value in the middle of the room, approximately 90 % RH, is reached. After additional minutes the maximum value under the bath , 70-80 % RH, is reached.

The humidity decreases faster in the exhaust air terminal device and in the middle of the room than under the bath.From approximately 15 minutes after the end of the shower the highest humidity level in the room is found under the bath.

This is an example of a typical test run, but the measurements show wide variations, especially under the bath. Droplets of water drain down the wall during and after the shower. Another difficulty is the influence of the air temperature and the humidity in the supplyair.

3.2 Airflow patterns

The airflow was supplied through a 32 mm slot under the door. The construction of the doorstep formed a large whirl which gave a wellmixed ventilation with an air-exchange efficiency of 55 to 60 %. The higher value was found when the supply air temperature difference was decreased from -0.5 to -2 °C below the room temperature tr1.1.

The local mean-age of the air showed small variations. in the heated and non-heated referance case it was calculated to be 0.22 hours except under the bath,where it was 0.24 hours.

The influence of the airflow is shown i figure 3.2

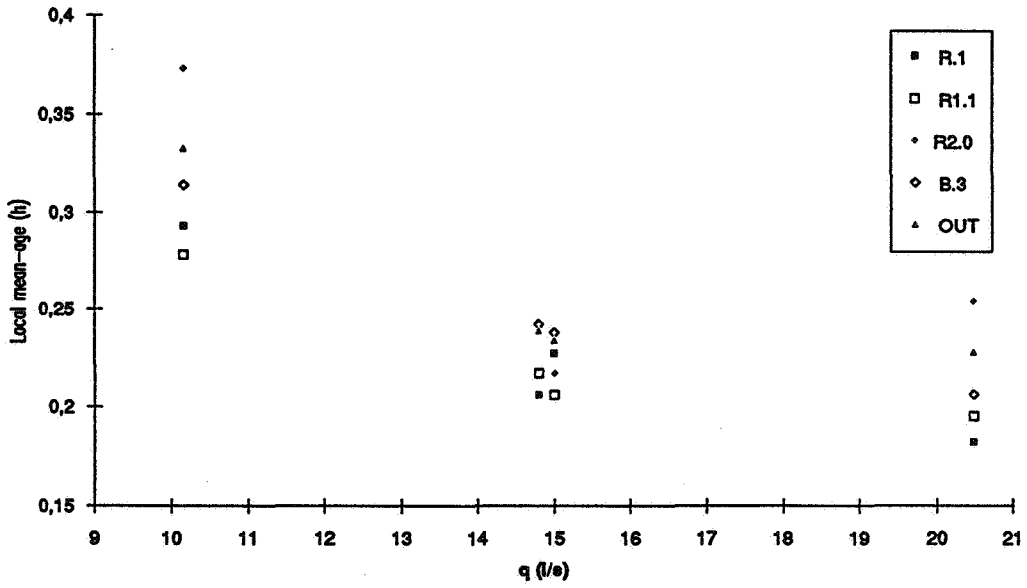

Figure 3.2 Measured mean-age of air, reference case i.e. no space heating.

3.3 Maximum moisture content directly after the shower

The majority of the measurements were made in the non heated bathroom with an airflow of 15 l/s (reference case). The water on the surface was measured to be approximately 0.3 kg after a standard shower.

The maximum moisture content in the air, at reference airflow, was compared with all the measurements .It was found that the level is a function of the room temperature and the moisture content in the supply air.The values are shown in figure 3.3.

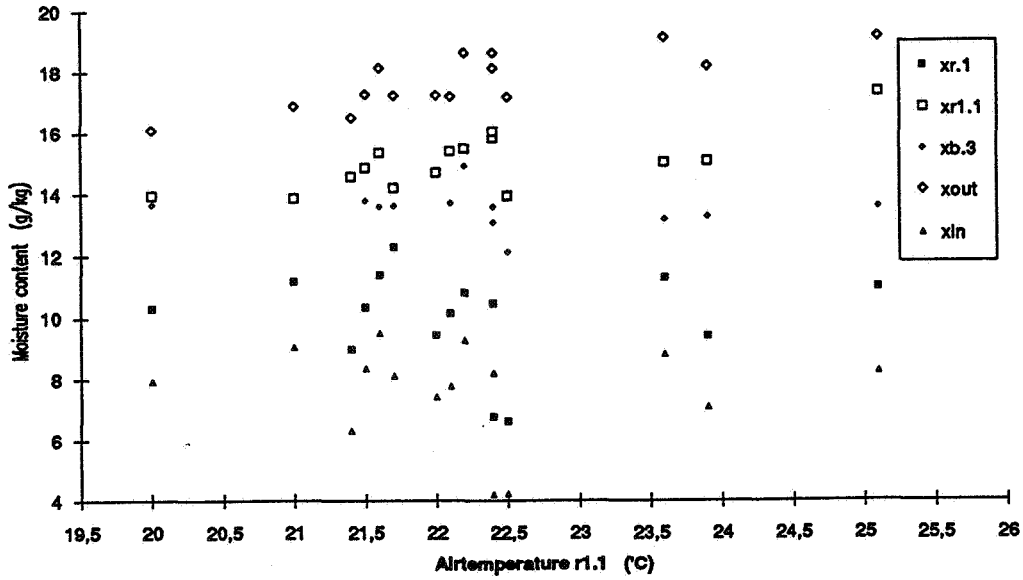

Figure 3.3 Maximum moisture content at different air temperature,exhaust airflow 15 l/s .

The maximum of relative humidity is approximately constant at a given air temperature except under bath where the maximum moisture content is constant ,14 g/kg .

The slope of the logarithmic added moisture-time curve was found to decrease with time.The first half an hour of the measurements showed the highest degree of accuracy.

If a mixed ventilation is assumed, the slope will correspond to the local mean-age of air. The values are shown in table 3.1

Table 3.1The inverted slope of the added moisture content

q	Heater	xaout	xab.3	xar1.1
(l/s)		(h)	(h)	(h)
10	---	0.8	2.6	1.2
15	---	0.6	1.2	0.8
20	---	0.3	1.3	0.8
15	IRH	0.4	?	0.4
15	R	0.6	?	0.3

The best results for the exhaust air terminal device were found when the airflow was increased and by use of a infrared heater. The effect of an increased airflow is much higher for the added moisture than for the local mean-age of air.

The slope in the middle of the room was highly affected in the radiator case and the infrared heater case. In two of the cases no valid slope was found according to the big variations.

3.4 Moisture content in the air with no space heating

One hour after the shower the variations of the slope for the same case increased.To investigate the continued process, the maximum and mean values of the added moisture content in the air were measured for the different positions of the bathroom. The values are shown in figure 3.4

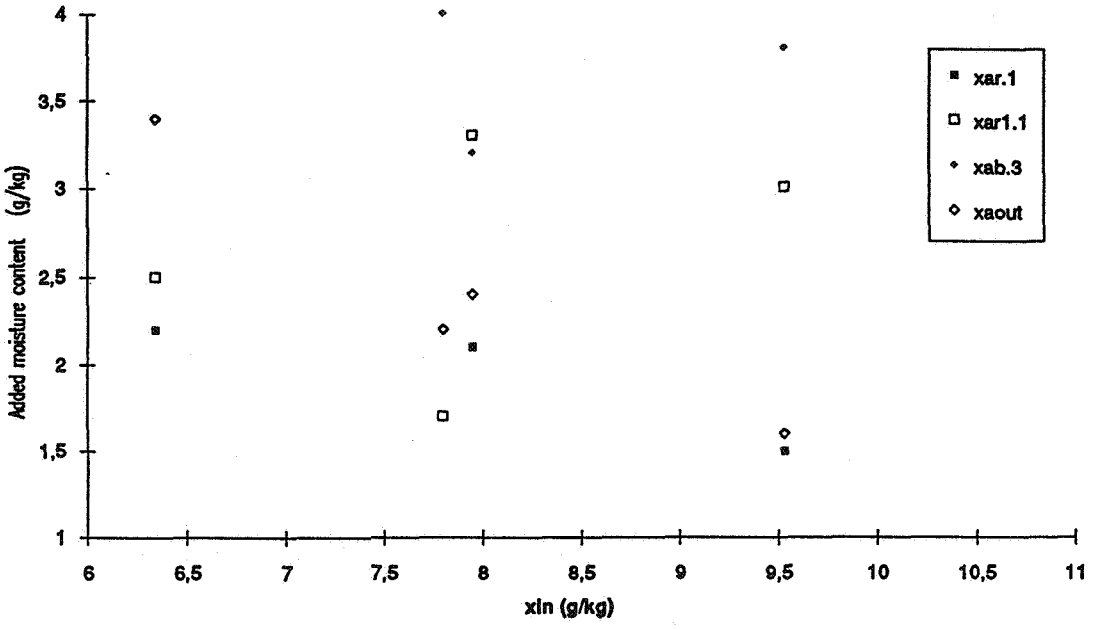

Figure 3.4 Moisture added to the air in the bathroom as a function of the moisture content in the supply air.The values is based on measurement, one hour after the shower for the reference case at an air temperature of 22 °C.

At 0.1 m in the room and in the exhaust ATD a high influence of the moisture content of the supplied air was observed. The measured values at 1.1 m in the room and under the bath were not affected by the supplied air to same extent , but the variation was bigger.

The totally extracted moisture content was calculated. This was repeated for a two hour mean value. The results are given in figure 3.5

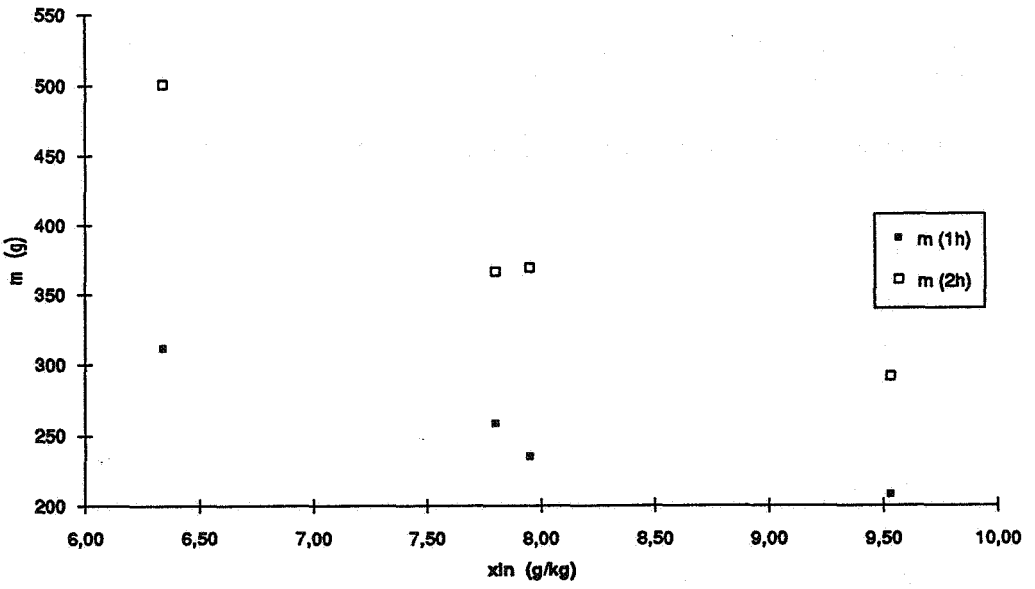

Figure 3.5 Totally extracted moisture as a function of the moisture in the supply air.The values is based on measurement, after one and two hour after the shower for the reference case at an air temperature of 22 °C

A simplified formula of the totally extracted moisture can be defined as

$$m = A \cdot xin^B \qquad (1)$$

The constants A and B are given in table 3.2

Table 3.2

Parameter	Constant	Constant
m	A	B
m (1h)	2000	-1.00
m (2h)	5500	-1.31

An air temperature of 22 °C and a relative humidity of 50% RH corresponds to a moisture content of 8.2 g/kg. One hour after the shower approximately 240 g moisture was extracted from the bathroom and after two hours approximately 340 g moisture was extracted.

In order to compare other results with this reference case a non-dimensional relationship is introduced as

$$F = \frac{\text{Measured value}}{\text{reference value*}} \quad \frac{(g/kg)}{(g/kg)} \quad (\%) \qquad (2)$$

* the reference value according to formula (1) for a certain moisture content in the supply air.

A decrease in airflow, to 10 l/s, was found to increase the variation in the measured points.

The opposite was found when the airflow increased.The reduction of relative humidity after one hour, was not easily observed except at 0.1 m in the room and in the exhaust air.

The airflow will effect the totally extracted moisture as shown in figure 3.6

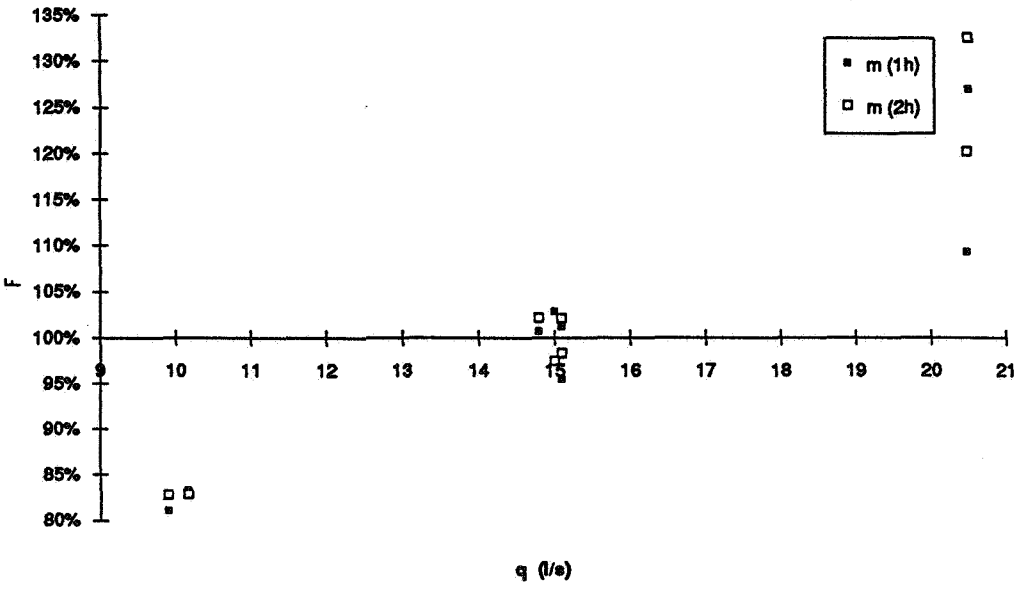

Figure 3.6 Totally extracted moisture (equation 2) after one and two hours as a function of airflows.

Increasing the airflow by 33% will give rise to an increase in the extracted moisture, after one hour with by 20% and after two hours 25% . A 33% decrease in airflow will reduce the extracted moisture with 17% compared with the extracted moisture for the reference airflow 15 l/s.

3.3 Moisture content in the air with space heating

The measurements were repeated with a centrally located infrared heater. As the bathroom module was not insulated these measurements do not have the same degree of accuracy. The extracted moisture content, in different locations, varied to a grat extent. The influence of totally extracted moisture and electric power is shown infigure 3.7

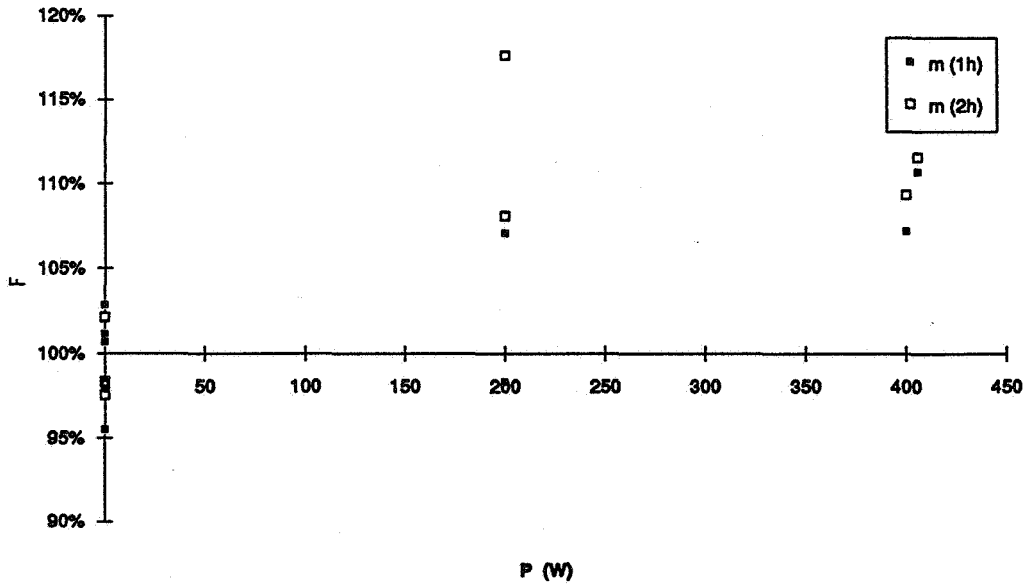

Figure 3.7 The relationship between the reference and the infrared heater case. Totally extracted moisture after one and two hours at different electrical power.

The electrical power corresponds to an air temperature , tr1.1 ,of 23 and 24 °C .

The measurements were also made with an electric radiator. As the moisture content in two of the measurements was very low, xin = 4.3 g/kg , the formula (1) will give higher inaccuracy. The influence of the air temperatures is shown in figure 3.8

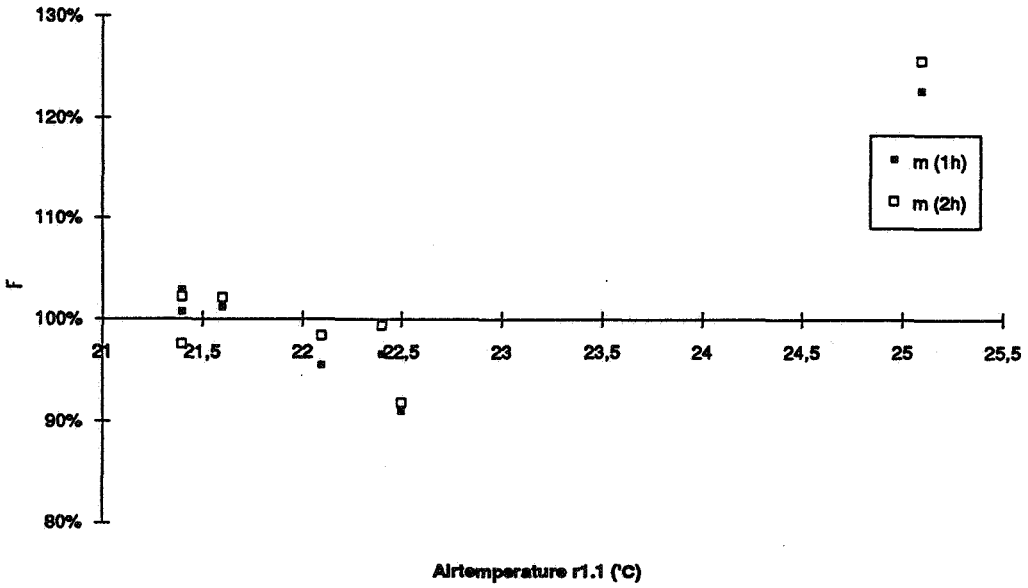

Figure 3.8 The relationship between the reference and the radiator case. Totally extracted moisture after one and two hours at different air temperature.(the air temperature of the radiator case is higher than 22.3 °C.

Between the cases with the infrared heater and the radiator only a small surface temperature difference was found.

4 Conclusions

The process of vafour production from the shower and evaporation from the wet surfaces will be different in different locations.

The maximum relative humidity, in a bathroom , is approximately constant at a given air temperature. This does not seem to be true for the measurement under the bath where the maximum moisture content was found constant. The test results also show that the moisture content , at one hour after a shower, is highly influenced by the moisture content in the supply air.

The most accurate measurement was made directly after the shower. The slope of the added moisture content show that the best results were found by increasing the airflow but the best advantage is the reduction of the vapour spread in the room.

The increased airflow did not have any effect of the moisture content in the middle of the room and under the bath. This was shown by the mean values of added moisture content in the air and in table 3.1 .

The totally extracted moisture was highly affected by an increased airflow as showed by the slope of the logarithmic added moisture-time curve.The use of an infrared heater also show a improved reduction of the moisture content in the middle the room and extracted moisture. No valid slope was found under the bath but the relative humidity found lower due to the increased temperature.The totally extracted moisture also indicate a smaller improvement.

The use of a radiator only showed a reduction of the moisture content in the middle of the room.

One hour after a shower approximately 240 g moisture is extracted and after two hours approximately 340 g moisture is extracted from the bathroom.

The extraction of moisture will be much lower during summer when the moisture content in the supply air is high.This will affect the time of wetness. The same amount of extracted moisture is achieved after one hour with a supply moisture content of 7 g/kg ,as after two hours with a moisture content of 9.5 g/kg.

To reduce the moisture problem in summertime it may be worth considering installing a dehumifier since an increased airflow only will give a small reduction.

Investigations have also been made to examine the effect of the supply air terminal device over the door,another location of the infrared heater and a reduction of the wet surface behind the bath by closing the slot around the bath. A final report is found in reference [4].

Further investigations are planed for a model of moisture content in the different locations of the room which combine the processes, ventilation, vapour from the shower and evaporation from the wet surfaces.

Acknowledgements

The author wishes to acknowledge the financial support of the Swedish Council for Building Research.

References

[1] Persson, Judit "Hygienrum etapp I" (An Investigation of different layouts of bathroom) Swedish Council for Building Research Report 6´88.

[2] Sundin, Johan "Ventilation i badrum" (An Investigation of ventilation in bathroom) KTH march 1989.

[3] Hansen Sten Olaf "Evaporation from swimming-pools" Proceeding of Roomvent, Oslo, Norway 1990.

[4] Fransson,Jan I "Hygienrum etapp II"(An Investigation of ventilation and humidity in a bathroom) Swedish Council for Building Research Report *´91.To be published.

[5]Nordtest Method "Buildings-Ventilation , local mean age"NT VVS 019

[6]Nordtest Method "Buildings-Ventilation , mean age of air"NT VVS 047

AIR MOVEMENT & VENTILATION CONTROL WITHIN BUILDINGS

12th AIVC Conference, Ottawa, Canada
24-27 September, 1991

POSTER 15

Demand Controlled Ventilation – Full Scale Tests in a Conference Room

Svein H Ruud, Per Fahlén, Helena Andersson

The Swedish National Testing and Research Institute
Box 857
S–501 15 Borås
Sweden
Tel: +46 33 165000 Fax: +46 33 131979

Synopsis

A conference room has been converted to temperature- and carbon dioxide controlled ventilation. A number of tests have been conducted with the system in different load conditions. The variables that have been measured are air flow rate, temperature and carbon dioxide concentration. The activity in the room during the measurements has also been well recorded. The main purpose has been to evaluate the ability of a demand controlled ventilation system to maintain a good indoor air quality.

The room is also acting as a reference field test installation for a simultaneously ongoing testprogram for sensors for demand controlled ventilation. From measurements on sensors for humidity and volatile organic compounds, conclusions have also been drawn about how suitable these sensors are for the purpose of demand controlled ventilation.

A simple system with temperature controlled air flow rate can in many cases be sufficient to achieve a well functioning demand controlled ventilation.

Carbon dioxide control seems to work very well and the output of the sensors has a very distinct and good correlation with the number of persons present in the room. The measured background/outdoor level is quite stable and the sensors do not show any great sensitivity to changes in temperatur, humidity or any other contamination in the air.

The relative humidity sensors are quite accurate and seem to bee very suitable for humidity control , but as their output is only slightly increased even for a large number of persons present and as the background/outdoor level can vary substantially and rapidly, they do not seem suitable for this type of demand controlled ventilation.

The sensors for volatile organic compounds are quite sensitive to the presence of persons, tobacco smoke and other contaminants produced in the room, but they are also very sensitive to changes in temperature/humidity and to changes in the contamination level in the outdoor air. Different sensors also have quite different outputs for the same air. The sensors seem to have a potential for demand controlled ventilation, especially when the main load is something other than heat sources and human related production of carbon dioxide, but further development of sensors and/or control system software is needed.

List of Abbreviations

AQ	Air Quality
CO_2	Carbon Dioxide
DCV	Demand Controlled Ventilation
IEA	International Energy Agency
RH	Relative Humidity
HVAC	Heating, Ventilation and Air Conditioning
VOC	Volatile Organic Compounds

1 Background

Within the framework of IEA Annex 18 "Demand Controlled Ventilating Systems" a number of research projects are being operated at present. The aim is to investigate the possibility to reduce energy consumption while maintaining a good indoor AQ. One of these projects is a full scale test of a DCV-system in a conference room situated at The Swedish National Testing & Research Institute.

2 Project Description

The conference room has been in use for about eight years. All furniture and other inventories are of about the same age. The room has a mixed ventilation system designed for a maximum of about 20 persons. A new HVAC-system, separated from the rest of the building, has been installed. The system is equipped with devices for heating, cooling and heat recovery. It has been especially designed to give a larger than usual span between maximum and minimum air flow rate. To regulate the air flow rate, the system is equipped with sensors for both temperature and CO_2. It is normally temperature regulated, but when the CO_2 concentration exceeds 700 ppm the system is CO_2 controlled. Both sensors are installed on one of the walls, 1.7 m above the floor. To avoid that the temperature sensor is influenced by heat from the CO_2-sensor, the sensors are placed several meters apart from each other.

A proposed "Method for Evaluation of Demand Controlled Ventilation" has been used as a guideline throughout the project. The above given air flow rates have been checked and the output voltage signal from the air terminal devices calibrated. The room-average air-change efficiency (RAACE) has been measured by means of CO_2-decline at two different air flow rates. RH- and CO_2-sensors have also been calibrated in the beginning and the end of the project. The VOC-sensors have only been checked functionally. These sensors all give an output signal between 0 and 10 volts, which we in the following will refer to as an indicated AQ of 0-100%. The energy consumption of the lighting can vary from 160 to1200 W.

Area:	43 m^2
Volume:	115m^3
Air flow span:	170-1000 m^3/h
RAACE:	46% (900 m^3/h), 64% (300 m^3/h)
(inlet temperature 5 °C below room temperature)	

The room has also been acting as a reference field test installation for a simultaneously ongoing testprogram for DCV-sensors. CO_2-sensors, RH-sensors and VOC-sensors have therefore been installed in a chamber connected to the exhaust air duct. It was planned to control the system with some of these sensors as well, but due to problems in getting a stable baselevel to regulate against these plans had to be abandoned.

The main purpose has been to evaluate the ability of a DCV-system to maintain a good indoor AQ. Measurements have only been made on the temperature- and CO_2 controlled system, but from simultaneous measurements on sensors for RH and VOC, conclusions have also been

drawn about how suitable these sensors are for the purpose of DCV.

The conference room is in rather limited use. Most of the time it is empty and when in use there are very seldom more than 10 persons present. Because of this the threshold level for CO_2–control is rarely exceeded. Instead of making long time measurements we have there–fore concentrated our measurements to 12 shorter periods of 6–12 hours. These periods have been chosen to cover different load conditions that are of interest. During the test periods the following parameters have been measured:

Air flow rate:	exhaust air
Temperatures:	inlet air, exhaust air, on one of the walls
RH:	exhaust air (9 sensors)
CO_2:	exhaust air (2 sensors), on one of the walls (1 sensor)
VOC:	exhaust air (6 sensors)

As most of the time the system is only temperature controlled, we have decided to include some results and conclusions from measurements on this as well.

A test is also conducted where the reaction of the sensors to tobacco smoke is studied. This is done at three different manually chosen air flow rates.

Calculations on energy savings are very much dependent on other system components than the DCV itself, what system you are comparing with and also how often the system is in use. Because of the very limited use of the actual system it has not been considered worthwhile to make any such calculations.

3 Full Scale Tests

3.1 Temperature Controlled Ventilation

Due to the heat produced by the human body itself and other heatsources that are activated when people are in the room, in this case mainly electric lighting, the system will react by in–creasing the air flow rate and decreasing the inlet air temperature. If the increase in air flow rate, due to the influence of the human body as a heat source, corresponds to the human need of fresh air, then a temperature controlled system vill theortically act just as a CO_2 controlled system. The problem is that the human beeing is very seldom the only heat source in a room and that these other heat sources can vary quite differently from the number of persons present. But if the main load is due to heat sources, then a simple temperature control is probably the best system and other more sofisticated systems are superfluous. We have in our case also noticed that the lighting is a heat source of the same magnitude as the heat from 10–15 persons. The lighting is therefore such a large heat source that it can force the system to increase the air flow rate all on its own.
Test No.7, that is shown in diagrams 1–3 below, is a good example of how the temperature control is working. During the test there was first a meeting with 4 persons going on for two hours, then a lunch break for one hour, then another meeting with 3 persons for one hour followed by a third meeting with 8 persons going on for half an hour. The lighting was

then turned off and the room was empty for the rest of the measurement periode. The lighting was also lowered after one hour of the first meeting and throughout the lunch break. Although the air flow rate never exceeded 350 m³/h the CO_2 concentration was always below 700 ppm and both the air quality and the thermal comfort were considered as good.

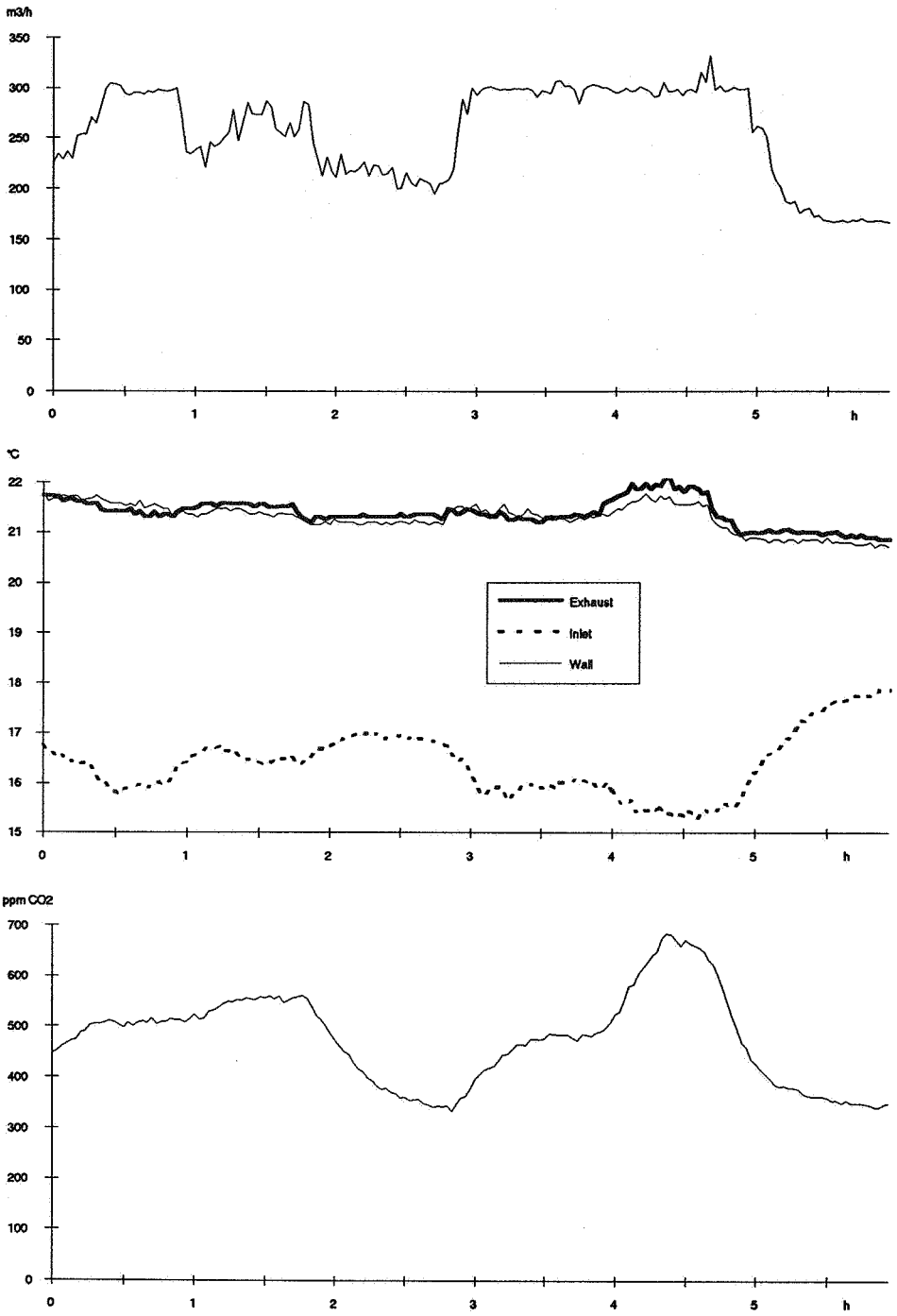

Diagrams 1–3; Air flow rate, temperatures and CO_2 concentration (test No.7).

The test presented above is for a low heat load condition. At medium loads we have had some problems with instability. Changes between half and full speed of the fans can then occur up to 6 times per hour, resulting in unpleasent sound and pressure shocks.In the next test that is

presented (No.11) this is exemplified by the system behaviour during the lunch break and for two hours after the last meeting.

3.2 Temperature- and CO_2 Controlled Ventilation

Test No.11, that is shown in the diagams 4–5 below, is a good example of how this system is working . When the measurment starts the room is empty, but people have been in the room for a very short while about half an hour before. This can bee seen on the CO_2 concentration which is a little bit higher than the background level (335 ppm according to the sensor) and slowly declining. After a little bit more than one hour and a half 24 persons enter the room attending a meeting for nearly two hours. Then there is a lunch break for one hour and a half, followed by a second meeting with the same people, going on for slightly more than one hour. The room is then left empty for the rest of the day. Lighting is on during the first 9 hours of measurement. The AQ and thermalcomfort are also this time considered as good.

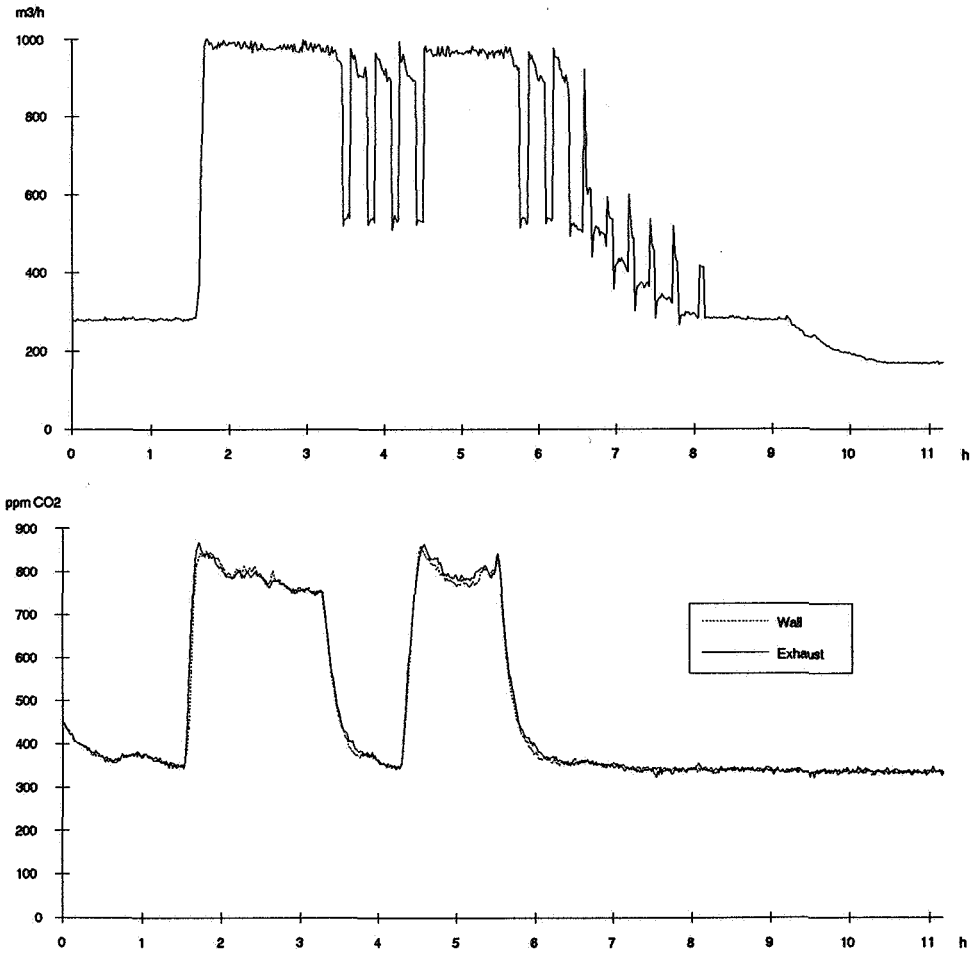

Diagrams 4–5; Air flow rate and CO_2 concentration (test No.11).

In diagram 5 above one can clearly see when people are entering and leaving the room. One can also see that there is no great difference between the sensor placed in the exhaust air duct and the one that is placed on one of the walls. This difference (exhaust conc. minus wall conc.) is more clearly shown in diagram 6 below.

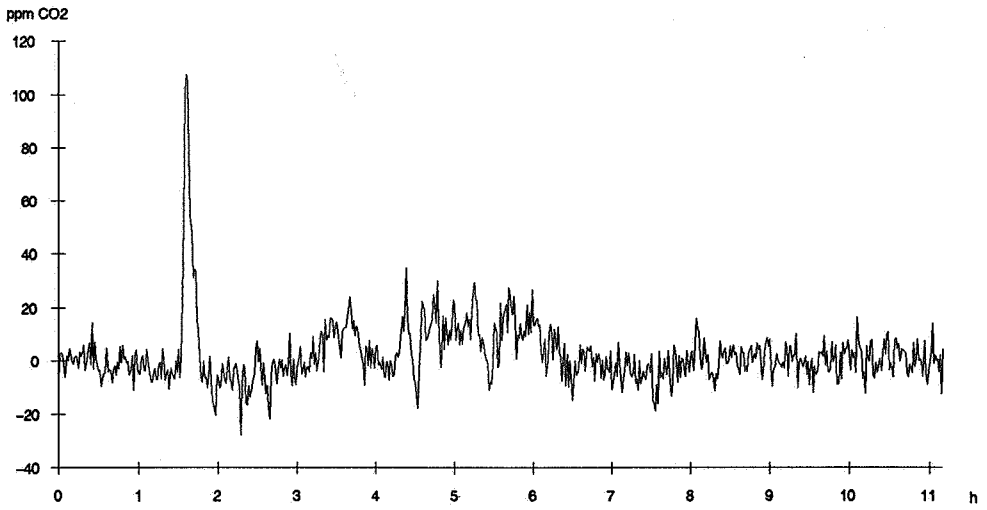

Diagram 6; Difference between CO_2–sensors in two different positions (test No.11).

This diagram shows that the difference between the two sensors most of the time is less than ±20 ppm. It is only during the beginning of the first meeting that the difference for a short while is a little bit more than 100 ppm. This particular sequence is more clearly seen in diagram 7 below. From this diagram one can see that the wall–mounted sensor has a delay of about 2 minutes.

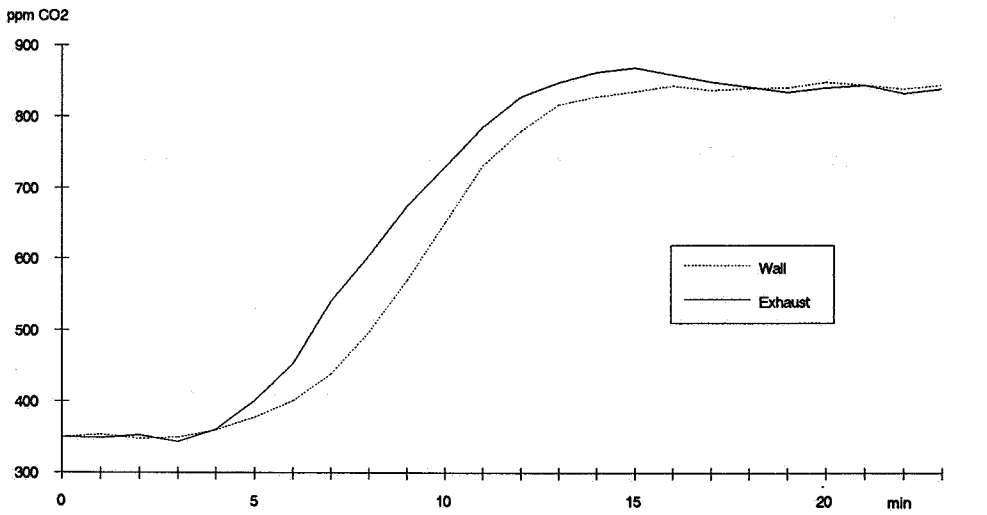

Diagram 7; Step–up for CO_2 –sensors in two different positions (test No.11).

In diagram 8 below the response curve of the flow rate is given together with the CO_2 concentration in the exhaust air. The result must be considered as very good. Especially as the system is controlled by the delayed sensor on the wall. A test with a simulated heatsource (1200 W lighting + 1200 W heat fan) does not give the same quick response at all.

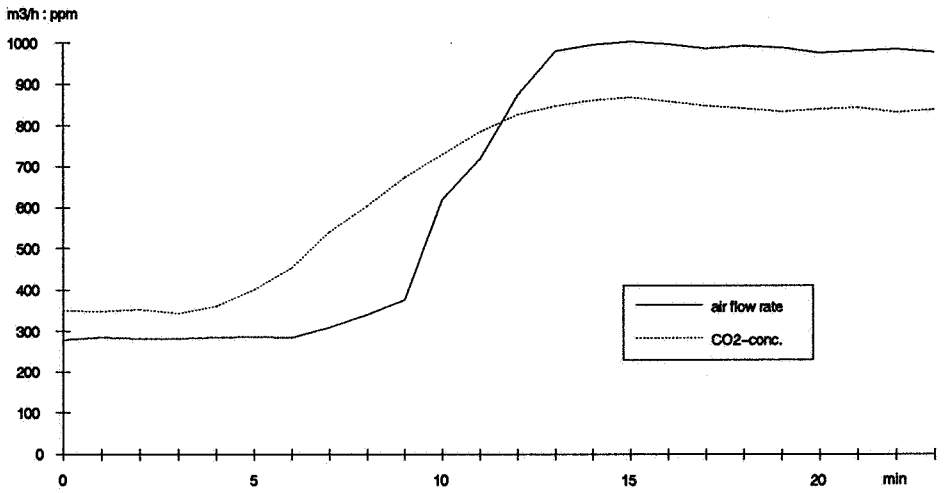

Diagram 8; Air flow rate and CO_2 conc., 24 persons enter the room (test No.11).

In diagram 9 below the measured background/outdoor CO_2 concentration during two different tests are shown. To what extent this variation is due to variations of the real concentration or variations in the sensor itself we do not know. The difference is in any case so small, compared with the response due to human presence, that it almost can be neglected.

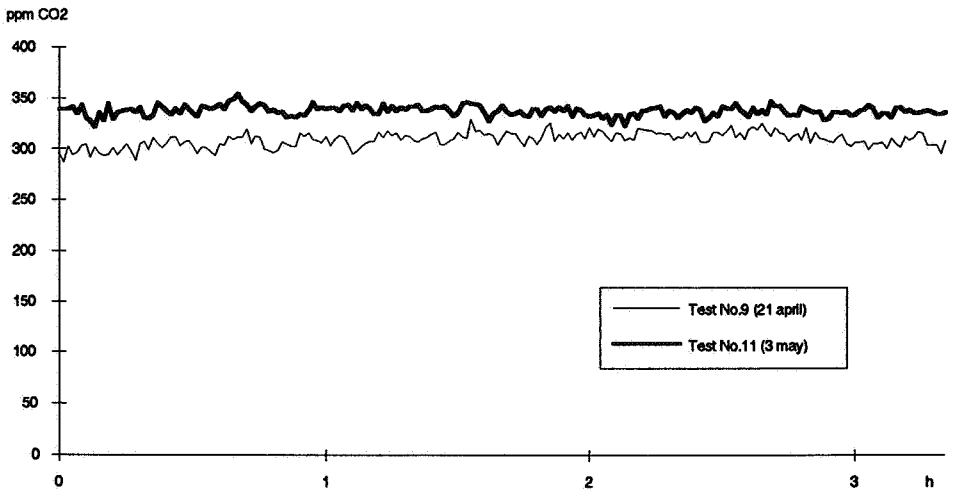

Diagram 9; Measured outdoor background CO_2 conc. during two different tests.

Note: We have in this context noticed some problems with one of the CO_2 sensor types. It has to be connected to the supply voltage for several days before the output signal reaches a long term stability. If the supply voltage exceeds the nominal voltage by more than 10% (not unusual), then it can cease to function. We therefore had to install a power resistor to keep the supply voltage down.

3.2 Humidity-sensor Measurements

Most of the RH-sensors have in the parallel laboratory testing project proven to be quite accurate. In our measurements all factory calibrated sensors but one are within a span of ± 5%RH. After our own calibration and curve fitting the results are even better. We have therefore chosen to present only curves for one sensor, but for three different tests. The results are given in diagram 10 below.

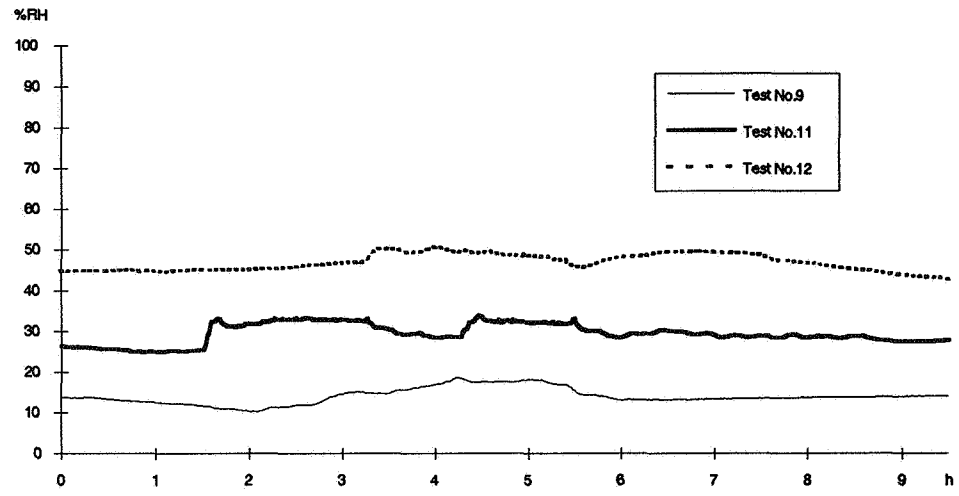

Diagram 10; Relative humidity during three different tests.

One can here clearly see the effect of human related humidificatin during test No.11. Calculations on the results indicates that about one third of the human energy consumption (30-40 W) goes into humidification of the air. During this test we have only very little variation in the background/outdoor RH level.

In test No. 9 the room is empty during the whole test. The variation in the background level is in this case of the same magnitude as was the effect of as many as 24 persons i test No.11.

Test No.12 is similar to test No.11, but the number of persons is now only 13-14 and due to simultaneous changes in the background level it is now impossible to distinguish when the meetings took place.

If one compares the different curves one can also see how much the background level can vary over a longer period of time.

If one wants to regulate the air flow rate with RH-sensors according to the number of persons present, then the RH and temperature must probably be measured both in the inlet and the exhaust air. The sensors will also have to be extremely sensitive and accurate. Finally some software must calculate the amount of humidity produced and regulate the air flow rate accordingly. One problem is that the humidification per person can vary quite much.

Another disadvantage with RH controlled DCV is that it does not react to smoke or any other source of contamination in the room.

3.3 VOC-sensor Measurements

A rather representative set of VOC-sensor curves are shown in diagram 11 below. They are also taken from test No.11 and one can clearly see the response to human presence. Sensors 4 and 16 represent more or less the behaviour of all but one VOC-sensor. That is, they have the same kind of response but at different levels and with different sensitivities. Sensor 3 behaves a little bit differently. It seems to react negatively to something that is produced in the room and is therefore going down to a lower level when the air flow rate is decreased. It can also bee of interest to notice that all sensors indicate lower AQ after lunch.

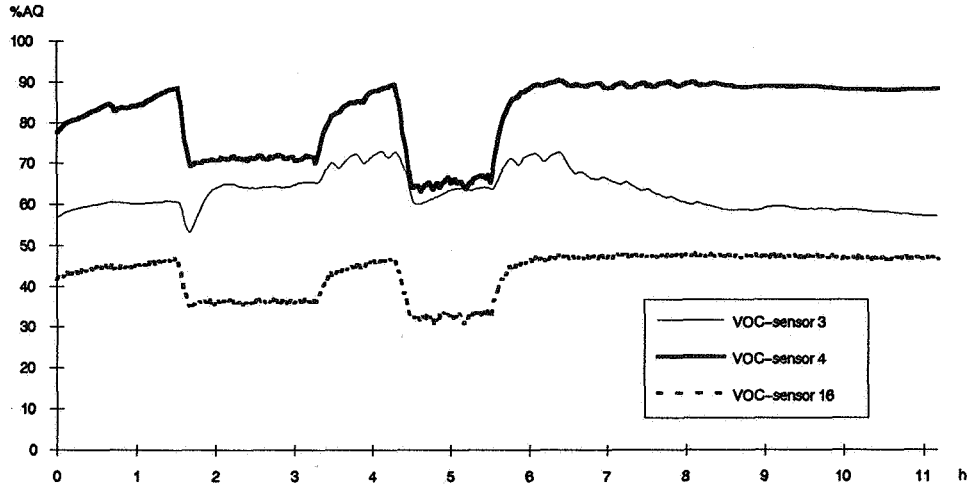

Diagram 11; The response of VOC-sensors to to human "load" (test No.11).

In diagram 12 below one can see that the sensors are sensitive to changes in temperature and RH. During the first two hours the temperature is increased, then for three hours everything but the RH (and possibly the outdoor AQ) is constant. One can also see that an overall decrease in RH results in an increased sensor-indicated AQ. For sensor 4 a RH below 20% makes it constantly indicate 100%AQ. Compare with diagrams 10-11.

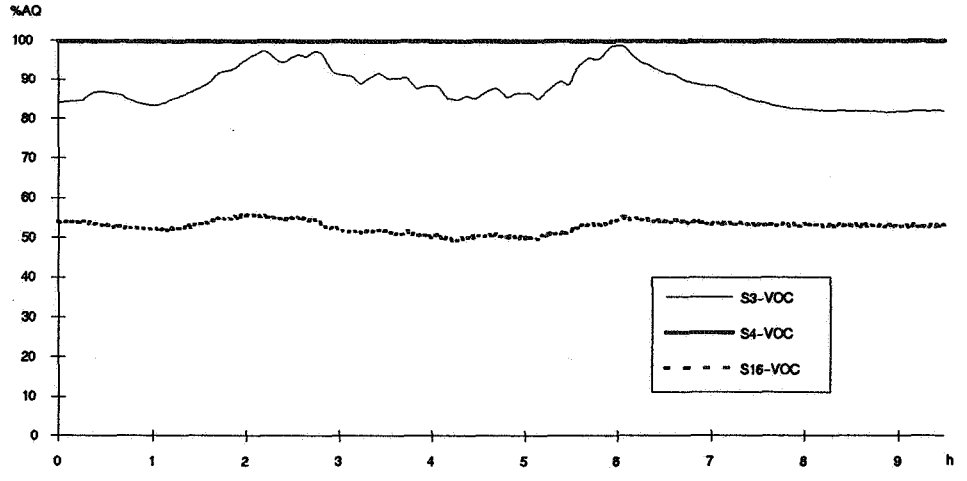

Diagram 12; The sensitivity of VOC-sensors to temperature and humidity (test No.9).

In diagram 13 below all other parameters (temperature, CO_2 concentration and RH) are held constant. This means that the variations of the VOC-sensors must be due to variations in the outdoor air. And if we look at the time when a decrease in AQ has occured, it correlates very well to people finishing their jobs in the afternoon. The decrease is therefore probably caused by contamination from cars that just have started up. There is a parking lot just outside the building and also a road with busy traffic at 16 pm and 17 pm. Sensor 3 is, unlike the other VOC-sensors, not sensitive to those outdoor variations. During functional tests with outdoor air, we have had atmospheric inversion and all sensors including sensor 3 were negatively affected (sensor3: 38%AQ, sensor4: 63%AQ, sensor 16: 26%AQ).

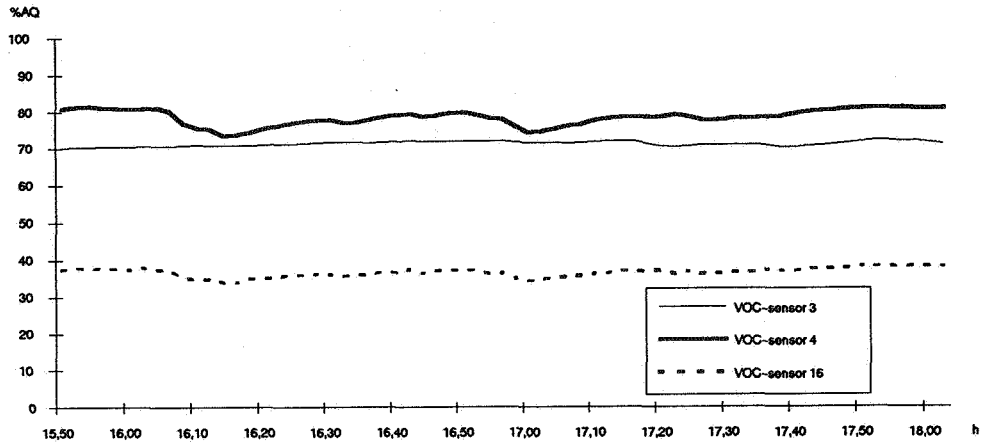

Diagram 13; Sensitivity of VOC-sensors to changes in the outdoor AQ (test No.2).

Sensor 16 was also equipped with a software that changes the output in three different steps. This can then be used to regulate the speed of the ventilation fans. Monitoring the outputs and recalculating them into three air flow rate steps in the range of 250 to 1000 m^3/h gives for test No.11 the result given in diagram 14 below. This indcates that there is room for improvements on the software. (See top of page 5 for explaination of the curve for the real air flow).

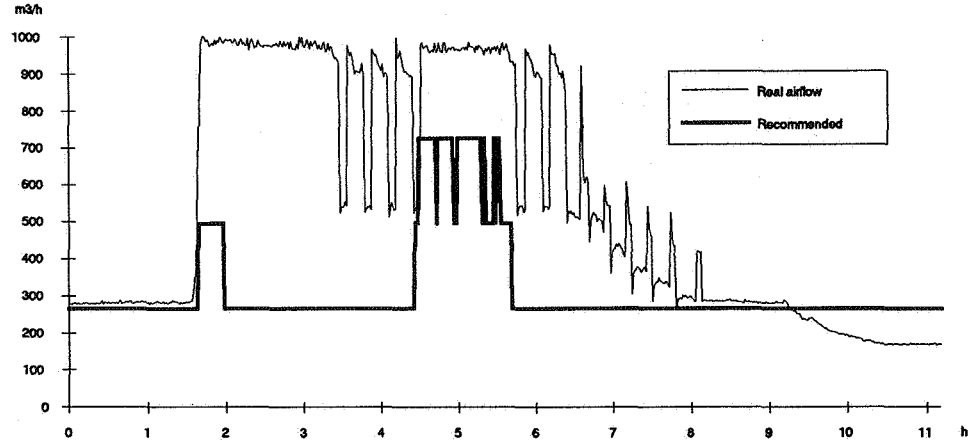

Diagram 14; Real air flow rate compared to that recommended by VOC-sensor 16 (test No.11).

VOC-sensors will probably have to be installed both in the inlet and the outlet air. Each pair (or more) of sensors will also have to be either nearly identical in behaviour or calibrated in such a way that some software can take care of the differences.

3.4 Smoke Test

A has been conducted with tobacco smoke. The temperature and RH were nearly constant during the whole test (20–21°C and 35–37%). The air flow rate was manually controlled to three different levels. The air flow rate, VOC–sensor output and CO_2 concentration during the test is shown in diagram 15–17 below. The test can be divided into 10 periods with different load conditions according to the following table.

period	1	2	3	4	5	6	7	8	9	10
start (hour.minute)	0.00	0.50	1.00	1.20	1.55	2.40	2.50	3.35	3.55	4.35
duration (minutes)	50	10	20	35	45	10	45	20	40	60
number of persons	0	0–7	7	7	6–7	7	5–7	6–7	7	0
number of cigarettes	0	0	0	12	0	0	10	0	8	0

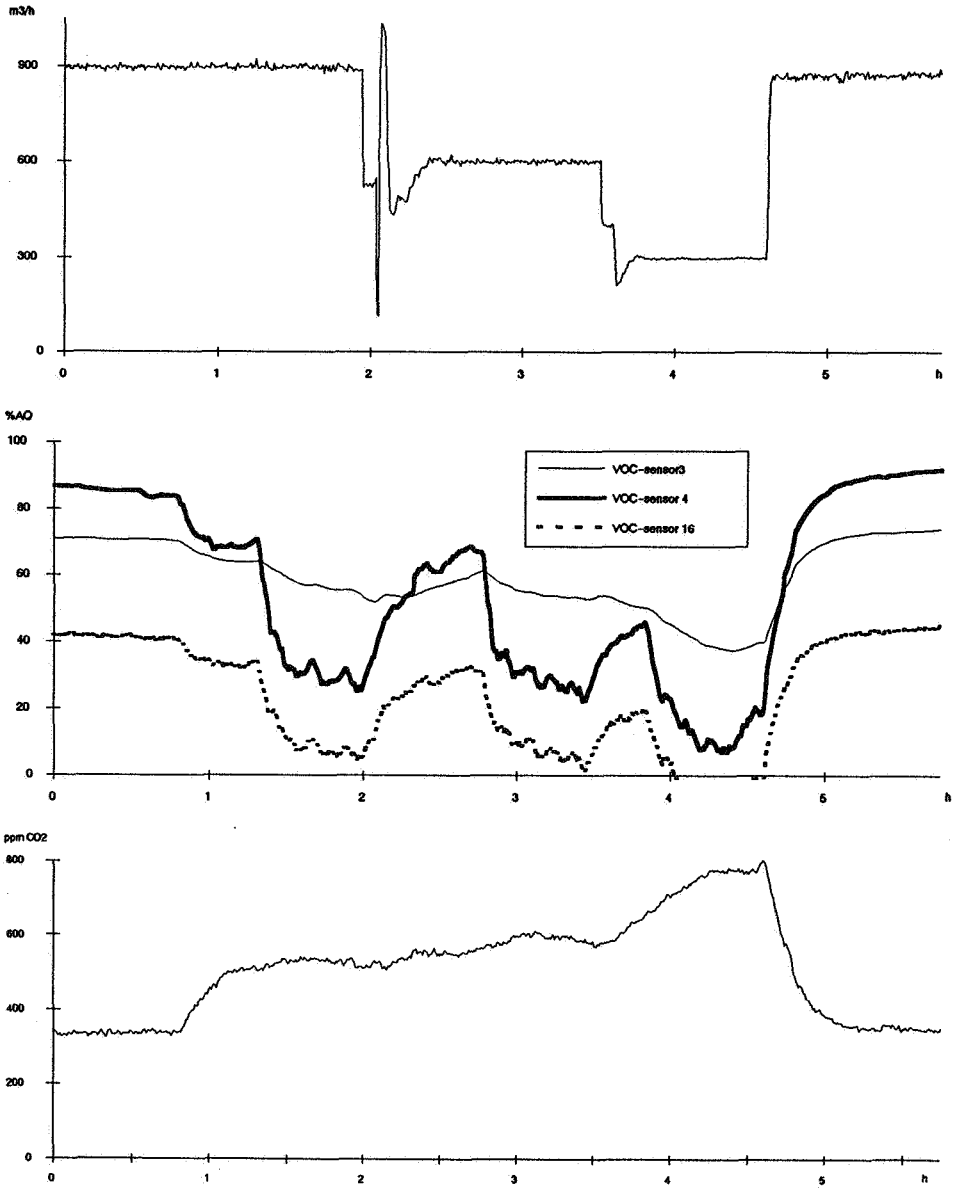

Diagrams 15–17; Air flow rate, VOC–sensor response and CO_2 conc. (test No.4)

One can clearly see the decrease in indicated AQ during the smoking periods. The AQ was considered as very poor during periode 7 and especially during periode 9.

Calculations on the response of the VOC–sensors give the result that the presence of one human beeing corresponds to smoking in the range of 0.2 to 1.0 cigarettes per hour.

It is also of interest to notice that the CO_2–sensor during the same period of time gave no significant indication about how poor the AQ really was. If the CO_2 control had been turned on it would only have been activated during period 9 and the increase in air flow rate to decrease the CO_2 concentration to 700 ppm would only result in a slight and insufficient increase of the AQ.

4 Conclusions

The sudied system seems to have a very good ability to maintain a good indoor AQ. The main problem with the system has been instability at medium heat loads.

The usefulness of DCV are very dependent on what kind of system it is installed in and how the system is used. Furthermore the kind of DCV–system that is the best depends on what the main load is.

If the main load may be of different types at different times, then a combination of different control variables can be necessary.

A simple system with temperature controlled air flow rate can in many cases be sufficient to achieve a well functioning DCV. If the main load is due to heat sources, then a simple temperature control is probably the best system and other more sofisticated systems superfluous.

The lighting and other heatsources are often of such a magnitude that they can not be neglected, especially if the air flow rate is temperature controlled.

The output of a CO_2–sensors has a very distinct and good correlation with the number of persons present in the room. The measured background/outdoor level is quite stable and the sensors does not show any great sensitivity to changes in temperatur, humidity or any other contamination in the air. The latter can be both good and bad. Insensitivity to tobacco smoke is, as we have seen, not a good desired characteristic in DCV–systems where smoking may occur..

The RH sensors are quite accurate and seem to bee very suiteable for humidity control, but as their output is only slightly increased even for a large number of persons present and as the background/outdoor level can vary substantially and rapidly they do not seem to be suitable for the kind of DCV that we have studed. The requirements on sensitivity and accuracy will probably be too extreme, making sensors to expensive.

The sensors for VOC are quite sensitive to the presence of persons, tobacco smoke and other contaminants produced in the room, but they are also very sensitive to changes in temperature/humidity and to changes in the contamination level in the outdoor air. Different sensors also have quite different outputs for the same air. The sensors seem to have a potential for demand controlled ventilation, especially when the main load is something other than heat sources and human related production of carbon dioxide, but further development of sensors and/or control system software is needed.

Except for simple temperature control, CO_2-sensor controlled systems seem to be the only on the market today that have been developed enough to be recommended.

Having a well functioning mixed ventilation system, it does not seem to matter much whether the sensor is placed in the exhaust air or on one of the walls.

Acknowledgements

The authors wish to acknowledge the financial support of the Swedish Council for Building Research and the Swedish National Board for Technical Development. The authors would also like to express their gratitude to the participating manufacturers of sensors as well as to the Fläkt AB who has delivered the ventilation system. Finally the authors would like to thank all those who have voluntarily participated as "loads" during the tests.

Note: A more detailed report from the measurements will be published later this year.

AIR MOVEMENT & VENTILATION CONTROL WITHIN BUILDINGS

12th AIVC Conference, Ottawa, Canada
24-27 September, 1991

POSTER 16

Demand Controlled Ventilation - Evaluation of commercially available sensors

Per Fahlén, Helena Andersson, Svein Ruud

The Swedish National Testing & Research Institute
Box 857
S-501 15 Borås
Sweden
Tel: +46 33 165000 Fax: +46 33 131979

Synopsis

A test programme has been designed to evaluate the performance characteristics of sensors for the automatic control of ventilation rates. The test programme consists of two main parts, one being the evaluation of sensor performance in laboratory tests and the other referring to long term characteristics of sensors in actual buildings. Included in the present evaluation are eight different types of humidity sensors, two carbon dioxide sensors and five mixed gas sensors.

The test results indicate that capacitive humidity sensors are well suited for the control of humidity levels in buildings. The combined error of linearity, hysteresis and repeatability is normally below 5% RH at 20 °C. The cross-sensitivity to variations in the ambient temperature and power supply (voltage and frequency) are acceptable and the cross sensitivity to hydrocarbons, carbon dioxide and tobacco smoke is negligible. A plastic stripe humidity sensor on the other hand proved unsuitable due to excessive hysteresis and linearity errors.

Carbon dioxide sensors show acceptable performance for control purposes but sensor calibration and/or adjustment is a time consuming process. These sensors are sensitive to humidity below a threshold value. The mixed gas sensors show a mixed behaviour. Some react strongly to tobacco smoke, some slightly and one hardly at all. The characteristic curve was determined using a gas cocktail consiting of equal parts of one alifatic HC, one aromatic HC and one aldehyde. Tests were also made with one component at a time but there was little difference in the response to the individual components.

All sensors endured the climatic tests reasonably well. Mechanical vibration on the other hand caused some of the sensors to break. Radiated electromagnetic fields affected all sensors and electric shocks, due to a simulated strike of lightning, proved too much for most of the sensors.

List of symbols and abbreviations

AQ	Air quality
ASD	Acceleration spectral density
DPT	Dew point temperature
f	frequency
HC	Hydrocarbon
IEA	International Energy Agency
RH	Relative humidity
RMS	Root mean square
SP	The Swedish National Testing & Research Institute
U	Voltage
VOC	Volatile organic compounds
WBT	Wet bulb temperature

1 Background

A fundamental prerequisite for demand controlled ventilation systems is the possibility to find a measurable "indicator" of the air quality. Another important factor is the existence of commercially available sensors for the measurand, which have acceptable sensitivity, accuracy, long term characteristica and price level.

Different types of "indicators" can provide different types of information concerning the ventilation requirements of a specific building. Furthermore, different types of sensors for the same "indicator" can give different results. Such sensors must be sensitive enough to detect changes in the air quality requiring increased or decreased supplies of outdoor air and simultaneously be stable enough to function satisfactorily over long periods in varying environments.

Hence it is of great value to increase our knowledge concerning questions such as

1) which "indicators" are suitable
2) which sensors are possible for the planned "indicators"
3) how do the different "indicators" read relative to each other
4) how do different sensors for one particular "indicator" read in the short term as well as in the long term.

2 Project description

Sensors for the following types of indicators (in accordance with the scope of IEA Annex 18) were included in a laboratory performance test:

* Water vapour (RH, WBT, DPT)
* Carbon dioxide
* Non-oxidized gases (VOC, e.g. C_mH_n, CO, etc).

The tests consist of two main parts. In the first part one specimen of each sensor type is extensively laboratory tested and in the second part one specimen of each sensor type is exposed to normal indoor climatic conditions (e g in an office building).

Thus two specimens of each sensor type are included. To limit the size and cost of the project, testing was planned for a maximum of fifteen sensors (seven for water vapour, three for carbon dioxide and five for non-oxidized gases). In the actual test it was not possible to include more than two carbon dioxide sensors due to time considerations. Several suppliers expressed an interest to participate in the test but only two actually delivered any sensors. Instead another humidity sensor was included to give the same total number of sensors.

This presentation pertains only to the laboratory part of the test program. The experience in using this test procedure has been reasonably good and thus a continuation of the project with other types of sensors is possible. Feed back from the tests however indicate a need to revise some of the procedures.

The laboratory tests consist of four main parts (see separate detailed description in chapter 3).

* Checking of the manufacturers' data sheets and instructions

* Determination of the performance of new sensors including comparisons with data sheets

* Determination of the cross-sensitivity of sensors exposed to various combinations of the three chosen indicators as well as variations in the power supply, atmospheric pressure, temperature and air velocity

* Environmental tests concerning exposure to dry heat, dry cold, humidity, temperature change, vibration, electromagnetic radiation and electrostatic discharge.

Results relating to the specific makes of sensors will be published when the entire project has been terminated. Before publication of the test results, the supplier/manufacturer of a sensor shall however be permitted to study the results and express his opinion.

3 Laboratory testing of DCV sensors

The test procedure consisted of four main parts as described in 2.1. In this chapter the detailed test procedure is described including presentation of some results. Sensors for the following indicators were tested:

* Water vapour (8 types)
* Carbon dioxide (2 types)
* Non-oxidized gases (5 types)

3.1 Sampling and preparation

Sensors were selected and tested by the respective manufacturer prior to delivery to SP. Special care was asked for regarding packaging and handling of the selected sensors in order to avoid unrepresentative test results due to delivery mishaps. All necessary instructions concerning general descriptions, installation, operation and maintenance were to be included in the delivery of the sensors. The sensors were installed in the laboratory as described by the manufacturer's instructions. The reference ambient testing conditions were considered to be (unless other values were specified in the individual test procedures):

Temperature: 20 ± 2 °C
Relative humidity: 40 ± 10 %
Pressure: 101 ± 1 kPa(a)
Air velocity: < 0.5 m/s
Supply voltage: Nominal ± 5 %
Supply frequency: Nominal ± 5 %
Air quality: Normal indoor air (CO_2 = 350 ± 50 ppm, VOC < 0.4 mg/m^3)

The test room was kept free of strong electric or magnetic fields and the input power to the sensors was supplied via magnetic stabilizers (except during tests with electromagnetic radiation).

The reference gas for testing VOC-sensors was composed of the following constituents:

1 aldehyde (Octanal, $C_7H_{15}CHO$):
1 aromatic HC (Toluene, C_7H_8)
1 aliphatic HC (Nonane, C_9H_{20})

These substances were intended to represent organic compounds that are frequently found in the analysis of air from e.g. office buildings.

3.2 Data sheets and general information

A standardized data sheet for the presentation of sensor characteristica was proposed. Prior to the test the manufacturers were asked to fill in the data asked for in this data sheet. This information was noted as background information to be compared with the test results.

3.3 Determination of the performance of new sensors

The sensor performance has been defined in terms of the following parameters,

* Warming up time
* Zero drift
* Linearity
* Repeatability
* Hysteresis
* Stability
* Accuracy
* Sensitivity
* Rise time
* Sensitivity to influence factors (cross-sensitivity).

3.3.1 Warming up time

The intention was to measure the warming up time by inserting the sensor into a test chamber with all parameters, except for the primary measurand, at the reference conditions (see 3.1). The measurand (e.g. humidity) was held constant at a value corresponding to an output signal of 40-60 % of the measuring range of the sensor. The sensor was then left 24 h with the power switched off. The power was then switched on and the sensor output was measured. The time from switching on the power supply until the output was stable within the claimed uncertainty of measurement was recorded as the warming up time.

One half of the humidity sensors had negligible warming up times (less than 30 s). The other half of the humidity sensors had sizeable warming up times, e.g. no. S9 (2000 s), S12 (4000 s), S14 (1800 s) and S15 (4000 s). The VOC-sensors on the other hand have two different warming up times, one after a short interruption of the power supply and one after the heated sensing element has been permitted to cool down. These were not determined in this investigation but the long term warming up time may be as long as a fortnight or even up to a month according to the manufacturer.

3.3.2 Determination of the sensor characteristic curve

The output from the tested sensors were recorded for values of the measurand according to table 3.1.

Table 3.1. Values for determination of the sensor characteristic curve

Measurand	1	2	3	4	5	6	7	8	9
Relative humidity (%)	-	20	40	60	80	60	40	20	-
Carbon dioxide (ppm)	200	500	1000	1500	2000	1500	1000	500	200
VOC (mg/m^3)	0	0.5	1.0	1.5	2.0	1.5	1.0	0.5	0

The VOC-cocktail is normally composed of equal parts of the three constituents. At test point 3 (1.0 mg/m^3) tests were also performed with the total concentration consisting of only one of the reference gases at a time. It was found that for this particular cocktail, and with these particular sensor types, changing the composition had no significant influence on the result.

The VOC-sensors were not possible to test in a closed system as planned originally. The sensors were encased in plastic housings with emissions substantial enough to cause a continuous increase in the VOC-level if left in a closed tank. Instead outdoor air was supplied continually to the tank and a specified amount of the VOC-cocktail was evaporated into this air flow. As can be seen from examples of the characteristic curves for VOC-sensors in diagram 3.1 the behaviour of different sensors may be markedly different even though the sensing elements come from the same manufacturer.

Linearity is calculated as the maximum deviation between any measured value and a straight line between points 2 and 5 in table 3.1. Hysteresis is calculated as the maximum deviation between points 2 and 8, 3 and 7, 4 and 6. Finally the sensitivity is calculated as the change in output between points 3 and 4 in table 3.1, divided by the corresponding change in input (e.g. V/% RH). The results obtained are presented in table 3.2 below. Sensor no. S14 is equipped with two sensing elements, one for humidity and one for VOC.

Table 3.2. Results from determinations of the sensor characteristic curve.

Sensor no.	Linearity	Hysteresis	Sensitivity
S1 VOC	1 (%AQ)	0.9 (%AQ)	0.28 (V/ mg/ m^3)
S2 VOC	-*	-*	-*
S3 VOC	-*	-*	-*
S4 VOC	3.5 (%AQ)	0.3 (%AQ)	0.046 (V/ mg/ m^3)
S5 CO2	98 (ppm CO_2)	18 (ppm CO_2)	0.0038 (V/ ppm CO_2)
S6 CO2	26 (ppm CO_2)	21 (ppm CO_2)	0.0047 (V/ ppm CO_2)
S7 RH	0.9 (%RH)	0.8 (%RH)	0.15 (mA/ %RH)
S8 RH	0.6 (%RH)	0.8 (%RH)	0.0097 (V/ %RH)
S9 RH	0.1 (%RH)	3 (%RH)	0.084 (V/ %RH)
S10 RH	11 (%RH)	15 (%RH)	0.071 (V/ %RH)
S11 RH	0.4 (%RH)	1 (%RH)	0.15 (mA/ %RH)
S12 RH	0.3 (%RH)	0.9 (%RH)	0.16 (mA/ %RH)
S13 RH	0.4 (%RH)	0.8 (%RH)	0.15 (mA/ %RH)
S14 RH/ VOC	3.5 / 2.2 (%RH / ppm CO_2)	0.3 / 1.4 (%RH / ppm CO_2)	0.0073 (V/ %RH)/ 0.098 (V/mg/m^3)
S15 RH	2.4 (%RH)	2.3 (%RH)	0.098 (V/ %RH)

* The response of the sensor was too small to be significant or the results were inconclusive.

A special problem with the use of an open system is that the the quality of the outdoor air is beyond the control of the experimenter. Figure 3.2 illustrates this problem clearly. The supply air to the test set up is being fed with a constant level of 3.5 mg/m^3 of toluene. Initially the output of the sensor is constant but at a specific time, which corresponds to the end of the working day, the indicated air quality deteriorates. This is the result of people starting their cars to go home. This is also an illustration of one of the problems in controlling ventilation flowrates using a VOC-sensor. In this case the sensor would have signalled to the ventilation system to increase the outdoor air flow even though the outdoor air was the source of the decreased air quality.

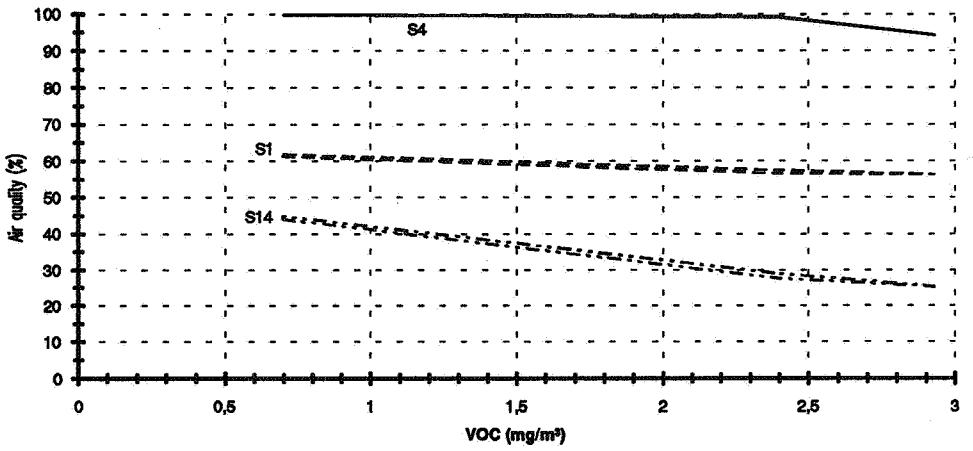

Figure 3.1. One example of output signals in terms of "percentage air quality" for sensors S1 , S4 and S14 as a function of the VOC-level in mg/m^3.

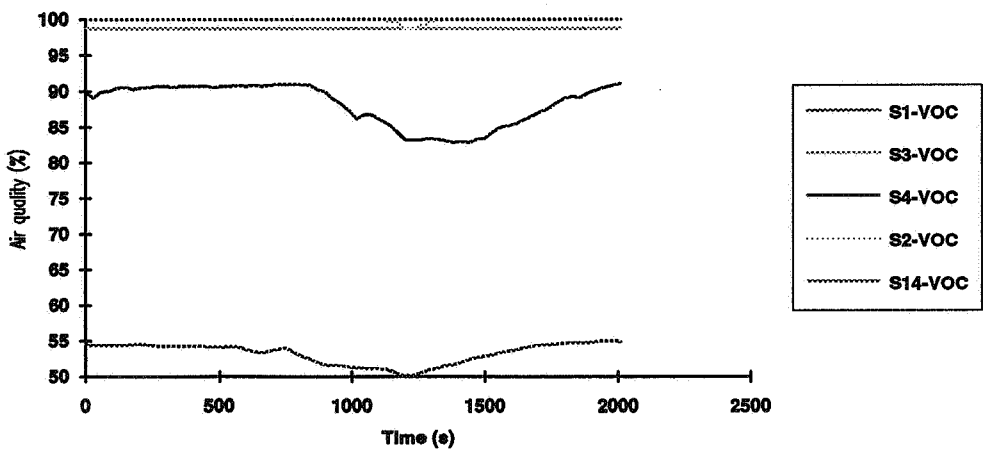

Figure 3.2. Output signals in terms of "percentage air quality" for sensors S1-S4 and S14 as a function of time. The VOC-level was aimed at 3.5 mg/m^3 but the background level changes after 800 s.

VOC-sensors were also tested with tobacco smoke corresponding to two levels of smoke concentration at each of three different flowrates (minimum flow for a non-smoking environment, minimum flow for a smoking environment and the maximum flowrate of the system). Cigarettes were smoked by an "artificial smoker" to achieve a reproducible test. In figure 3.3 the response of CO_2-sensors (S0, S5 and S6) and VOC-sensors (S1, S2, S3, and S4) are shown for the case of 1 0 cigarettes smoked simultaneously at a condition of minimum ventilation rate for a non-smoking environment. The diagram indicates that although this is a case of extreme smoke pollution one of the VOC-sensors does not react at all and one only reacts to a very small extent.

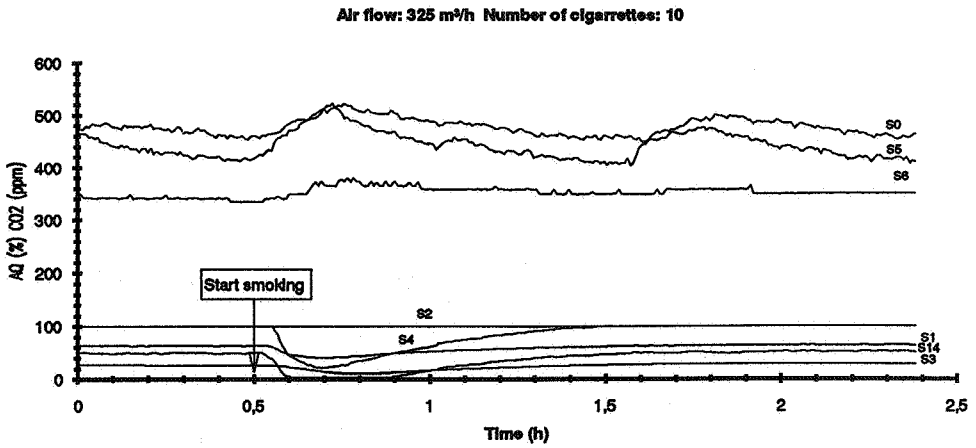

Figure 3.3. Response of CO_2-sensors (S0, S5 and S6) and VOC-sensors (S1, S2, S3, and S4) when 10 cigarettes are smoked simultaneously at a condition of minimum ventilation rate for a non-smoking environment.

In figure 3.4 the characteristic curve for the two CO_2-sensors are shown and in figure 3.5 results for three of the humidity sensors are presented. As can be seen in figure 3.5 there is a considerable difference in linearity and hysteresis between sensors S7 and S8 (capacitive) on the one hand and sensor S10 (plastic stripe) on the other hand.

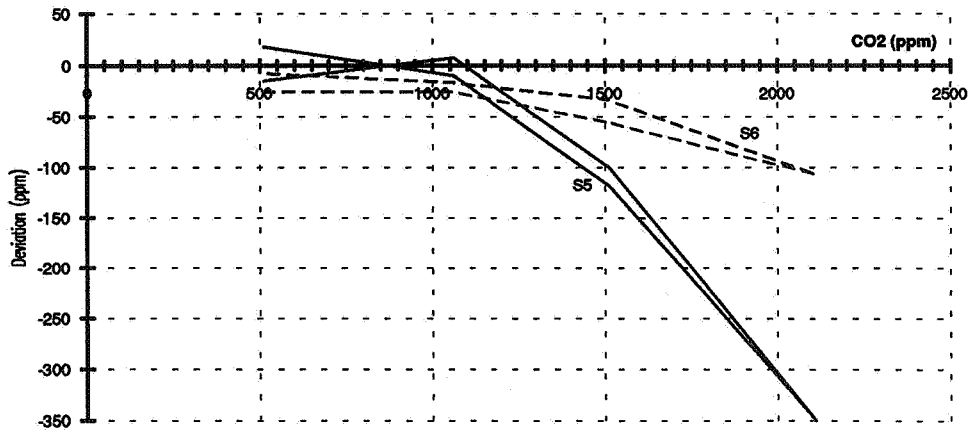

Figure 3.4. Characteristic curves for the two CO_2-sensors S5 and S6.

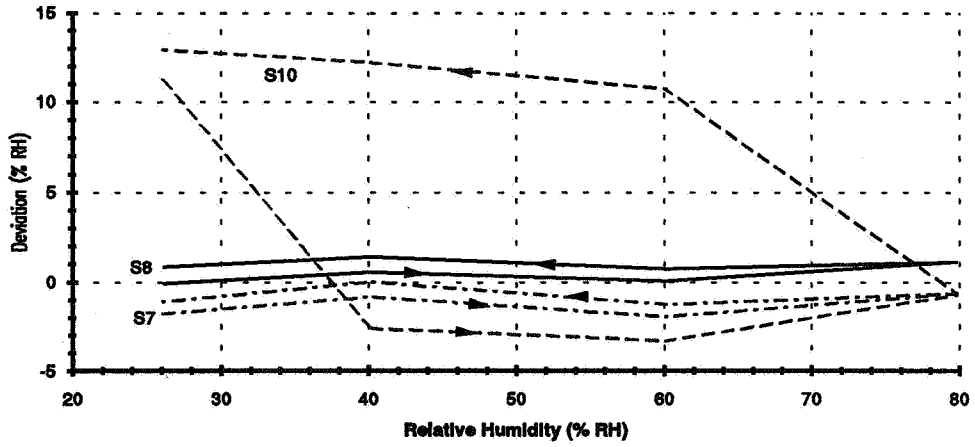

Figure 3.5. Characteristic curves for three humidity sensors (S7, S8 and S10).

3.3.3 Repeatability and stability

The sensors were tested at points 2 and 5 in table 3.1 alternatively 5 times. The repeatability is the maximum deviation between any measured value and the corresponding measured value in 3.3.2. To evaluate the stability of the sensors they were kept at point 4 in table 3.1 for 24 hours. The stability is the maximum deviation between any measured value and the initial value. Results from determinations of repeatability and stability for humidity sensors are presented in table 3.3.

Table 3.3. Results from determinations of repeatability and stability.

Sensor no.	Repeatability (%RH)	Stability (%RH)
S7 RH	0.3	0.3
S8 RH	0.3	0.2
S9 RH	1.9	0.2
S10 RH	0.8	0.2
S11 RH	0.9	0.6
S12 RH	0.6	0.3
S13 RH	0.3	0.3
S14 RH/ VOC	0.3 / -	0.4 / -
S15 RH	0.2	0.1

3.3.4 Rise time

The sensor input was changed from point 2 to point 4 and then from point 4 to point 2. The rise time and fall time respectively were calculated as the time between a change of input until the output has changed to 90 % of the steady state value. The air flowrate passing the sensor during the test was to be specified by the manufacturer. If no specification was made, the flowrate used was 3 m/s for sensors mounted in ducts and less than 0.15 m/s for wall mounted units.

The rise times of most humidity sensors were quite short. Therefore the test will have to be repeated with a measuring system using a higher time resolution. Rise times for carbon dioxide and VOC-sensors have not yet been evaluated.

3.3.6 Cross-sensitivity

The sensitivity of the sensor to various influence quantities is tested by varying each influence quantity, one at a time, according to table 3.4.

Table 3.4. Variation of influence factors.

Influence factor	1	2	3	4	5	6	7	8	9	10	11	12	13	14
Temp., (°C)	20	30	10	20	20	20	20	20	20	20	20	20	20	20
RH, (%)	40	40	40	80	20	40	40	40	40	40	40	40	40	40
Voltage, (U/Un)	1.0	1.0	1.0	1.0	1.0	1.2	0.8	1.0	1.0	1.0	1.0	1.0	1.0	1.0
Freq., (f/fn)	1.0	1.0	1.0	1.0	1.0	1.0	1.0	1.1	0.9	1.0	1.0	1.0	1.0	1.0
Pressure, (kPa)	101	101	101	101	101	101	101	101	101	105	97	101	101	101
CO_2, (ppm)	500	500	500	500	500	500	500	500	500	500	500	1000	500	500
VOC, (mg/m^3)	0	0	0	0	0	0	0	0	0	0	0	0	1	0
Tobacco smoke	No	No	No	No	No	No	No	No	No	No	No	No	No	Yes

The cross-sensitivity is given for each influence factor as the ratio between total change in output and total change in input. Test results are indicated in table 3.5 expressed as the change in output relative to the nominal operating point. The response to tobacco smoke is only indicated qualitatively by "yes" or "no".

Table 3.5. Results from the cross-sensitivity test.

Sensor no.	Voltage (unit/ V)	Frequency (unit/ Hz)	Temperature (unit/ K)	Rel. humidity (unit/ % RH)	Air pressure (unit/ hPa)	CO_2 (unit/ ppm CO2)	VOC (unit/ mg/ m^3)	Cig. smoke (yes or no)
S1 VOC (%AQ)	0.2	0.1	0.1	0.2	-*	-*	-	yes
S2 VOC (%AQ)	-*	-*	-*	-*	-*	-*	-	yes?
S3 VOC (%AQ)	-*	-*	-*	-*	-*	-*	-	yes
S4 VOC (%AQ)	0.7	0.3	1.5	0.6	-*	-*	-	yes
S5 CO2 (ppm)	3.2	-18	7.1	2.6	0.0	-	-*	yes
S6 CO2 (ppm)	-57	-0.2	4.7	0.1	0.4	-	-*	yes
S7 RH (%RH)	0.0	0.0	0.1	-	0.0	0.0	0.0	no
S8 RH (%RH)	0.0	0.0	0.1	-	0.0	0.0	0.0	no
S9 RH (%RH)	0.1	0.0	0.2	-	0.0	0.0	0.1	no
S10 RH (%RH)	0.0	0.0	0.4	-	0.0	0.0	0.0	no
S11 RH (%RH)	0.1	0.0	0.1	-	0.0	0.0	0.1	no
S12 RH (%RH)	0.0	0.0	0.0	-	0.0	0.0	0.0	no
S13 RH (%RH)	0.0	0.0	-0.1	-	0.0	0.0	0.0	no
S14 (%RH) /(%AQ)	0.0 /0.0	0 /0.3	0.1 /0.0	- /0.0	0 /-	0.0 /-	0.1 /-	no / yes
S15 RH	4.9	0.0	0.3	-	0.0	0.0	0.1	no

* The response of the sensor was too small to be significant or the results were inconclusive.

3.4 Environmental tests

Environmental tests were performed to check the resistance of a sensor to possible extreme situations in the environment within the field of application of the sensor. Tests were carried out concerning

* Climatic parameters
* Mechanical parameters
* Electrical parameters.

3.4.1 Climatic parameters

Climatic tests were performed in accordance with IEC standards on low temperature, dry heat, damp heat and change of temperature. **IEC 68-2-1, Test Ad**, was used for the low temperature test. The sensors were exposed to a temperature of +5 °C for a duration of 16 hours.

This test seemed to have little effect on the sensors and all survived. Concerning the sensitivity of the actual output signal reference is made to table 3.5 regarding temperature as an influence parameter.

The next step was to expose the sensors to a temperature of 55 °C for a duration of 72 hours as specified in **IEC 68-2-2, Test Bd**, dry heat. Functional tests were carried out at an intermediate temperature of 40 °C. This test also seemed to have little effect on the sensors and all were still functioning after the test. Concerning the sensitivity of the actual output signal reference is again made to table 3.5, this time regarding temperature as an influence parameter.

Damp heat was tested as prescribed by **IEC 68-2, steady state, Test Ca**. The temperature selected was 40 °C at a humidity level of 93 %. The duration of the test was 21 days. None of the sensors showed any signs of significant deterioration due to this test. Concerning the sensitivity of the actual output signal reference is made to table 3.5 regarding humidity as an influence parameter.

The effect of a cyclic change in temperature was investigated according to **IEC 68-2-14, Test Nb**. The temperature was cycled between a low level of +5 °C and a high level of + 40 °C. The rate of change of temperature was 5 °C/min, the number of cycles was 5 and the exposure time was 3 h. Results show that all sensors pulled through also during this test.

In addition humidity sensors will be checked functionally after storing the sensors at -10 °C with the power switched off for 24 h. The ambient conditions will then be changed to +20 °C with a relative humidity of 80 % in less than 10 minutes. This test is yet to be carried out.

3.4.2 Mechanical parameters

Mechanical tests were performed in accordance with the IEC standard on random vibration, **IEC 68-2-36, Test Fdb.** The equipment was mounted on the vibrator using its normal means of mounting, e.g. flanges and screws. Tests were repeated for each of the three perpendicular axes of the equipment and a functional check was performed after exposure to:

ASD 10-20 Hz: 0.5 g^2/Hz
ASD 20-500 Hz: -3 dB/octave.

The total rms acceleration was 1.9 g for a duration per axis of 90 minutes. One CO_2-sensor (S5) and two humidity sensors (S12 and S14) broke during this test.

3.4.3 Electrical parameters

Electrical tests were performed in accordance with IEC standards on conducted bursts, electrostatic discharge, electromagnetic radiation and surge voltage immunity. Conducted transient bursts were tested according to **IEC 801-4.** In this test each group of signal cables was exposed to transients using capacitive coupling boxes for each group. At least 2 minutes of both polarities were used for testing of each group. All exposures were repeated for each specified functional mode of the equipment with a voltage amplitude of 4 kV.

Most sensors were greatly affected during the actual transient burst. The output of one humidity sensor (S15) changed from 1 V to -10 V and another (S13) changed from 3.8 V to 25 V. The remaining CO_2-sensor changed its output from 10.3 V to 40 V and then slowly died altogether. Humidity sensor no S10 was also irretrievably damaged by this test.

Electrostatic discharges were applied as described by **IEC 801-2.** The test generator, charged to a voltage of 8 kV, was approached to points on the test object normally accessible to the operator. Ten discharges were applied on each preselected point and the test was repeated for each functional mode of the equipment. During the electrostatic discharge there was little change in the output signals of the sensors. However three further sensors (S3, S9 and S13) did not pass this test and thus only seven of the fifteen sensors remained for the test with radiated interference.

This test consisted of exposing the sensors to radiated electromagnetic fields as specified in **IEC 801-3.** The sensors were submitted to electromagnetic radiation with a field strength of 10 V/m with the frequency changing from 27 to 500 MHz while the correct function was checked continuously. When disturbances occured the frequency was recorded. The test was repeated for each functional mode. The results clearly indicate that this type of interference is a potential source of trouble. Even though the behaviour of individual sensors was quite different in detail all of them changed their outputs by several orders of magnitude at specific frequencies or frequency ranges.

For the final electrical test, i.e. surge voltage immunity ("thunder"), seven sensors (S1, S2, S4, S7, S8, S11 and S15) remained. The test was carried out as outlined in the draft proposal IEC 801-5 DP and the voltage used was 2 kV.

As a result of this final test three more sensors (S2, S4 and S15) were irrevocably damaged. Thus as a final result of all the environmental testing there was a total of four surviving sensors.

3.5 Final test

The sensor outputs of the surviving four sensors were checked in accordance with table 1 in chapter 3. The results for two of the sensors are shown in figure 3.6 . Sensor no. S8 has endured all tests extremely well whereas sensor no. S7 has survived but changed its output at low humidities considerably. This is probably due to a change in off-set voltage.

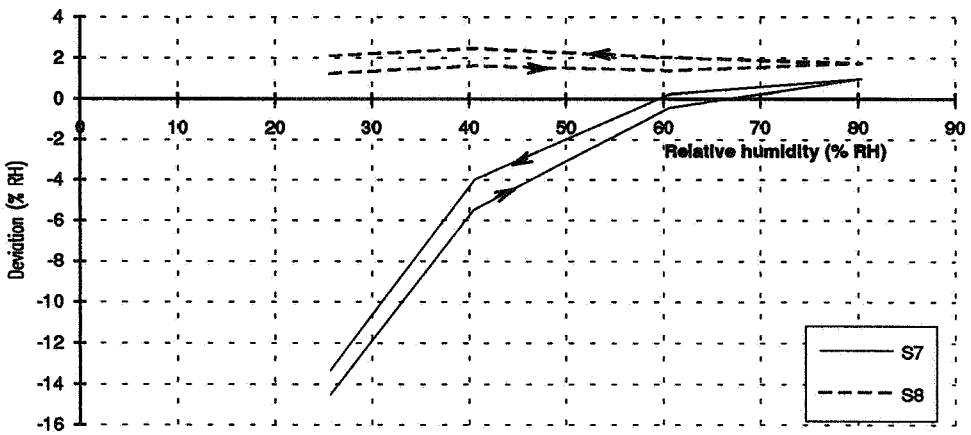

Figure 3.6. The characteristic curves of humidity sensors S7 and S8 after the environmental testing. These curves can be compared with the corresponding curves in figure 3.5.

4 Conclusion

The test results indicate that capacitive humidity sensors are well suited for the control of humidity levels in buildings. The combined error of linearity, hysteresis and repeatability is normally below 5% RH at 20 °C. The cross-sensitivity to variations in the ambient temperature and power supply (voltage and frequency) are acceptable and the cross-sensitivity to hydrocarbons, carbon dioxide and tobacco smoke is negligible. A plastic stripe humidity sensor on the other hand proved less suitable due to excessive hysteresis and linearity errors.

Carbon dioxide sensors show acceptable performance for control purposes with a deviation of less than 30 ppm at a level of 1000 ppm. Sensor calibration and/or adjustment is however a time consuming process. These sensors are also sensitive to humidity below a threshold carbon dioxide level. The mixed gas sensors show a mixed behaviour. Some react strongly to tobacco smoke, some slightly and one hardly at all. On the other hand all of them seem quite sensitive to humidity. Tests with varying compositions of the chosen VOC-cocktail indicated little difference in the response to the individual components.

All sensors endured the climatic tests reasonably well. Mechanical vibration on the other hand caused some of the sensors to break. Radiated electromagnetic fields affected all sensors and the electric shock due to a simulated strike of lightning proved too much for most of the sensors.

The environmental tests were decisive in the respect that only four out of fifteen sensors survived all of the tests. These results notwithstanding the test conditions were chosen to represent favourable operating situations that e.g. household electronics may encounter. It must however be born in mind that laboratory tests are one thing and the facts of real world situations may be quite a different cup of tea. Future in situ evaluations will hopefully provide further useful information in this respect.

Acknowledgements

The authors wish to acknowlege the financial support of the Swedish Council for Building Research and the Swedish National Board for Technical Development. The authors would also like to express their gratitude to the participating manufacturers of sensors as well as to the Swedish Tobacco Company for the use of the "artificial smoker".

AIR MOVEMENT & VENTILATION CONTROL WITHIN BUILDINGS

12th AIVC Conference, Ottawa, Canada
24-27 September, 1991

POSTER 17

Should Future HVAC-Systems be Demand Controlled?

W. Braun

Geilinger Ldt
Grüzefeldstr. 47
CH-8401 Winterthur, Switzerland

Should Future HVAC-Systems be Demand Controlled?

W. Braun, Geilinger Ldt
Grüzefeldstr. 47
CH-8401 Winterthur, Switzerland

Abstract

Demand controlled HVAC-systems have many advantages. The principle is to optimize comfort and to minimize energy consumption simultaneously.

In modern office buildings, indoor temperature is very often a useful control parameter. The question is, wheather it should govern the system for each room individually or for a zone. In the latter case: how shall the zones be defined? Above all, performance criteria have to be weighed against the investment cost.

This paper discusses different strategies, which have been or are going to be realized for office buildings. The results are from computer simulations and show the fields of application. The investigation concentrates on ceiling cooling by a water system (which is part of combined water/air HVAC-system).

1. Introduction

In this paper it is looked at up-to-date and future office buildings which offer a high standard of user comfort and minimized energy consumption [1]. Both principles may be fullfilled at the same time relaying on a building concept which incorporates excellent thermal insulation of the envelope and soft HVAC-technology [2]. If the internal heat loads exceed 30 W/m^2, it might be appropriate to use combined water-air systems [3].

In large office buildings, a variety of activities take place. Some of them result in high internal heat loads, but others doen't. For this reason, the control of the HVAC-system is an important part of an integral building concept. Many kinds of control strategies can be thought of or have already been realized. Two diverging philosophies are known: one is to use highly sophisticated demand control. On the other side, one can try to avoid control as far as possible.

Both principles have already been put to practise. But comparable results are not available up to now. In this paper, a theoretical investigation on the problem of control of water cooling systems is presented.

2. Type of Building and HVAC-System

This study concentrates to a specific type of building [4]. Nevertheless, the results may be generalized. We assume that the building has an airtight envelope with windows with an outstanding thermal insulation (U-value below 0.8 W/m^2K), and a soft climatisation, which meets the requirements of comfort and energy saving. Although there are no radiators below the windows, there is no sensible downdraft in the environment of the window and a nearly symmetrical infrared radiation field even in strong winters. The user experiences a very pleasant indoor climate throughout the year.

The large variety of performance purposes has brought up a number of different control types for the HVAC-system. Control parameters are time,

temperature, humidity, CO_2, etc. Since control equipment raises the investment costs, rooms with similar load profiles are often bound together to control-zones. Unfortunately, the result of this procedure is in many cases unsatisfactory.

For this study, we assume to deal with mechanical climatisation of the combined type: the air system is a displacement ventilation with a rather limited, constant air change rate, so that time is the only control parameter - a simple on-off-function. (Clearly, auditora are excluded from this study). Its purpose is solely given by the requirements of air quality.

A water system acts as energy transport system, predominantly in the mode of cooling. The heat energy exchange between room and water takes place by the ceiling: water pipes are integrated in the concrete (this study). Other possibilities are to use ceiling mounted radiators or capillary networks attached to the concrete [5]. In any case, the infrared radiation exchange plays an important role.

Outstanding advantages of a system with splitted functions are the high energy transport capacity of water (this lowers the air duct sizes and also the investment costs drastically), and the possibilty to avoid the variable control of an air duct network.

Principally, there are three possibilities to control a water cooling system, namley:

- time (exclusively)
- temperature (exclusively)
- time and temperature

Further, the control function must be defined: it may simply be the on/off-function or it may be the water temperature (three way valves).

If temperature acts as control parameter, it's still the question: which temperature should be used? It may be:

- room temperatures (room individual control)
- mean temperature of a zone (control of zones)
- temperature of a reference room (control of zones)
- outdoor temperature (not very helpfull within this context)

Defining a control strategy, a variety of criterias must be observed. Among others, these are:

- comfort requirements (temperature range)
- variablilty of heat load profiles within the whole building (or zone)
- flexibility (modification of the ground-plan or purposes)
- investment costs
- energy consumption
- system behavior (time constants of the building mass, type of cooler)

A number of buildings based on the splitted concept have been planed by our company and have shortly been constructed or are still under construction. For this reason, practical experience is still missing. But with the help of numerical simulations, the fields of application of the different solutions have been checked. Some of the results are presented here.

3. Dynamic Simulation Models

Two different numerical models have been developped to specifically conduct investigations on the above described type of office building. Both are single room models with periodic boundry conditions. In order to simulate also thermal charge/discharge processes, the time step is 6 minutes only.

Although the physical concepts of the two models are different (e.g. in only one of the models the room air is incorporated), the same conclusions are obtained.

The model used in this study has the following features. The basic idea was to simulate in detail the two physical processes: infrared radiation between all surfaces of the room and heat energy conductance inside the thermal masses (floor, walls, ceiling).

The air is not simulated in this model. For the validity of this hypothesis, one can argue as follows:

- With the above defined concept (mechanical ventilation with a low air change rate and inlet air temperature at comfort level) only a small fraction of the heat energy produced by the sources is removed directly by the ventilation system. This fraction can be subtracted from the heat load prescribed in the model. The major part of the heat load is transferred from the sources to the surrounding surfaces by radiation and convection.

- Preliminary studies have shown that the heat removal process is not very sensitive to the distribution pattern of the sources (the reason is, that energy exchange by radiation is very efficient). Therefore, it can be assumed, that radiation is the only transfer mechanism from the sources to the surfaces.

- The time constant of the room air is in the range of 10 to 20 minutes. The mean room air temperature is strongly correlated to the wall surface temperatures.

The perceived temperature is a function of the radiative temperature and the air temperature. In this study, the area weighed average of all surface temperatures is taken instead.

The internal heat loads are held constant during 8 hours of each of the 5 work days. This simple assumption is dictated by the goals of the simulation: investigation of the fields of application of several control strategies means to look for the limitations.

The water cooling system is simulated by a parametrized model which has the vertical temperature gradient of the cooling ceiling as input. The on/off-function is controlled in four different modes:

- *permanent*:
  The cooling system is running permenantly (= no control).

- *temperature*:
  Cooling is swichted on if a wall surface temperature exceeds 21.0°C and is swichted off if it undergoes 20.7°C.

- *time*:
  Cooling is on during working time (8 hours, 5 days), or, alternatively at night (12 hours, 7 days).

4. Parametric Studies

The simulated room has a ground floor of 20m^2. Floor and ceiling are assumed to be built of concrete (each 15cm thick, periodic boundry conditions). Two types of wall constructions are assumed: light walls (very common in office buildings) and concrete walls (10cm). The stationary key values of the two room types are given in table 1.

Type	Capacity [MJ/K]	Temp.diff. [K]
light	19.9	1.45
heavy	30.1	0.96

Table 1: Heat capacity of the thermal masses for the two types of room. The "temperature difference" is the result of a 1000 W source acting for 8 hours without cooling.

Heat loads of 200 or 1000 W, respectively, represent a low type and a high type case. The sources are switched on for 8 hours from the beginning of each work day.

At the start of each simulation, all temperatures are set to 20°C. The first day will therefore not represent a common performance. In the following, the third or fifth day is looked at. In some cases, one has to look for a steady state, which is reached after a few days up to two weeks, depending on heat load, wall mass, control strategy and water temperature.

Table 2 gives an overview of the three cases presented in this paper. Each case was done with the two wall types and the two heat loads as defined above. The water temperature is set to 18°C or 20°C, respectively. "Active part" means percentage of the ceiling surface, which acts as cooling ceiling. (For the case of suspended radiators, this is necessarily less than 100%, but here, 100% active part can be realized).

No.	Control strategy	Water temp.	Active part
1	temperature or time	18°C	100%
2	permanent	20°C	60 ... 100%
3	time (night)	20°C	100%

Table 2: List of cases discussed in this paper.

With figure 1, the effect of the temperature control shall be demonstrated. Its a simulation of case 1 with light walls and low type heat source. During the first 8 hours of the second day, temperatures increase as a consequence of the heat energy input. But since the wall surface temperature doesn't reach 21.0°C, the ceiling remains passiv. After the work time, the internal heat source is switched off. The surface temperatures begin to sink because of the equalizing effect of thermal conductance (thermal charge of the masses) and radiation. At the end of the second day, the heat energy is more or less equally distributed. The temperature is now 0.29 K higher than 24 hours before (Table 1, but 200 W only). - During the third day, the source is again active (hours 48 to 56). In the time span from hour 51 to hour 54, the temperature control puts the ceiling to the active cooling mode (water in circulation). After that, the active mode is turned off, but since the volume mean temperature of the concrete ceiling is well below the actual equilibrium temperature, the ceiling acts in a passive mode for the rest of the day. The next day begins with a room temperature slightly below 20°C.

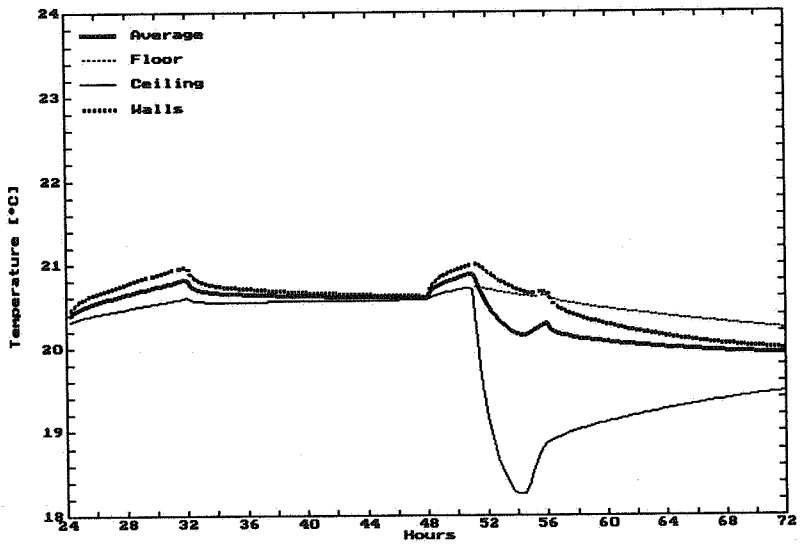

Figure 1: Surface temperatures for days 2 and 3 for case 1 with temperature control, light wall construction and 200 W heat load.

The type of wall construction has an important effect on the temperature behavior of the room. This is demonstrated with two simulations of case 1, both temperature controlled and with 1000 W internal heat sources: one room with light walls, the other with concrete. The differences can be seen in figure 2. Expressed with the mean values of the room temperature (work time, third day), the difference is 0.5 K. The maximum temperatures are 21.6°C (light type) and 20.8°C. Light walls react to heat sources with higher temperatures compared to concret walls. Since in our model the wall temperature is taken as control parameter, the resulting time schedules of active cooling is different for the two rooms: In the room with the light walls, the system is switched on 30 minutes after the sources have started to operate, in the other room after 2.5 hours. (In practical applications, one would certainly choose different threshold temperatures for the two wall types).

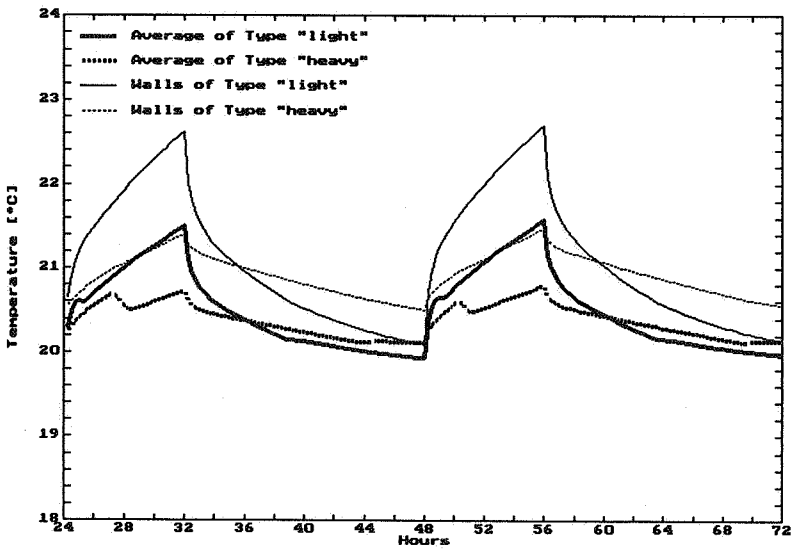

Figure 2: Room temperature and wall temperature for days 2 and 3 for two simulation of case 1, both with temperature control and 1000 W internal heat loads: light or heavy wall type, respectively.

In the examples given so far, the effect of thermal inertia of the masses could be seen. This is especially true for the next case. In practice, it might be an advantage to run the cooler during night time only. Therefore, the concrete ceiling acts as a buffer. Here, a simulation of case 3 is looked at: light wall construction, 1000 W internal heat load, cooling ceiling active during 12 hours each night. The process of thermal charge and discharge of the masses is shown in figure 3.

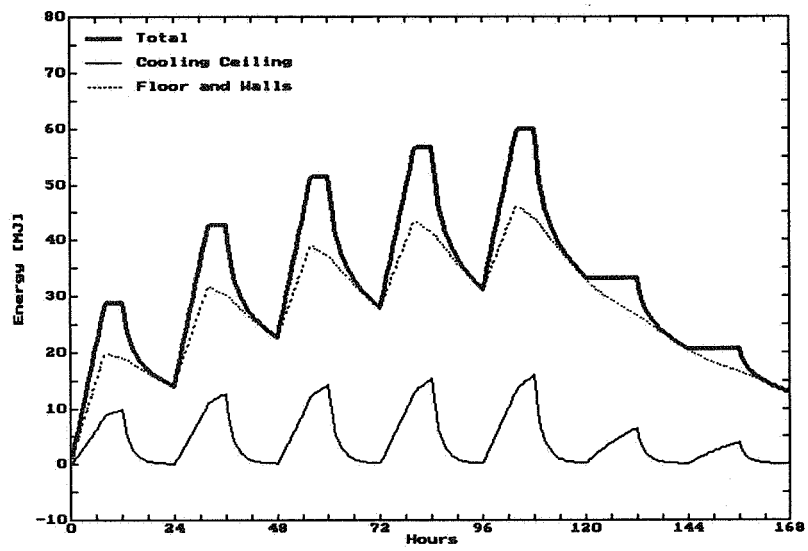

Figure 3: Energy contents of the thermal masses over one week. It's a case with light wall construction, 1000 W internal heat load, cooling ceiling active during 12 hours each night.

5. Results

The aim of this study is to come to an idea of the fields of operation for the different control strategies. Clearly, the power of the heat loads is a very important parameter. In many office buildings, the load profiles differ from room to room to a large extent. In any case, one must declare an upper limit of heat loads to which the comfort requirements have to be met. With some systems, it might also be necessary to define a minimum temperature.

Case 1

The two control strategies "temperature" and "time", as defined in chapter 3, are compared. Figure 4 shows the daily mean room temperatures (work time, third day) as a function of the heat load power. The four curves represent the combination of the two wall types with both control types. With temperature control and heavy walls, the mean temperature is practically independent of the heat load, with light walls, the dependance is minor. The situation becomes very different with the fixed time control. Either, the rooms with low heat loads are too cool, or, if the water temperature is shifted, rooms with substancial loads are critical to become unacceptably warm. Consequently, this type of control may be applied in buildings with minor variety.

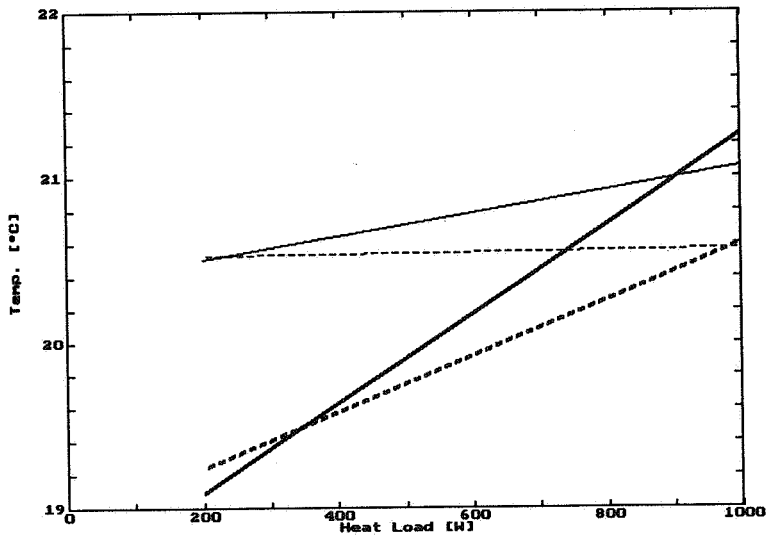

Figure 4: Daily mean room temperatures (work time, third day) as a function of the heat load power. The curves represent the four cases:

——— light walls, temperature control
▬▬▬ light walls, time control
------ concrete walls, temperature control
▪▪▪▪▪▪ concrete walls, time control

Case 2

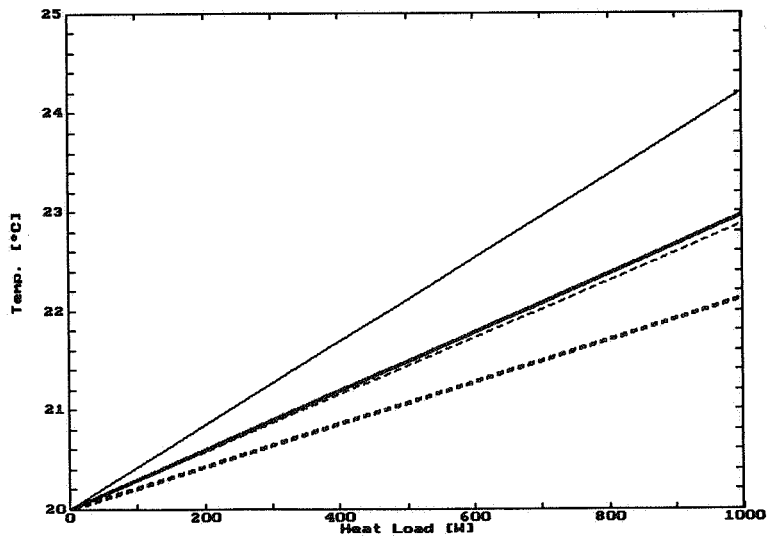

Figure 5: Daily mean room temperatures (work time, fifth day) as a function of the heat load power for permanently active cooling systems. The curves represent the four cases:

——— light walls, 60% active part
------ light walls, 100% active part
▬▬▬ concrete walls, 60% active part
▪▪▪▪▪▪ concrete walls, 100% active part

Case 2 demonstrates the ability of systems without any control of the cooling ceiling (strategy: permanent). The water temperature is held at

20°C in order to prevent undertemperature. Again, for four situations (light and concrete walls, 60 and 100% active part) the daily mean room temperatures are shown as a function of the heat load (figure 5). Day 5 is chosen for the following reasons: within the first week, the state of dynamic equilibrium is nearly reached in the cases "100% active part", but is not reached in the 60%-cases. So, the temperatures given in figure 5 are typical in the latter cases, but they represent an upper region for 100% active part. - The result is, that with 100% active part, the cooling ceiling can keep an acceptable indoor temperature throughout a large range of heat loads, whereas with a limited active part restrictions must be accepted.

Case 3

In this case, night cooling with fixed times (12 hours each night) is simulated. The results given in figure 6 are for the third and the fifth day of the first week (the argumentation of case 2 is again valid). Although the comfort conditions taken over the whole range are not as favorable as with permanent cooling, they are nevertheless acceptable.

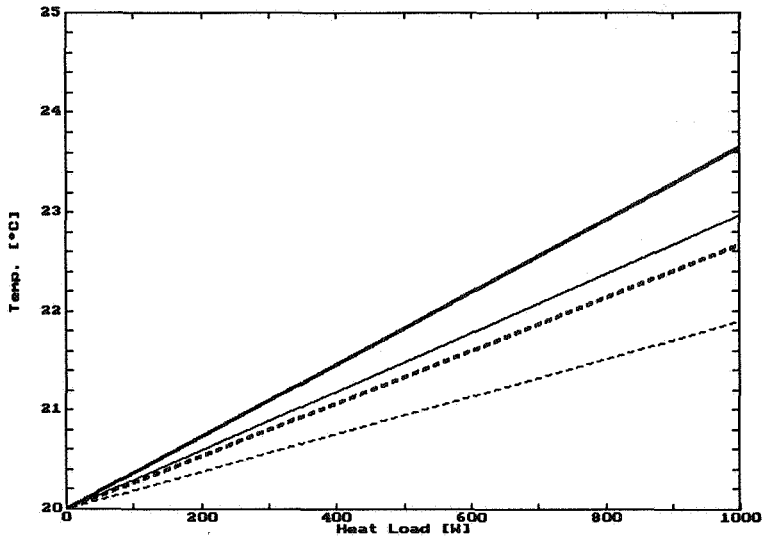

Figure 6: Daily mean room temperatures (work time, third and fifth day) as a function of the heat load power for night cooling systems. The curves represent the four cases:

——— light walls, third day
▬▬▬ light walls, fifth day
------ concrete walls, third day
▪▪▪▪▪▪ concrete walls, fifth day

The figures 4 to 6 show daily mean temperatures. Sometimes, limits for maximum temperatures have to be respected. Since the variation throughout a day depends on heat load, wall type, control strategy and water temperature, the same kind of investigation should be conducted for maximum temperatures.

6. Conclusions

Dynamic computer simulations demonstrate, that acceptable comfort conditions can be achieved with different or even opposing control strategies. In this paper it is looked to ceiling cooling systems with demand control by temperature, and, on the opposite side, to systems without any control.

Demand controled systems principally offer more flexibility than time controlled or permanently running systems. Nevertheless, there exist many situations in which the less sophisticated systems are attractive.

References:

[1] WIDMER F.
Raumlufthygiene und rationelle Energieverwendung sind kein Widerspruch
Heizung Klima Nr. 1/2, 1989

[2] BRAUN W.
Building Performance and Ventilation System
11th AIVC Conference, Italy, 1990

[3] ESDORN H., KÜLPMANN R.
Deckenkühlung in Verbindung mit Verdrängungslüftung: Hohe Einsparungen bei der Förderenergie
CCI 4, 1989

[4] BRAUN W.
Experiences with High Tech Buildings
CIB W67, Rotterdam, 1990

[5] ESDORN H., ITTNER M.
Betriebsverhalten von Deckenkühlsystemen

AIR MOVEMENT & VENTILATION CONTROL WITHIN BUILDINGS

12th AIVC Conference, Ottawa, Canada
24-27 September, 1991

POSTER 18

PERFORMANCE ANALYSIS OF DEMAND CONTROLLED VENTILATION SYSTEM USING RELATIVE HUMIDITY AS SENSING ELEMENT

A.J. Parekh

Research Engineer
Scanada Consultants Limited
436 MacLaren Street
Ottawa, Ontario
K2P 0M8

M.A. Riley

Chief, Buildings Group
Energy Efficiency and Alternate Energy Branch
Energy, Mines and Resources Canada
580 Booth Street, 7th Floor
Ottawa, Ontario K1A 0E4

PERFORMANCE ANALYSIS OF DEMAND CONTROLLED VENTILATION SYSTEM USING RELATIVE HUMIDITY AS SENSING ELEMENT

SYNOPSIS

This paper evaluates the suitability of humidity-controlled house ventilation system to determine (i) the effectiveness of relative humidity as a sensing element, and (ii) the operating and performance characteristics of such ventilation strategy. The ventilation system consists of continuously running "mechanical" air extractor units and "passive" air inlet units equipped with humidity sensors. The ventilation system was installed in two single storey houses which were monitored during November 1989 to April 1990. Results showed that the changes in the relative humidity did not appear to track the levels of normal human activity accurately. The difference in air in-flow through each passive air inlet due to changes in RH (2 to 10%) varied from 0.8 L/s to a maximum of 1.7 L/s, which was found to be insufficient based on high CO_2 levels (> 1200 ppm) in occupied rooms. The humidity-controlled mechanical exhaust system was found satisfactory in maintaining the level of exhaust air-flow with changes in RH. The air in-flow and out-flow analyses showed that the air leakage though the house envelope remained as a predominant form of fresh air supply to the house, thus defeating the purpose of demand controlled ventilation. The energy consumption of these two houses reduced by more than 8% by cutting down the fresh air provided to house during un-occupied periods. Relative humidity as an exclusive sensing element may not be sufficient enough to achieve required quality ventilation in houses.

1. INTRODUCTION

Modern houses have significantly improved building envelopes in terms of insulation and airtightness to improve energy efficiency and human comfort. Given the current trend towards increased airtightness of house envelopes, it is recognized that houses now being built in North America will have to incorporate some form of controlled mechanical or passive ventilation. The controlled ventilation should assist in removing the moisture source as well as providing sufficient fresh air to occupants [CMHC 1990].

In Canada, the CSA Standard F326 - *Residential Mechanical Ventilation Requirements* - defines the requirements for mechanical ventilation systems for providing minimum controlled rates of ventilation air to habitable spaces by using continuous or intermittent air supply and exhaust devices [CSA 1989]. It is likely that the F326 Ventilation Standard will be referenced, as mandatory, in the upcoming 1995 National Building Code and in those provincial codes based on it. The minimum mechanical ventilation requirement is 0.3 air changes per hour (ach), which is similar to ASHRAE Standard 62-1989 [ASHRAE 1989].

One such controlled ventilation strategy is based on humidity sensing passive air inlets and humidity-controlled mechanical exhaust system. The humidity-controlled ventilation (HCV) systems rely on humidity levels generated by the occupants as being the controlling variable determining the necessary ventilation rate. In this way it attempts to follow a "demand-controlled ventilation" strategy (DCV): ventilate the house when and as needed. The HCV system was installed in two single storey detached houses located near Ottawa, Ontario which were monitored during the winter months of November 1989 to April 1990. The study objectives were to (i) to gauge how well the ventilation system responded to changes in indoor humidity, and (ii) to determine the response of air inlets and extractors to indoor RH and occupancy. The ventilation system was evaluated using two criteria: (i) the occupant related pollutants dominate house related pollutants; and (ii) the house envelope is sufficiently air-tight that some form of passive or mechanical ventilation is required.

2. HUMIDITY-CONTROLLED HOUSE VENTILATION (HCV) SYSTEM

The indoor humidity levels depend on the following factors: (i) the number of people in the house (a person at rest emits roughly 40 grams of water vapour per hour); (ii) the occupancy level in the room (a vacant room will have a lower humidity level than when occupied); (iii) the utilization of each room (level of human activity, laundry, cooking, bathing, dishwashing, etc.); and (iv) the effect of air infiltration and ambient air temperature and humidity. The indoor humidity level seems to vary according to occupancy and level of utilization of space. Therefore, a ventilation system designed to respond according to the changes in indoor relative humidity have seemingly good potential to supply fresh air and exhaust stale air according to occupancy when and as needed.

The humidity sensor in HCV system is composed of polyamide tissue (nylon strips) which responds to changes in humidity with shrinking or stretching. The movements of the nylon strips are amplified and transmitted by a system of actuator to the movable shutter. The air-inlets and extractor units are composed of humidity sensor, actuator, movable shutter and deflector. Fresh air is introduced through air-inlets into the main rooms such as the living and dining areas, family rooms, and bedrooms according to the relative humidity in each room. The exhaust outlets are located close to the source of pollutant generation such as kitchen, bathrooms and laundry room.

Extractor Units: The extractor units control the rate of exhaust by automatically varying the size of the extractor opening in proportion to the level of indoor relative humidity (RH). The extractor opening contains an inflatable rubber tube/spring assembly, which controls the dimension of the opening pneumatically. As the relative humidity in the room rises, the pneumatic circuit closes, causing the tube to lengthen and allowing greater air flow through the extractor. As the relative humidity drops, the tube shortens and widens, reducing air flow through the extractor. In this way, the exhaust rate is proportioned according to the relative humidity. Air extractors are hooked to the 100 L/s (208 cfm) central exhaust fan, which are placed in rooms where humidity is produced such as bathrooms, kitchens and laundry rooms. The exhaust fan runs 24 hours a day at slow speed and continually maintains a slight negative pressure across the building envelope.

Air Inlets: The air inlets are installed with through-the-wall supply diffusers, placed in each bedroom and the main living area in the house. The air flow into the house through the supply diffusers is controlled by the relative humidity of each room or space. The air inlets provide a variable free opening of 5 to 30 cm^2 (0.78 to 4.65 in^2), adjusting the opening by means of a humidity sensing element that sets the damper position. Two humidity ranges can be selected on the fixture: 25% to 60% RH, for cold climates, and 40% to 70% RH for milder climates. The humidity sensor is located in the fixture, but away from the incoming fresh airstream, so that it senses the average room humidity level [Baets and Dietz 1986]. Figure 1 shows the schematic of an air inlet.

3. HOUSE DESCRIPTION AND CHARACTERISTICS

Two test houses are located near Ottawa, Ontario. These houses are designated as House A and House B.

House A: This house is a split entrance, raised bungalow with three bedrooms, a dining room, living room, kitchen and unfinished basement. The electric baseboard heaters are controlled by individual wall mounted thermostats. This house has 109.7 m^2 (1,137 ft^2) of heated floor space and volume of 460.2 m^3 (16,243 ft^3). The estimated airflow to cause at 10 Pa pressure difference is 88 L/s (184 cfm). The measured airtightness was 3.18 air changes per hour at 50 Pa.

House B: This house is a three bedroom bungalow with eat-in kitchen, and living room as shown in Figure 2. It has a floor area of 101.8 m^2 (1,056 ft^2) and volume of 414.9 m^3 (14,644 ft^3). The estimated airflow to cause at 10 Pa pressure difference is 84 L/s (175 cfm). The electric baseboard heaters with wall mounted thermostats are located in each room and wherever necessary. The measured airtightness was 3.03 air changes per hour at 50 Pa.

4. RESULTS AND DISCUSSION

Monitored data was examined and "typical" snapshots of three to four days were selected to determine the performance of the HCV components and system as a whole. The following operating conditions were used in evaluating the HCV system: (i) periods of normal house occupancy and non-occupancy; (ii) the outdoor temperature: below -10 C (14 F), between 0 (32 F) and -10 C (14 F), between 0 C (32 F) and 10 C (50 F); and (iii) surge loads such as when several people enter (or leave) a room at the same time.

4.1 Relative Humidity and Air Inlet Response

Analysis of air inlet response to relative humidity was performed for two scenarios using several snapshots: (i) during the normal occupancy periods, and (ii) surge loads.

Normal Occupancy: With variation in human activity, in most cases, the RH changes by 1 to 10%. The HCV system is a humidity-controlled system and in its current configuration the air inlets do not show *instant* response of air inlet to the changes in room humidity. When there is a small increase in RH (1 to 3%) due to normal human activity, as shown in Figure 3, the air inlet response times are slow and the resulting increases in ventilation rates are very slight; however, CO_2 level indicate increase by more than 15%. Air flow through the individual air inlet vary from 0.8 L/s (1.7 cfm) to a maximum of 1.7 L/s (3.5 cfm). The time-referenced data on RH and air inlet position did not necessarily followed each other, for example, a slight increase in RH might have been followed by the closing of the air inlet rather than the opening. The relative humidity levels do not appear to track the levels of human activity in any significant way during normal occupancy.

Surge Loads: Several snapshots were observed to see the effect of "surge" loads on the HCV system to evaluate its "quick" response. The ventilation system showed quick response to changes when several people entered the room at the same time; however, it was sluggish to respond to changes when several people left the room at the same time as shown in Figure 4. The quick response of the air inlets opening when a sudden increase in the occupancy increased the air flow from 0.8 (1.7 cfm) to 3.5 L/s (7.3 cfm) in most cases. The CO_2 levels increased heavily during "surge" loads and remained high (more than 1000 ppm) for a period of more than 2 hours. This indicates that the air flow through the air inlets during sudden "loading" may not be sufficient to meet the ventilation requirements of occupants at that time.

Relative humidity is found to be a poor indicator of occupancy. Response times are slow and often there is no discernable change in RH despite major changes in occupancy and CO_2 concentrations. Relative humidity displays lag time with changes in occupancy due to absorption and desorption characteristics.

4.2 Carbon Dioxide and Air Inlet Response

The carbon dioxide (CO_2) is commonly used as an indicator of air quality in buildings. The time-referenced snapshots of CO_2 are shown in Fig 4 and 6. Unlike relative humidity, CO_2 levels do appear to track the human presence and levels of activity very well during normal occupancy and for the "surge" loads. A rise in CO_2 consistently occurs at the times of

maximum activity. During unoccupied periods, CO_2 levels decay, as indoor air is continuously exhausted from house by the extractor units. Presumably, CO_2 can be a good indicator of occupancy and indoor air quality with demand-controlled ventilation systems.

In both houses, the CO_2 levels in the master bedrooms peaked at more than 1200 ppm and remained above this level for a period of three to seven hours during the night time. The higher CO_2 levels indicate the lack of supply of fresh ventilation air to the house. It is probable, therefore, that the current air inlet system is not providing adequate fresh air supply to the house.

Since CO_2 appears to be a good indicator of occupancy, the demand-controlled ventilation systems, like HCV, might require a combination of CO_2 and indoor relative humidity sensors to provide good air quality and moisture control in cold climate houses.

4.3 Comparison of Indoor Carbon Dioxide and Relative Humidity

Figure 5 shows the comparison of CO_2 and RH. It shows that variations in RH are more stable and smaller than changes in CO_2. The CO_2 tends to indicate *instant* changes in the occupancy while the RH lags about 15 to 30 minutes behind changes in occupancy. The time-referenced comparison of CO_2 and air inlet response do not track each other well. However, one or two hour averaged variations in CO_2 and RH response can be compared well in either increasing or decreasing trends. This observation raises the question regarding whether the humidity-controlled air supply inlets are effective in demand-controlled situations where the supply of fresh air is supposed to be provided on a room by room basis when necessary.

4.4 Performance of Humidity-Controlled Ventilation System

In both houses, an intentional opening area (IOA of air inlets) to the total house leakage area (ELA) ratio varied approximately from a minimum of 12% (all air inlets in minimum position) to a maximum of 35% (inlets in maximum position). This suggests that a significant amount of ventilation air is entering the house through non-intentional openings.

The in-flow and out-flow calculations showed the following results for both houses: The fresh air flow through air inlets varied from a minimum of 12% during non occupancy periods to a maximum of 27% of the total air in-flow during full occupancy. Estimated total air flow through all air inlets varied from 6.5 L/s (13.5 cfm) to 16 L/s (33.3 cfm). The air leakage through the house envelope remained as a predominant means of supplying fresh air to the house. Therefore, even if all air inlets were fully opened (say 90 to 95%), it would not substantially increase the fresh air supply to the rooms. The air inlets do not seem to have control over where fresh air is supplied. The fresh air will most likely be supplied to the basement where the majority of the leaks occur. In this regard, the air inlets are of questionable value except where the air leakage patterns are uneven and require additional leakage in a specific applications such as in a small isolated room.

The performance analysis of exhaust system showed that the continuous air exhaust was maintained adequately by the air extractors. The flow measurement results showed that these units were working according to their settings and on an average provided required 37 L/s (77 cfm) of exhaust in both houses. These extractors were constantly exhausting air from the house and kept the house depressurized.

The energy consumption monitoring and data analysis showed that the HCV system reduced the energy consumption by more than 8% when compared to forced air system. The energy efficiency of the HCV system is achieved by cutting back the fresh air provided to the house occupants, presumably at times when it is not required). However, the results of air quality

monitoring (CO_2) in both houses raise questions about the suitability of humidity control as an exclusive control for ventilation rates.

5. CONCLUSIONS

This paper has attempted to describe the performance of the most recent approach to house ventilation using the indoor humidity level as a sensing element. The following conclusions are drawn from the monitoring results of humidity-controlled ventilation system installed in two houses:

- In most cases the indoor relative humidity changes by 1 to 10% with the changes in occupancy. The change in air in-flow through individual air inlet varies from 0.8 L/s (1.7 cfm) to 1.7 L/s (3.5 cfm), which was found to be insufficient based on high CO_2 levels in occupied rooms.
- Air inlets supply approximately 12 to 27% of the total fresh air. Remaining fresh air supply is through the envelope leaks.
- Air extractor units were working according to their settings and on an average provided the necessary 37 L/s (77 cfm) of exhaust.
- Relative humidity does not appear to reflect the levels of human activity accurately. Hence, the use of humidity as an exclusive sensing element for ventilation control may not be suitable in cold climates.
- Carbon dioxide levels do appear to track human presence and activity very well. Since CO_2 appears to be a good indicator of occupancy, the demand-controlled ventilation systems, like HCV, might require a combination of CO_2 and indoor relative humidity sensors to provide good air quality and moisture control in cold climate houses.

ACKNOWLEDGEMENTS

The authors would like to acknowledge the financial assistance of Energy, Mines and Resources Canada. The humidity-controlled ventilation system was installed by CAN-AERECO Ventilation Inc.

REFERENCES

1. ASHRAE 1989. *ASHRAE Standard 62-1989, Ventilation for Acceptable Indoor Air Quality*, American Society of Heating, Refrigerating, and Air-Conditioning Engineers, Inc., Atlanta, Ga.
2. F.A. Baets and D.R. Dietz, "Humidity Controlled Ventilation", Symposium on Air Infiltration, Ventilation and Moisture Transfer, Building Thermal Envelope Coordinating Council, Fort Worth, Texas, December 1986.
3. CMHC 1990. *How to Comply with Residential Ventilation Requirements of the 1990 National Building Code*, Canada Mortgage and Housing Corporation, Ottawa, Ontario.
4. CSA 1989. *CSA Standard F326.1-M1989, Residential Mechanical Ventilation Requirements*, Energy Efficiency in Housing, Canadian Standards Association, Rexdale, Ontario.
5. Scanada 1989. *To Study and Monitor the Operating Characteristics and Performance of the AERECO Humidity-Controlled Ventilation System*, Phase I Report Prepared by Scanada Consultants Limited for Energy, Mines and Resources Canada, Ottawa, Ontario, December 1989.
6. Scanada 1990. *Operating Characteristics and Performance of Humidity-Controlled House Ventilation System - Phase II: Monitoring and Performance Analysis*, Report prepared by Scanada Consultants Limited for Energy, Mines and Resources Canada, Ottawa, Ontario.

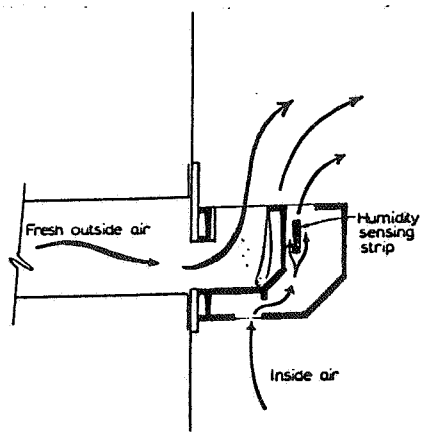

Figure 1: Humidity-controlled air-inlet.

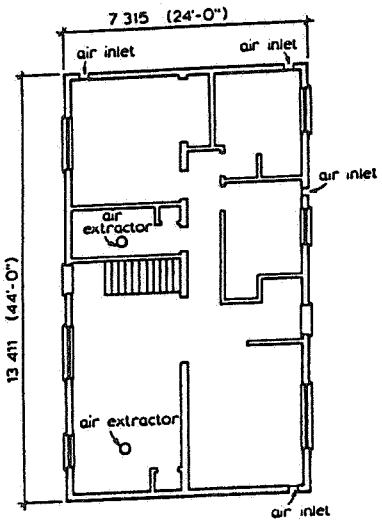

Figure 2: Description of house ventilation system.

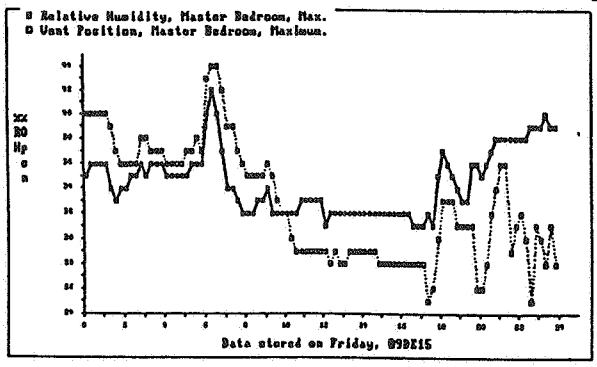

Figure 3: Relative humidity and air-inlet response.

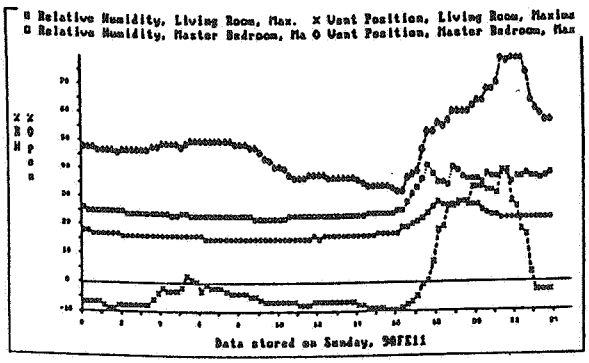

Figure 4: Effect of surge loads on RH and air-inlet opening.

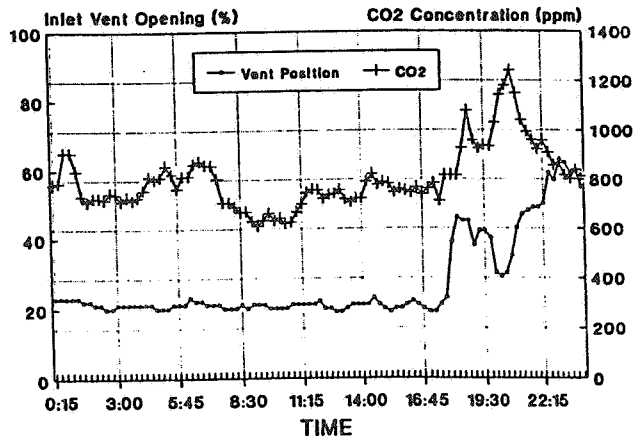

Figure 5: Response of air inlets to occupancy. Comparison of CO_2 measurements with air-inlet position.

AIR MOVEMENT & VENTILATION CONTROL WITHIN BUILDINGS

12th AIVC Conference, Ottawa, Canada
24-27 September, 1991

POSTER 19

The Potential for Residential Demand Controlled Ventilation

Tom Hamlin
Canada Mortgage and Housing Corporation
Ottawa, Ontario

Ken Cooper
SAR Engineering Ltd
Burnaby, British Columbia

Synopsis

A literature search was performed to gain as much knowledge as was available on ventilation, indoor air quality sensors and demand controlled ventilation (DCV) strategies. Field data was gathered on the time and spatial variation of indoor air quality in houses.

Appropriate designs were then developed. Design strategies are discussed elsewhere (1). Hour by hour simulations of the performance of several ventilation systems in various Canadian climates were done. Energy savings were then estimated for DCV and heat recovery ventilation with air to air heat exchange. These were compared to a base case of continuous exhaust ventilation. All systems utilized air recirculation.

Introduction

Demand Controlled Ventilation (DCV) is the control of ventilation air supply rates to the minimal rate required to control indoor air quality. These systems can reduce energy requirements and/or improve indoor air quality. The designs examined in this study are orientated primarily toward energy efficiency.

Analysis Technique

An hour-by-hour multi-zone thermal simulation program ENERPASS (2) was combined with the National Institute of Standards and Technology contaminant simulation program CONTAM87 (3). This new program ENERPASS/CONTAM was used to estimate energy use and carbon dioxide concentrations for various systems in various locations. The program allowed the ventilation system airflow to be controlled as a function of pollutant concentration. Because the two programs had to pass data between them, execution time was slow at 7 to 10 minutes per day of simulation on an IBM AT compatible with math coprocessor. Most of the annual energy performance results were projected based on simulations of January to March weather data. Fifty percent of the space heating was found to occur in this period. Results were extrapolated to annual savings from the base case.

Simulations were performed for Vancouver, Winnipeg and Toronto for a base case of continuous mechanical exhaust only ventilation, continuous balanced flow heat recovery ventilation, and DCV using carbon dioxide as the control parameter. See Tables 1 and 2. Some demand controlled heat recovery ventilation systems were also simulated. Simulations were performed with three and six occupants. Canada has an average of 2.9 occupants per dwelling. Two demand control modes were simulated - match peak and match average. The match average mode consisted of performing multiple runs to find the

carbon dioxide setpoint that would result in the same heating season average carbon dioxide concentration as the base case. Similarly, for the match peak mode of control, multiple runs were carried out to find the set point which matched DCV peak concentrations with those of the non-DCV base case. It is assumed that acceptable CO2 levels lie in this range. A DCV system with matched average CO2 is a conservative comparison which results in an indoor environment with the same average CO2 levels but reduced peaks - a more comfortable environment than continuous ventilation. A matched peak mode allows the DCV system to achieve significantly greater cost savings by reducing ventilation at all times, except during periods with highest pollutant activity or occupancy.

Results

All houses simulated were assumed to have relatively large air recirculation systems. Air recirculation within dwelling units reduces the local concentration of occupant generated pollutants and thus reduces the amount of ventilation required. This would not be true in conventional housing with high building generated pollutants.

The house is a bungalow with full basement and 123 m2 per floor. Fan capacities and other information is in Tables 1 and 2. Electrical fan energy savings were assumed to be 25%. Field trials (1) showed non-optimized savings of 23 and 24% suggesting more was possible. The simulations performed were for houses that were sufficiently airtight to benefit from controlled ventilation. All houses were run using a 0.1 air changes per hour natural air leakage rate. This corresponds to houses with equivalent sharp edged orifice sizes at 10 Pascals pressure of 200 cm2 in Vancouver, 170 cm2 in Toronto, and 150 cm2 in Winnipeg.

Simulated carbon dioxide levels are shown in Figure 1, for continuous fan (base case) versus match average and match peak DCV control modes. The results are for two days one being a weekend day with higher occupancy.

Simulation results are presented in the following figures and tables. DCV rates were reduced by about 25% for match peak mode and 10% for match average from a base case level of 0.32 air changes per hour.

With DCV was able to save 9.6 Gj/yr (Vancouver) to 15.7 Gj/yr (Winnipeg). Based on local energy prices the savings were from $46 (Vancouver) to $69 (Toronto) per year. With a ten year system life, these savings could translate into an allowable economic investment opportunity of $460 to $690. These savings are about the same as current heat recovery ventilation using air to air heat exchange.

The matched average CO2 case demonstrates that DCV can improve comfort by reducing the peaks in concentration and still provide some savings. Savings ranged from $19 per year (Vancouver) to $37 per year (Toronto) translating into an allowable economic 10 year investment of $190 to $370. All

space heating energy was costed as natural gas. Electrical space heating energy savings would be about double.

The DCV system as modelled would require 22 L/s more capacity than the continuous exhaust fan, wiring from a sensor in the recirculation system to a controller and a controller. Potential exists for lowering the cost of DCV controllers by integration with thermostat and home security functions.

A factor which became apparent during economic analysis is the importance of efficient fans. While the amount of energy was not large, the dollar value of fan energy became quite significant due to the disparity between natural gas and electricity rates.

For comparison purposes, a number of simulations were performed with heat recovery ventilation. Higher efficiency runs used values of about 70% heat recovery effectiveness depending upon outside temperature while lower efficiency runs used 50% without a temperature dependence.

Conclusions

The scenario examined for DCV potential is as follows; Building related pollutants such as formaldehyde are minimized, the pollutants resulting from events such as showers and cooking are removed (1), and occupant related pollutants as indicated by carbon dioxide concentration dominates the indoor pollution load. The dwellings were also assumed to be tight enough to avoid excessive air leakage. Air recirculation was then used as a mechanism to dilute occupant related pollutants. If this scenario is satisfied, it was estimated that there is a good opportunity for the reduction of ventilation air flow by demand control. DCV can use measurements of carbon dioxide concentration to control air flow rates.

Demand controlled ventilation has the potential to reduce ventilation energy consumption by about the same amount as typical heat recovery ventilators. Although the energy efficiency of heat recovery systems could be improved, demand controllers have more potential for cost reduction. Further field demonstration should be undertaken to improve the understanding of the performance of these systems.

References

(1) Moffatt, S., Moffatt, P. "A Demonstration of Low Cost DCV Technology on Five Canadian Houses" 12th AIVC Conference, Ottawa, 1991.

(2) Enermodal Engineering, "Enerpass Version 3.0" Waterloo, Ontario, 1990.

(3) Axley, J. "Progress Toward a General Analytical Method for Predicting Indoor Air Pollution in Buildings" IAQ Modelling phase III report. NBSIR 88-3814. Washington, National Institute for Science and Technology.

Figure 1 **CO_2 Comparison - 3 Simulation Scenarios**

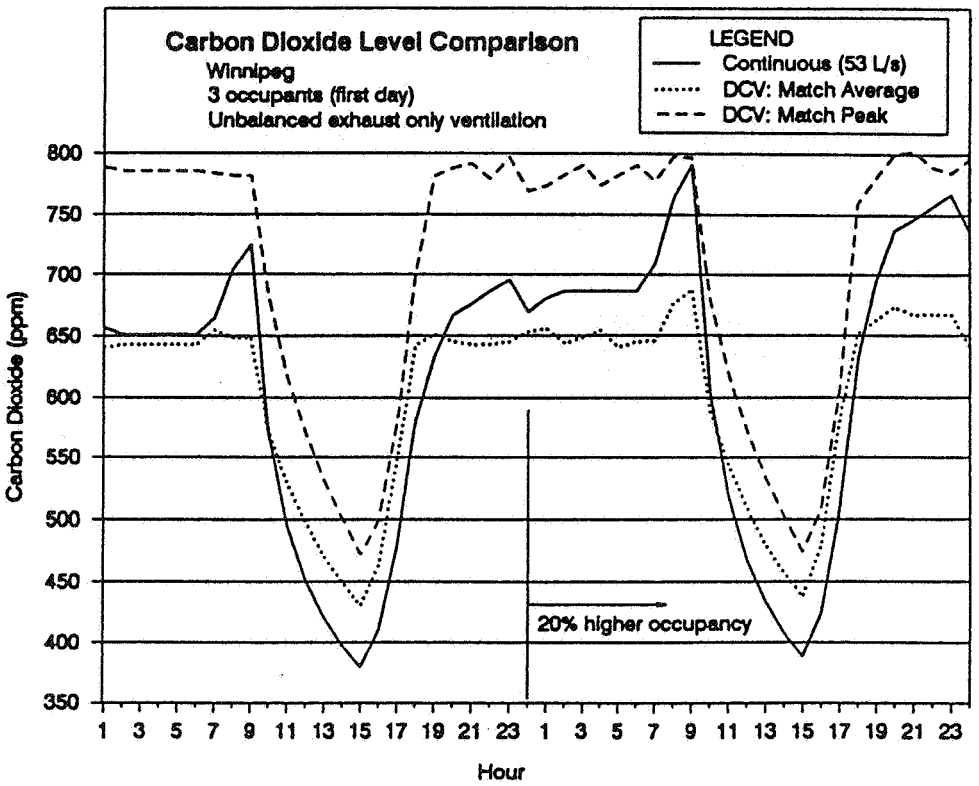

Figure 2 **Comparison of DCV and HRV for Vancouver**

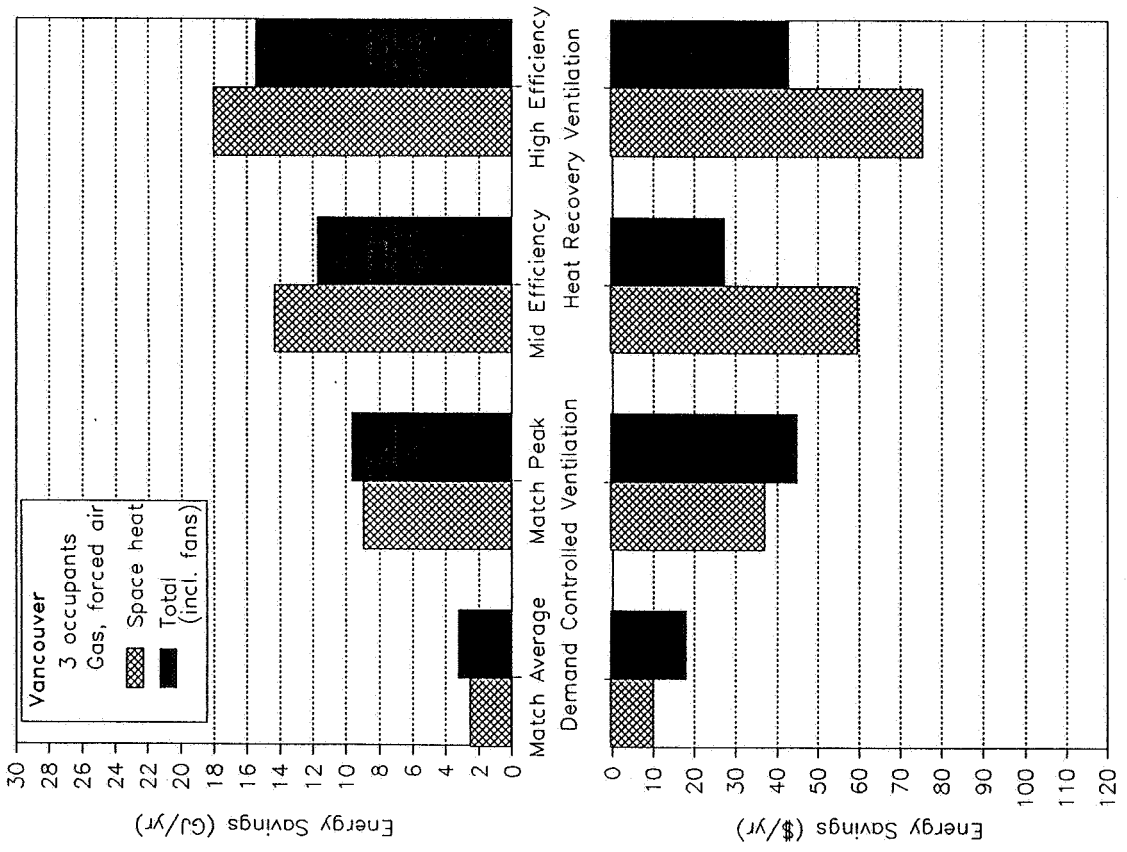

Figure 4 **Comparison of DCV and HRV for Toronto**

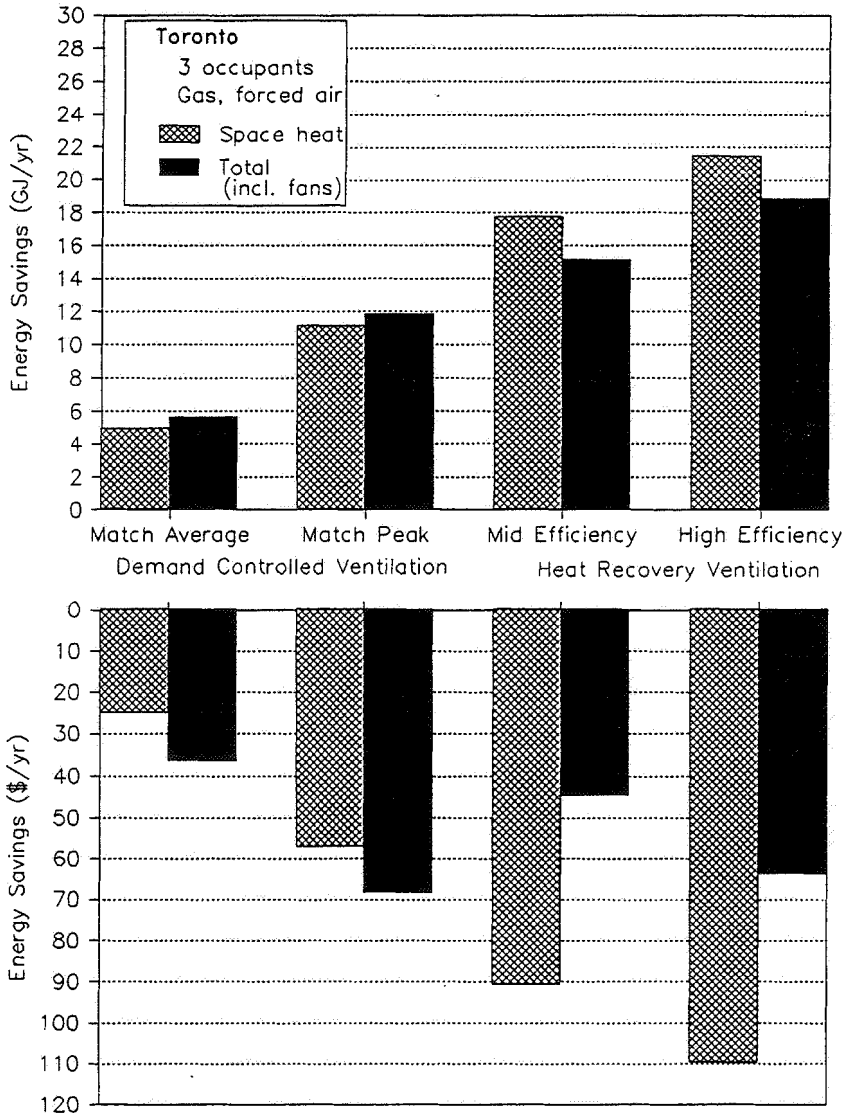

Figure 3 **Comparison of DCV and HRV for Winnipeg**

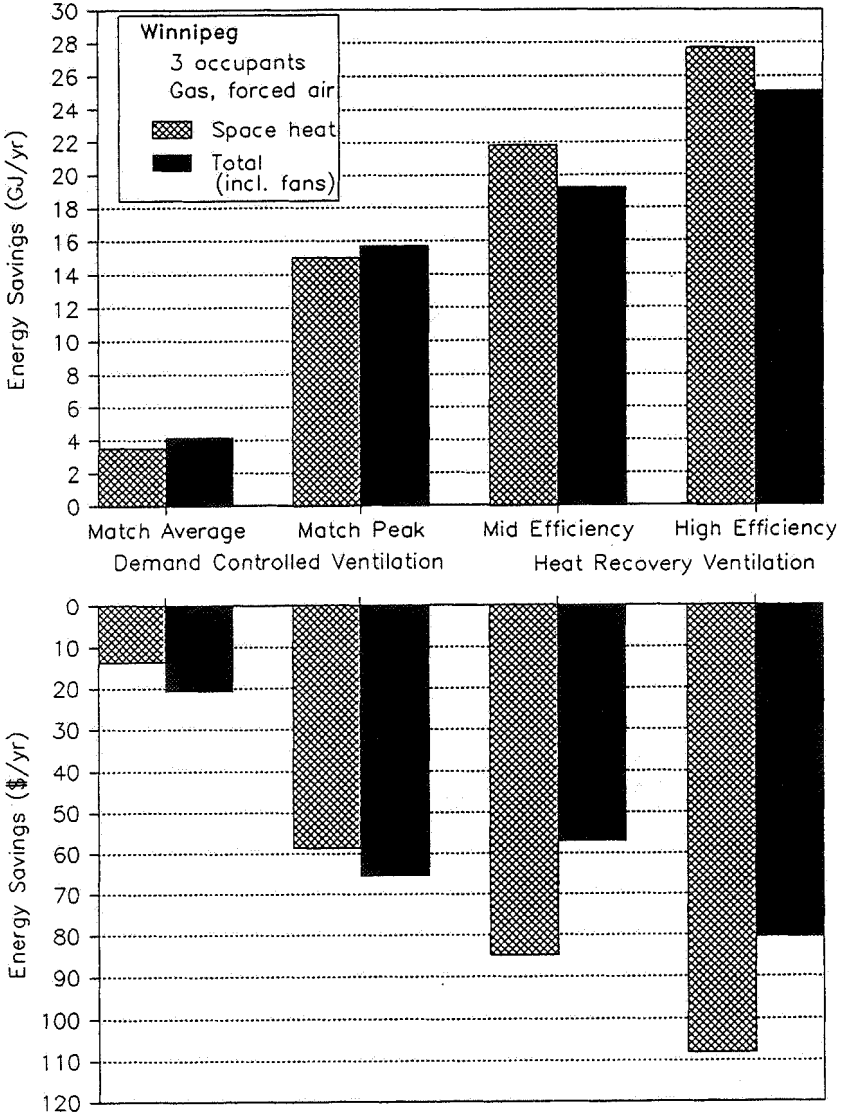

Table 1 **Simulation Results**

Gas forced air heating, 3 occupants

VANCOUVER:			BASE (continuous exhaust fan)			
	Fan Capacity	(L/s)	53			
	Ventilation + Infiltration	(ach)	0.32			
	CO2 - average	(ppm)	571			
	- maximum	(ppm)	802			
	Space Heat Energy	(GJ/yr)	59.5			
	Ventilation Fan Energy	(GJ/yr)	2.6			
			DCV:		Continuous HRV:	
			Match avg.	Match peak	low effic.	high effic.
	Fan Capacity	(L/s)	25/75	25/75		
	Ventilation + Infiltration	(ach)	0.30	0.23	0.31	0.31
	CO2 set-point	(ppm)	655	790		
	CO2 - average	(ppm)	574	659	589	589
	- maximum	(ppm)	694	804	835	835
	Space Heat savings	(GJ/yr)	2.5	8.9	14.3	18
	Fan savings*	(GJ/yr)	0.7	0.7	-2.6	-2.6
	TOTAL DCV SAVINGS	(GJ/yr)	3.2	9.6	11.7	15.4
		($/yr)	$18.60	$45.55	$27.89	$43.47
TORONTO:			BASE (continuous exhaust fan)			
	Fan Capacity	(L/s)	53			
	Ventilation + Infiltration	(ach)	0.32			
	CO2 - average	(ppm)	571			
	- maximum	(ppm)	802			
	Space Heat Energy	(GJ/yr)	82.0			
	Ventilation Fan Energy	(GJ/yr)	2.6			
			DCV:		Continuous HRV:	
			Match avg.	Match peak	low effic.	high effic.
	Fan Capacity	(L/s)	25/75	25/75		
	Ventilation + Infiltration	(ach)	0.29	0.24	0.31	0.31
	CO2 set-point	(ppm)	645	770		
	CO2 - average	(ppm)	560	695	589	589
	- maximum	(ppm)	658	801	835	835
	Space Heat savings	(GJ/yr)	4.9	11.1	17.7	21.4
	Fan savings*	(GJ/yr)	0.7	0.7	-2.6	-2.6
	TOTAL DCV SAVINGS	(GJ/yr)	5.6	11.8	15.1	18.8
		($/yr)	$36.66	$68.66	$44.94	$63.94
WINNIPEG:			BASE (continuous exhaust fan)			
	Fan Capacity	(L/s)	53			
	Ventilation + Infiltration	(ach)	0.32			
	CO2 - average	(ppm)	571			
	- maximum	(ppm)	802			
	Space Heat Energy	(GJ/yr)	112.6			
	Ventilation Fan Energy	(GJ/yr)	2.6			
			DCV:		Continuous HRV:	
			Match avg.	Match peak	low effic.	high effic.
	Fan Capacity	(L/s)	25/75	25/75		
	Ventilation + Infiltration	(ach)	0.29	0.23	0.31	0.31
	CO2 set-point	(ppm)	645	790		
	CO2 - average	(ppm)	562	707	589	589
	- maximum	(ppm)	655	823	835	835
	Space Heat savings	(GJ/yr)	3.5	15.0	21.8	27.7
	Fan savings*	(GJ/yr)	0.7	0.7	-2.6	-2.6
	TOTAL DCV SAVINGS	(GJ/yr)	4.2	15.7	19.2	25.1
		($/yr)	$20.69	$65.58	$57.16	$80.52

*based on 25% off-time

Table 2 **DCV Simulation Results**

Gas forced air heating

VANCOUVER:			Exhaust Fan		HRV	
	Occupants:		3	6	3	6
Continuous	Fan Capacity	(L/s)	53	53	39	
(base case)	Ventilation + Infiltration	(ach)	0.32	0.32	0.31	
	CO2 - average	(ppm)	571	816	589	
	- maximum	(ppm)	802	1276	835	
	Space Heat Energy	(GJ/yr)	59.5	49.7	41.5	
	Ventilation Fan Energy	(GJ/yr)	2.6	2.6	5.2	
Demand						
Controlled:	Fan Capacity	(L/s)	25/75	25/75	19/57	
(match avg.)	Ventilation + Infiltration	(ach)	0.30	0.29	0.31	
	CO2 set-point	(ppm)	655	995	675	
	CO2 - average	(ppm)	574	823	581	
	- maximum	(ppm)	694	1066	726	
	Space Heat savings	(GJ/yr)	2.5	2.6	0.3	
	Fan savings*	(GJ/yr)	0.7	0.7	1.3	
	TOTAL DCV SAVINGS	(GJ/yr)	3.2	3.3	1.6	
		($/yr)	$18.60	$19.19	$17.35	

TORONTO:			Exhaust Fan		HRV	
	Occupants:		3	6	3	6
Continuous	Fan Capacity	(L/s)	53	53	39	39
(base case)	Ventilation + Infiltration	(ach)	0.32	0.32	0.31	0.31
	CO2 - average	(ppm)	571	816	589	851
	- maximum	(ppm)	802	1276	835	1339
	Space Heat Energy	(GJ/yr)	82.0	73.3	60.6	52.2
	Ventilation Fan Energy	(GJ/yr)	2.6	2.6	5.2	5.2
Demand						
Controlled:	Fan Capacity	(L/s)	25/75	25/75	19/57	19/57
(match avg.)	Ventilation + Infiltration	(ach)	0.29	0.28	0.29	0.3
	CO2 set-point	(ppm)	645	995	675	1025
	CO2 - average	(ppm)	560	818	581	837
	- maximum	(ppm)	658	1025	726	1127
	Space Heat savings	(GJ/yr)	4.9	5.8	-0.1	0.3
	Fan savings*	(GJ/yr)	0.7	0.7	1.3	1.3
	TOTAL DCV SAVINGS	(GJ/yr)	5.6	6.5	1.2	1.6
		($/yr)	$36.66	$41.37	$22.67	$24.64
Demand						
Controlled:	Fan Capacity	(L/s)			25/75	
	Ventilation + Infiltration	(ach)			0.20	
	CO2 set-point	(ppm)			1000	
	CO2 - average	(ppm)			797	
	- maximum	(ppm)			1005	
	Space Heat savings	(GJ/yr)			5.1	
	Fan savings*	(GJ/yr)			1.4	
	TOTAL DCV SAVINGS	(GJ/yr)			6.5	
		($/yr)			$50.59	

*based on 25% off-time

DCV Simulation Results

Gas forced air heating

WINNIPEG:			Exhaust Fan		HRV
	Occupants:		3	6	3
Continuous	Fan Capacity	(L/s)	53	53	39
(base case)	Ventilation + Infiltration	(ach)	0.32	0.32	0.31
	CO2 - average	(ppm)	571	816	589
	- maximum	(ppm)	802	1276	835
	Space Heat Energy	(GJ/yr)	112.6	103.7	86.1
	Ventilation Fan Energy	(GJ/yr)	2.6	2.6	5.2
Demand					
Controlled:	Fan Capacity	(L/s)	25/75	25/75	19/57
(match avg.)	Ventilation + Infiltration	(ach)	0.30	0.29	0.31
	CO2 set-point	(ppm)	645	995	675
	CO2 - average	(ppm)	562	823	593
	- maximum	(ppm)	655	1066	735
	Space Heat savings	(GJ/yr)	3.5	4.8	1.4
	Fan savings*	(GJ/yr)	0.7	0.7	1.3
	TOTAL DCV SAVINGS	(GJ/yr)	4.2	5.4	2.7
		($/yr)	$20.69	$25.55	$12.78
Demand					
Controlled:	Fan Capacity	(L/s)	25/75		
	Ventilation + Infiltration	(ach)	0.28		
	CO2 set-point	(ppm)	675		
	CO2 - average	(ppm)	585		
	- maximum	(ppm)	700		
	Space Heat savings	(GJ/yr)	6.6		
	Fan savings*	(GJ/yr)	0.7		
	TOTAL DCV SAVINGS	(GJ/yr)	7.2		
		($/yr)	$32.53		
Demand					
Controlled:	Fan Capacity	(L/s)	25/75		
	Ventilation + Infiltration	(ach)	0.18		
	CO2 set-point	(ppm)	1000		
	CO2 - average	(ppm)	830		
	- maximum	(ppm)	1004		
	Space Heat savings	(GJ/yr)	20.5		
	Fan savings*	(GJ/yr)	0.7		
	TOTAL DCV SAVINGS	(GJ/yr)	21.2		
		($/yr)	$87.06		

Acknowledgements

This project from which this work was drawn was partially funded by the Panel for Energy Research and Development and formed part of Canada's contribution to the International Energy Agency. The project was performed by Peter Moffatt, and Sebastian Moffatt of Sheltair Scientific Ltd., Ken Cooper of SAR engineering ltd. with Tom Hamlin of Canada Mortgage and Housing Corporation.

AIR MOVEMENT & VENTILATION CONTROL WITHIN BUILDINGS

12th AIVC Conference, Ottawa, Canada
24-27 September, 1991

POSTER 20

A Demonstration of Low Cost DCV Technology on Five Canadian Houses

Peter Moffatt

Sheltair Scientific Ltd
Vancouver, British Columbia
Canada

Abstract

Field investigations were undertaken on five houses to determine the potential for improved performance and lower costs through the use of a demand controlled ventilation (DCV) systems. All 5 houses were energy efficient, low toxicity construction, and were chosen to reflect a range of mechanical systems consistent with Canada's new ventilation standard (CSA F326). Three of the test houses were extensively monitored and, after 90 days of conventional operation, were converted to DCV using a wide variety of sensors and controls. A fourth house with a previously installed DCV system was submitted to a series of "activity scenarios" to evaluate the performance of a DCV system based on extractors and inlets that respond to indoor relative humidity. The fifth house was a new house, designed to demonstrate DCV technology, and to validate the insights obtained from the other 4 houses. Commissioning of the new DCV house showed the suitability of using low cost sensors for detecting VOCs, absolute humidity, air flow and activity levels. A low-cost but sophisticated computerized control and monitoring system was used to analyze the ventilation needs and to switch fan motor windings and speeds to create a range of "operating modes" for the ventilation system. A video monitor display with occupant control added a further measure of demand control. The result was a successful demonstration of how currently available and affordable sensors and controls can be used to improve the performance of typical ventilation systems.

1.0 Introduction

This research project was completed for the Research Division of Canada Mortgage and Housing Corporation, and is part of Canada's contribution to an international research effort on Demand Control Ventilation (DCV). The research took place between September 1989 and December 1990.

The primary objective for the project was to determine if DCV can improve the way in which Canadian houses are ventilated, while lowering the operating or capital cost of ventilating systems. A further objective was to provide guidance for home builders and ventilation system designers on what DCV strategies might be most appropriate for near term applications.

The project was completed in five separate phases described in Table 1.

Table 1: Phases of CMHC Funded DCV Research

Phase 1	Literature Survey
Phase 2	Preparation of a Primer for Builders and Designers
Phase 3	Field Research on Five Canadian Houses
Phase 4	Computer Simulations of Ventilation Rates
Phase 5	Economic Analysis of DCV

The results of the first two phases have been combined into a separate publication - A DCV Primer for Builders and System Designers, which provides a popular explanation of ventilation strategies, and identifies many types of sensor technologies and DCV hardware that are currently available or under development. This paper summarizes the findings from the field investigations on the five research houses. A companion paper, also prepared for AIVC 1991, summarizes the results from the computer simulations and economic analysis.

Field investigations were intentionally designed to test ventilation systems compatible with the new CSA F326 Ventilation Standard for Canadian houses. Four of the five research houses were energy efficient, low toxicity construction. The houses were located in both coastal and interior climatic zones. The variety of systems was intended to reflect the most common approaches applied in new energy efficient Canadian housing.

Table 2: Description of ventilation systems in the Five Research Houses

Sue house	HRV with recirculating system
Jones house	HRV without a recirculation system
Smith house	Exhaust only ventilation with recirculating system
Morewood house	Exhaust only ventilation without a recirculating system
Helma house	Multiple sensor DCV system, HRV with recirculating system

The Sue, Jones and Smith houses were extensively monitored and retrofitted as part of the research. The Morewood house had an existing DCV system which was tested as found. The Helma house was new construction, and incorporated ventilation design specifications prepared as part of this project.

Field investigations began with extensive commissioning tests on existing ventilation systems, followed by minor up-grades and installation of long term monitoring equipment. After three months of monitoring house performance and air quality without DCV, each house was retrofitted with a new DCV system.

The new DCV systems employed a variety of sensors, to permit continuous measurement of such parameters as CO2 levels, pressure differentials, temperatures indoors and out, relative humidity, absolute humidity, air flow through the ventilation system, activity levels within the house, operation of heating equipment and clothes dryers, and air flows through variable exhaust equipment and furnace blowers. Several patented devices for gauging air quality measurement were also employed in the houses, including the Massawa Vital Air Purity meter (with sensors for oxygen, particles and humidity), and the Halitech Sensor (for odours and combustibles). Different combinations of sensors were used in each house, as dictated by the type of systems. Spot measurements were also conducted for measuring formaldehyde, organics and other pollutants.

Intensive monitoring of activity scenarios was conducted in four of the research houses, to measure how the systems responded to very different kinds of activities within the home. The intensive monitoring included: a tracer gas growth test in each house, to measure ventilation effectiveness; a tracer gas decay test, to measure ventilation efficiency; a mass balance moisture test, to measure the capture efficiency of the exhaust inlets; and a multi-point absolute humidity test, to measure the moisture absorption and desorption rates of the entire house.

During the intensive monitoring, Co-pilot, a program designed for MSDOS computers, was successfully used as a sophisticated controller and data acquisition system. A new version of Co-pilot, written for this project, was capable of simulating many different DCV control strategies.

An additional two months of monitoring was conducted on the Sue, Jones and Smith houses, following the installation of DCV systems. This approach provided extensive data for comparison with the earlier pre-DCV configurations.

2.0 Results

The results of field monitoring on three of the research houses is presented in the following table.

Table 3: Summary of Low Level Monitoring - Before and After DCV

	Sue house		Jones house		Smith house	
DCV Control Strategies	Before RH	After Activ.	Before RH	After CO2	Before RH	After AbsH
Hours of Monitoring Data	856	580	1168	189	1385	846
Outside Temperature (C)	3.8	10.5	2.7	n.a.	7.1	13.4
Inside Temperature (C)	20.9	21.4	21.2	22.1	24.4	24.0
Relative Humidity (%)	40	42	38	n.a.	31	n.a.
Average CO2 (ppm)	571	544	584	558	542	472
Max. Hourly CO2 (ppm)	2250	948	996	726	2767	1028
Ventilation Flow Rate (L/s)	80	75	62	49	25	32
Ventilation - Time Off (%)	0	23	0	34	0	0
Activity Counts Family Rm	75	67	39	35	79	68
Activity Counts Bedroom	4	4	15	13	4	5

Note: n.a. - not available due to data collection problems

With demand control, ventilation reductions of 6% to 21% resulted for the period monitored. This will result in a corresponding reduction in energy required to heat

the ventilation air. In addition, fan electrical energy was reduced from 23% to 34%.

While generally reducing energy use, all three DCV systems achieved slight reductions in average CO2 levels, and significant reductions in peak CO2 levels.

3.0 Jones house

Three figures from the Jones houses are presented as an example of the data that was analyzed prior to choosing a DCV strategy for this house. A similar procedure was followed for the Sue house and the Smith house.

Figure 1: Typical Working Day presents a typical working day in the Jones house. The house has 335 square meters of living area and is rated as a super energy efficient home under the Canadian R2000 Program. The house is heated with a hot water radiant boiler and is ventilated with a fully ducted HRV running continuously. Two adults and four children live in the Jones house. The mother works at a nearby school and the children are all school age.

CO2 levels slowly rise during the night with 6 people sleeping with a ventilation rate at 62 L/s. CO2 levels are constant through the night and peak at 8:30 AM as the family prepares to start the day.

The HRV is activated either by relative humidity sensors or by manual controls. The maximum HRV flow is at 7:30 AM and likely corresponds to showers. CO2 levels decay slowly over the day but begin to rise when the children first arrive home from school at 3:00 PM. The maximum peak for CO2 (850 ppm) is reached at 11:00 PM just before bedtime. Activity Sensors detect some slight movement during the night as occupants use the washroom and a burst of activity in the morning. Activity sensors detect the arrival home of the youngest children in the early afternoon. Weekends were found to only vary slightly from this typical working day.

Figure 2: Evaluation of Absolute Humidity Sensor for DCV Control presents intensive monitoring of the same house at the same time of year, but over several days. Absolute humidity and CO2 are being sampled every 5 seconds and averaged and stored on a 3 minute basis by the data acquisition system. Only a rough visual correlation exists between peaks in CO2 and absolute humidity. Humidity and CO2 peaks tend to coincide, however the CO2 peaks are usually one to three hours later. During unoccupied periods, CO2 concentrations drop from peaks of 800 - 900 ppm to 500 - 600 ppm (about 35%). For the same period, absolute humidity drops about 15% to 20%. At night, when the six occupants are sleeping, CO2 concentrations remains relatively stable, while the absolute humidity tends to fall.

Figure 3: CO-Pilot CO2 DCV Control shows the Co-pilot data acquisition control program acting as a DCV controller in the Jones house. This trial of the software shows that the feedback gain set for the ventilation system controller was to high,

causing an erratic fluctuation in the ventilation rates. Further experimentation was required to obtain a smooth transition. With a CO2 set point of 650 ppm the DCV system was unable to match the load during breakfast. However, during most of the night flows of either 40 L/s or 88 L/s were able to control the load.

4.0 New DCV House

The Helma house was a new house, designed to demonstrate DCV technology, and to validate the insights obtained from the other 4 houses. Commissioning of the new DCV house showed the suitability of using low cost sensors for detecting VOCs, absolute humidity, air flow and activity levels. The Helma house DCV system has five main features that are presented in Table 4.

Table 4: Features of DCV Control Strategy in Helma House

Feature 1	The system automatically turns on when people are at home and cycles on and off when people are away. The ventilation rate is calculated by the software program based on activity levels and the number of people at home. (Alternatively, a CO2 sensor could have been used.)
Feature 2	An air quality sensor will detect when pollutants are produced and will increase ventilation rates. The Figaro semi-conductor sensor operating in AC mode with a breather will sense toxic cleaning chemicals, off-gassing from construction materials and cigar smoke.
Feature 3	The system automatically monitors moisture levels in the home and outdoor temperatures. The system will automatically lower humidity levels to prevent condensation form occurring on window surfaces if outdoor temperatures drop.
Feature 4	The information that is being monitored is continuously displayed on a video monitor in the living room. The occupant can always be aware of how the system and the house is performing.
Feature 5	The software written to control the system is able to achieve any ventilation rate by switching between two motor windings and four motor speeds. Moving averages are used to dampen variability and slowly target a given ventilation rate.
Feature 6	The occupant can override the system at any time to set minimum and maximum ventilation rates by turning a dial and flicking switches. The occupant can choose when to rely on the automatic system.

5.0 Conclusions and Recommendations

A number of useful guidelines for designing DCV systems in Canadian housing were discovered by analyzing data from the before and after low level and intensive monitoring. The guidelines apply to the 5 research houses and we believe can be safely applied to other Canadian homes.

- DCV offers benefits only when time-varying occupant generated pollutants exceed building related pollutants

- Source control of building generated pollutants at the construction stage is essential for applying DCV control strategies in new Canadian homes.

- CO2 is an excellent indicator of occupancy and ventilation requirements in residential buildings. A small, moderately priced passive CO2 gas analyzer performed well in three research houses. However, the cost of the technology is too expensive for the bulk of Canadian houses.

- Activity related pollutants are best controlled by special purpose high capacity, directly vented, exhaust fans with high capture efficiencies.

- Relative humidity is a poor indicator of occupancy. Response times are slow and often there is no discernable change in RH despite major changes in occupancy and CO2 concentrations. Absolute humidity is a much better indicator of occupancy than relative humidity but still displays a lag time that is due to absorption and desorption characteristics of the house. Ventilation control based on absolute humidity is limited to the heating season, and is best combined with a window inside surface temperature to provide condensation control.

- The dehumidistats commonly employed for RH control were found to be grossly inaccurate as supplied by the manufacturers, subject to drift over time, and lacking any convenient means for re-calibration.

- Passive Infra red (PIR) activity sensors proved low cost and reliable during the field trials. They have a poor short term correlation with CO2 but excellent long term correlation. The poor short term correlation is due to the fact that activity is sensed instantly whereas pollutant concentrations rise over time. Short term correlations could be improved with more sampling points, and a software program that is able to gauge the level of activity over time and allow the system to respond to the rhythms of the household.

- Semi-conductor sensors (e.g. Figaro T68800) appear to have potential as an overall IAQ indicator if used in alternating operation with a breather that periodically flushes the sampling chamber to automatically zero the sensor.

- High mixing rates in residential houses are preferable to zoning and can greatly reduce the ventilation requirements on a room by room basis. In an energy efficient home, the ventilation requirements - not the heating load - should dominate the design specifications for air moving and distribution systems.

- DCV systems are particularly effective at reducing peak pollutants concentrations. This offers improved health and comfort, even if the mean level of pollutants are similar for systems without DCV.

- Further research, including theoretical work and chamber testing, is needed to develop a simple and reliable performance test capable of describing the effectiveness of fresh air distribution, and the response time of systems to fresh air demands. The development of these tests could greatly facilitate the evolution of ventilation systems and the incorporation of minimum standards within the building code.

- Inlets equipped with humidity controlled bladders were found to be particularly ineffective for DCV application, both in coastal climates and in central Canada.

- DCV system design can be simplified by defining the most common operating modes for the house, and configuring the air mixing and air change rates accordingly. Typical operating modes could be: standby (with timer activated intervals of operation); occupant arrival; high activity; odour control: and sleep.

- A potential exists for lowering the capital costs of sophisticated DCV systems by using a multipurpose home computer.

- Occupants should not be relied upon to optimize the operation of ventilation systems, although occupants must have the ability to interpret and override automatic controls

- DCV systems have the potential to become highly visible sales features in new homes, especially if occupants are provided with continuous feedback on their indoor and outdoor environments.

References:

1. Moffatt, P., Moffatt, S., and Cooper, K. "Demand Controlled Ventilation", Final Report - March 1991, Canadian Mortgage and Housing Corporation, Ottawa, Canada.

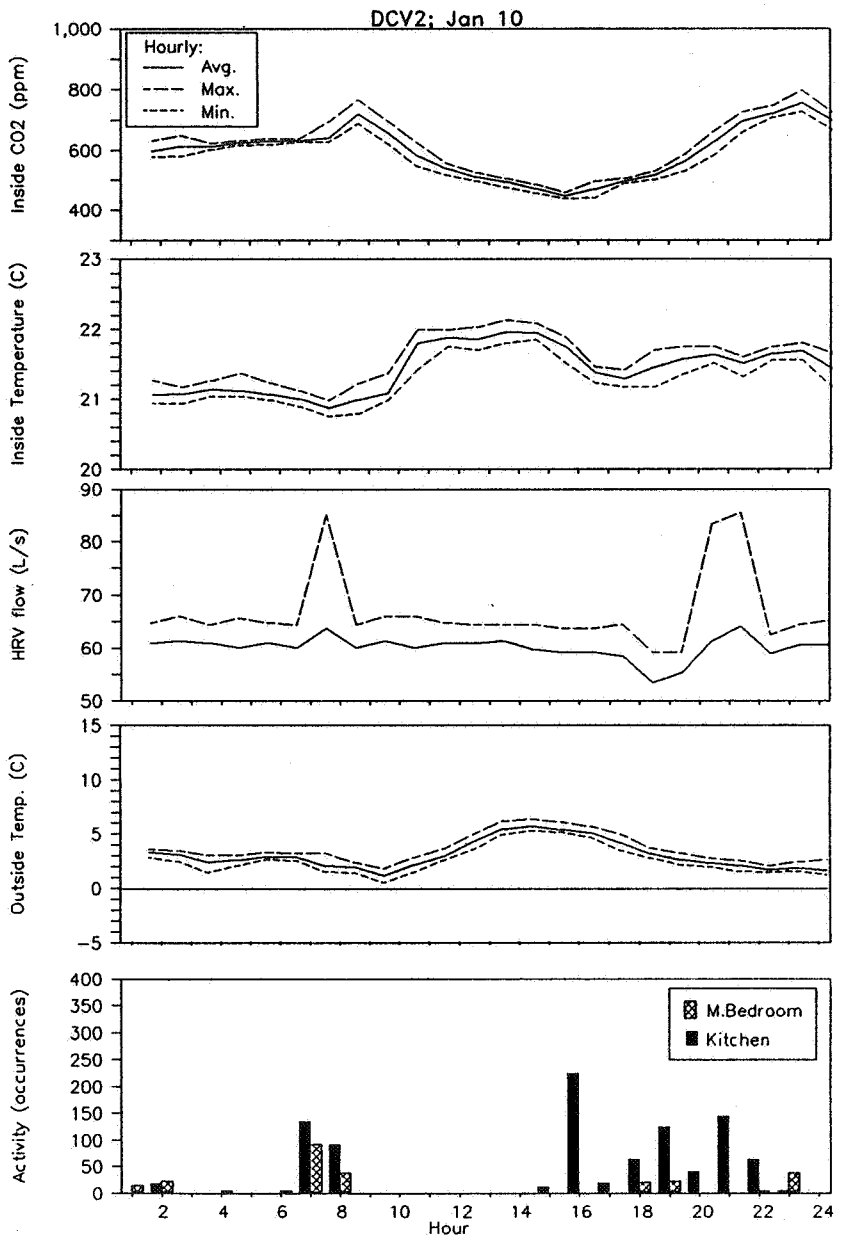

Figure 1: Jones house - Typical Working Day

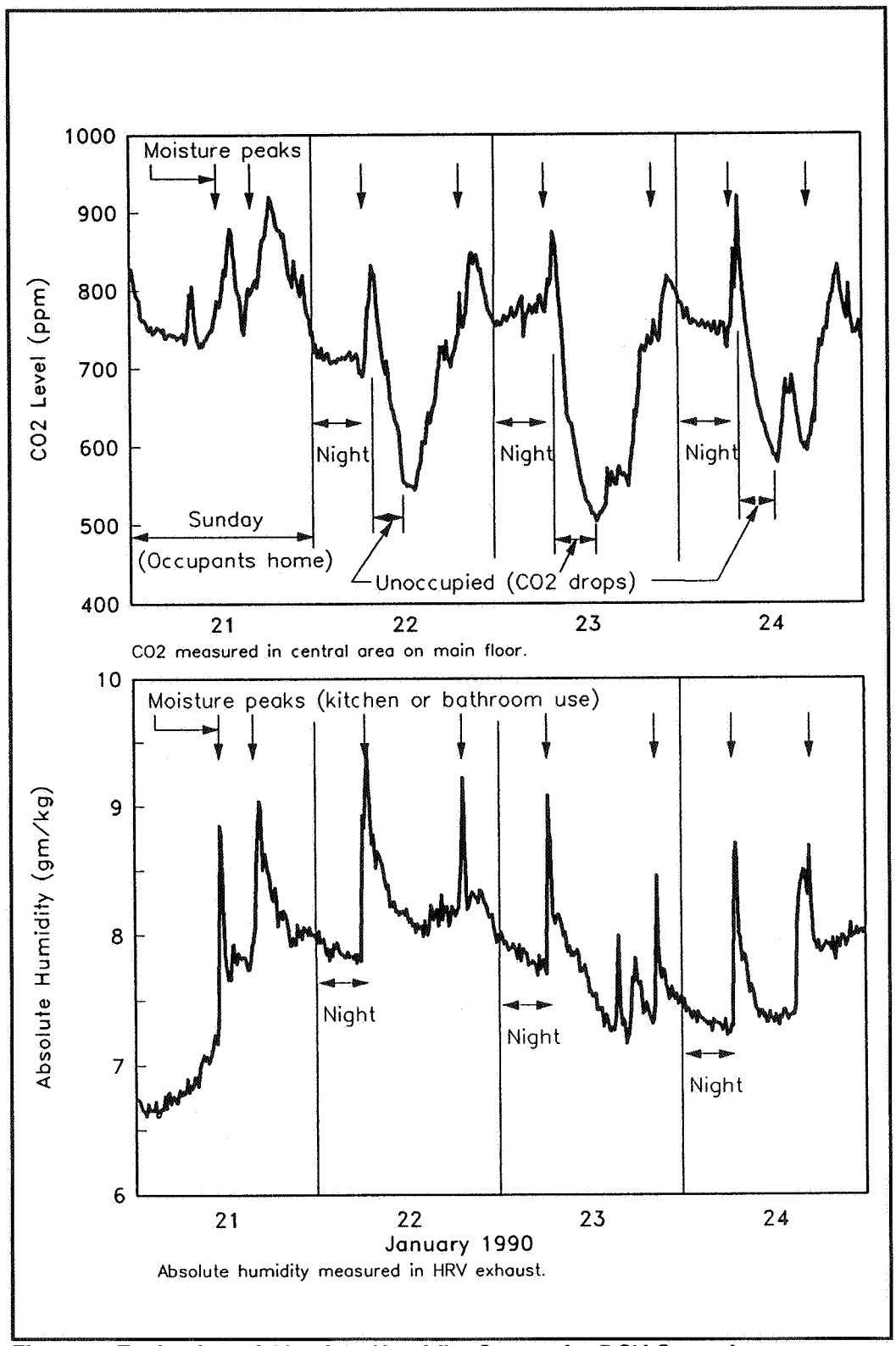

Figure 2: Evaluation of Absolute Humidity Sensor for DCV Control

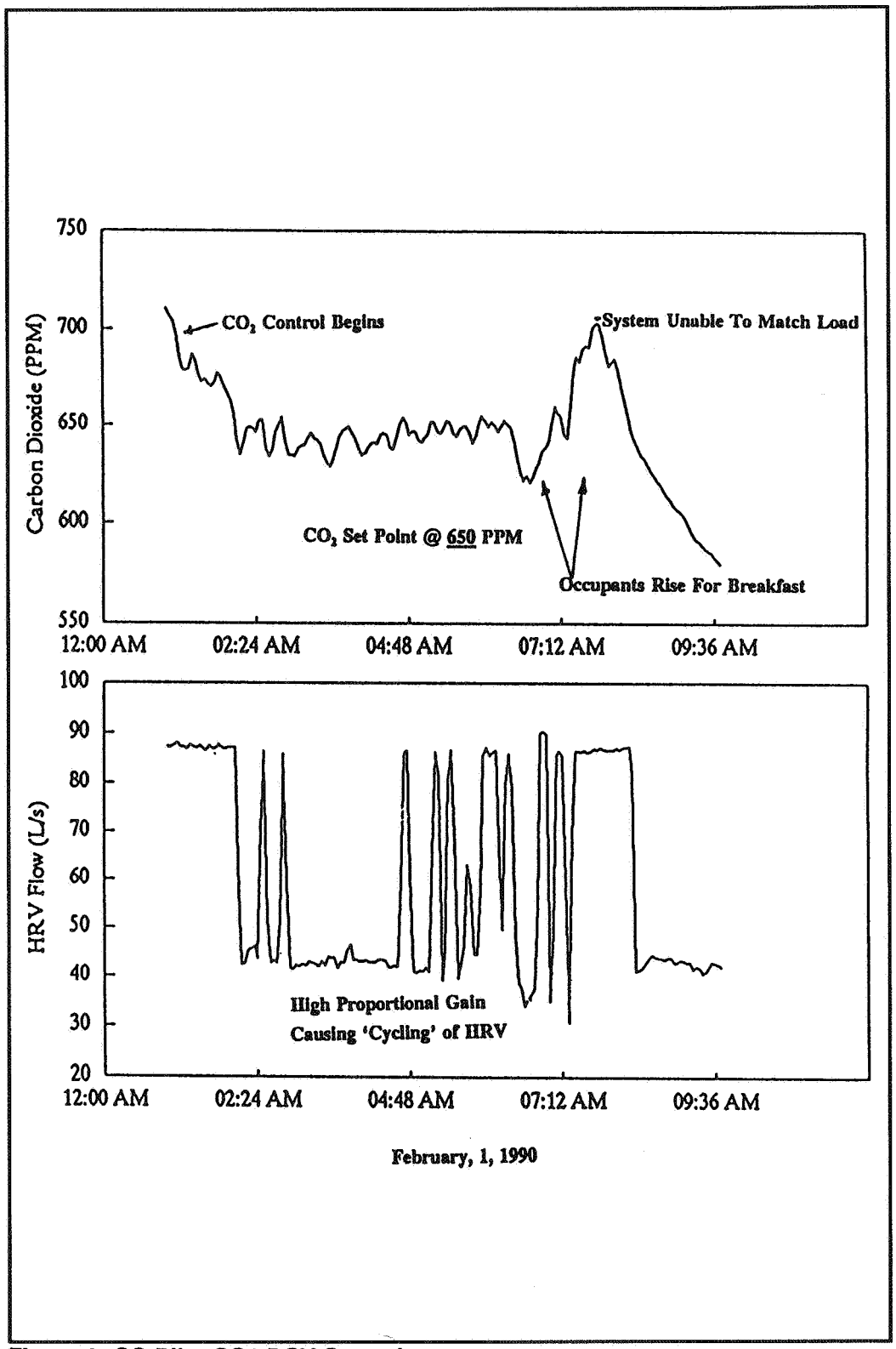

Figure 3: CO-Pilot CO2 DCV Control

AIR MOVEMENT & VENTILATION CONTROL WITHIN BUILDINGS
12th AIVC Conference, Ottawa, Canada
24-27 September, 1991

POSTER 21

DEMAND-CONTROLLED VENTILATION IN A SCHOOL

L. Norell, M.Sc.
Fläkt Indoor Climate AB,
S-120 86 Stockholm, Sweden

Summary

The performance of a system for demand-controlled ventilation was investigated for a period of 1.5 years. Presence sensors of the passive infrared type are used to control the ventilation rate in each classroom. The signal from the presence sensors was recorded, as well as the CO_2 concentration in the classrooms.

One of the classrooms was equipped with displacement ventilation. A comparison was made between displacement and mixing ventilation to investigate the CO_2 concentration in the stay zone. A significantly lower CO_2 concentration was measured in the case of displacement ventilation.

Project description

In 1988, the rebuilding and renovation of an elementary school was planned in the Municipality of Nacka outside Stockholm, Sweden.

Fig 1. Järla school in Nacka

The most important part of the renovation project concerned an improvement of the ventilation in the school. One objective was to provide good air quality in the classrooms. A low energy consumption was also desired.

The purpose of this project was to demonstrate that it is possible to maintain better air quality in the classrooms by means of demand-controlled ventilation when the rooms are in use, and that this can be achieved at lower energy consumption, compared with the dimensioning of fresh air flows in accordance with current building codes.

Measurements and calculations also showed that this was a profitable measure.

The installation and test measurements were funded by the Swedish Council for Building Research (BFR).

Building form

The schools consists of two buildings joined together by a common stairwell. The buildings were constructed at different times. The older section, which has four floors and contains six classrooms, a cafeteria and administrative offices, was built in the 1920s, while the newer building dates from the beginning of the 1940s and has three floors and six classrooms.

The classrooms face the south and southeast. The height from floor to ceiling is approximately 360 cm in the older section, and 310 cm in the newer section. The floor measures 9 m x 6.5 m in the classrooms.

Building services.
Heating and ventilation before renovation.

The school has a radiator system for heating that is connected to the Nacka district heating system. When the school was renovated, the

radiators were equipped with thermostat valves. Before the renovation, the ventilation system consisted of a natural draft system in the older section of the school. The new building had a mechanical exhaust air system, in which the fan operated 24 hours a day.

Before the renovation, tests were conducted to test the tightness of the buildings and the air change situation. In the building with the natural draft system, as well as in the section with mechanical exhaust air ventilation, carbon dioxide measurements were conducted in the classrooms to determine how the air was changed. At the end of a lesson, the CO_2 concentration was between 2000 and 3000 ppm.

In the newer section of the school, the CO_2 concentration normally stayed below 2000 ppm, provided that windows were opened during recesses.

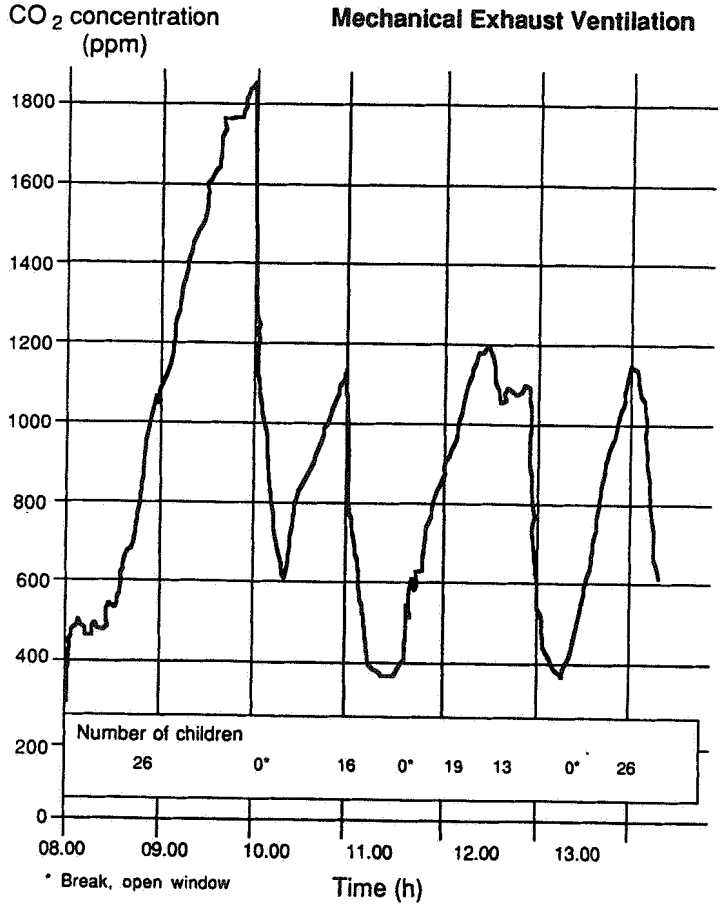

Fig 2. CO_2-concentration in a classroom before renovation

Air flow tests indicated air changes corresponding to a fresh air flow of approximately 2 l/s per student. Thus, earlier complaints about the ventilation system were justified.

Heating and ventilation after renovation

The existing radiator system was kept. The radiators were equipped with thermostat valves. When the school was renovated, the six classrooms in the older section were equipped with a supply and exhaust air system that was dimensioned in compliance with existing building codes (5 l/s of fresh air per student).

The six classrooms in the newer wing were equipped with a demand-controlled ventilation system connected to a separate AHU, as shown in Fig. 3. The objective was to prevent the carbon dioxide concentration from exceeding 1000 ppm in the stay zone.

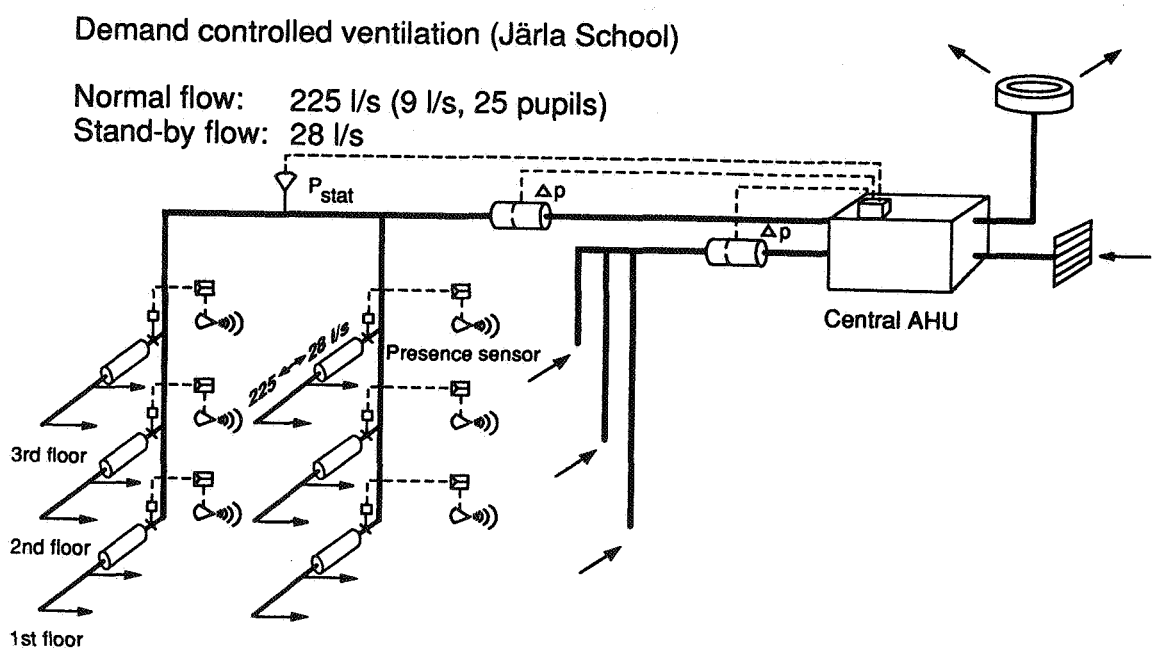

Fig 3. System principle

The system functions as follows:

- Each classroom is equipped with a presence sensor of the passive infrared type. When the device senses that someone is in the classroom, a supply air damper opens and closes ten minutes after the presence sensor picks up the last movement in the room.

- When the damper opens, the supply air to the classroom increases from approximately 28 l/s to about 225 l/s. This corresponds to 7.5 l/s per student, with 30 students in the class (grades 4-6), or 9 l/s per student, with 25 students in the classroom (grades 1-3).

- The general ventilation (basic flow) system operates 24 hours a day.

- Air exhausted into the corridor outside the classrooms is evacuated through exhaust air devices on each floor.

- The central air handling unit for supply and exhaust air is equipped with fans with guide vane control. The supply air is controlled by maintaining a constant pressure in the supply air duct system The exhaust air follows the supply air flow.

- The AHU is equipped with a plate heat exchanger for heat recovery, as well as a microprocessor-based controller that makes it possible to easily monitor the AHU's function. No air is recirculated.

- Five classrooms have traditional mixing air distribution with air being supplied at the front end of the ceiling. One room has displacement ventilation, with the supply air terminals positioned at floor level at the two corners in the front of the classroom. The supply air temperature is 18°C.

Measurements after the renovation

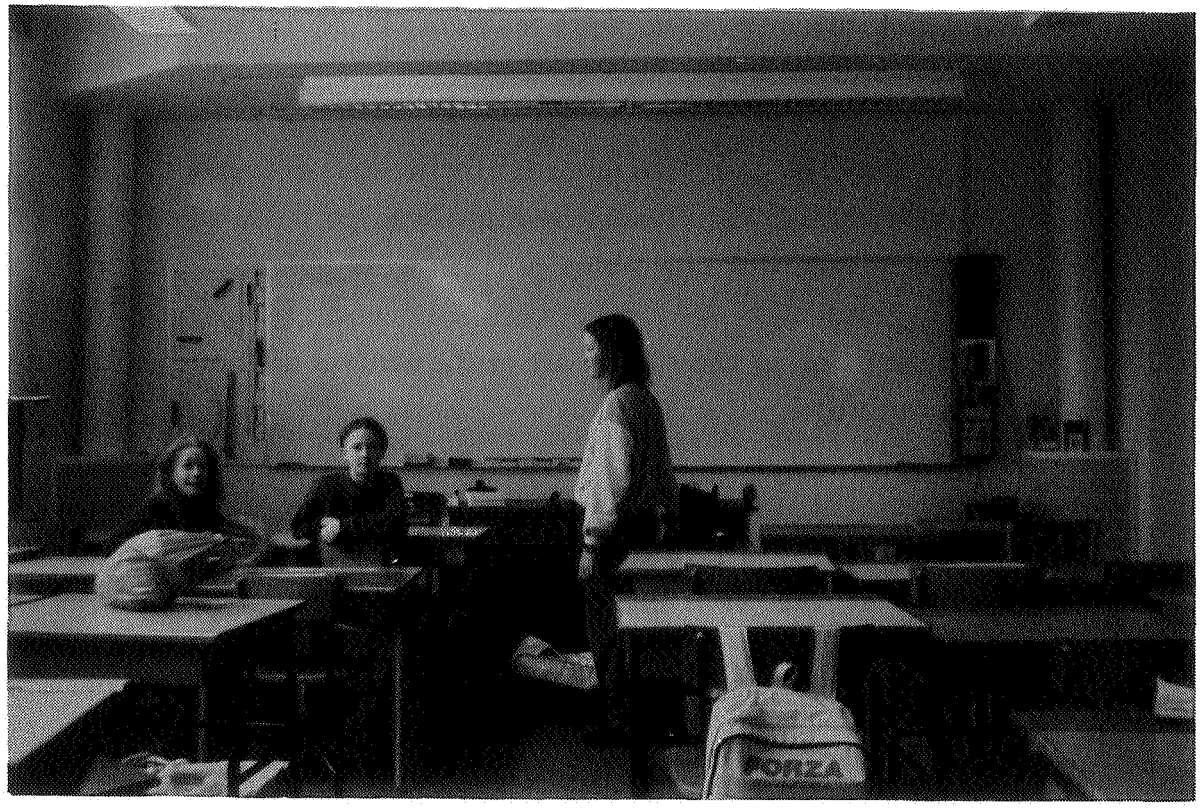

Fig 4. Classroom (306) with displacement ventilation

Measurements were conducted in three classrooms after the renovation was completed. One classroom had displacement ventilation and five had mixing air distribution.

The following measurements were made during 1990-91.

- The CO_2 concentration was recorded on a continuous basis for about two months.

- The signals (supply air flow) from the presence sensors were recorded in conjunction with the CO_2 measurements.

- Fresh air and exhaust air temperatures were recorded.

- Detailed measurements were made of horizontal and vertical CO_2 gradients in two classrooms over a period of several days.

- The supply air flow was measured when the detailed measurements were made. During these periods, teachers or students recorded how many persons were present in the room.

- The variation in the supply air in the central air handling unit was recorded.

Results of the measurements

Function of the ventilation system. Room function.

During the 1.5 years the system has been in operation, the measurements have shown that the demand-controlled system has functioned as planned. An example of this is shown in Fig. 5.

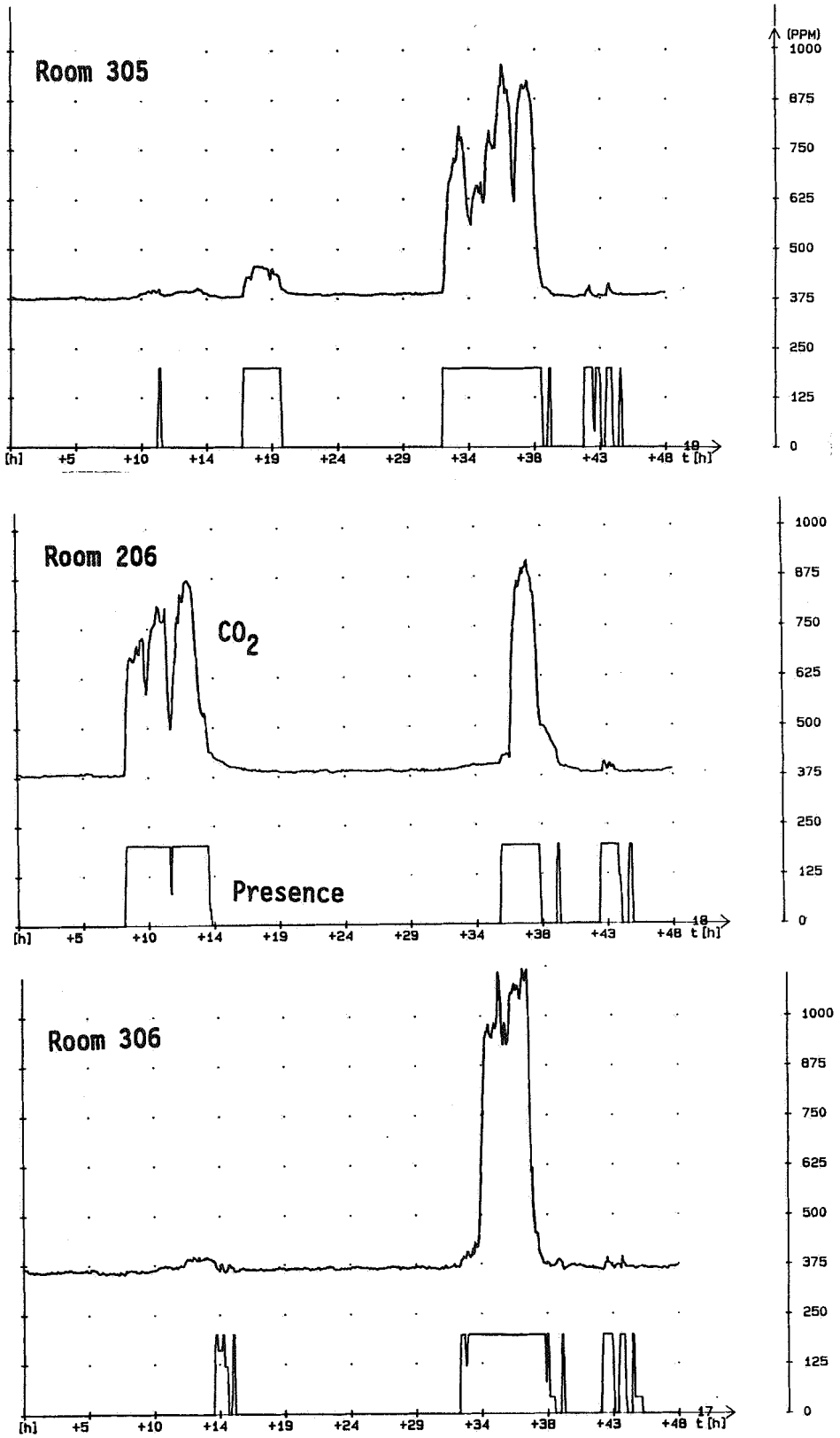

Fig 5. Presence and CO_2-concentration Monday and Tuesday, May 14th and 15th 1990

Here the carbon dioxide concentration and signal from the presence sensor have been measured for the three classrooms over a 48-hour period. The figure shows

- that only one of the three classrooms was in normal use on Monday, May 14, 1990.

- that in the other classrooms, some one entered the rooms to get books or other materials on a few occasions.

- that a small class meeting was probably held one evening in one of the classrooms.

- that the classrooms were cleaned on Tuesday evening.

The fact that two of the classrooms were not used on Monday was not in agreement with the ordinary schedule. In general, the signal of the presence sensor followed the respective class schedules closely.

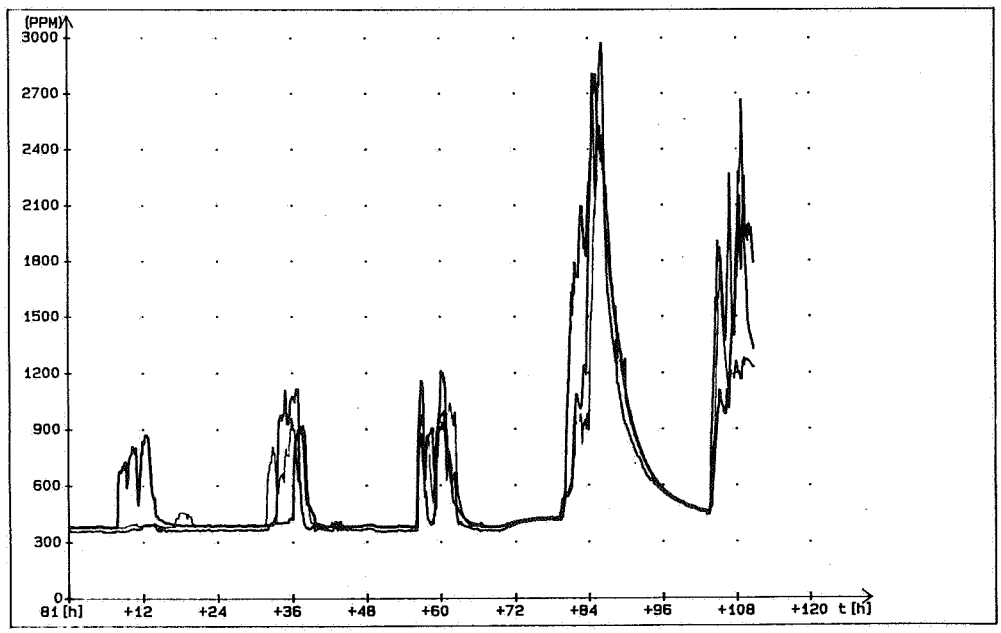

Fig 6. Power supply cut off

During the same week referred to above, the operation of the ventilation system was disturbed at the end of the week, due to the ongoing renovation work in the school. On Thursday and Friday the power was cut off completely to the AHU. The consequences of this disturbance are shown in Fig. 6.

Central Air Handling Unit

The following was recorded in the central air handling unit:

- the control signal to the guide vanes for supply air: 100% = full flow.
- the static pressure in the duct system (supply air): set value 310 Pa.
- the control signal for the air heater: 100% = open valve.
- the supply air temperature: set value = 18°C.

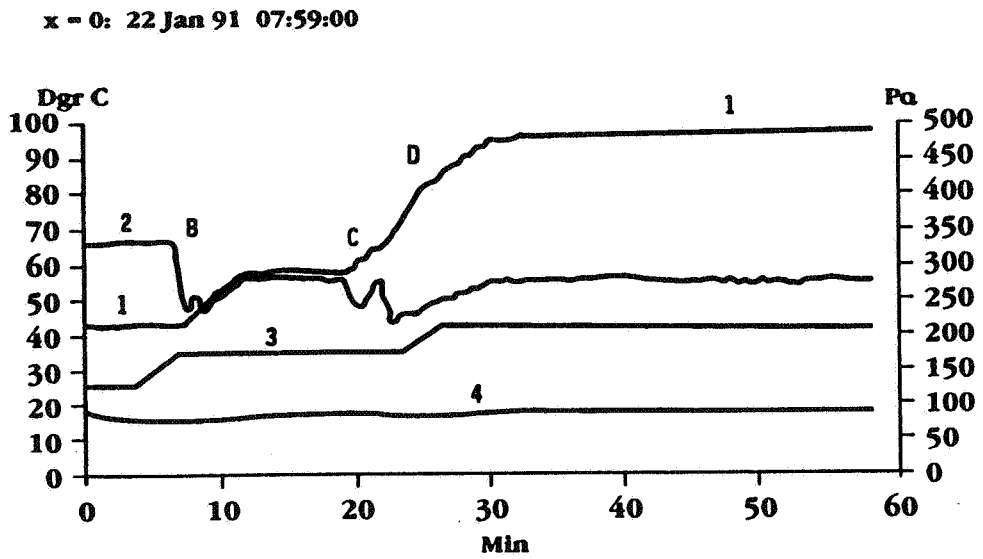

Fig 7. Measured values in central AHU

Fig. 7 shows how the air flow increases as the classroom is used. Only about 50% of the total air flow in the AHU is affected by demand control, since the remaining 50% is supplied to two workshops and to teacher rooms.

It is possible to see that:

- at 8.00 a.m. students arrive at one of the classrooms.
- the presence sensor in the classroom opens a damper.
- the pressure decreases. Guide vane B compensates the pressure drop.
- another classroom starts to be used, C and D, and the signal to the guide vane increases.
- at 100% all classrooms are being used.

Air quality

During the longer measurement periods, the CO_2 concentration was recorded in the exhaust air from the three classrooms.

The goal to keep the CO_2 concentration below 1000 ppm in the stay zone was achieved. This could be expected, considering the actual supply air flows being used.

The air quality was also considered good by students and teachers, despite the fact that measurements were made during the outgasing period, when solvents were being emitted by new building materials. The interior of the school was also painted and fitted with an acoustic ceiling.

Comparison between mixing and displacement air distribution

In two classrooms, one with displacement air distribution (306), and one with mixing air distribution (206), detailed measurements were made of the CO_2 concentration vertically. In room 306 (displacement ventilation), the CO_2 concentration was also measured horizontally at floor level.

When measuring the CO_2 gradient vertically, two measuring bars with sensors were used at 0.1, 1.1 and 2.1 m above the floor. The bars were placed about 2 m from the rear wall of the classroom as shown in Fig. 8. Thus, measurements were made at six points in all.

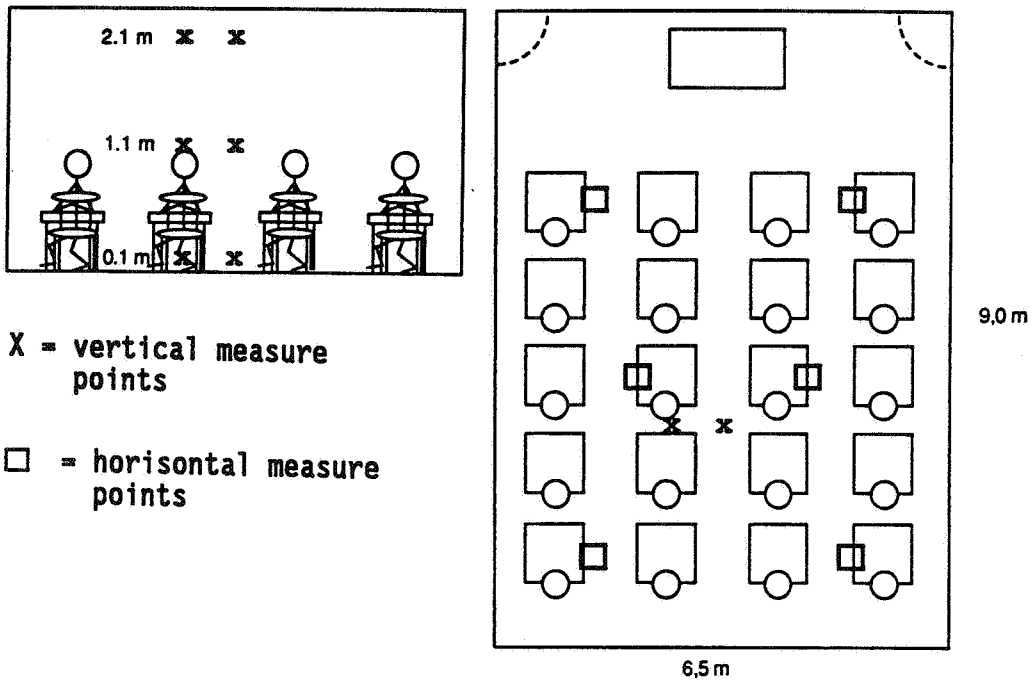

During the measurements, activity was normal in the classroom, meaning that students moved between their desks and the blackboard, and between groups.

The results from the two *vertical* measurements are shown in Fig. 9. After a recess, the measurements were carried out over a double lesson (about 90 minutes in length).

Depending on the actual number of students in the classrooms, the fresh air flow corresponded to 8.0 l/s per student in the room with displacement ventilation, and 9.2 l/s per student in the room with mixing ventilation. If the measurement values are corrected to take this into account, the measured concentration at the 2.1 m level coincides in both classrooms, which, theoretically, should be the case.

As can be seen from the diagrams, the CO_2 concentration in the mixing air distribution case (206) is largely the same at all measurement points. But in the classroom (306) with displacement air distribution, a clear difference can be seen between the CO_2 concentration at the three different levels.

Here, the mean concentration in the breathing zone (1.1 m) is approximately 750 ppm, while the concentration at 2.1 m is about 1000 ppm.

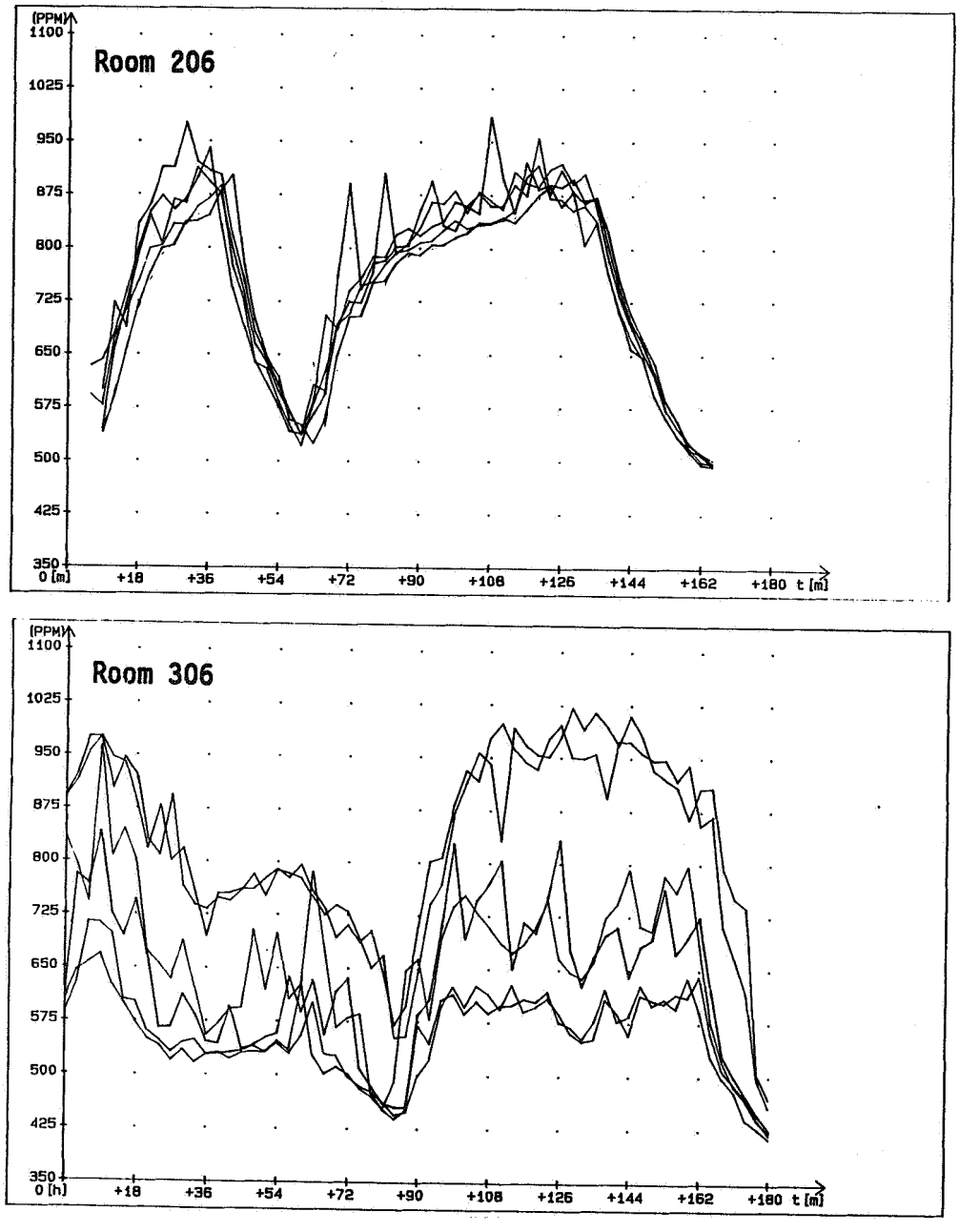

Fig 9. Mixing vs displacement ventilation

Thus in classrooms, displacement air distribution improves air quality in the breathing zone corresponding to about 250 ppm of CO_2, compared with mixing air distribution and a similar air flow.

It can also be stated that, with displacement air distribution, it is possible to decrease the fresh air flow, and thereby lower the energy requirement for heating air, by about 25 percent, and still retain air quality.

In general, it can be noted that the measured concentrations (206) indicate that the children (ages 7-13) exhale about 18 l of CO_2 per hour. This is otherwise a value considered typical for adults performing office work.

The *horizontal* measurements were also made at six points at floor level (0.1 m).

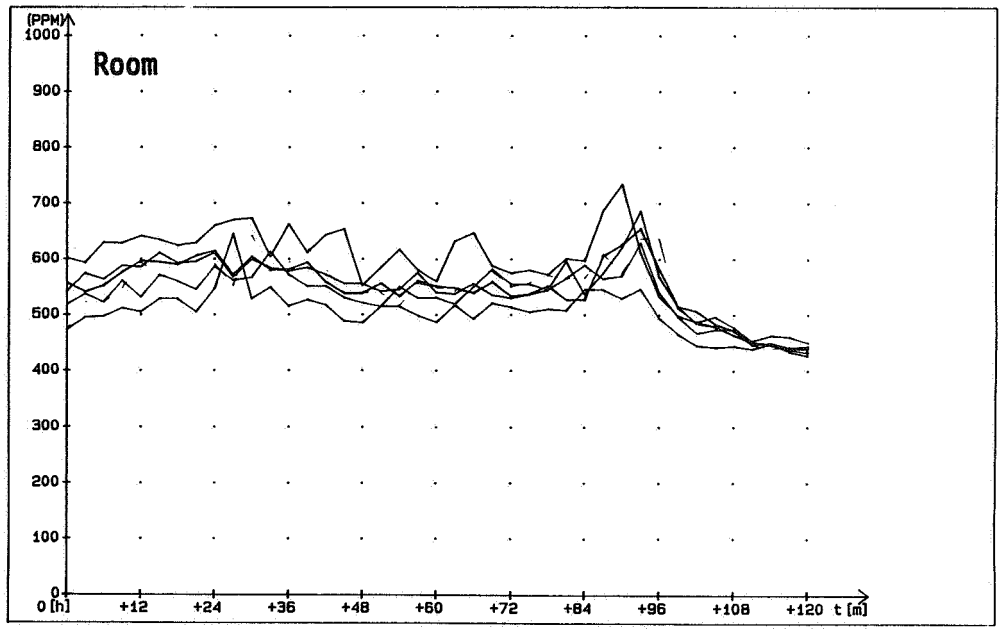

Fig 10. CO_2-concentration in 6 points at 0.1 m level

The measuring points and results are shown in Fig. 10. As indicated by the results, the supply air, which was cooler than the

room air temperature, was distributed effectively throughout the classroom. The radiators were not on when the measurements were made.

Energy performance

The measurements confirmed that the air flow to the classrooms met the requirements shown on the respective schedules. Based on the schedule for the six classrooms with demand-controlled ventilation, the system's function and energy requirement for heating can be simulated. Climate data were used for Stockholm.

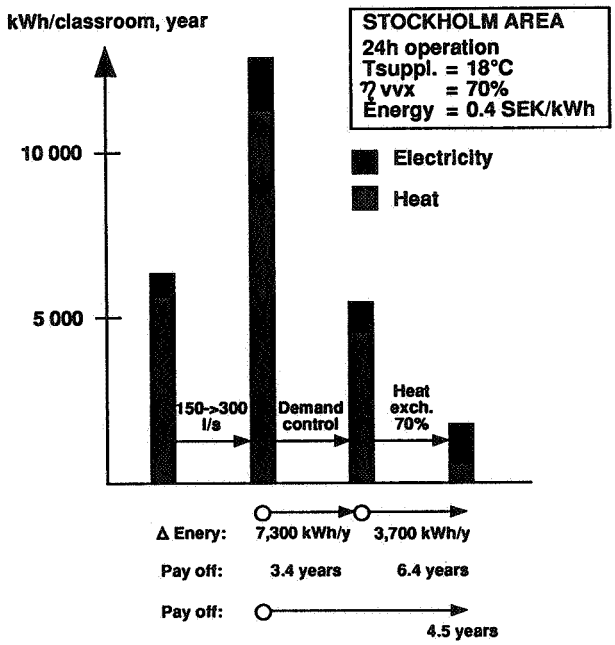

As shown in Fig. 11, increasing the fresh air flow specified in the existing building code (5 l/s per student, 150 l per class) to a fresh air floor guaranteeing good air quality – for example, a maximum of 800 ppm of CO_2 (10 l/s per student, 300 l per class), doubles the energy requirement for air handling.

By using demand-controlled ventilation, however, the energy requirement is reduced by more than half. The use of heat recovery further decreases the amount of energy required. Based on the

demand-controlled ventilation and heat recovery system used in this project, the payoff period has been estimated at about 4.5 years for both measures.

Conclusions

When the air flow is 8-9 l/s per student, the student feel the air quality is sufficient during those months of the year when the room temperature is at an acceptable level.

In the autumn and spring, an increase in the fresh air flow, using air cooler than room air, is desirable to keep the room temperature down. It is not always possible to open windows to air out the classrooms because of noise, or because of pollen, for example. A high room temperature is one of the main reasons why the students feel the air is dry and of "poor" quality.

In a VAV system controlled on the basis of air quality, the air flow can vary between 100-10% at any time of the year.

This places special demands on the control of the heating coil in the central air handling unit.

The classroom ventilation system controlled by presence sensors has functioned reliably. The estimated energy savings were confirmed. In a centralized ventilation system, equivalent savings can almost be achieved by using a more efficient heat recovery system. This should be a more profitable solution in systems with short operating times, such as in schools.

AIR MOVEMENT & VENTILATION CONTROL WITHIN BUILDINGS

12th AIVC Conference, Ottawa, Canada
24-27 September, 1991

POSTER 22

Warm Air Heating with a Constant High Supply Air Flow Rate without Recirculation

Thomas Carlsson

The Swedish National Testing and Research Institute
Box 857
S-501 15 BORÅS
Sweden
Tel: +46 33 165000 Fax: +46 331979

Synopsis

In Halmstad a multi-apartment house has been built with air carried heating. Fresh air was used as the only heat carrier. To improve the air quality it was decided to not use circulation flow, which is normally required for air carried heating. The heating requirement was obtained with a higher air flow than what the standard requires. This also implied improved air quality. The standard specification states 0.5 changes per hour as the minimum requirement, but in Halmstad the house was ventilated with 0.7 - 1.0 changes per hour. The drawbacks resulting for this (greater ventilation losses, with operating faults to fans) have been solved with a high degree of heat recovery and frequency control of the fans.

The measurement results indicate that the increased ventilation losses on the basis of a higher ventilation flow were 11 kWh/year m^2. The operating faults for the fans increased from 60 W to 110 W per apartment. The tenants experienced an improved air quality in comparison with a control group. All the air in the apartments was replaced with fresh air within two hours. Despite that the installed system is not fully commercially developed the costs for installation and operation were the same as for conventional heating and ventilation systems.

In the next generation of similar systems the experience of this project will enable the reduction of the safety margins during planning. During the planning it was decided to dimension the system for 1.3 changes per hour. During practical operations 1.0 changes per hour has proved to be sufficient. This implies that it is possible to reduce the duct dimensions, use smaller fans, smaller air-to-air heat exchangers, and remove the frequency controls on the fans. This enables a considerably cheaper system and a better acoustic climate.

1. Background

1.1 Ventilation

In Sweden the minimum requirement with respect to the ventilation (see Ref. 1) of apartments is regulated for the different types of rooms and the activity which takes place. In addition there are requirements as to which type of air is to be supplied to the different rooms.

In living rooms the "outdoor air flow rate" shall be at least 0.35 ltr/sec m^2 of the floor area.

Even in bedrooms the "outdoor air flow rate" shall be 0.35 ltr/sec m^2 of the floor area. However, in addition to the requirement for outdoor air flow there is a requirement on an "air flow rate" of 4 ltr/sec per bed. The concept of air exchange includes both outdoor flow and transferred air.

Other apartment areas can be ventilated with "transmitted air" only. Depending on the type of room there are different requirements as to how large the flow shall be.

Example

A three-room apartment is to have the following ventilation flows and types of air.

Example

Type of room	*Living area* m^2	*Outdoor air* l/s	*Transferred air* l/s	*Exhaust air* l/s
Bedroom 1*	12.6	4.4		
Bedroom 2**	12.8	4.5	3.5	
- Living room	30.7	10.7		
- Kitchen	13.4			10.0
- Bathroom	4.2			10.0
- Hall	7.7		2.7	

*) one bed
**) two beds

In the example above it was the exhaust air for the kitchen and bathroom which were critical for the dimensioning of the apartment, the total outdoor flow rate was 20 ltr/sec. This corresponds to 0.4 air turnovers per hour. A typical value for the number of turnovers per hour is 0.5 as per Swedish standard requirements.

During the last five years the debate in Sweden has been intensive as to how much we should ventilate our apartments, and on the use of circulation air.

The reason why the use of circulation air is not favoured is that impurities are thereby distributed to the entire apartment. Arguments that the ducts for circulation air are dirty and contaminate the air have also been presented.

1.2 Heat recovery

Since the end of the 70' s the majority of buildings have been provided with some form of heat recovery. The two methods which have been used for the recovery of the ventilation air are air heat exchangers or exhaust air heat pumps. The different systems are estimated to have an equal share of the market.

The reasons that buildings were provided with heat recovery were on the one hand rising energy prices. and on the other the modified standards (Ref. 2) which required heat recovery when the heat content in the exhaust air was > 50 MW hours/year.

1.3 Insulation

In the standard requirement for the insulation of external walls the requirement for U was up to 1975 0.58 W/m^2 °C. The new standard the next year almost halved the U value to 0.3 W/m^2.

2.1 Test object

In Halmstad a multi-apartment house with 14 apartments has been built during 1989. Since the building is well insulated the power requirement for heating is low. By reasonably increasing the ventilation flows it is possible to supply heat via the ventilation system. The air which is used for heating is outdoor air only. There is no circulation air in the system. To meet the heating requirement of design temperature (-16°C) with a max supply air temperature of 50°C one air change per hour is needed. Depending on the outdoor temperature the number of air changes varies steplessly between 0.7 - 1.0 / hour. In the system there is an air to air heat exchanger. The temperature efficiency capacity of the unit is 67%. The unit is placed in the fan room and supplies all the apartments. Each apartment is provided with a follow-up heating battery which enables the regulation of the temperature in each apartment up to 22°C.

The house is well insulated, the heat transmission ratio of the outer walls in 0.17 W/m^2.

2.2 Results and discussion

The Swedish National Testing and Research Institute (SP) were commissioned by Swedish Council for Building Research (BFR) to make an evaluation during the period Feb 1990 to April 1991 as to how the system functioned with respect to:

- Greater ventilation losses on the basis of higher ventilation flow.

- The air quality.

- The air exchange efficiency.

- Noise from fans.

- Greater operating faults to fans as a result of higher flow.

- Poll investigation of the experience of the tenants as to the indoor environment.

- Economical yield of the system.

The measurements were initiated in connection with occupation of the building in December 1989.

- Function check in connection with occupation.

- Long-term measurements.

- Function check at he end of the project.

The measurements in connection with the function checks have been carried out with intensive measurements. The objective of these measurements was to ensure that the system functioned as intended at the planning stage.

The long-term measurements have been carried out with a data logger which was installed in the building. Via a modem the measurement values have been transferred to a mini computer (VAX) to SP every day. The objective of these measurement was to follow-up energy/power consumption for electricity and heating.

The results form the project are presented in a report, see reference 5.

Measurement results

3.1 Greater ventilation losses on the basis of a higher ventilation flow.

The total air flows to the building and the sub-air flows to the apartments have been measured continuously during the measurement period.
The measurements indicate that the ventilation flow to the building has varied between 0.7 - 1.0 changes per hour.
The mean value for the ventilation was 0.9 changes per hour over the measurement period.

The heat recovery unit's temperature efficiency has been measured up to 67%.

To study the differences in the ventilation losses between a ventilation system which complies with the minimum requirements as per Swedish standards (0.5 changes per hour) and the air exchange which has taken place in the building (0.7 - 1.0), calculations were made in the computer program AXSEL; see reference 6.

From these calculations it was revealed that the ventilation losses increased by 5200 kWh/year for the whole building. The total living area in the building is 475 m^2. The increase in ventilation losses per year thus becomes 11 kWh/m^2 floor area.

3.2 Volatile organic substances

The building's air quality with respect to volatile organic substances was established by absorbing the substances on tenax tubes for a period of one hour. This measurement was carried out in the fresh air duct and in an apartment. The measurements were carried out 16 months after occupation.

These measurements indicated that the VOC content was 170 µg/m^3.
Several of the substances which were identification the indoor air were 2-(epoxyethexy) ethanol, one of many glycol ethers, used in water diluted paints. Phenol, included in different binder agents in flooring of PVC.

In order to study differences in VOC in the outdoor air, measurements were made for one week. These measurements were carried out with the aid of a photo-acoustic
method which registered VOC in the form of methane equivalents every 12 minutes. The measurements were made in the fresh air duct to the building.

The content of VOC proved to vary between 50-65 µg/m^3 of air during the measurement period.

The content of VOC in indoor air is usually less than 200 µg/m^3 as per the experience have of measurements in Swedish apartments.

3.3 Relative humidity content in the indoor environment

The relative humidity content was measured continuously during the measurement period in four apartments. During a three week period in February 91 the RH values read off were registered. During this period the RH was between 30-35%; the indoor temperature was 23°C and the outdoor temperature was -4 °C. The highest level on RH was registered in Aµgust -90. During a couple of weeks in August the RH value was 60%, the indoor temperature was 23 °C and the outdoor temperature was 19 °C.

The discomfort limits which we have in Sweden indicate that RH should lie between 30 - 60%.

3.4 Air exchange efficiency

A measure of how efficiently the ventilation air is entered into all the areas in an apartment is the "air exchange efficiency" (see Ref. 3). The efficiency is given in per cent of the theoretical min time taken to exchange all the air in a room. If the efficiency is less than 40%, and the number of changes is 0.5 hour, it will take 5 hours before the air is exchange in the apartment.

The air exchange efficiency was measured in one apartment in the building to 50%. Since the number of changes per hour is 1.0, the air will be exchanged every other hour in the apartment.

A typical value of the air exchange efficiency in a conventional ventilation system is 40 - 50%.

3.5 Noise from fans

The system is dimensioned to handle up to 1.3 changes per hour. The reason for this is that a safety margin was required in the event that the heating did not work as intended. The sound level was measured in two apartments, in the bedrooms and living rooms. The measurements were carried out for the max installed flow of 1.3 changes per hour. The following results were obtained:

Bedroom 1	23 dBA
Bedroom 2	23 dBA
Living room 1	26 dBA
Living room 2	31 dBA

The max permissible sound pressure level as per the Swedish Standard is 30 dBA in bedrooms and living rooms, but since in practical operations 1.0 turnovers/hour has proved to be sufficient the sound requirements have been met.

3.6 Greater operating faults for fans on the basis of the higher flows

To counteract the negative effects of a higher power consumption for the fans they were provided with frequency control. A standard ventilation with 0.5 changes per hour in a building with 14 apartments (the same as the experimental building) requires a fan effect of 400 W per fan.

In view of the fact that the adjustment of the air flows was incorrect during a part of the measurement period there are no measurement results for the fan consumptions during a one year period. But with the experience we have obtained from the measurements during the period when the flows were correctly adjusted we can confirm that a good mean value for the year as to the number of changes per hour is 0.9. With this flow the exhaust air fans consume 600 W and the supply air fans 850 W.

The extra fan effect resulting from the increase of the fresh air flow by almost half in comparison with the Swedish Standard thus becomes 50 W per apartment.

3.7 Polling of the experience of the tenants as to the indoor climate

A poll developed by Örebro's Industrial Medicine department was used to investigate the subjective experience of the tenants as to the indoor climate. The investigation was addressed to adults only. There were too few children for them to be included in the investigation. The response frequency was very high, a full 95%. The investigation was made seven months after occupation. There was a check group of 292 persons for the poll. The poll was divided into two main headings: "environmental factors" and "complaint symptoms".

Environmental factors were dust and dirt, noise, tobacco fumes from others, static electricity, unpleasant smells, dry air, stuffy air, too low room temperature, varying room temperature, too high room temperature, and draughts.

The characteristics which were investigated with respect to "complaints and symptoms" were dry itching, red skin on hands or face, coughing, hoarse throat, irritated or blocked nose, eye irritation, concentration difficulties, off-colour, headache, heavy head, and tiredness.

The investigation indicated that there were more persons with tiredness, heavy heads and headaches than in the check group. The increase was between 20 - 30% of these complaints.

The reason for the complaints could possibly be the result of high contents of volatile organic substances VOC or noise. If the problem is the result of VOC the complains should become alleviated since these diminish powerfully during the first two years.

That noise can result in the type of problems experienced by the tenants is confirmed in other investigations (see Ref. 4).
In the check group, 20% of the persons consider themselves to have complaints with "stuffy bad air". In the experimental building 10% experienced these problems. This would indicate that the tenants noticed a positive effect of the increased fresh air flow with respect to the detectable air quality.

3.8 Economic yield of the system

3.8.1 Investment costs

In the area where the experimental building is located there is a similar building with conventional heating system. A comparison between the investment costs between the conventional system and the experimental building indicates that the cost structures remain the same.

The air heating system which was installed in the experimental building was not commercially tested in any previous installation. During the installation of techniques which are relatively untested in a commercial sense, the cost structure in comparison with more tradition techniques usually tends to favour the traditional system. This relationship usually changes when the techniques have become more generally available, and commercially developed. This is what has occurred in the Swedish small house industry, where today 50% of the buildings have air carried heating where the ventilation system is integrated with the heating system.

3.8.2 Costs for operation and maintenance

Previous multi-apartment buildings which have tested air heating on an experimental scale have in several cases utilized units placed in the apartments. This has proved to imply increased costs for operation and maintenance since the administrator has been obliged to go into every apartment and replace filters. In the building in Halmstad there is only two filters in place in the fan room. Replacement of these filters take place as often as normally required in a balanced ventilation system. According to the administrator the system has not contributed towards the increase of costs for operating and maintenance in comparison with a traditional heating system.

4.1 Conclusion

The general conclusions which can be drawn from the project of heating apartment buildings with fresh air only and an air changes per of 1.0 hour are:

- The increased ventilation losses become less (in this project it became 11 kW hours/year floor area).

- The tenants experienced an improved air quality.

- The relative humidity content lies within comfort limits (30 - 60%).

- The increase in operating faults for the fans does not need to exceed 50 W per apartment.

- A fully developed commercial system will be cheaper than a conventional heating system.

5 Recommendations

In the next generation of similar systems the experience of this project will enable the reduction of the safety margins during planing. During the planning it was decided to dimension the system for 1.3 changes per hour. During practical operations 1.0 changes per hour has proved to be sufficient. This implies that it is possible to reduce the duct dimensions, use smaller fans, smaller air-to-air heat exchangers, and remove the frequency controls on the fans. This enables a considerably cheaper system and a better acoustic climate.

References:

Ref. 1 New building regulations BFS 1988:18
Ref. 2 Swedish Building Standard 1980
Ref. 3 Building-Ventilation Air NT VVS 047
Ref. 4 Journal of Sound and Vibration (1989) 133 (1), 117-128
Ref. 5 Luftburen värme i kvarteret klotet SP-RAPP 1991 E20013
Ref. 6 Computer program AXSEL, Stratos Ventilation

The Swedish National Testing and Research Institute

Thomas Carlsson

AIR MOVEMENT & VENTILATION CONTROL WITHIN BUILDINGS

12th AIVC Conference, Ottawa, Canada
24-27 September, 1991

POSTER 23

VENTILATION CONTROL WITHIN EXHAUST FAN VENTILATED HOUSES

Åke Blomsterberg

Department of Building Science
Lund University
P.O. Box 118
S-221 00 LUND
Sweden

SYNOPSIS

Modern one-family houses in Scandinavia are often ventilated by an exhaust fan. Most of the outdoor air probably enters through whatever cracks and openings there are and only a small part enters through the supply vents in many of these houses. The overall supply of outdoor air might be adequate, but some rooms often do not get enough of outdoor air.

The constant concentration tracer gas technique was used to examine the supply of outdoor air. Fan pressurization combined with infrared photography were employed to characterize the air leakage of the building. A multi-zone network model was used to further evaluate the measurements.

A reasonable level of outdoor air, upstairs in an airtight two-storey house, can be ensured by locating the supply vents upstairs close to the floor. If that is not possible additional exhaust vents can be installed. If more than 3/4 of the outdoor air is to enter through the the supply vents, then the airtightness should be better than 1.0 air changes per hour at 50 Pa. The performance of an exhaust fan system is very much dependant upon the overall airtightness (including open supply vents) and the distribution of the airtightness of the building.

1. INTRODUCTION

A common ventilation system in modern Scandinavian one-family house is exhaust fan ventilation. An important issue for these houses is where the outdoor air enters and thereby how much outdoor air individual rooms gains. Does the outdoor air enter through the supply vents in the building envelope or does most of it enter through whatever cracks and openings there are in the building envelope? There are reasons to believe that supply vents can act as exhaust vents when it is cold. This is especially true for two-storey houses, where the total supply of outdoor air upstairs is reduced when the outdoor temperature is lowered.

The overall supply of outdoor air might be adequate, but are there long periods of time when too little outdoor air enters some rooms? The air exfiltration is often difficult to determine for a house with exhaust fan ventilation. It is usually given a constant value or neglected. Is that correct?

This paper is based on a report, where the relationship between ventilation and airtightness is examined (Blomsterberg 1990).

2. THE HOUSES TESTED

A group of 18 identical well-insulated experimental houses (Lättbygg 85) in Täby 30 km north of Stockholm, utilizing uncomplicated construction techniques, was built during 1984 and was monitored during 1985 and 1986 (Blomsterberg 1989). Two of the houses (No. 3 and No. 14) are examined in this paper .

The principle ideas governing the design of the houses were to build energy efficient, inexpensive, and uncomplicated houses with.

- a well-insulated and tight building envelope
- a resource efficient light construction technique
- an uncomplicated foundation
- an uncomplicated heating system with individual thermostats
- energy and water efficient appliances
- an instructive owner's manual
- an uncomplicated ventilation system

All houses are modern wood frame constructions employing I-beams made of wood and masonite throughout the construction. Wall, ceiling, roof, and floor elements are prefabricated. Space heating is provided with electric baseboards heaters. The houses are 119 m^2, with three bedrooms upstairs, a kitchen, and a living room downstairs (see figure 1 and 2).

The houses have an exhaust fan ventilation system. There are exhaust air terminal devices in bathrooms, laundry, and kitchen. This kind of system is common in modern one-family houses in Scandianvia. Nine of the experimental houses (e.g. house no 3) have additional exhaust air terminal devices in the bedrooms. Every house has seven special vents, in the exterior walls above the windows, for supplying outdoor air. The ventilation rate can be controlled by the user by adjusting a conveniently located three-way switch: no one at home = 0.1 air changes per hour, at home = 0.3 changes per hour, maximum = 0.5 air changes per hour (120 m^3/h) . The distribution of outdoor air within the house can to some extent be determined by opening and closing the supply vents.

The average mechanical ventilation rate during the heating season of 1986 was 0.35air changes per hourfor the experimental houses. During the summer the average ventilation rate was somewhat higher, 0.40 ach. These values are based on recorded values of run times for the different settings of the fan speed and one-time tests of the exhaust ventilation rates (Blomsterberg 1986). The recorded run times showed that the occupants did use the different fan speeds.

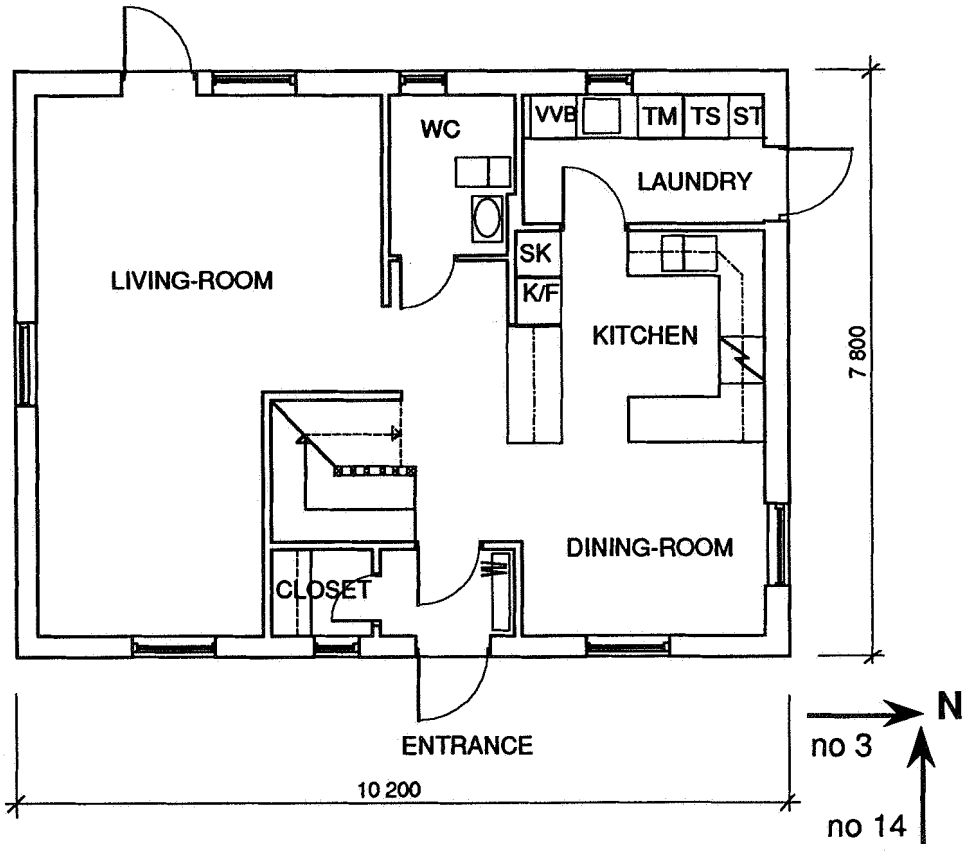

Figure 1. Plan of Lättbygg 85 house, downstairs.

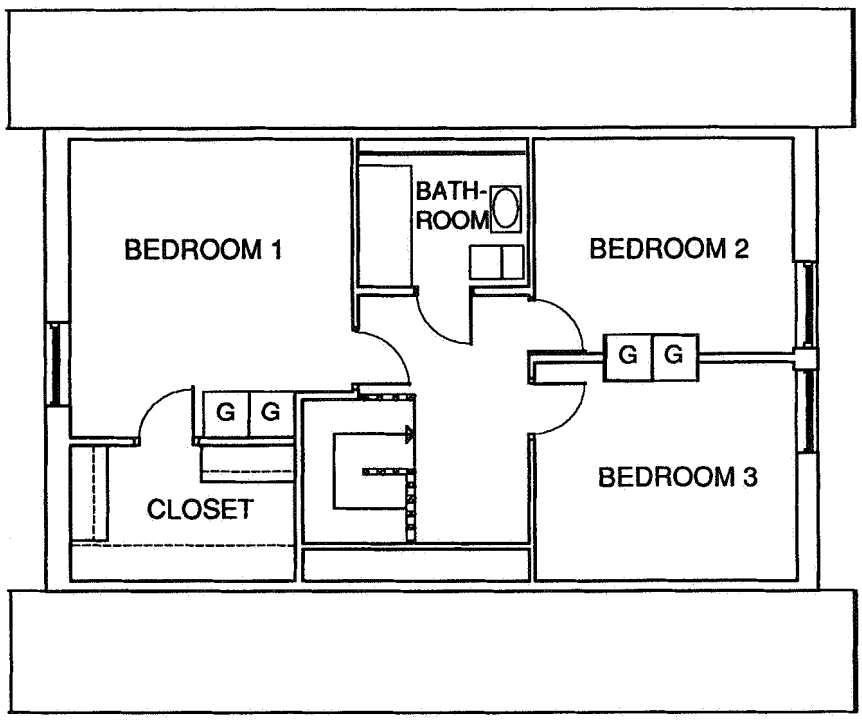

Figure 2. Plan of Lättbygg 85 house, upstairs.

3. TEST METHODS

3.1 Airtightness

The standard method for finding the leakage function of a building is fan pressurization. According to the Swedish standard for fan pressurization all openings in the exterior envelope intended for ventilation purposes must be sealed before the test is performed. Other openings are kept closed. For the purpose of modelling air infiltration and exfiltration it is advantageous to also make a test with open supply vents part of an exhaust fan ventilation system. The exhaust fan is supposed to draw air through the supply vents and cracks and openings in the building envelope.

All rooms which are heated to more than 10 °C are included in the test. A doorleaf or a window is replaced by a sheet of plywood or airtight plastic film which is fixed to the frame and sealed. An air flow generating and metering system is connected through the sheet. The air flow rate is recorded at a number of pressure differences, positive and negative, and the test results are presented in a diagram with pressure difference and air flow/air change rate on the axes.

3.2 Ventilation

The most straightforward method of measuring the total ventilation rate i.e. the combined effect of mechanical ventilation and natural ventilation is to measure it directly (Blomsterberg 1990). In a mechanical ventilation system the air flow in the ducts can be measured with different techniques for volume and mass flow rate measurements. There are many ways of measuring total ventilation, and almost all of them involve a tracer gas, which permits the indoor air to be labelled so that the outdoor air ventilation can be traced.

The tracer gas is injected into and mixed with the indoor air and its concentration is monitored. The mixing is assumed to be complete, which is probabaly the largest single source of error in tracer gas measurements. There are three different schemes; decay, constant concentration, and constant flow of a tracer gas.

All measurements are governed by the continuity equation. The single-chamber continuity equation is given here:

$$V\,dC/dt + Q\,C = F$$

where V is the effective volume, m^3
dC/dt is the time rate of change of concentration
Q is the outdoor air ventilation rate, m^3/s

C is the concentration and
F is the effective injected tracer gas flow rate, m^3/s

In the two houses tested a constant concentration of tracer gas was maintained in order to measure of the ventilation rate. One of the principle advantages with this tehnique is that it eliminates the problem of estimating the effective volume as the effective volume is eliminated from the continuity equation:

$$Q\,C = F$$

The outdoor air ventilation is obtained directly. The field of application for hte constant concentration technique is to continuously monitor the supply of outdoor air to several individual rooms simultaneously, i.e. outdoor air which enters an individual room directly instead of first passing through an adjacent room. The estimated inaccuracy in the measured outdoor air ventilation rate is ± 10 %.

4. MULTI-ZONE MODEL

A multi-zone model, which has been developed at the Royal Institute of Technology in Stockholm was used as a tool for further evaluating the measurements (Herrlin 1987). The PC research version of the program was used MOVECOMP-PC(R) (Bring 1988). In the program the building and its ventilation system is modelled. The model consists of pressure nodes connected to each other with flow paths. The nodes are different zones and duct components, while the flow paths are different leakage paths and ducts. The air flows are calculated by seeking a flow balance in each node. Mass balance has to be achieved.

The mass flow through leakage openings and ducts/ducts components, which is a function of the pressure difference, is throughout the model approximated with a power function. The flow through a leakage opening is calculated using the same flow exponent throughout the entire flow intervall. The Reynholds number correction of the air flow coefficient is done for the actual condition.

The system of simultaneous equations describing the flow balance is solved with a modified Newton-Rapson method. The method avoids on most cases otherwise common problems with convergence. As a result of a simulation all air flows and the pressure conditions within the simulated building are given.

How different ventilation systems work in different buildings can be studied. Almost any kind of combination of zones and leakage openings can be simulated.

The main disadvantage with the multi-zone approach is that it requires substantial inputs to describe the flow network. It is often also difficult to find reliable data e.g. wind pressure distributions and internal leakage characteristics (e.g. between rooms).

5. ANALYSIS

All tracer gas measurements of ventilation rates are only valid for the range of weather conditions, which prevailed during the measurements. The important questions are what happens if the weather conditions are changed, the building moved to another location or even the building itself modified. To answer some of these questions the two houses tested were modelled (Blomsterberg 1990).

The first step was to examine how good the agreement is, between predicted ventilation rates and ventilation rates measured using tracer gas. Each room was modelled as a separate zone, and each leakage path was modelled with the same air flow exponent.
As inputs were used:

- the results from the fan pressurization tests,
- the leakage function of the supply vents
- the distribution of leakage openings according to infrared photography scans,
- the actual locak shielding conditions,
- the measured indoor and outdoor temperatures (hourly averages),
- the on site measured wind velocity (hourly averages), not taking into account the fluctuations,
- the terrain roughness,
- the measured mechanical ventilation rates (i.e. air flows in ventilation system),
- the on site measured wind direction (hourly averages),
- wind pressure coefficients from windtunnel studies,
- the measured geometry of door crackage (which was converted to a leakage function),

The second step was to make predictions for an entire heating season (assumed to start on the 24th of September and end on the 8th of May). Weather data was taken from the reference year 1971 of Stockholm.

5.1 House no 3.

The prediction of the overall outdoor air ventilation rate (80 m^3/h) for house no 3 is close to the tracer gas measurement (70 m^3/h) (see table 1). One reason for the difference is that in the model the boundary between different zones is clearly defined, which is not the case in the measurements due to the fact that measurements in different rooms can influence each other. Only three interior doors were closed, the bathroom, the WC and the closet upstairs. As the house is very tight (1.3 air changes per hour at 50 Pa, 2.3 including supply vents) there is no air exfiltration during the measuring period according to the multi-zone model or the tracer gas measurements. The measured average air exfiltration was -10 ± 10 m^3/h i.e. the difference between measured mechanical air flow (80± 8 m^3/h) and tracer gas measurements (71± 4 m^3/h).

The multi-zone model also shows that only 40 % of the outdoor air enters the house through the supply vents during a typical winter day, the remainder enters through all the leakage openings. A similar result was obtained for similar weather conditions, when the pressure drop across the supply vents was measured and the air flow through them was calculated. The designer of the ventilation system presumably expected all air to enter through the supply vents. The air is mostly infiltrated through the facades and the floor. The higher above the floor the lower the air infiltration rates through the openings.

The discrepancy between prediction and measurements can partly be explained by the fact that the outdoor air supplied directly to the bathroom and the WC probably wasn't measured by the tracer gas technique. Adding these two air flows to the measured ventilation rate brings the overall outdoor air ventilation rate to 74 m^3/h.

Table 1 Multi-zone model predicitions vs tracer gas measurements for house no 3. Average air flows for a 15 hour period, m^3/h. For detailed information on air flows for individual rooms, see Blomsterberg 1990. The average outdoor temperature was 1 °C and the average wind velocity 0.5 m/s. The exhaust air flow was 80 m^3/h, 37 m^3/h upstairs and 43 m^3/h downstairs. There is no air exfiltration.

	Multi-zone model		Tracer gas measurement
	Supply vents	Total	Total
Overall supply outdoor air	33	80	71
Downstairs	22	61	52
Upstairs	11	19	19

During the heating season the variation in air exfiltration rate is very large according to the multi-zone model, if the exhaust air flow is 0.35air changes per hour(84 m^3/h) i.e. according to the measured average during the heating season. The maximum rate, 73 m^3/h, is very high and the minimum rate 0 m^3/h. The average rate is 9 m^3/h. The maximum value, 73 m^3/h, occurs at high wind velocities and is therefore uncertain, as high wind speeds never occured during the tracer gas measurements. If the ventilation is raised to 0.5 air changes per hour, then the average air exfiltration is lowered to 1 m^3/h (or 1 % of the total ventilation) and the maximum to 46 m^3/h. The house is obviously tight enough. With an airtightness level according to the Swedish Building Code 1980 (3.0 air changes per hour at 50 Pa) the average air exfiltration would have been raised very much, to 18 m^3/h (or 13 %).

In order to clarify where the outdoor enters house no 3 a parametric study was carried out using the multi-zone model. The following assumptions were made: the air flow through the exhaust fan is 0.5 ach, the airtightness of the house is equal to the fan pressurization result (1.3 air changes per hour at 50 Pa, 2.3 incl. supply vents) and the supply vents are adjusted according to the design by the HVAC consultant. The predictions show clearly how the outdoor air ventilation rate downstairs is increased from 60 m^3/h to 95 m^3/h and how the outdoor air ventilation rate upstairs is decreased from 60 m^3/h to 25 m^3/h when the outdoor temperature drops from + 20 °C to - 15 °C (see figure 3). A similar result was obtained during the tracer gas measurements in house no 14 (see section 5.2). Less than half of the outdoor air enters through the supply vents. When the outdoor temperature drops the pressure drop across the supply vents upstairs is reduced from 4 Pa to 1 Pa. A pressure difference of 1 Pa corresponds to a wind velocity of 1,5 m/s i.e. the direction of the air flow through the vent can easily change. A minimum air exchange rate is ensured in the bedrooms by the added exhaust air terminal devices there. When it is cold outside, part of the outdoor air to the bedrooms will sometimes be transfered air i.e. enter through the rooms downstairs.

A slight improvement in the distribution of outdoor air can be obtained by a better adjustment of the supply vents. The outdoor air ventilation rate upstairs will then vary between 63 m^3/h and 32 m^3/h , instead of between 60 m^3/h and 25 m^3/h (see figure 4). The pressure drop across the supply vents increases slightly and thereby the air flows are less sensitive to the influence of wind (see figure 4). The adjustment has been made in such manner that the house is depressurized at 4 Pa, when there is no wind and the indoor temperature is equal to the outdoor temperature. The adjustment was made using the air leakage function of the house and the supply vents. 4 Pa was chosen as being a representative value of the pressure difference caused by wind and temperature. The part of the outdoor air which enters through the supply vents is still almost the same.

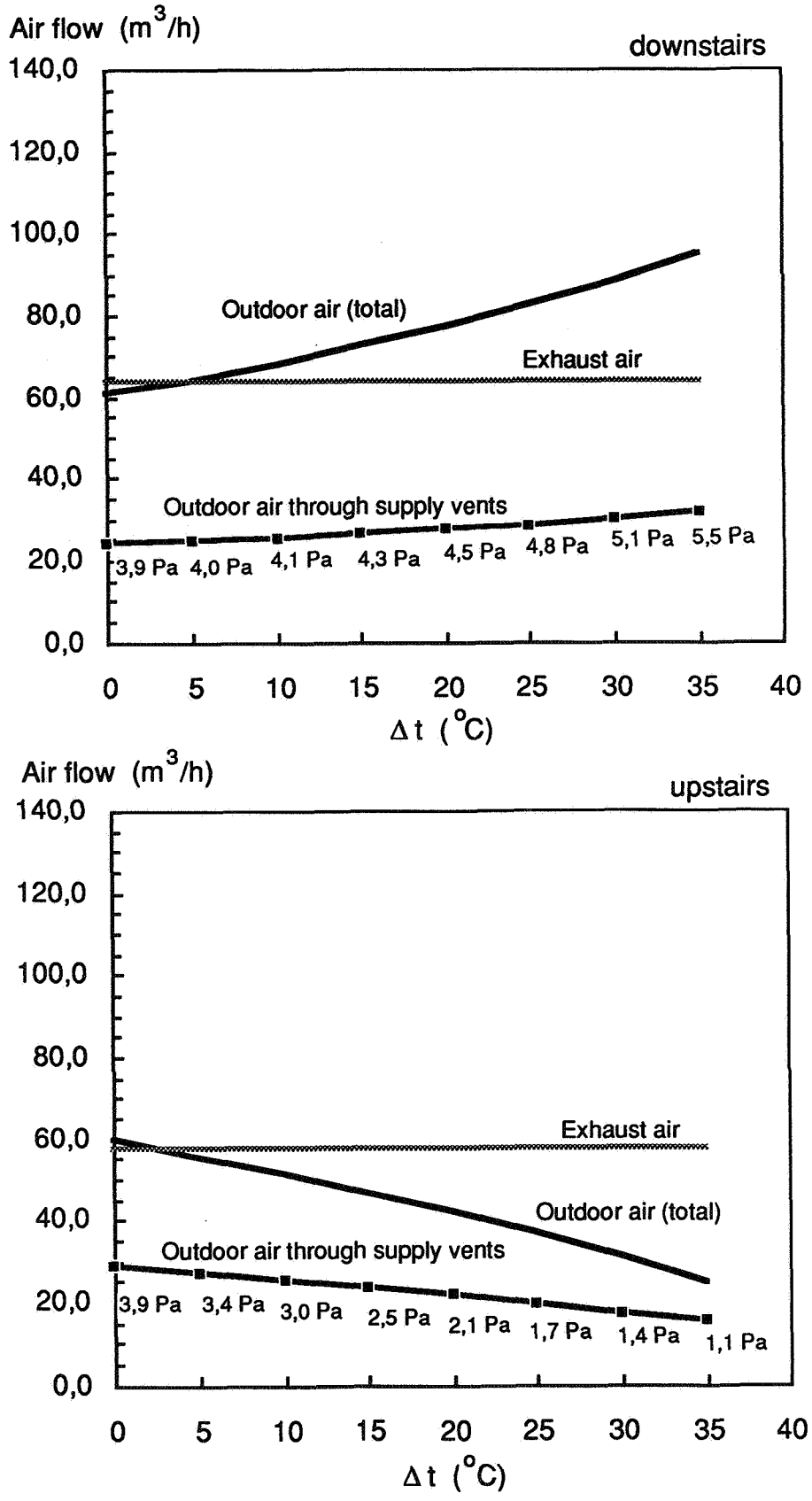

Figure 3. Predicted outdoor air ventilation rate as a function of inside-outside temperature difference, downstairs and upstairs in house no 3. For the supply vents the pressure drop is given. Airtightness = 1.3 ach at 50 Pa. Adjustment, HVAC-consultant. Wind = 0 m/s.

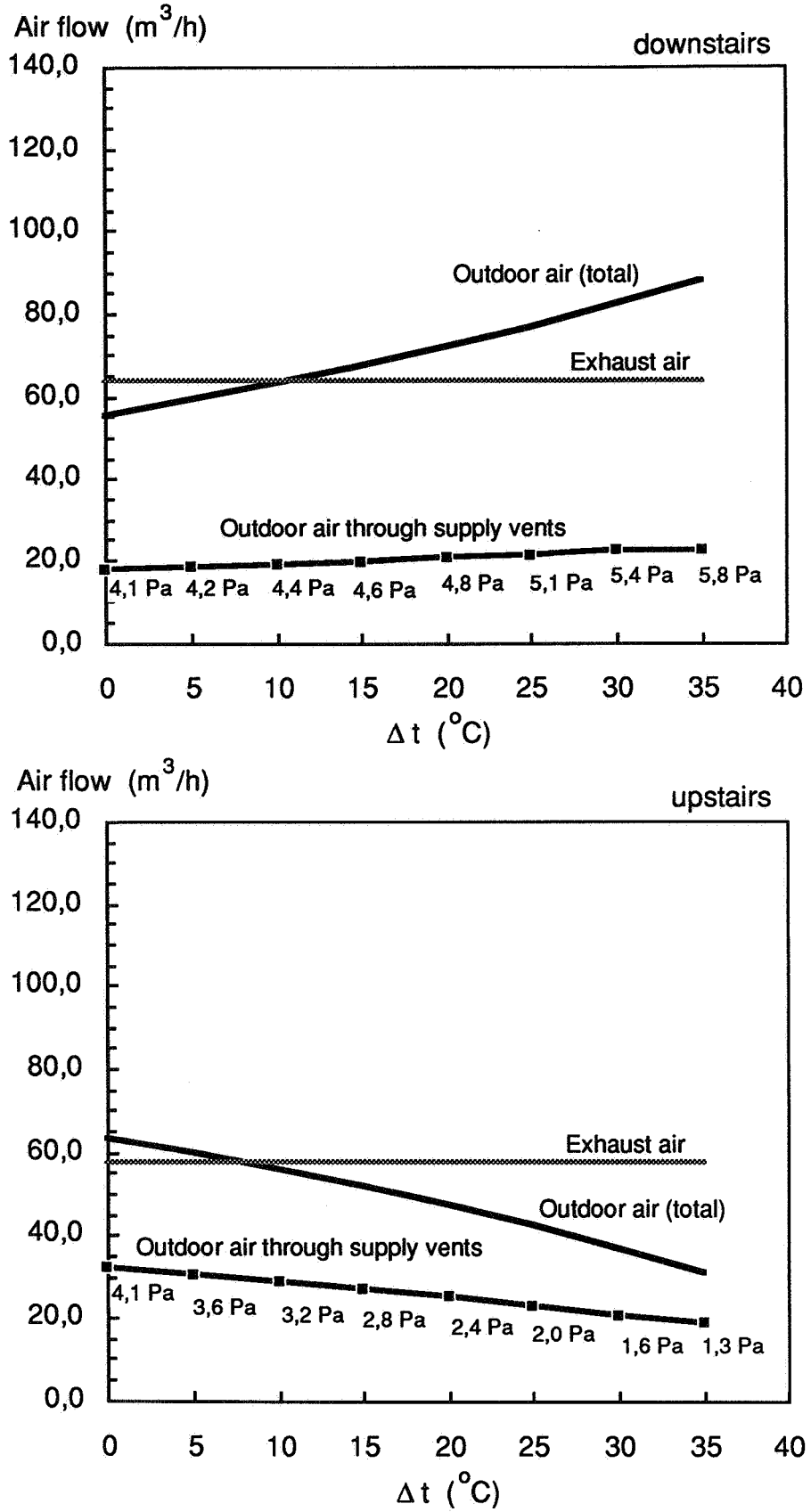

Figure 4. Predicted outdoor air ventilation rate as a function of inside-outside temperature difference, downstairs and upstairs in house no 3. For the supply vents the pressure drop is given. Airtightness = 1.3 ach at 50 Pa. Adjustment at 4 Pa. Wind = 0 m/s.

In order to further improve the distribution of outdoor air the house has to be tightened. If the house was as tight as some experimental houses e.g. 0.8 air changes per hour at 50 Pa and the adjustment was made at 4 Pa, then more than 3/4 of the outdoor air would enter through the supply vents. The total outdoor air ventilation rate upstairs will increase with 20 % (at + 20 °C) to 60 % (at - 15 °C), but will still be reduced when the outdoor temperature drops. The pressure drop across the supply vents is slightly increased by the tightening of the house.

There are two techniques of reducing the dependance upon the outdoor air temperature of the distribution of the outdoor air flow between upstairs and downstairs. One alternative is to increase the pressure drop by choking the supply vents. With this technique the air flow through the vents will be reduced. Another alternative is to move the openings vertically by locating the supply vents upstairs close to the supply vents downstairs (see Fahlén 1991). If the supply vents upstairs are located close to the floor level and the supply vents downtairs close to the ceiling level, then the distribution of the outdoor air flow will be less affected by the outdoor air temperature and will be almost constant (see figure 5). The total outdoor air flow upstairs will vary between 63 m^3/h and 41 m^3/h. In the real house the calculated minimum was 25 m^3/h. Furthermore the pressure drop across the supply vents will be higher than 4 Pa, i.e. the air flow will be less sensitive to wind. The calculations are based an airtightness equal to the fan depressurization result and an adjustment at 4 Pa.

5.2 House no 14

Predictions were also made for house no 14. This house is identical to no 3 with a few exceptions, it is less airtight (2.2 air changes per hour at 50 Pa, 3.1 including supply vents), it has a slightly different ventilation system and the weather during the measuring period was much colder. There is a large discrepancy between prediction and measurement. The overprediction is close to 70 % (see table 2). There are reasons to believe that there was a constant background leakage of tracer gas from the equipment located on the first floor during the tracer gas measurements. This would mean that the measured ventilation rate would be too low with almost a constant amount, as the overall ventilation rate is dominated by the exhaust air flow, which can be assumed to be constant over time.

The overall predicted and measured ventilation rate varies almost to the same extent over time. During the measuring period the variation is between 92 and 129 m^3/h (± 11 %) resp. 60 and 73 m^3/h (± 9 %). Based on these findings and the findings for house no 3, the multi-zone model was used for predictions for the heating season.

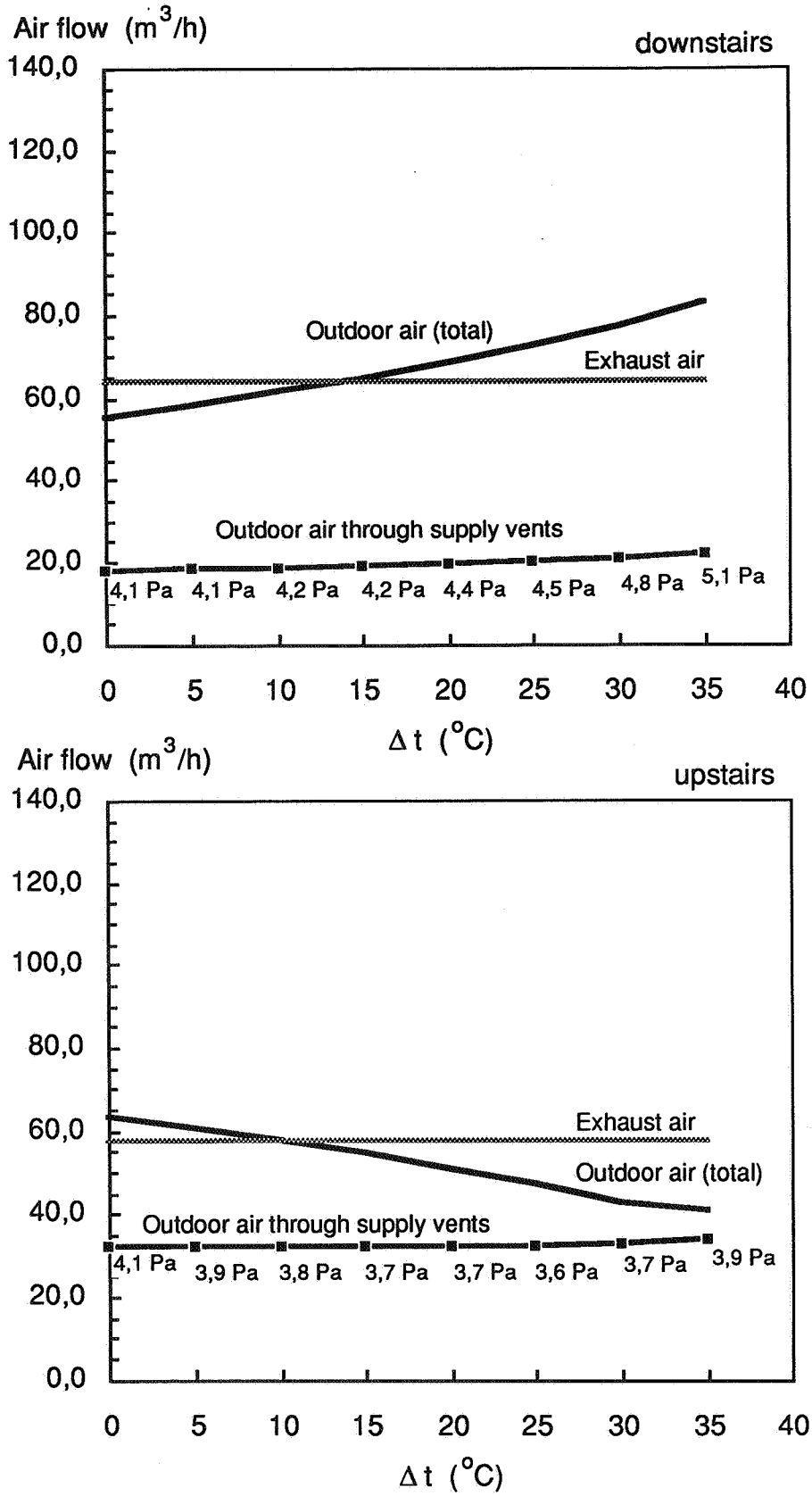

Figure 5. Predicted outdoor air ventilation rate as a function of inside-outside temperature difference, downstairs and upstairs in house no 3. For the supply vents the pressure drop is given. Airtightness = 1.3 ach at 50 Pa. Adjustment at 4 Pa. Wind = 0 m/s. The supply vents upstairs are located 0.2 m above the floor level.

As can be determined from the prediction there is an air exfiltration rate of between 2 and 39 m³/h in house no 14, while there was no air exfiltration in house no 3. This can partly be explained by the fact that house no 3 is tighter and was subject to a milder climate. One might also believe that the upstairs of house no 14 doesn't get very much air. Air is leaving the house through the supply vents, when the outdoor temperature drops below the freezing point. In both houses air is exhausted through the exhaust air terminal devices located upstairs. The upstairs of both houses gets replacement air from downstairs. The amount of replacement air to the bedrooms upstairs in house no 14 would have been larger, if there had been exhaust air terminal devices in the bedrooms as in house no 3. Close to 50 % of all air entering the house enters through the envelope below the windows downstairs. Particularly during the measuring period it might create some discomfort as it is cold air entering. Most of the exfiltration takes place through the ceiling.

If during the measuring period the exhaust air flow is raised from 0.4 air changes per hour to 0.5 air changes per hour, then the air exfiltration is reduced from 29 m³/h to 13 m³/h and air enters through all supply vents.

Table 2 Multi-zone model predictions vs tracer gas measurements for the house no 14. Average air flows for a 108 hour period, m³/h. For detailed information on air flows for individual rooms, see Blomsterberg 1990. The average outdoor tempe- rature was -14 °C and the average wind velocity 0.2 m/s. The exhaust air flow is 90 m³/h, 24 m³/h upstairs and 66 m³/h downstairs. Inside parenthesis is given the air exfiltration.

	Multi-zone model		Tracer gas measurement
	Supply vents	Total	Total
Overall supply outdoor air	16	118 (-28)	69
Downstairs	24.4	109	61
Upstairs	-8.3	9 (-28)	8

The variation in air exfiltration rate during the heating season is larger for house no 14 than for house no 3. The main reason is that house no 14 is less airtight. The maximum air exfiltration rate is almost two times higher, 136 m³/h com- pared with 73 m³/h. The average rate is two times higher, 21 m³/h (or 20 % of the total ventilation) vs. 9 m³/h. The maximum values occur at high wind velocities and are therefore uncertain, as high wind speeds never occured during the tracer gas measurements. If the air flow through the exhaust fan was the required 0.5 air changes per hour, then the average air exfiltration is reduced to 10 m³/h (or 8 % of the total

ventilation). The maximum rate is reduced to 116 m^3/h. The house needs tightening to arrive at an air exfiltration rate of 5 % (6 m^3/h) of the total ventilation . The air leakage at 50 Pa has to be lowered by 15 % from 2.2 air changes per hour to 1.9. The house would have experienced an average air exfiltration rate of 15 % (20 m^3/h), if the air leakage had been as in the Swedish Building Code 1980.

In order to clarify where the outdoor enters house no 14 a parametric study, like the one for house no 3, was carried out using the multi-zone model. The following assumptions were made: the air flow through the exhaust fan is 0.5 ach, the airtightness of the house is equal to the fan pressurization result (2.2 air changes per hour at 50 Pa, 3.1 incl. supply vents) and the supply vents are adjusted according to the design by the HVAC consultant. The predictions show clearly how the outdoor air ventilation rate downstairs is increased from 63 m^3/h to 128 m^3/h and how the outdoor air ventilation rate upstairs is decreased from 58 m^3/h to 7 m^3/h when the outdoor temperature drops from + 20 °C to - 15 °C (see figure 6). A similar result was obtained during the above mentioned tracer gas measurements (see figure 7). Less than 1/3 of the outdoor air enters through the supply vents. When the outdoor temperature drops the pressure drop across the supply vents is reduced from 2 Pa to 0 Pa. A pressure difference of 1 Pa corresponds to a wind velocity of 1,5 m/s i.e. the direction of the air flow through the vent can easily change. A minimum air exchange rate is not ensured in the bedrooms as in house no 3, as there are no added exhaust air terminal devices there.

A slight improvement in the distribution of outdoor air can be obtained by a better adjustment of the supply vents. The outdoor air ventilation rate upstairs will then vary between 60 m^3/h and 12 m^3/h , instead of between 58 m^3/h and 7 m^3/h (see figure 8). The pressure drop across the supply vents increases slightly and thereby the air flows are less sensitive to the influence of wind (see figure 8). The adjustment has been made in such manner that the house is depressurized at 4 Pa, when there is no wind and the indoor temperature is equal to the outdoor temperature. The adjustment was made using the air leakage function of the house and the supply vents. 4 Pa was chosen as being a representative value of the pressure difference caused by wind and temperature. The part of the outdoor air which enters through the supply vents does not change very much due to the better adjustment.

In order to further improve the distribution of outdoor air the house has to be tightened (see house no 3).

There are two techniques of reducing the dependance upon the outdoor air temperature of the distribution of the outdoor air flow between upstairs and downstairs. One alternative is to increase the pressure drop by choking the supply vents. With this technique the air flow through the

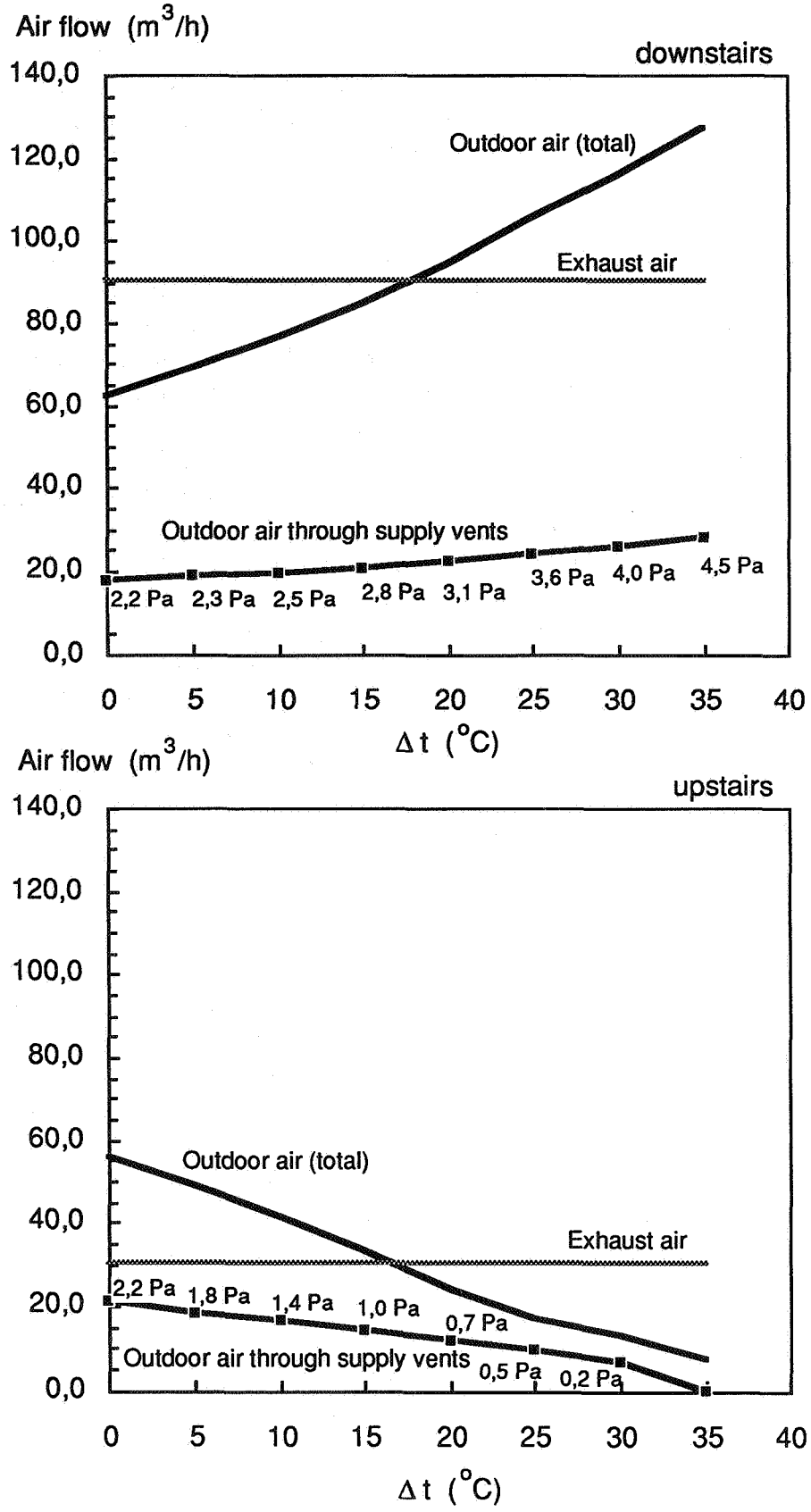

Figure 6. Predicted outdoor air ventilation rate as a function of inside-outside temperature difference, house no 14 downstairs and upstairs. For the supply vents the pressure drop is given. Airtightness = 2.2 ach at 50 Pa. Adjustment, HVAC-consultant. Wind = 0 m/s.

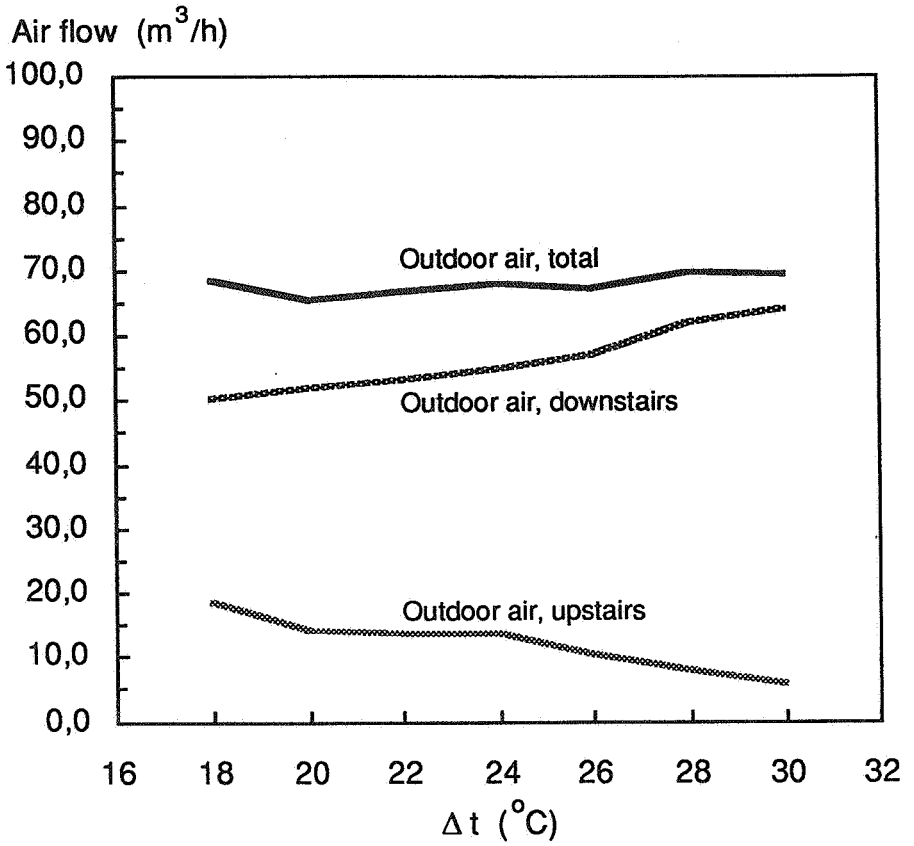

Figure 7. Measured outdoor air ventilation rate as a function of inside-outside temperature difference, for house no 14. The wind speed was 0.5 m/s. The exhaust fan was set on "at home" position. The constant concentration tracer gas technique was used.

vents will be reduced. Another alternative is to move the openings vertically by locating the supply vents upstairs close to the supply vents downstairs (see Fahlén 1991). If the supply vents upstairs are located close to the floor level and the supply vents downtairs close the ceiling level, then distribution of the outdoor air flow will be less affected outdoor air temperature and will be almost constant (see figure 9). The total outdoor air flow upstairs will vary between 63 m^3/h and 41 m^3/h. Furthermore the pressure drop across the supply vents will be higher than 2 Pa, compared with 4 Pa in the tighter house no 3. The calculations are based an airtightness equal to the fan depressurization result and an adjustment at 4 Pa.

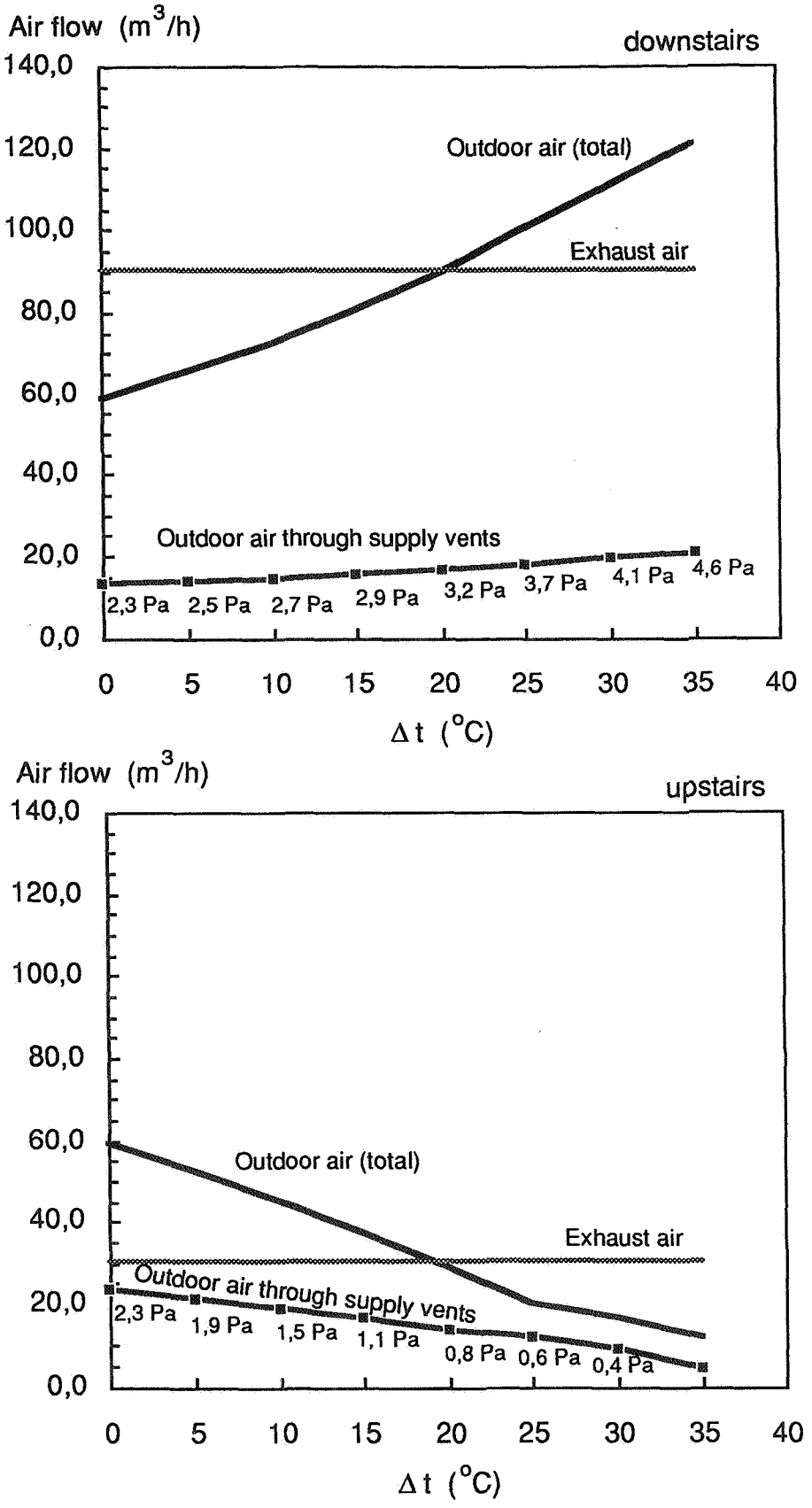

Figure 8. Predicted outdoor air ventilation rate as a function of inside-outside temperature difference, downstairs and upstairs in house no 14. For the supply vents the pressure drop is given. Airtightness = 2.2 ach at 50 Pa. Adjustment at 4 Pa. Wind = 0 m/s.

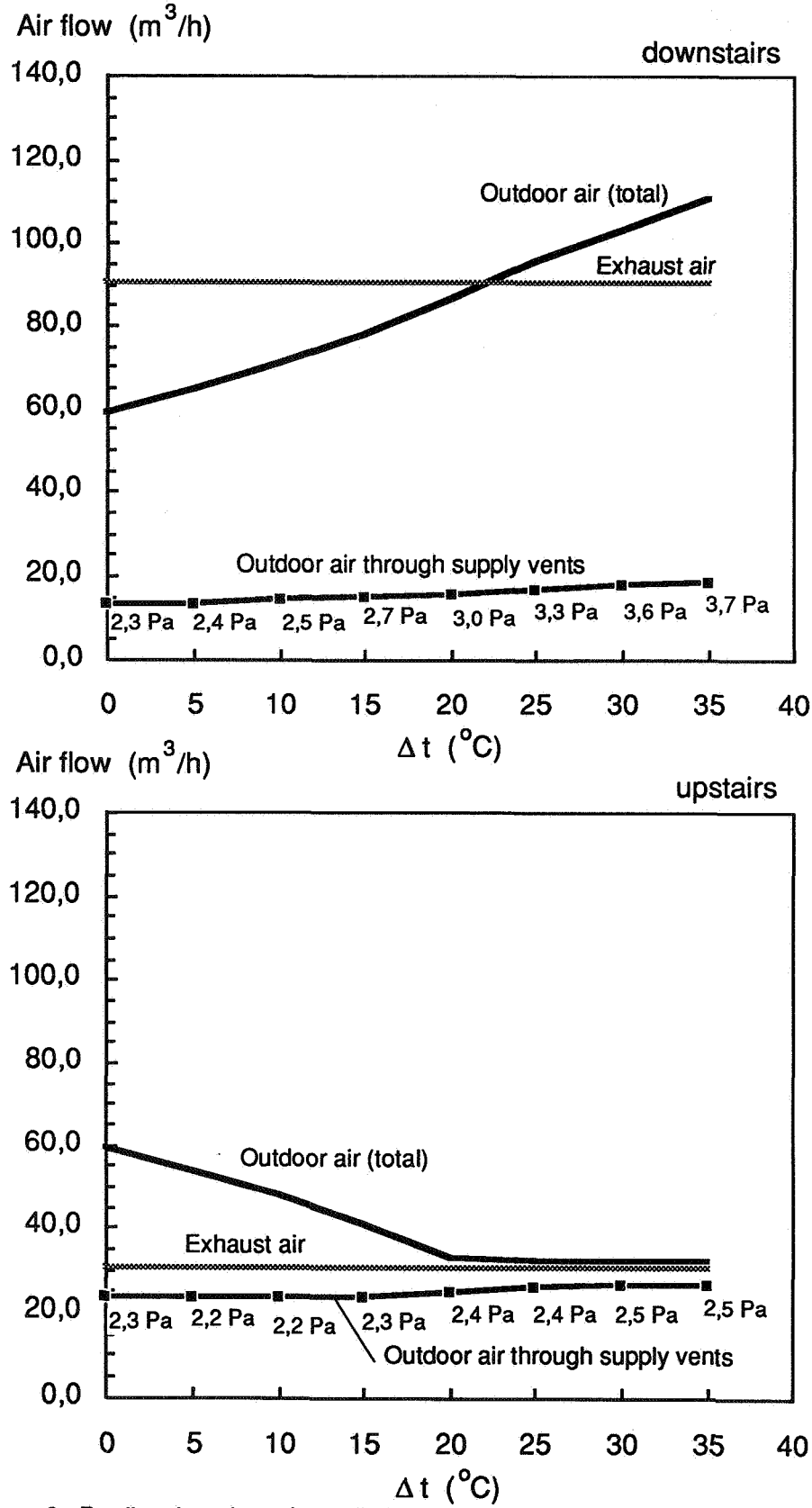

Figure 9. Predicted outdoor air ventilation rate as a function of inside-outside temperature difference, house no 14 downstairs and upstairs. For the supply vents the pressure drop is given. Airtightness = 2.2 ach at 50 Pa. Adjustment at 4 Pa. The supply vents upstairs are located 0.2 m above the floor level. Wind = 0 m/s.

6. CONCLUSIONS

The Lättbygg 85 houses had a correct distribution of air flows between the exhaust air terminal devices. One of the ideas behind the ventilation system in these houses was that the occupants should be able to control where the outdoor air enters the house. Vents which can easily be closed and opened were incorporated in the building envelope. Measurements and calculations show that although the two Lättbygg 85 houses tested are tighter than most modern houses only 1/3 of the air enters through the vents if all of them are open. The remainder of the outdoor air enters through whatever cracks or openings there are. If the cracks are located at floor level cold air can enter during the winter and impair the thermal comfort. An uneven distribution of cracks can cause an uneven distribution of outdoor air i.e. some rooms might get too little outdoor air.

For the least airtight house (2.2 air changes per hour at 50 Pa) the air is actually leaving the house through the supply vents in the bedrooms upstairs, when the outdoor temperature falls below the freezing point. The exhaust air flow was 0.35 air changes per hour. Raising the air flow lowers that critical temperature. It would therefore make sense to raise the fan speed to arrive at the stipulated 0.5 air changes per hour.

The mechanical ventilation rate in the Lättbygg 85 houses is controlled by the occupants (0.1 ach, 0.3 ach or 0.5 ach) and is therefore often below 0.5 ach. This increases the air exfiltration and makes the ventilation more sensitive to the influence of wind and temperature.

A reasonable level of outdoor air, upstairs in an airtight two-storey house, can be ensured by locating the supply vents upstairs close to the floor and the supply vents downstairs close to the ceiling. The outdoor air flow through the vents will then also be only marginally affected by the outdoor temperature. If the relocation of the supply vents is not possible, then in order to get at least transferred air to the rooms upstairs from the rooms downstairs exhaust air terminals can be installed in each room upstairs.

If more than 3/4 of the outdoor air is to enter through the the supply vents, then the airtightness of the building envelope must be better than 1.0 air changes per hour at 50 Pa. The adjustment of the supply vents should be done at a pressure difference of 4 Pa.

If the average air exfiltration during the heating season is to be lower than 5 % of the overall outdoor air ventilation, then the airtightness (incl. open supply vents) should be better than appr. 3.0 air changes per hour at 50 Pa.

The performance of an exhaust fan system is very much dependant upon the overall airtighness and the distribution of the airtightness of the building. Many existing modern houses are less airtight than the two houses tested i.e. only a small part of the outdoor enters through the supply vents and the direct supply of outdoor air to individual rooms is strongly affected by the natural driving forces. Most of the time there will probably be some air exchange in the individual rooms, but it will be a varying combination of outdoor and transferred air.

7. REFERENCES

BLOMSTERBERG, Å. "User controlled exhaust fan ventilation in one-family houses" Proceedings of the 7th AIVC Conference, Coventry, Great Britain, 1986.

BLOMSTERBERG, Å. "Lättbygg 85 - Energy and resource efficient one-family houses with a low annual cost" Swedish Council for Building Research, R41:1989, Stockholm, Sweden, 1990.

BLOMSTERBERG, Å. "Ventilation and airtightness in low-rise residential buildings - Analyses and full-scale measurements" Ph. d. thesis, Swedish Council for Building Research, D10:1990, Stockholm, Sweden, 1990.

BRING A., HERRLIN M. "User's Manual - MOVECOMP-PC(R) - An Air Infiltration and Ventilation System Simulation Program" Bris Data AB, Saltsjöbaden, Sweden, 1988.

FAHLÉN, P. , personal communication, Swedish National Testing and Research Institute, Borås, Sweden, 1991.

HERRLIN, M. "Air Flows in Buildings - A Calculation Model" Royal Institute of Technology, Division of Building Services Engineering, Stockholm, Sweden, 1987 (in Swedish).

AIR MOVEMENT & VENTILATION CONTROL WITHIN BUILDINGS

12th AIVC Conference, Ottawa, Canada
24-27 September, 1991

POSTER 24

Control Algorithms for Rooms with Displacement Ventilation System.

V.Prochaska, A.Schreiber, B.Kegel.

Sulzer Infra Group
Laboratory
8401 Winterthur
Switzerland

ABSTRACT

A test room with a Displacement Ventilation System was built. Temperature control was provided with a DDC (Direct Digital Control) System, controlling the air volume and the air inlet temperature. Air velocity and temperature profiles were measured at different locations in the room for various internal loads.

The aim of the control was not only to provide a constant temperature but also comfortable conditions. the temperature gradient, the air velocity and the radiant heat exchange were taken into consideration for the comfort condition in the space.

It is found that the influence of the building structure is more important for displacement systems than for mixing systems. Tests were carried out with various thermal masses of the room. Due to the vertical temperature distribution especially the mass of the ceiling has a great influence on the storage capacity.

For displacement systems, VAV proved to be very efficient over the whole range of the load. there is satisfactory air movement in the room even with a reduced air change rate of 1 to 2 per hour.

Adapted control algorithms allow to reduce the energy consumption of the ventilation system. Further investigations will consider the optimization of the use of energy.

AIR MOVEMENT & VENTILATION CONTROL WITHIN BUILDINGS

12th AIVC Conference, Ottawa, Canada
24-27 September, 1991

POSTER 25

Performance Evaluation of Kitchen Hoods

P.Wouters, B.Geerinckx*, B.Vandermarcke**

* Belgian Building Research Institute
Aarlenstraat 53/10
B-1040 Brussels
Belgium

**Sint Lucas Instituut for Architecture
B-9000 Gent
Belgium

12th AIVC CONFERENCE

AIR MOVEMENT AND VENTILATION CONTROL
WITHIN BUILDINGS

TITLE : Performance evaluation of kitchen hoods

AUTHORS : P. Wouters, B. Geerinckx, B. Vandermarcke*
ADDRESS : Belgian Building Research Institute
Aarlenstraat 53/10 B-1040 Brussels
tel : +32.2.653.88.01 fax : +32.2.653.07.29

* Sint Lucas Instituut for Architecture
B-9000 Gent

Abstract

Kitchen hoods are frequently found in Belgian kitchens. Most of them have as only function intensive ventilation during certain cooking activities. It is expected that kitchen hoods with appropriate performances can also play an important role as device for guaranteeing basic ventilation.

The aims of the research can be summarized as follows :

- How do occupants evaluate the performances of existing kitchen hoods?
- What are the sound levels (dB(A)) in various locations in theses dwellings due to the kitchen hood?
- What are the flow rate performances of old and new kitchen hoods in occupied dwellings and in the laboratory?
- What are the measured ventilation efficiencies in the laboratory?

The project focusses as well on existing kitchen hoods as on the most recent models of kitchen hoods.
In order to come to representative answers, the following actions are planned (they will be largely finished at the time of the conference) :

- an enquiry in some 200 randomly selected dwellings and some 50 dwellings with new kitchen hoods. These 50 dwellings were suggested by the manufacturers.
- Sound level measurements in 4 locations of each dwellings as well as flow rate measurements (with compensated flow meter and/or tracer gas) in occupied dwellings.
- FLow rate and ventilation efficiency measurements in the laboratory on common and new kitchen hoods.

The results till now indicate that often very high sound levels are found (up to 80 db(A)) and that there are a lot complaints about noise problems. Fortunately, several good systems allowing to achieve the required flow rates at very low sound levels exist.

AIR MOVEMENT & VENTILATION CONTROL WITHIN BUILDINGS

12th AIVC Conference, Ottawa, Canada
24-27 September, 1991

POSTER 26

VENTILATION CONTROL OF INDOOR AIR QUALITY, THERMAL COMFORT, AND ENERGY CONSERVATION BY CO_2 MEASUREMENT

GIOVANNA DONNINI
IRRST, MONTREAL, CANADA

FARIBORZ HAGHIGHAT
CENTRE FOR BUILDING STUDIES
CONCORDIA UNIVERSITY
MONTREAL, CANADA

VAN HIEP NGUYEN
IRRST, MONTREAL, CANADA

SYNOPSIS

The use of indoor carbon dioxide levels is a good method for controlling indoor air quality in office buildings. The measured CO_2 is used to determine the amount of outdoor air needed to purge air contaminants and to obtain the desired CO_2 indoors. Two floors of a commercial building in Montreal were used in the study. Since both floors were identical in architectural layout, type of work being done, and in population density, and since they had identical yet separate ventilation systems, one floor was used as a control, and the other was modified to include a CO_2 and temperature control system. The strategy complies with the requirements of the ventilation, indoor air quality, and thermal comfort standards. The discomfort that did exist was due to HVAC system repairs. It also performs the ventilation service in an energy effective manner, with an annual saving of 12%, and a payback period of 0,4 years. However, the occupants' perception of their working environment does not reflect the measured results. They perceived that their productivity is proportional to their perception of the indoor environment. The DCV floor occupants complained significantly more of their indoor environment than the occupants of the other floor.

1. INTRODUCTION

The following study compares the indoor environment created by two different types of ventilation control systems in an eleven-storey office building, located along the St. Lawrence river, in Montreal. Experiments were conducted during an entire year. The two systems were electrically operated: a conventional system was controlled by outdoor temperatures, and a demand-controlled system used carbon dioxide and supply temperature as an indicator (see Figure 1). The main objective was to compare the air quality, thermal comfort, energy demands, and occupant satisfaction resulting from the two different controls, in two separate floors of an office building, and to rate these results according to their respective criteria, since operation of a ventilating system should always keep all of the contaminants and thermal comfort parameters within acceptable limits. Considerable research has gone into DCV systems over the past 10 years. Up until 1983, most papers on DCV systems stressed energy savings and pay-back times, but it is indoor air quality that is being emphasized in more recent works [1]. This studies emphasizes the impact on the indoor environment.

2. METHOD

Actual test data was obtained over four seasons--spring, summer, fall, and winter. Each scheduled test period consisted of one week per month, for 12 consecutive months. This plan was set up to evaluate system performance under different weather conditions. The testing was performed simultaneously on two floors of an office building--one floor operating under the normal mode, and the other floor operating under the carbon dioxide control mode. These two types of control were in operation throughout the total testing year (including the time between the scheduled test periods).

A set of relays was installed to enable the 8th floor system to be operated in a "CO_2 mode"; while the 9th floor system operated under the "normal mode". Under the CO_2 control the CO_2 state kept the outdoor air damper closed until the CO_2 level in the space reached the lower control point (600 ppm). The outdoor air dampers would open to a minimum when the CO_2 did reach 600 ppm. As the CO_2 increased further, so did the opening of the dampers, up to a maximum opening when the CO_2 reached the upper limit of 1000 ppm. The lower limit of 600 ppm was chosen due to the recent findings that headaches start at this point [2]. The upper limit of 1000 ppm was chosen since it is the ASHRAE recommendation [3]. The code-specified amount of outdoor air was provided under the normal mode (i.e. based on temperature demand). An indoor temperature control was installed to override the CO_2-control system, to certify that the indoor temperature would not exceed the comfort limits [4].

The following parameters were measured for one week per month, for 12 consecutive months: indoor air quality parameters (carbon dioxide, formaldehyde, volatile organic compounds, particles and ventilation performance); thermal comfort parameters (dry-bulb and operative temperature, relative humidity, vertical temperature gradients, air velocity, and thermal comfort PMV and PPD); and occupant perception. The energy demand was monitored continuously throughout the 12 months, i.e. 365 days. The sampling stations are shown in Figure 2 (both floors' stations are directly one above the other).

To verify if there was any significant difference between the variables, the confidence interval of $\mu_D = \mu_1 - \mu_2$ for paired observations was used. If $\bar{d}$ and s_d are the mean and standard deviation of the normally distributed differences of n random pairs of measurements, a $(1 - \alpha)100\%$ confidence interval for $\mu_D = \mu_1 - \mu_2$ is

$$\bar{d} - t_{\alpha/2}\frac{s_d}{\sqrt{n}} < \mu_D < \bar{d} + t_{\alpha/2}\frac{s_d}{\sqrt{n}},$$

where $t_{\alpha/2}$ is the t value with $v = n - 1$ degrees of freedom, leaving an area of $\alpha/2$ to the right [5].

2.1 Indoor Air Quality Parameters

Ten CO_2 sampling stations were chosen as per Figure 2. A direct reading instrument (ADC, range 0-5000 ppm, infrared gas analyzer) was used to measure CO_2 hourly from 7:00 to 19:00, for three consecutive working days each month. The IRSST method #34-A was followed [6].

Three formaldehyde sampling stations were chosen as per Figure 2 (stations 1, 5, and 7). A sampling duration of three working days was used each month. The IRSST method # 216-1 was followed [6]. The formaldehyde was collected on orbo adsorbent tubes, impregnated with N-benzylethanolamine. These were attached to personal air pumps sampling at a frequency of 0,5 l/min. The tubes were then analyzed by gas chromatography.

Three VOC sampling stations were chosen as per Figure 2 (stations 1, 5, and 7). A sampling duration of three working days was used each month. The IRSST methods # 80-1, 16-1, and 101-1 for stoddard solvent, toluene, and xylenes (o,m,p), respectively, were used [6]. The VOC's were collected on activated charcoal tubes attached to personal air pumps sampling at a frequency of 0,2 l/min. These were then analyzed by gas chromatography.

Three dust sampling stations were chosen as per Figure 2 (stations 1, 5, and 7). The dust was sampled for a period of 3, 10-hour working days each month. The IRSST method # 48-1 was followed [6]. Personal air pumps at about 1,5 l/min air flow rates with pre-weighed filters were used to collect total dust. The filters were then weighed in a laboratory.

The decay tracer gas technique was used to measure air change rates during our monthly testing periods. The 9^{th} floor was tested on the first of three days, while the 8^{th} was tested on the third; to avoid the interzonal air movement problem from the 8^{th} up to the 9^{th} floor (due to the pressure differential). Approximately 4 liters of SF_6 was injected at the outdoor air dampers of the floor under study. A mixing period of about 30 minutes was allotted. Air samples were then taken at 5 locations throughout the floor (stations 1, 3, 5, 7, and 9, from Figure 2), in 9 continuous sequences, so as to average a time period of about 8 minutes between sequences (a total of about 80 minutes of sampling). These air samples were then sent to a laboratory for the SF_6 concentration. This method of calculating the rate of indoor-outdoor air exchange does not differentiate between the mechanisms of exchange (mechanical or infiltration) but includes both.

Analysis of the system performance was centred around evaluating the ability of the CO_2-based ventilation system to control the CO_2 concentration in the occupied spaces of the test site building.

2.2 Thermal Comfort

Operative temperature readings were taken at 9 locations per floor (see stations 1 to 6, and 8 to 10, in Figure 2), for 20 minutes per station, over a period of 3 working days, once a month. These were coupled with relative humidity and dry bulb temperature readings taken with a psychrometer.

A Thermal Comfort Meter was used to measure thermal comfort levels. Nine sampling stations per floor were chosen as in Figure 2 (stations 1 to 6, and 8 to 10), for 20 minutes per station, over a period of 3 working days, once a month.

2.3 Occupant Perception

The subjective response of the occupants to the environment was measured with a questionnaire. No behavioral questions were asked.

The questionnaire was distributed throughout the two floors, to all occupants in the open-area offices, every 3rd Wednesday morning of every month. These were then collected that same afternoon.

2.4 Energy Demand

Separate electric power meters were installed in all four ventilation systems; to measure all power used for heating and cooling.

Four XT-103 Electrical Current Stick-On Loggers were used. Each one has a range of 0 to 250 Amps (AC). The two loggers for each floor were added so as to arrive at a total energy consumption for each floor.

3. RESULTS

The system generally performed as expected. Under the CO_2 control mode, the outdoor air dampers remained closed for most of the year. The system is normally operated with the outdoor air dampers opened in cold weather because of the overheating inside (due to the poorly designed HVAC system location). There were never enough people at one time or for long enough to raise the CO_2 level to the control point. Operation of the overriding temperature control kept the building well ventilated (thermally). It was clear that the normal mode of control produced excess ventilation.

The ASHRAE ventilation standard offers two methods for controlling indoor air quality [3]. The first is to prescribe various amounts of outdoor air per person for different settings. The second allows the building operation personnel to reduce the outdoor air intake as long as there are no known contaminants at harmful concentrations. This project indeed showed that a CO_2 and temperature control was able to limit the amount of outdoor air and still keep all of the contaminants below the recommended maximum limits. Even though the contaminant levels were similar on both floors, the control system was able to save a significant amount of energy.

This control system had no real effect on indoor air quality and thermal comfort (similar levels are found on both floors), but it had a great effect on energy consumption. The main reason is probably the low occupant density.

The air quality, as expected, was generally good. No significant contaminant concentrations were found. Carbon dioxide, formaldehyde, and VOC levels were all well below the recommended limits. Total dust levels exceeded the ASHRAE recommended maximum for three months of the year, on the CO_2-controlled floor.

The thermal comfort was generally adequate on both floors. Dry-bulb temperatures and air velocities satisfied the recommended levels. Discomfort would be felt during the winter months when very low relative humidities were recorded [7]. Very warm operative temperatures were also recorded during the summer months. Vertical temperature gradients exceeded the recommended level due to very warm air temperatures at the neck level. However, this discomfort was almost always due to some HVAC mechanical repair being done at that time. The Predicted Percentage of Dissatisfied was above the recommended maximum more than one third of the time due to a slightly cool to cool environment.

The occupants' responses did not correspond to the measurements taken objectively [8]. This may put in evidence the inadequacy of the "state-of-the-art" measuring equipment to read much lower levels. Also, it may indicate that the occupants are much more sensitive to irritants than the general population. The occupants perceived that their productivity is proportional to their perception of the indoor environment; indicating that higher productivity rates can be achieved by better controlling the working environment above satisfactory levels (see Figure 3). Finally, more than 20% of the occupants were unsatisfied with their working environment (indoor air quality and thermal comfort) all of the time (see Figure 4). The 8th floor occupants complained much more of both indoor air quality and thermal comfort, however, the same significant differences could not be found in the measured data, indicating that other "global" factors may be influencing their environmental satisfaction [8].

A significant annual difference in energy consumption was found between both floors (see Figure 5). An energy savings of 12% was found by using the temperature and CO_2-control system. The payback period was calculated using a pre-determined cost schedule, and was found to be 0,4 years.

ACKNOWLEDGEMENTS

Financial support through grants from the Department of Energy, Mines and Resources of Canada and from the Natural Sciences and Engineering Research Council of Canada to one of the authors is acknowledged with thanks.

REFERENCES

1. International Energy Agency (IEA), "Demand Controlled Ventilating System--State of the Art Review. Annex 18: Energy Conservation in Buildings and Community Systems Programme", Raatschen, W. Ed, Swedish Council for Building Research, Sweden 1990.

2. "Draft Report of the Inter-Ministerial Committee on Indoor Air Quality (Ontario) by Rajhans, G.S., Ontario Ministry of Labour, presented at the ASHRAE/SOEH Conference IAQ'89, April 17-20, 1989."

3. ASHRAE (1989) *ASHRAE Standard 62-1989 Ventilation for Acceptable Indoor Air Quality*, Atlanta.

4. G. Donnini, V.H. Nguyen and F. Haghighat, "Ventilation Control and Building Dynamics by CO_2 measurement", The Fifth International Conference on Indoor Air Quality and Climate, Toronto, Canada, July 26-August 3, 1990, Indoor Air '90, vol. 4, pp 257-262.2.

5. R.E. Walpole and R.H. Myers, *Probability and Statistics for Engineers and Scientists*, 3rd ed., MacMillan Publishing Company, New York, 1985.

6. "Guide d'échantillonnage des contaminants de l'air en milieu de travail", IRSST, Direction des laboratoires, Montréal, Mars 1990.

7. F. Haghighat, G. Donnini and G. Bonofiglio, "Thermal Comfort and Indoor Air Quality Created by CO_2-Based Ventilation Control", Proc. of International Conference on Human-Environment System, Tokyo, 1991.

8. F. Haghighat, G. Donnini and R. D'Addario, "Relationship Between Occupants' Discomfort as Perceived and as Measured Objectively", The Journal of Indoor Air International, Indoor Environment, Vol. 2, 1992.

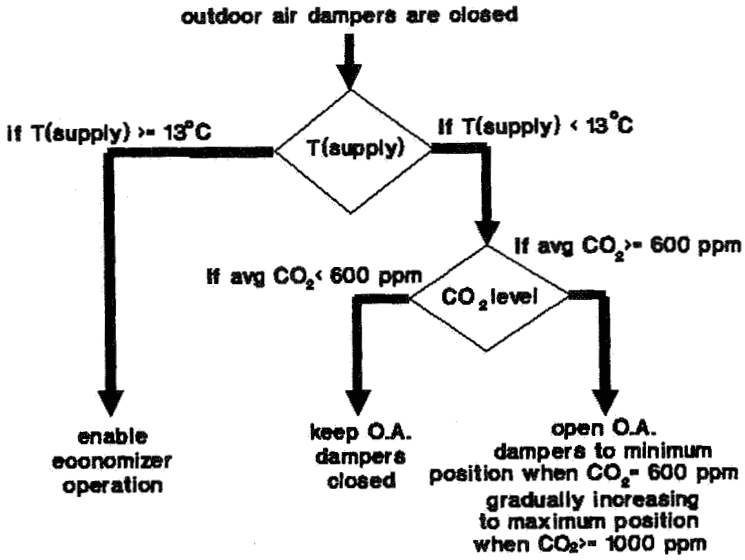

Figure 1. DCV system strategy

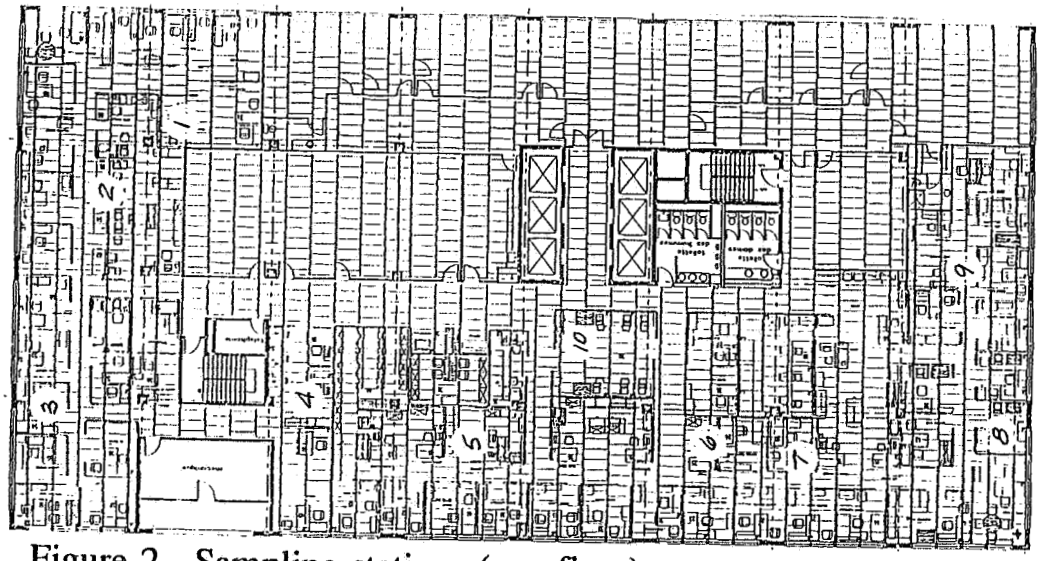

Figure 2. Sampling stations (one floor)

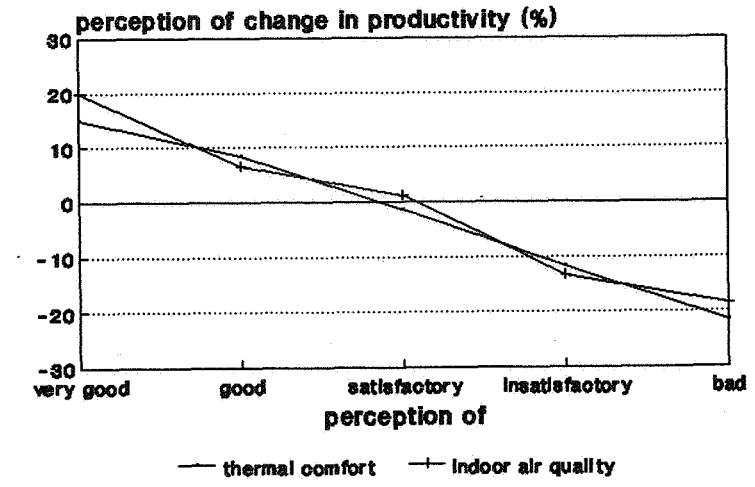

Figure 3. Occupant perception of productivity

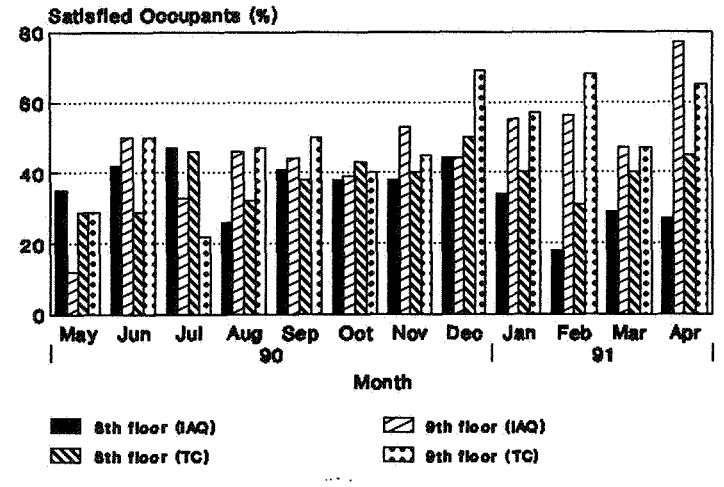

Figure 4. Percentage of satisfied occupants

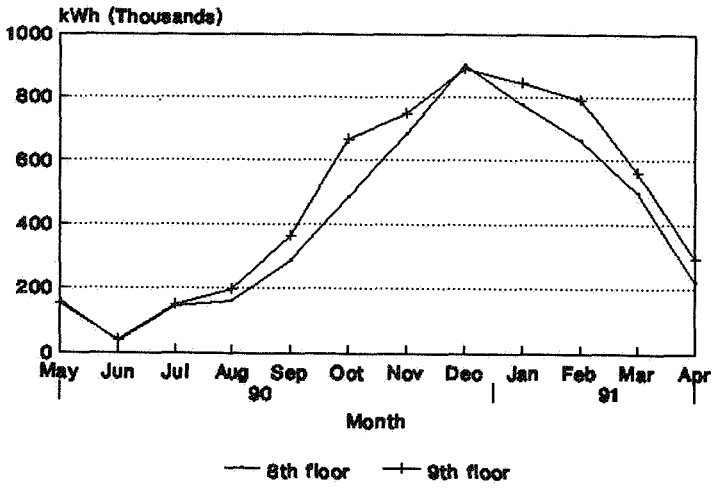

Figure 5. Difference in energy demand

AIR MOVEMENT & VENTILATION CONTROL WITHIN BUILDINGS

12th AIVC Conference, Ottawa, Canada
24-27 September, 1991

POSTER 27

MEASUREMENT OF ENTRANCE LENGTH AND FRICTION FACTOR OF DUCTS USING TRACER-GAS TECHNIQUES

S.B. Riffat and K.W. Cheong
Building Services Group
Department of Civil Engineering
Loughborough University of Technology
Loughborough
Leicestershire
LE11 3TU
United Kingdom

M. Holmes
Arup Research and Development
13 Fitzroy Street,
London
W1P 6BQ
United Kingdom

SYNOPSIS

We describe the use of constant injection and pulse injection techniques for measurement of airflow in a duct. Tracer-gas measurements were compared with measurements made using a pitot tube and a hot-wire anemometer. Tracer-gas concentration, air velocity and pressure distribution were measured at various distances from the duct wall and inlet. An empirical equation was obtained for the entrance length required to achieve fully-developed turbulent flow and this was compared with measurements made using a pitot tube and hot-wire anemometer. We present a relationship for the friction-factor and Reynolds number derived from tracer-gas measurements.

LIST OF SYMBOLS

C_c	Concentration of tracer gas; constant-injection technique (ppm)
C_p	Concentration of tracer gas; pulse-injection technique (ppm)
F_c	Airflow rate using constant-injection technique (m^3/s)
F_p	Airflow rate using pulse-injection technique (m^3/s)
F_u	Airflow rate using pitot tube (m^3/s)
F_h	Airflow rate using hot-wire anemometer (m^3/s)
q	Injection flow rate of tracer gas (m^3/s)
P_a	Pressure at point a (see Figure 9) (Pa)
P_x	Static pressure at point x (see Figure 8) (Pa)
U_b	Bulk velocity (m/s)
U_m	Maximum velocity (m/s)
U_τ	Shear velocity (m/s)
A_A	Cross-sectional area of the bellmouth (m^2)
A_B	Cross-sectional area of the duct (m^2)
f	Friction factor
Re	Reynolds number
L_e	Entrance length (m)
D_h	Hydraulic diameter of the duct (m)
X	Distance from the duct inlet in the direction of flow (m)
t	Time (s)
g	Acceleration due to gravity (m/s^2)
Z	Intercept of static pressure lines (Pa)
ρ	Air density (kg/m^3)
τ_w	Wall shear stress (Pa)

1. INTRODUCTION

Accurate measurement of airflow in ducts is important but often difficult to achieve using traditional instrumentation such as pitot tubes, hot-wire and vane anemometers. Limited access to the flow passage or short duct lengths could restrict measurements and flow velocities less than 3 m/s could lead to measurement inaccuracies if traditional instrumentation were employed. Tracer-gas techniques such as constant-injection and pulse injection offer an alternative approach for measuring airflow in ducts, and unlike traditional instrumentation, are not limited by the length or complexity of duct configuration. As gas chromatographs can detect tracer gas at low concentrations, tracer gas techniques can be used to measuring airflow over a wide range of values. Furthermore, tracer-gas techniques can be used to measure flow rates directly and do not require determination of the cross-sectional area of the duct or flow profile at the duct wall. One further advantage of tracer-gas techniques is that they can be used to determine the airtightness of ductwork. This is important if energy and noise resulting from air leakage are to be controlled.

The present study describes the use of constant-injection and pulse injection techniques for measuring airflow in a duct and compares the results with those obtained using a pitot tube and a hot-wire anemometer. We present an empirical equation for the entrance length required to achieve fully developed turbulent flow and a relationship for friction factor and Reynolds number.

2. THEORY

The following injection strategies were used to measure airflow in a duct:

2.1 Constant-Injection Technique

Tracer gas is injected into the duct at a constant rate and the resulting concentration response is measured. Assuming that the air and tracer gas are perfectly mixed within the duct, and that the concentration of tracer gas in outside air is zero, the following equation can be used for steady-state conditions[1]:

$$F_c = (q/C_c) \times 10^6 \qquad (1)$$

2.2 Pulse-Injection Technique

This technique is based upon the injection into the duct inlet of a short-duration pulse of tracer gas at a rate $G_{(t)}$. The variation of tracer concentration with time is measured at the duct exit. The amount of injected tracer gas is small, so it does not contribute significantly to the volume flow rate of air in the duct.

If we assume that the tracer gas is well mixed across the section of the duct, then the volume flow rate of tracer gas leaving the duct is equal to the product of the flow rate and the exit concentration. If the tracer gas is assumed to be purged from the duct after some time interval (t_1 to t_2) then the volume of tracer leaving the duct must equal to the amount injected. Applying the integral volume balance of tracer gas, we have:

$$F_p = [\int_{t1}^{t2} C_p(t)\,dt]^{-1} \int_{t1}^{t2} G_{(t)}\,dt \qquad (2)$$

3. EXPERIMENTAL

The experimental work was carried out using the duct system shown in Figure 1. The duct was constructed from galvanised mild steel and was 12m long with an internal diameter of 0.56m. The downstream end was connected to an axial fan by means of a diffuser. The flow rate through the duct was varied using a speed controller made by ABB Stromberg Drives, Finland. The fan was driven by an AC motor of 4 kW and with a maximum speed of 2880 rpm. The fan was manufactured by Elta Fan Ltd, UK.

Static, velocity pressure and tracer gas tappings were positioned along the duct. The velocity tappings allowed insertion of a pitot tube or a hot-wire anemometer which could be traversed across the duct cross-section in order to measure velocity at various distances from the duct wall. Velocity and static pressures were measured using an EMD 2500 micromanometer, made by Airflow Development, UK.

For the constant-injection technique (see Figure 2), SF_6 tracer gas was supplied at a constant rate into the duct inlet using a mass flow controller which had a maximum flow capability of 3.9 L/min. The measurement accuracy of the mass flow controller was ± 1%.

For the pulse-injection technique, tracer gas was injected at the inlet of the duct using a syringe (see Figure 3). Multipoint injection was necessary for the approximation of a uniform concentration across the cross-section of the duct at the measurement point. It was necessary to measure the concentration of tracer gas at the downstream point to determine the integral of the concentration. This was achieved by filling an air sample bag by means of a small pump. Sampling was begun 10 seconds before the pulse was injected, and continued until the pulse was completely purged from the duct.

The concentration of tracer gas was measured using an Infra-red gas analyser, type BINOS 1000, made by Rosemount GmbH & Co (RAE), Germany. The accuracy of analyser was estimated to be within ± 2%.

4. RESULTS AND DISCUSSION

4.1 Friction-Factor and Reynolds Number

The wall shear stress for steady, incompressible fully-developed flow in a duct is given by:

$$\tau_w = \frac{-D_h}{4}(\Delta P/\Delta X) \quad (3)$$

The friction factor may be defined as:

$$f = 2\,\tau_w/\rho U_b^2 \quad (4)$$

Measurement of airflow rate in the duct was carried out by means of the constant-injection and pulse injection techniques as well as using a pitot tube and hot-wire anemometer. SF_6 was injected at $X/D_h = 0.625$, and the concentration of tracer gas was monitored at various positions downstream. Figures 4 and 5 show the variation of tracer-gas concentration with X/D_h for Reynolds numbers in the range 76220 to 392850. The concentration of tracer gas was found to be large close to the injection point, and decreased as X/D_h increased. The tracer-gas concentration remained constant when X/D_h was greater than 15 (for constant-injection) and 8 (for pulse injection technique).

Figures 6 and 7 compare measurements of duct airflow rate made with the tracer-gas techniques, and a pitot tube and a hot-wire anemometer. General agreement was observed, and the best linear relationships were:

$$F_c = 1.05\,F_u + 0.112 \quad (5)$$

$$F_p = 1.062\,F_u - 9.12 \times 10^{-2} \quad (6)$$

$$F_c = 0.998\,F_h + 0.223 \quad (7)$$

$$F_p = 1.01\,F_h + 1.75 \times 10^{-2} \quad (8)$$

The above results indicate that the flow rate obtained using the pulse-injection technique is in closer agreement with values obtained using the pitot-tube and hot-wire anemometer than the flow rate obtained using the constant-injection technique.

The friction factor f of the duct was calculated using average velocity (based on the pulse-injection technique) and pressure gradient for the fully-developed flow (see Figure 8). The following relationship between f and Re was obtained:

$$f = 0.0124\,Re^{-0.13} \quad (9)$$

The friction factor obtained using equation (9) differs slightly from that obtained using Blasus[2] equation, probably as a result of the difference of the pipe characteristics and the inlet condition.

4.2 Entrance Length for Fully-Developed Flow

The formation of a boundary layer in a duct is shown in Figure 9. Air enters the duct at point a with a velocity U_a. At point b the velocity is uniform across the duct. At point f the boundary layer is completely formed. Further downstream from point f the boundary layer has a constant thickness. Here the influence of the entrance shape upon the airflow pattern has disappeared and fully-developed flow is said to exist.

We carried out measurements of tracer gas concentration and pressure distribution along the duct for a range of Reynolds numbers. Figures 8 and 10 were used to find an empirical expression (equation 10) for the entrance length required to achieve fully-developed flow (see Appendix for full derivation).

$$L_e/D_h = 2.315\ Re^{0.13} \qquad (10)$$

The entrance length derived from equation (10) is similar to that given by Hinze[3], i.e., $L_e/D_h = 0.693\ Re^{0.25}$, using the 1/7th power law approach.

5. CONCLUSIONS

The following conclusions are drawn:

1. Results indicate that the flow rate obtained using the pulse-injection technique is in closer agreement with values obtained using the pitot-tube and hot-wire anemometer than the flow rate obtained with the constant-injection technique.

2. The friction factor for the duct is given by $f = 0.124\ Re^{-0.13}$ and the entrance length required to achieve fully-developed flow is given by $Le/Dh = 2.315\ Re^{0.13}$.

ACKNOWLEDGEMENTS

The authors wish to acknowledge the financial support of the Science and Engineering Research Council for this project.

REFERENCES

1. RIFFAT, S.B. and HOLMES, M.
"Measurement of airflow in HVAC systems using tracer-gas techniques", Proceedings of the 11th AIVC Conference Ventilation System Performance, Belgirate, Italy, 18-21 September, 1990.

2. STREET, V.L. and WYLIE, E.B.
"Fluid mechanics", McGraw-Hill International Book Company Inc., 1983.

3. HINZE, J.O.
"Turbulence", McGraw-Hill International Book Bompany Inc., New York, 1959.

APPENDIX

Considering Figure 9, and applying the continuity equation to sections A and B, we have:

$$A_A U_A = A_B U_B \quad (A1)$$

But $U_A = U_a$ and $U_B = U_b$ and so equation A1 can be rewritten as

$$U_a = U_b A_B / A_A \quad (A2)$$

Applying Bernoulli's equation between points a and f (along the stream line abf, Figure 9) gives:

$$U_a^2/2g + P_a/\rho g = U_f^2/2g + P_f/\rho g \quad (A3)$$

But $U_f = U_m$

Substituting equation A2 into equation A3 and rearranging, we have:

$$(P_a - P_f)/\rho g = [U_m^2 - A_B/A_A)^2 U_b^2]/2g \quad (A4)$$

Dividing both sides of equation A4 by U_m^2 we have:

$$(P_a - P_f)/\rho U_m^2 = 0.5 - 0.5(A_B/A_A)^2(U_b/U_m)^2 \quad (A5)$$

But $A_B/A_A = 0.424$

Tracer-gas concentration was measured at different distances from the duct wall at the inlet of the duct and at the region of fully developed flow. This allowed the ratio C_m/C_b to be determined. Applying equation A4, we find that the flow rate ratio is given by:

$$F_b/F_m = C_m/C_b$$

since

$$F = AU$$

the velocity ratio U_b/U_m is given by:

$$U_b/U_m = F_b/F_m = C_m/C_b$$

The average value of U_b/U_m for the range of Reynolds numbers used in these experiments was 0.819.

Substituting the values of A_B/A_A and U_b/U_m into equation A5 gives:

$$(P_a - P_f)/\rho U_m^2 = 0.440 \quad (A6)$$

Consider the variation of static pressure with X, Figure 10. The difference between the static pressure at X = 0 (i.e. pressure ≈ atmospheric pressure) and the static pressure of fully developed flow, X = L_e is given by:

$$P_a - P_x = (Z + Y) = Z + L_e \tan\theta \quad \text{(A7)}$$

or

$$P_a - P_f = Z - L_e dP/dx \quad \text{(A8)}$$

$$\tau_w = -(D_h/4)dP/dx \quad \text{(A9)}$$

Equation A9 is normally applied to regions of fully developed flow but is also a very good approximation for the entrance region of the duct provided that $L/D_h > 1$. Experimental results (Figure 8) showed that dP/dx was constant along the length of the duct for the range of Reynolds numbers used.

Substituting equation A9 into A8 and dividing both sides of equation A8 by ρU_m^2, we have:

$$(P_a - P_f)/\rho U_m^2 = \rho_w g/\rho U_m^2 + 4 L_e \tau_w/D_h \rho U_m^2 \quad \text{(A10)}$$

$$U\tau = (\tau_w/\rho)^{0.5} \quad \text{(A11)}$$

and

$$U\tau = U_b(f/2)^{0.5} \quad \text{(A12)}$$

Substituting equations A11 and A12 into equation A10 and simplifying, we have:

$$(P_a - P_f)/\rho U_m^2$$

$$= Z/\rho U_m^2 + 2(L_e f/D_h)(U_b/U_m)^2 \quad \text{(A13)}$$

From tracer gas measurements, $U_b/U_m = 0.819$

$$f = 0.0124\ Re^{-0.13} \quad \text{(A14)}$$

Equation A14 is applicable when the velocity profile is fully developed. If the velocity profile is not fully developed but $L/D_h > 1$, then equation 14 is a good approximation.

Substituting the value of U_b/U_m and equation A14 into A13 and simplifying, we have

$$(P_a - P_f)/\rho U_m^2 = Z/\rho U_m^2$$

$$+ 0.0166\ (L_e/D_h)\ Re^{-01.3} \quad \text{(A15)}$$

Substituting equation A6 into A15 and simplifying, we have:

$$L_e/D_h = (26.42 - 60.1\ Z/\rho U_m^2)\ Re^{0.13} \qquad (A16)$$

The intercepts Z of the static pressure lines were found from Figure 8.

$$Z/\rho U_m^2 = 0.401 \qquad (A17)$$

Substituting equation A17 into equation A16 we obtain:

$$L_e/D_h = 2.32\ Re^{0.13} \qquad (A18)$$

This equation can be used to determine the entrance length L_e for fully developed turbulent flow.

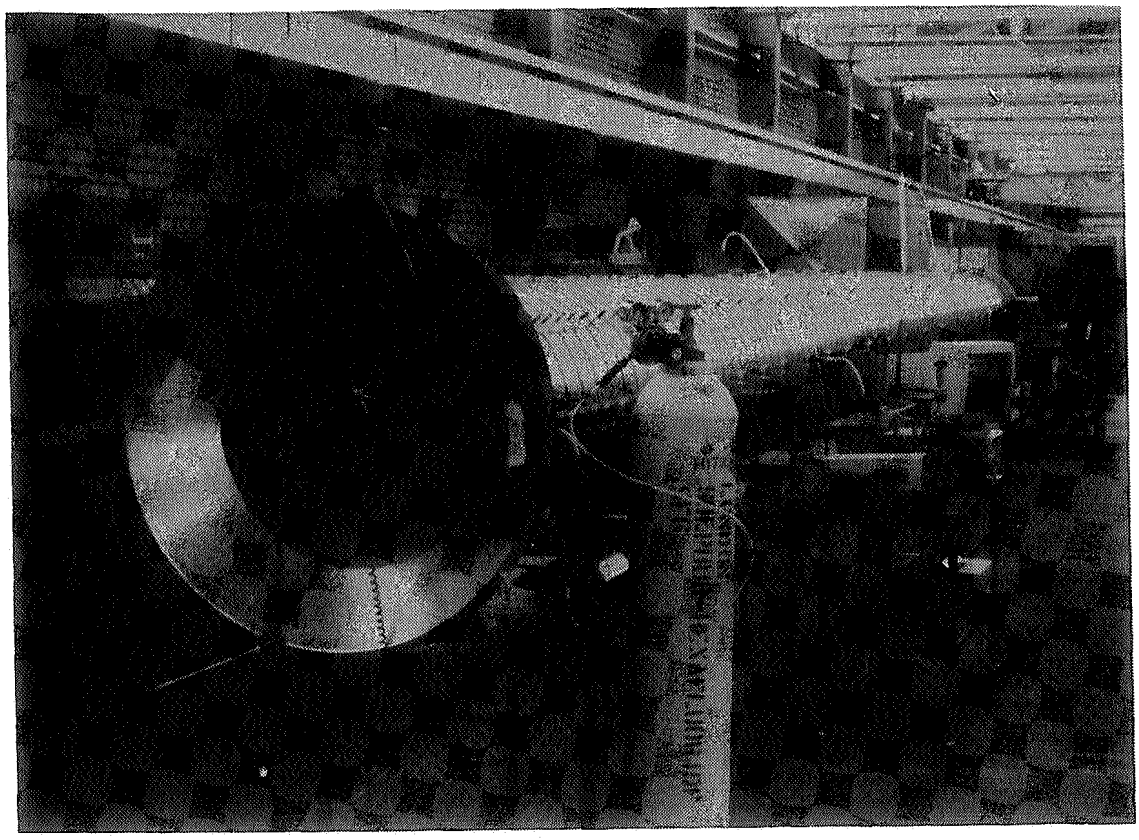

Figure 1 Experimental system for testing tracer-gas techniques

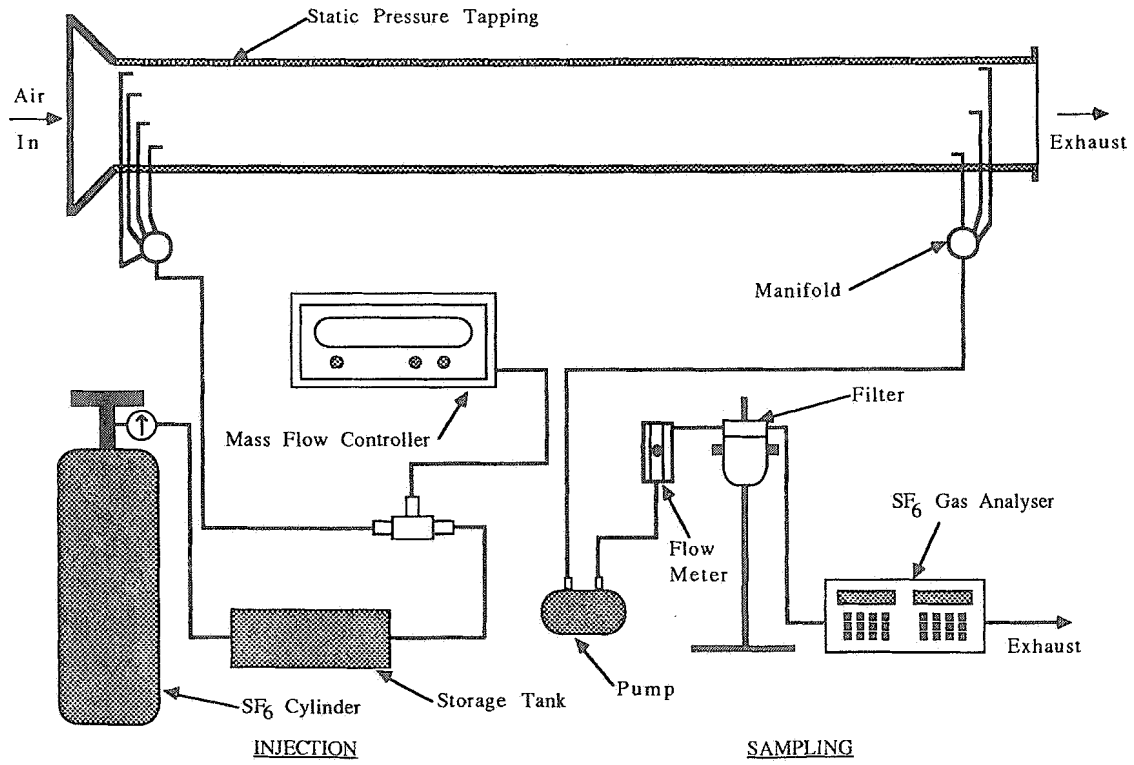

Figure 2 Instrumentation for the constant-injection technique

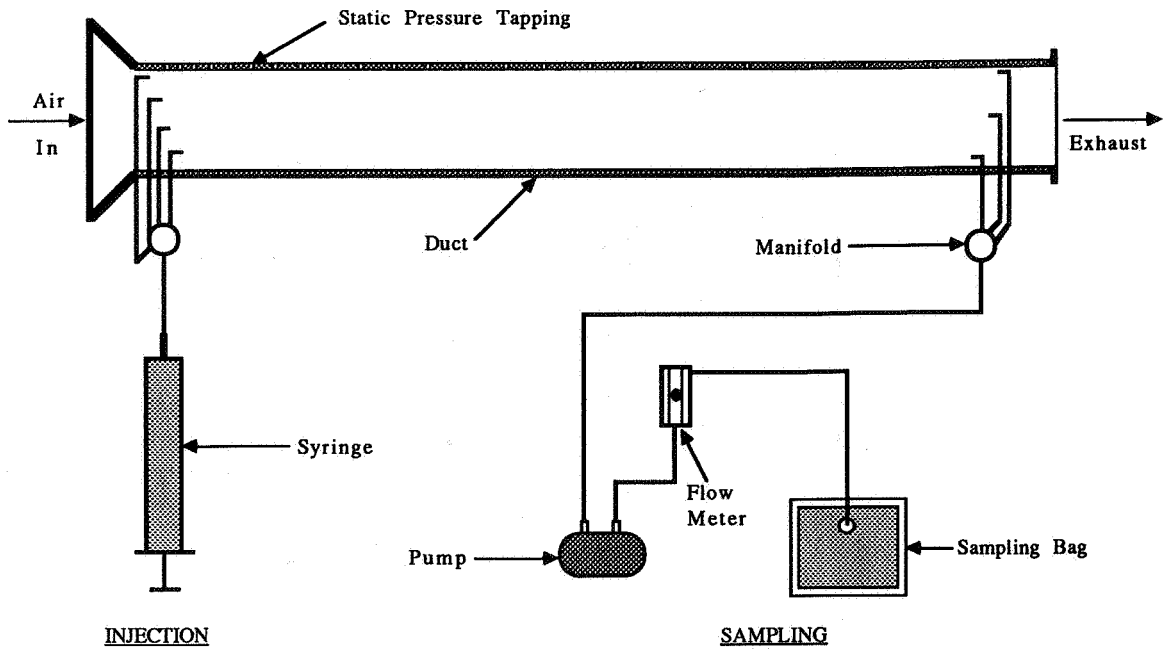

Figure 3 Instrumentation for the pulse-injection technique

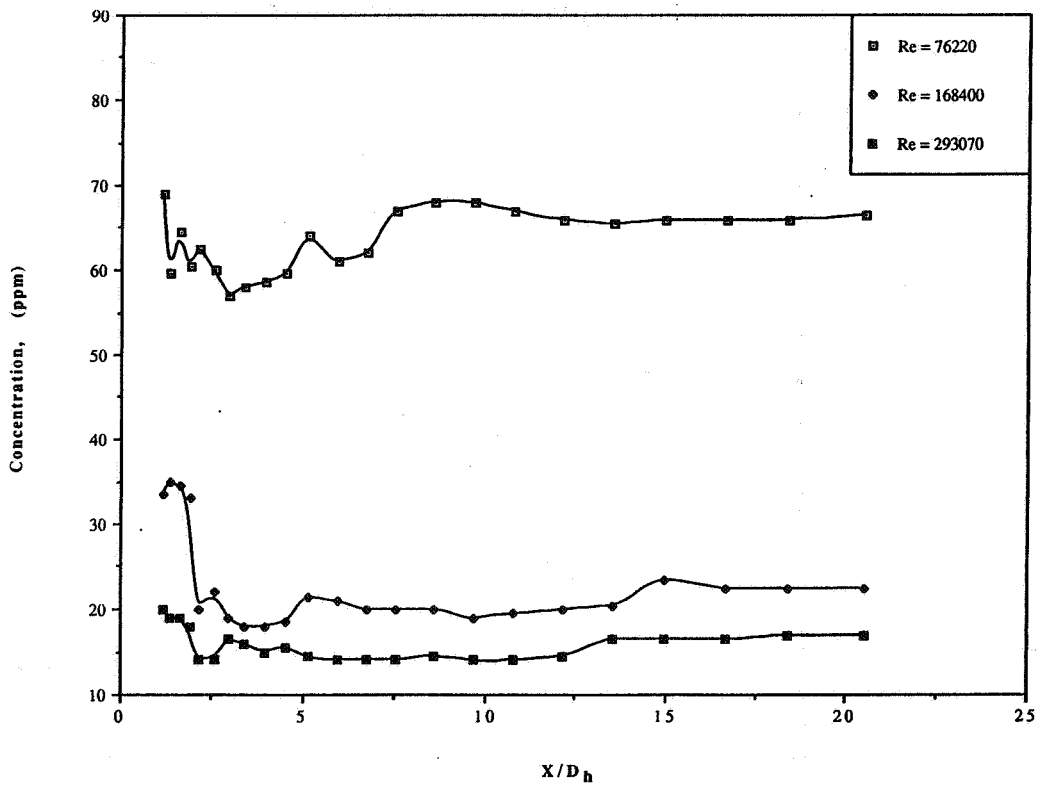

Figure 4 Variation of tracer-gas concentration with X/D_h, constant-injection technique

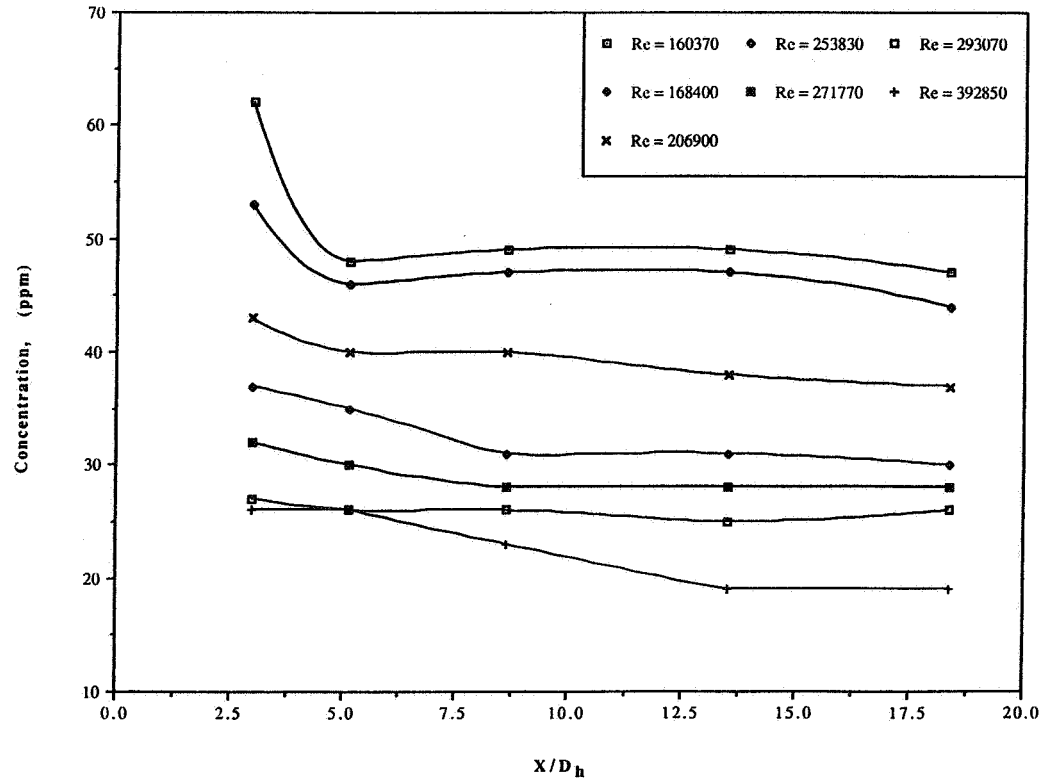

Figure 5 Variation of tracer-gas concentration with X/D_h, pulse-injection technique

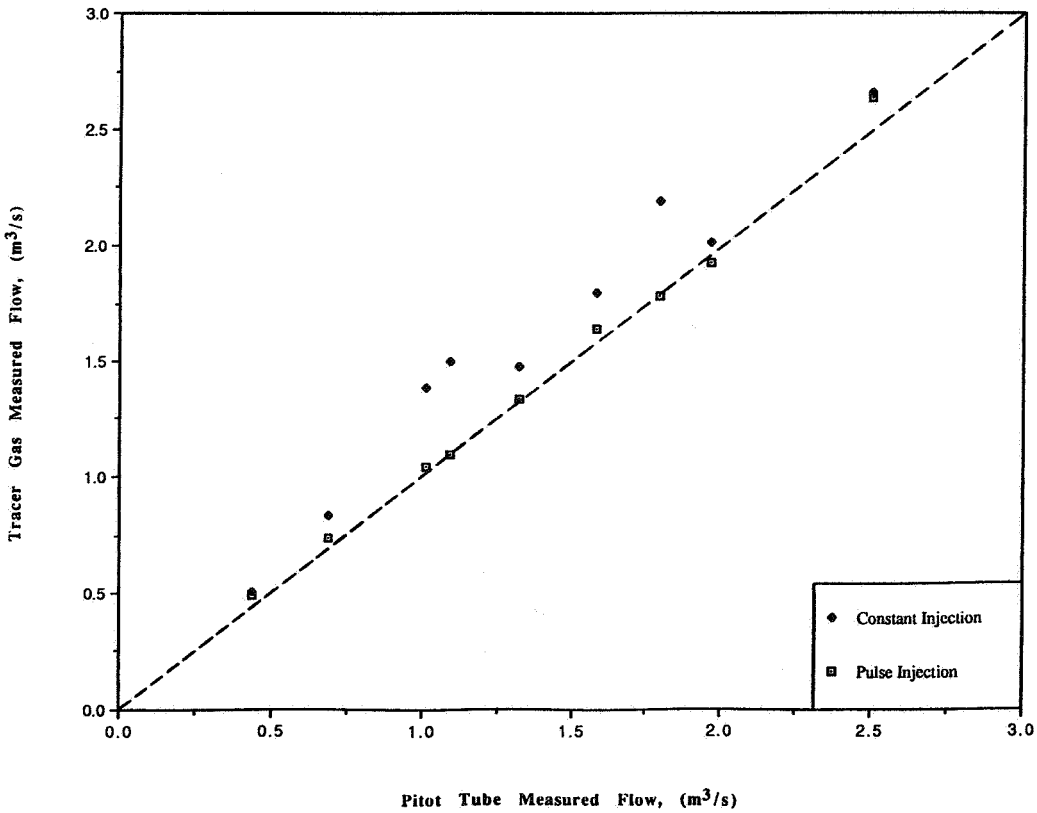

Figure 6 Comparison of tracer-gas airflow measurements with measurements made using a pitot tube

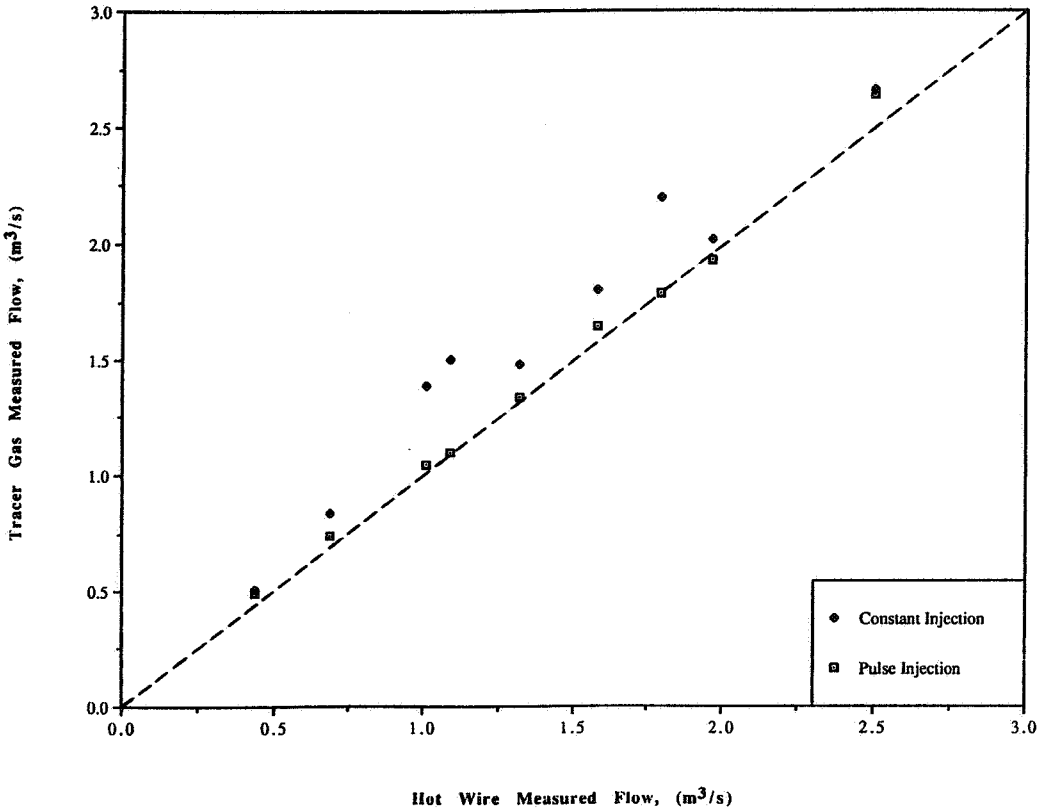

Figure 7 Comparison of tracer-gas airflow measurements with measurements made using a hot-wire anemometer

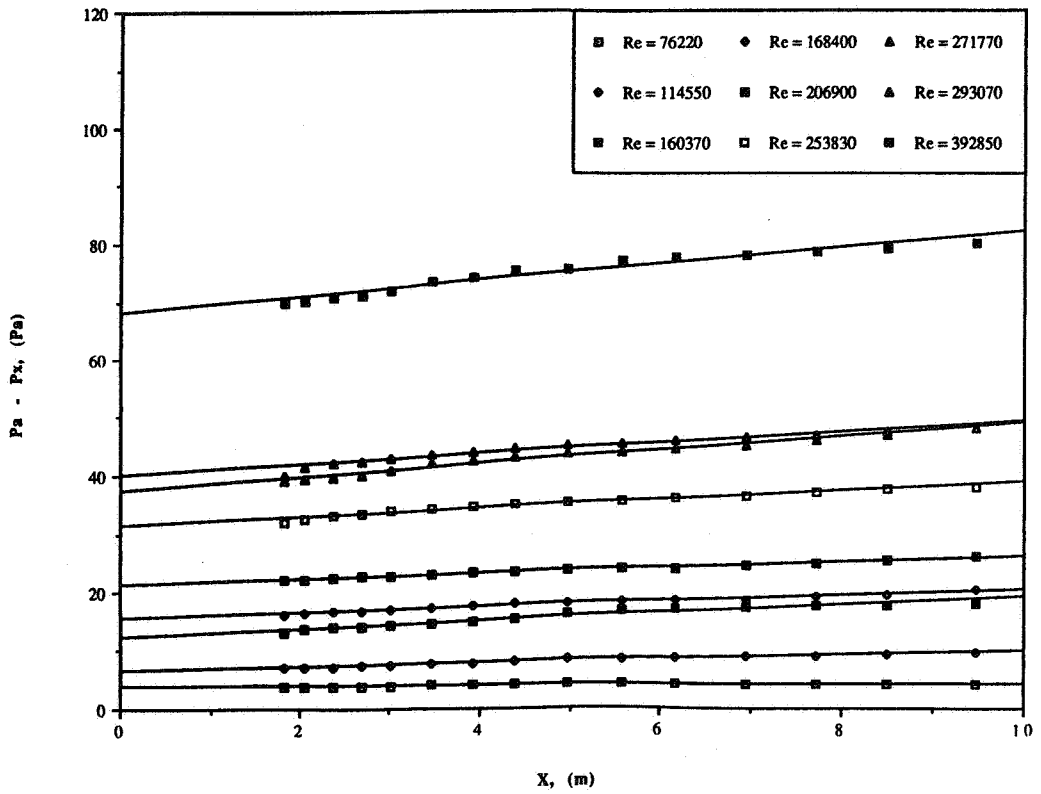

Figure 8 Static pressure distribution along the duct for various values of Re

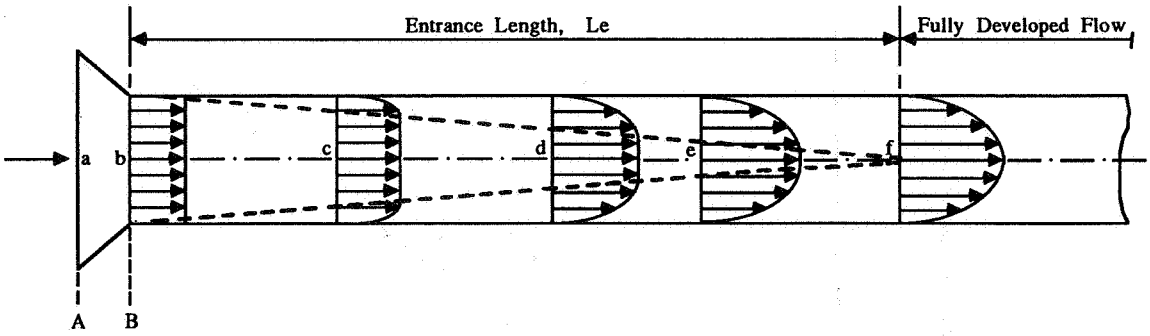

Figure 9 Formation of a boundary layer in a duct

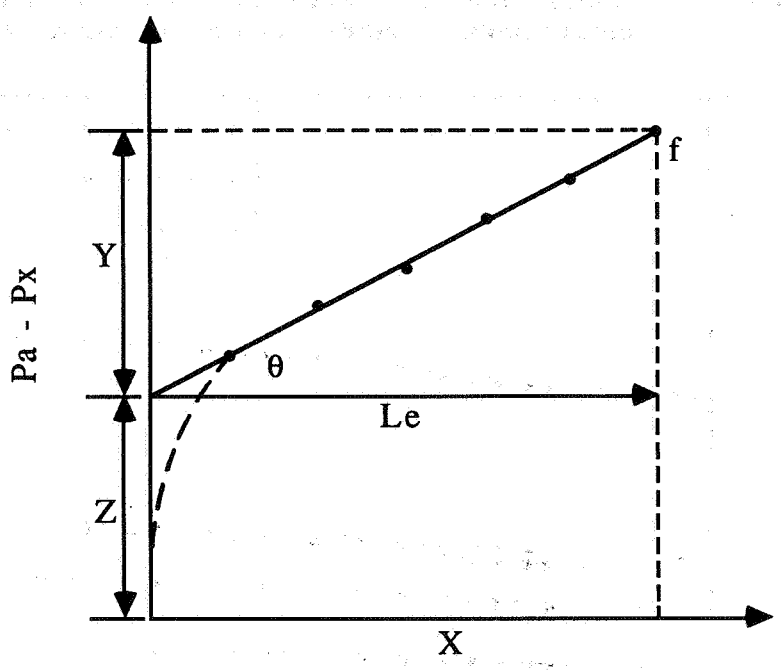

Figure 10 Variation of static pressure with X

AIR MOVEMENT & VENTILATION CONTROL WITHIN BUILDINGS

12th AIVC Conference, Ottawa, Canada
24-27 September, 1991

POSTER 28

INTERZONAL AIRFLOW MEASUREMENT - A TOOL TO SOLVE POLLUTION PROBLEMS.

BJØRN KVISGAARD[1], LARS SCHMIDT[2]

[1]Brüel & Kjær
DK-2850 Nærum
Denmark

[2]Thermal Insulation Laboratory
Technical University of Denmark
Building 118
DK-2800 Lyngby

ABSTRACT

Knowledge of air movement within a building is often a condition for solving problems with the spread of pollution. The internal airflow paterns are mostly very complex and a survey of the airflow normally demands that measurements are carried out.

Measuring equipment for defining air movement within buildings almost always uses the tracer gas technique. We have used two tracer gases and have kept a constant concentration of these in the polluted and the clean zones respectively. Thus enabling us to get a time history of the airflow between the two zones. Concurrently, with measurements of the airflow between clean and polluted zones, we have measured the concentration of pollution components.

The article describes both the results from testing the measurement method in an uninhabited test-house and the results from field measurements in a house and in a large factory building. From the results, the accuracy of the measurement method and the relationship between the calculated and actually measured pollution concentrations are discussed.

1. INTRODUCTION

Problems with the spread of pollution in buildings and problems in calculating the concentration of the pollution source are often so complex that simple measurement methods and common sense are not sufficient to achieve the correct results. Such problems require more advanced measurement techniques.

The tracer gas measurement methods are among the most effective and flexible tools available when you want to trace air movements. If you make use of several tracer gases you will come a long way in understanding the often very complex air movements in buildings. In our investigations we have used a measurement equipment capable of keeping a constant concentration of tracer gas in up to 12 rooms and handling 2 different tracer gases at the same time. With this equipment you will also be able to register the pollution concentrations and temperatures in the rooms.

The measurement equipment will calculate the outdoor air-exchange and make current print-outs, whereas the calculation of interzonal airflow must be done manually. In the following chapter the equations being used for calculating the interzonal airflow are explained. We are dealing with 2 different sets of equations, each related to the 2 main types of measurements. When performing the type of measurement we call split-measurement we keep a constant concentration of tracer gas A in one area of the building and a constant concentration of tracer gas B in the rest of the building. When performing the type of measurement we call supplement-measurement the concentration of tracer gas A is kept constant all over the building and in addition to this a constant concentration of tracer gas B is kept in a limited area of the house.

We have carried out three measurements, two of which are reported in the present text. One measurement in a factory hall is not included, as we have not been able to demonstrate any interzonal airflow between the polluted and the clean area of the building.

2. Calculation of Interzonal Airflow.

In figure 1 the flows which can be calculated by the split-measurement method are shown. The unknown values are the 6 flows marked with arrows, and the known values are the measured air-exchanges, concentrations and volumes. During the measurement the concentration of tracer gas A is kept constant in room 1, and the concentration of tracer gas B in room 2. Tracer gas A is not dosed in room 2, and tracer gas B is not dosed in room 1.

In figure 1 the 6 equations which are used for calculating the unknown airflow are stated. The 6 equations derive from stating a mass balance for tracer gas A, tracer gas B and the airflow for each room. The equation system is easily solved, especially if there is stationary flow and you wait until all tracer gas concentrations are stable.

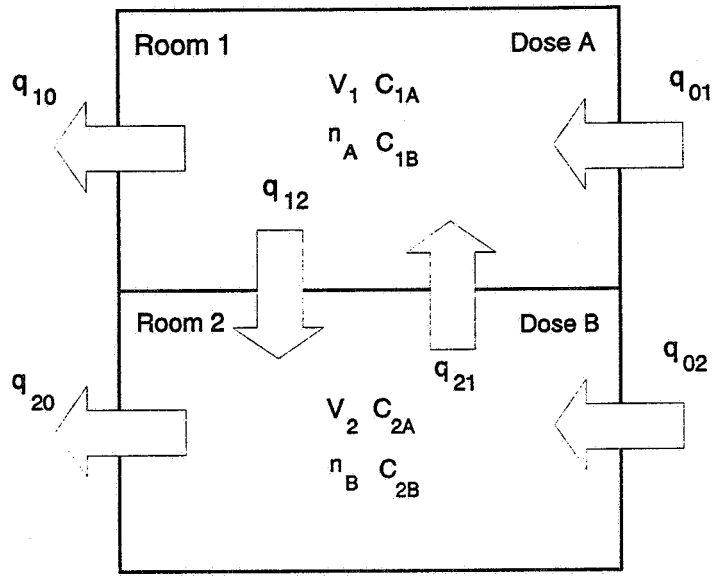

$$n_A \times V_1 = q_{01} + q_{21} \times (1-C_{2A}/C_{1A})$$

$$n_B \times V_2 = q_{02} + q_{12} \times (1-C_{1B}/C_{2B})$$

$$V_1 \times dC_{1B}/dt = q_{21} \times (C_{2B}-C_{1B}) - q_{01} \times C_{1B}$$

$$V_2 \times dC_{2A}/dt = q_{12} \times (C_{1A}-C_{2A}) - q_{02} \times C_{2A}$$

$$q_{10} = q_{01} + q_{21} - q_{12}$$

$$q_{20} = q_{02} + q_{12} - q_{21}$$

n = measured air-exchange
V = room volume
C = concentration of tracer gas
q = airflow
dC/dt = change in tracer gas concentration with respect to time.

Figure 1: Equations for calculation of interzonal airflow by split-measurements.

When using the supplement-measurement method we only have to calculate 4 unknown flows, as the flow of outdoor air into the two rooms is measured direct. In figure 2 the 4 unknown flows are marked with arrows out of and between the rooms. The known values are the measured air-exchanges, concentrations and volumes. During measurement a constant concentration of tracer gas A is kept in room 1 and 2, and a constant concentration of tracer gas B in room 2. Tracer gas B is not dosed in room 1.

In figure 2 the 4 equations used for calculation of the unknown airflow are stated. The 4 equations derive from stating a mass balance for tracer gas B and for the airflow for each room.

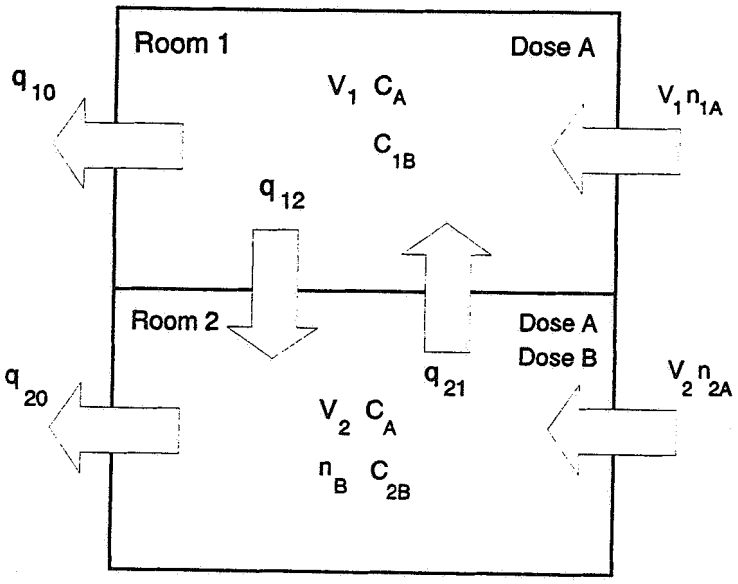

$$(n_B - n_{2A}) \times V_2 = q_{12} \times (1 - C_{1B}/C_{2B})$$

$$V_1 \times dC_{1B}/dt = q_{21} \times (C_{2B} - C_{1B}) - V_1 \times n_{1A} \times C_{1B}$$

$$q_{10} = V_1 \times n_{1A} + q_{21} - q_{12}$$

$$q_{20} = V_2 \times n_{2A} + q_{12} - q_{21}$$

Figure 2: Equations for calculation of interzonal airflow by supplement-measurements.

3. Measurement in Test-House.

As a control of the equipment a measurement was performed in a test-house at the Thermal Insulation Laboratory. It is a two-storied house with the size of a normal Danish one-family house. The measurements were carried out on the ground floor which consists of two almost equal-sized rooms of 135 m^3 and 142 m^3 respectively.

At first the leakage of the house was determined by the constant concentration measurement method. Tracer gas SF6 was used and the target for the tracer gas concentration was 1 ppm. The measurement was running during 12 hours and the following results were achieved:

Basic air-exchange rate = 0.01 1/h
Mean value SF6 concentration = 1.01 ppm
Spread in concentration = 0.02 ppm

The basic air-exchange is much lower than normally for Danish houses. However, in the test-house all joints was sealed very carefully. The outdoor climate during measurement of the basic air-exchange was:

Mean wind velocity = 6 m/s
Temperature = -3,0 ^{o}C

Then 3 ventilation plants were installed in the test-house, two of which were used to ventilate the two rooms with outdoor air and one to create an airflow between the two rooms. A plate orifice was installed in 3 of the ducts, enabling us to measure the exhaust airflow from each room and the flow from room 1 to room 2.

Four measurements were performed in the test-house with 4 different flow between room 1 and 2. They were all split-measurements and a concentration of the tracer gas Flourcarbon-22 was kept at 10 ppm in room 1 (vestrum), and a concentration of the tracer gas SF6 was kept at 1.0 ppm, in room 2 (oestrum). All measurements were running until all tracer gas concentrations were stable. In figure 3 an example of measured tracer gas concentrations and air-exchanges in the two rooms during a period of 12 hours is shown.

B K

7620
Tracer Gas
Measurement

SETTINGS:

Sampling Interval:		Cont.
Time bet. measurement	1570	s
Normalization temp.:	20.0	°C
Cross Compensation:		No
Water Vapour Compens:		Yes
Air Pressure:	101.30	kPa

GENERAL INFORMATION:

Start Time:	1991-02-16 20:00
Stop Time:	1991-02-17 10:00
Compression time:	None
Warning:	None
Data Edited:	No
Resolution:	11 %

COMMENTS:
Luftskiftet i oest- og vest-rummet.
Infiltration ca. 30 m3/h.

DATABASE: EXPHUS3
USER PRG: None

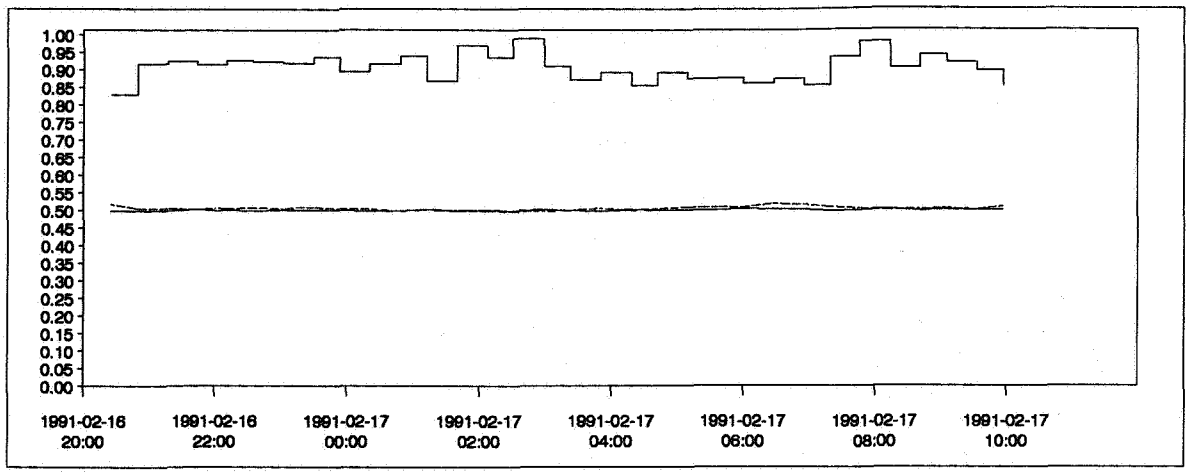

C	Location:	Measurement	Line	Scale	Unit	Room Vol.	Mean val.	Sprd. of c. p.
1	Vestrum	Flourocarbon 22	——	2E+01	ppm	135.00 m^3	9.99 ppm	2.97E-02 ppm
1	Vestrum	Sulphur Hexaflouride	---	5E-01	ppm	135.00 m^3	2.52E-01 ppm	2.55E-03 ppm
1	Vestrum	Air-change	_┌┐	1E+02	m^3/h	135.00 m^3	90.57 m3/h	3.79 m3/h

B K

7620
Tracer Gas
Measurement

SETTINGS:

Sampling Interval:		Cont.
Time bet. measurement	1578	s
Normalization temp.:	20.0	°C
Cross Compensation:		No
Water Vapour Compens:		Yes
Air Pressure:	101.30	kPa

GENERAL INFORMATION:

Start Time:	1991-02-16 20:00
Stop Time:	1991-02-17 10:00
Compression time:	None
Warning:	None
Data Edited:	No
Resolution:	11 %

COMMENTS:
Luftskiftet i oest- og vest-rummet.
Infiltration ca. 30 m3/h.

DATABASE: EXPHUS3
USER PRG: None

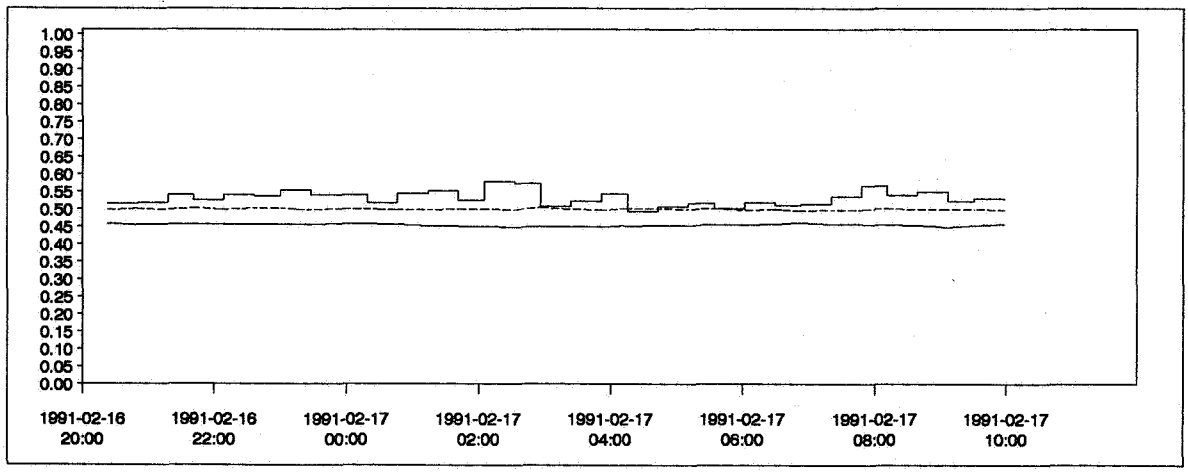

C	Location:	Measurement	Line	Scale	Unit	Room Vol.	Mean val.	Sprd. of c. p.
7	Oestrum	Flourocarbon 22	——	5E+00	ppm	142.00 m^3	2.27 ppm	1.54E-02 ppm
7	Oestrum	Sulphur Hexaflouride	---	2E+00	ppm	142.00 m^3	9.99E-01 ppm	3.06E-03 ppm
7	Oestrum	Air-change	_┌┐	2E+02	m^3/h	142.00 m^3	106.38 m3/h	3.99 m3/h

Figure 3: Tracer gas concentrations and air-exchange rate in test-house during test No. 3. Room 1 is location "Vestrum" and room 2 is location "Oestrum". The plotted values are half-hour mean values.

From the figure you can see that the tracer gas concentrations are very stable during the entire measurement, but the air-exchange rates vary. E.g. from 3.00 to 7.00 a.m. the air-exchange is lower than the average air-exchange which is equal for both rooms. We cannot explain any direct source to these variations. They are probably caused by variable outdoor climate, or changes in the ventilation fans' flow caused by variation in the mains voltage.

Table 1 shows a summary of the measurement results from the test-house. At the measurement method "Tracer gas corr." corrections are made for the set-off on concentrations measured from one channel to the other. E.g. if you measure on a very high concentration of tracer gas on one channel and afterwards on clean air on the next channel, the gas monitor will read out a few percentage of the last measured high concentration. This phenomenon we call the memory effect. How big the memory effect is, depends on the ability of the specific gas to stick to the surfaces in the sampling system. As for the tracer gas SF6 it is app. 3% and for Flourocarbon-22 it is 4-5%.

Test No.	Measurement Method.	Flow m^3/h			
		q_{10}	q_{20}	q_{12}	q_{21}
1	Tracer gas	75	89	4	2
	Tracer gas corr.	77	89	0	0
	Pitot Tube	73	81	0	
2	Tracer gas	67	82	17	16
	Tracer gas corr.	69	81	12	15
	Pitot Tube	72	75	11	
3	Tracer gas	70	88	26	24
	Tracer gas corr.	74	84	19	23
	Pitot Tube	71	81	23	
4	Tracer gas	68	87	32	31
	Tracer gas corr.	76	81	25	31
	Pitot Tube	70	80	30	

Table 1: Flow measured with Pitot tube and tracer gas in m^3/h and 4 different interzonal airflows. In fig. 1 you can see which flows are shown and how they are calculated. At the measurement method "Tracer gas corr." corrections for the memory effect in the measurement system have been made.

From the table you will find a mean difference of 4 m^3/h in the measurements on tracer gas and Pitot tube. The Pitot Tube measurements should result in somewhat lower values than the tracer gas measurements, as they do not compensate for airflow caused by leak in the construction.

4. Measurement in a one-family house.

Measurements were carried out in a typically Danish one-family house, see photo below. It is a one-storey house inhabited by 2 adults and 1 child. In figure 4 you will see a plan of the house.

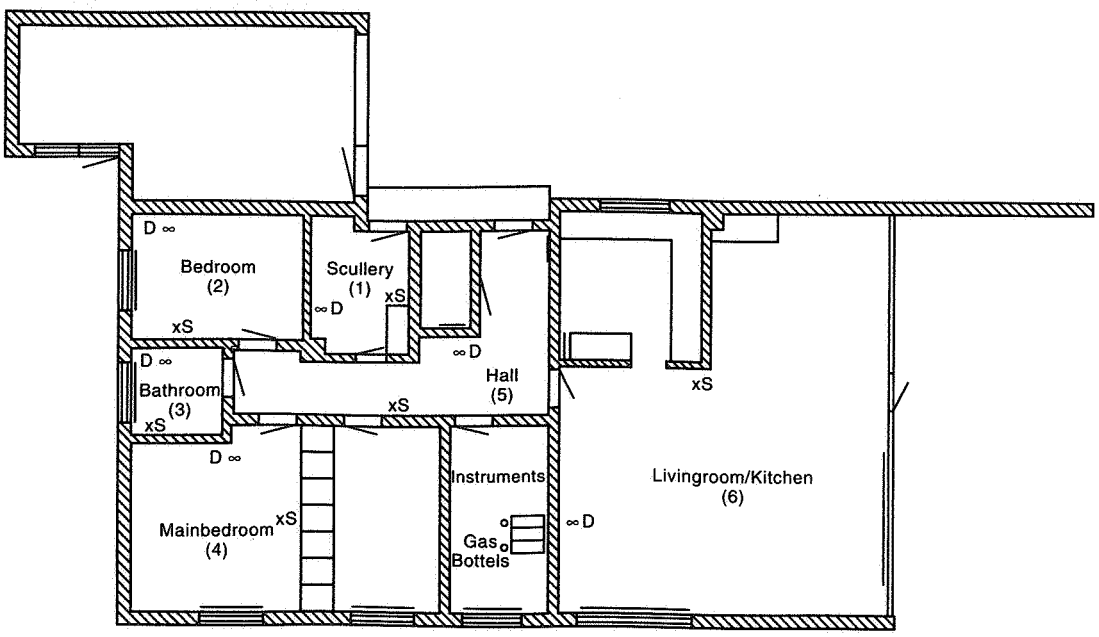

Figure 4: Plan of house with room numbers, dosing points and sampling points entered. During measurements the doors between the hall and the two rooms next to the living room were open.

The measurements were carried out as supplement-measurements. The tracer gas SF6 was used to measure the flow of outdoor air into each separate room, and the tracer gas R-22 was used to measure the total airexchange in one individual room, - as well the outdoor air entering direct from outdoor as the outdoor air entering from adjoining rooms. At this measurement especially the airflow to Main bedroom and Livingroom-Kitchen was examined. In addition to the measurement of airflow, the concentrations of carbon dioxide in the rooms and the temperatures in- and out-door were registered.

Below is shown a photo of the measurement equipment set-up in one of the guestrooms in the house. All tube connections to the equipment were placed so that the family was able to live as always in the house, and we asked the family to act as they used to with regard to airing and opening and closing of internal doors.

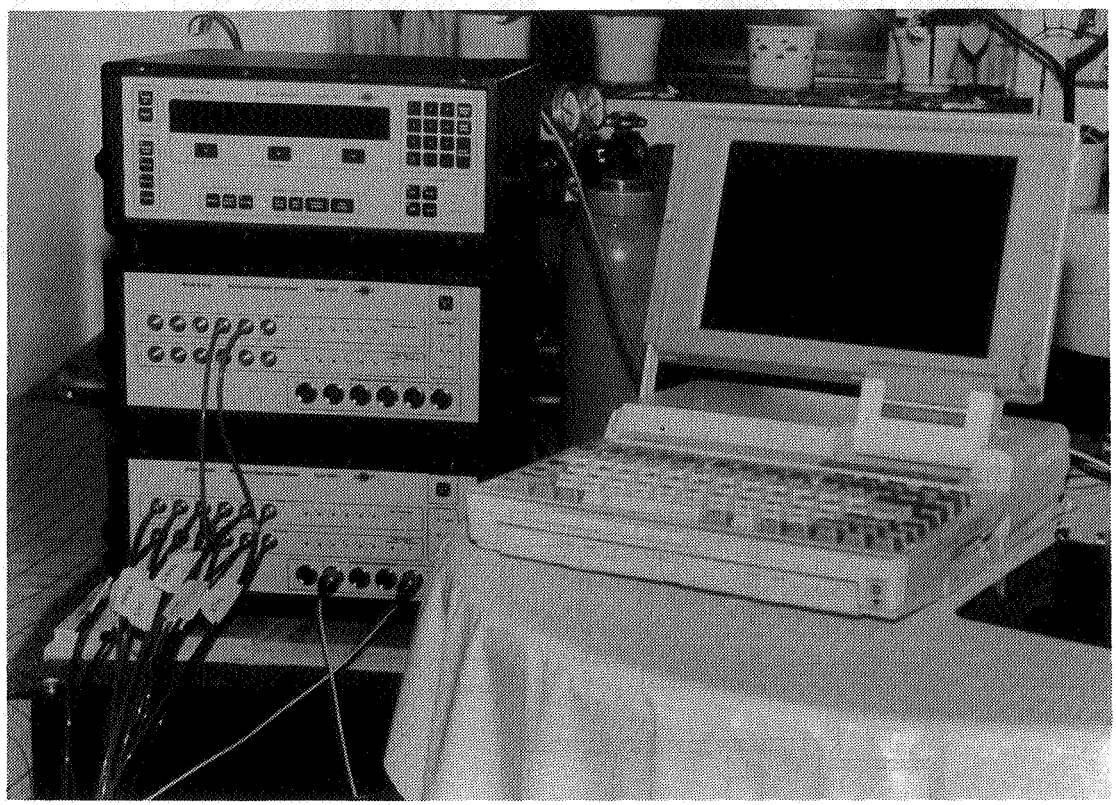

In figure 5 you will see the total air-exchange as function of time. Especially the most variable air-exchange is significant, and this is typically for a naturally ventilated house (ref. 1 and 2), with a very low air-exchange during night and some peaks during the day caused by airing.

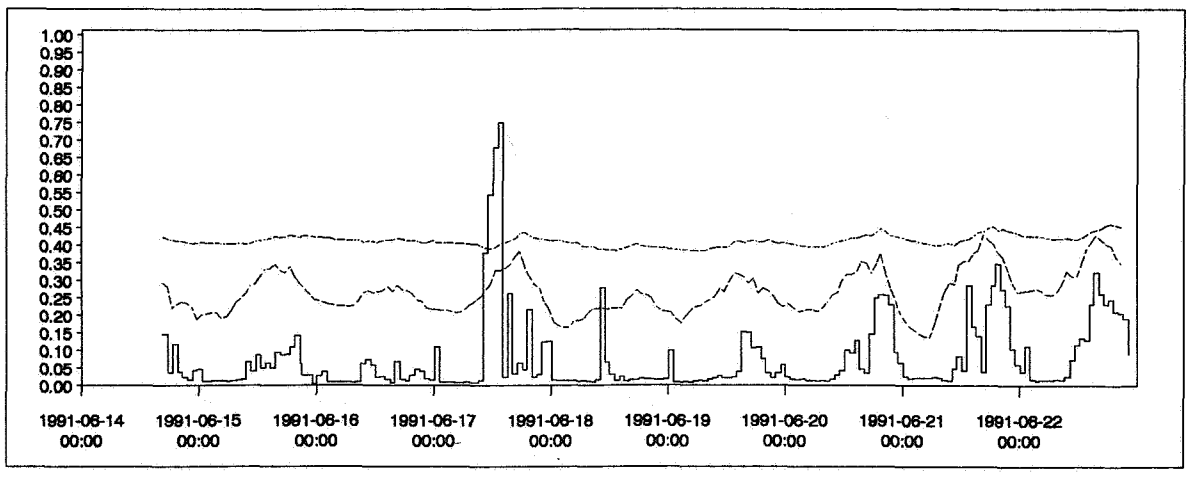

C	Location:	Measurement	Line	Scale	Unit	Room Vol.	Min.Val.	Max.val.	Mean val. of c.p.
W	Weighted mean	Air-change		1E+01	h-1	278.10 m^3	3.05E-02 h-1	7.48 h-1	7.38E-01 h-1
5	Hall	Temperature		5E+01	^{0}C	72.00 m^3	19.15 C	22.95 C	20.56 C
2	Bedroom	Temperature		5E+01	^{0}C	23.00 m^3	6.85 C	21.45 C	13.27 C

Figure 5: The air-exchange in the house and in- and out-door temperatures as function of time.

In the upper plot of figure 6 "C 4" states the measured airflow of outdoor air into the main bedroom, and "C 10" states the total measured air-exchange in the same room. The equations in figure 2 have been used to calculate the flow from the hall into the main bedroom during the period from 11 p.m. to 8 a.m. The flow calculated is shown in the upper plot.

On the second plot you can see how the air from the bedroom is circulated to the rest of the house, and e.g. a low air-exchange between the main bedroom and the livingroom/kitchen is seen.

If you compare the three graphs in the figure you will see that the door between the main bedroom and the hall has been left open from 1 p.m. to 5 p.m., then it has been closed until 11 p.m., and then again it has been partly open during the night.

At some occasions it could be very useful to combine measurement of air-exchanges with measurement of pollution concentrations, as this will give you the possibility to determine the source strength of a pollutant in a certain room. In this example we will calculate the produced volume of carbon dioxide during the night in the main bedroom.

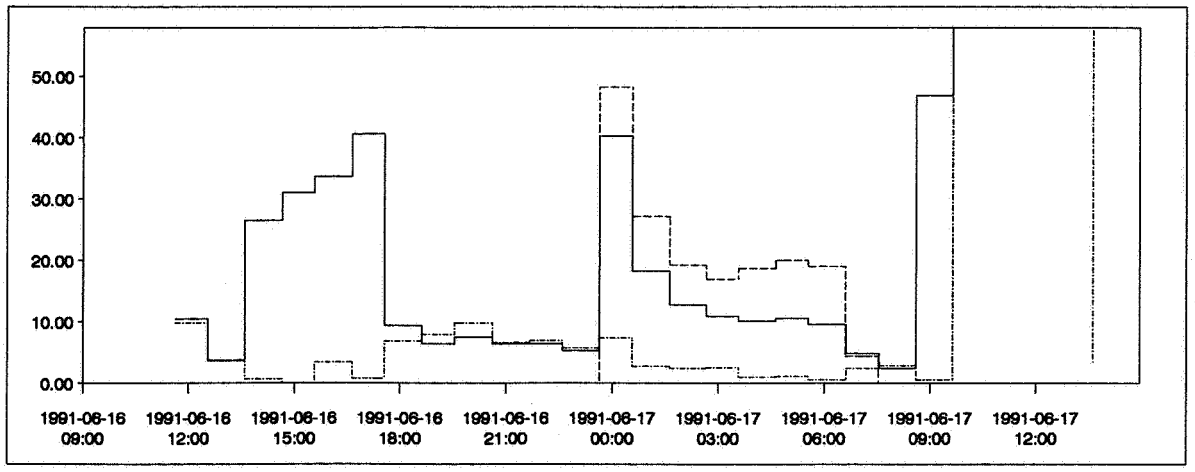

C	Location:	Measurement	Line	Scale	Unit	Room Vol.
4	Main bedroom	Air-change		1E+00	m^3/h	34.00 m^3
10	Main bedroom	Air-change		1E+00	m^3/h	34.00 m^3
1	User index 1	Calculated		1E+00	m3/h	

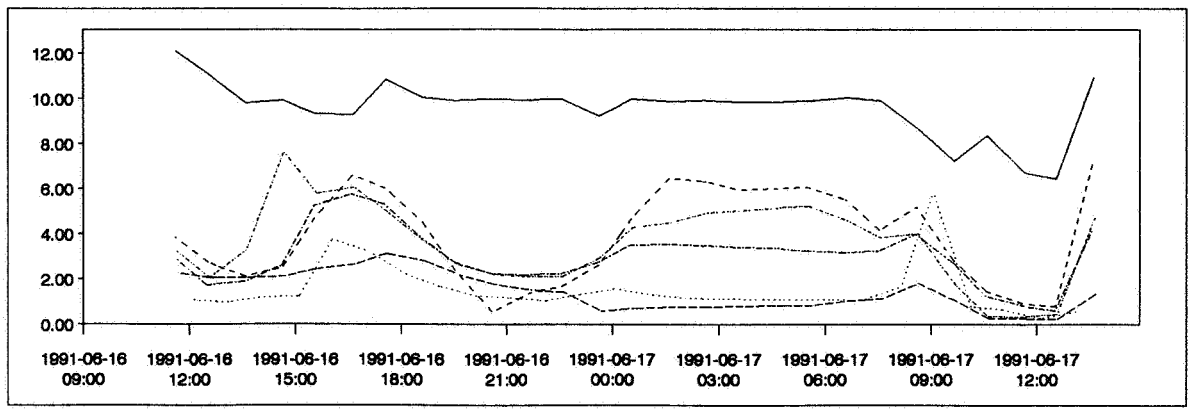

C	Location:	Measurement	Line	Scale	Unit	Room Vol.	Mean val. of c.p.
1	Scullery	R22		1E+00	ppm	14.00 m^3	1.52 ppm
2	Bedroom	R22		1E+00	ppm	23.00 m^3	3.04 ppm
3	Bathroom	R22		1E+00	ppm	8.10 m^3	3.90 ppm
4	Main bedroom	R22		1E+00	ppm	34.00 m^3	9.59 ppm
5	Hall	R22		1E+00	ppm	72.00 m^3	3.63 ppm
6	Livingroom-Kitc	R22		1E+00	ppm	127.00 m^3	1.44 ppm

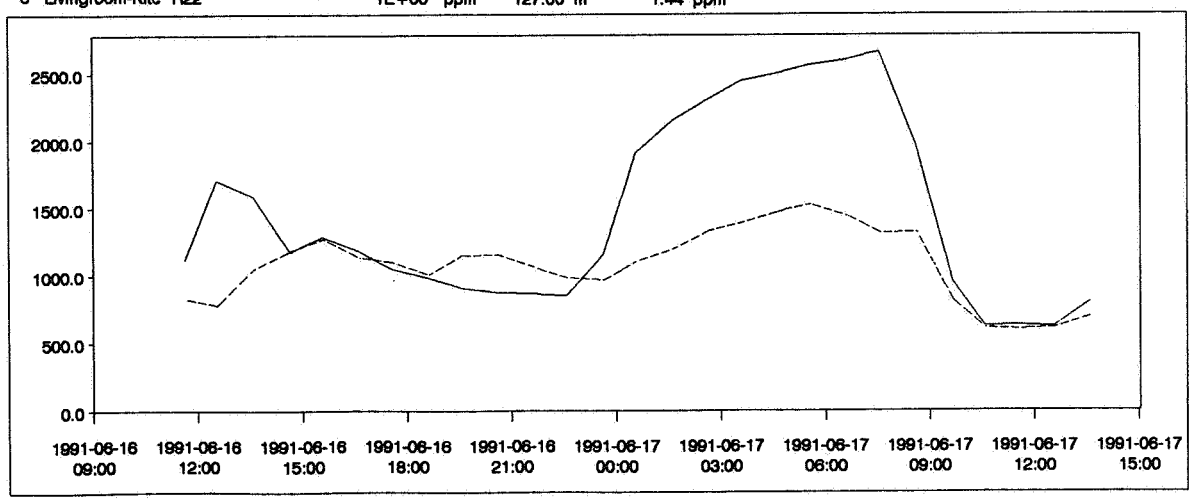

C	Location:	Measurement	Line	Scale	Unit	Room Vol.	Max.val.	Mean val. of c.p.
4	Main bedroom	Carbon Dioxide		1E+00	ppm	34.00 m^3	2.66E+03 ppm	1.46E+03 ppm
5	Hall	Carbon Dioxide		1E+00	ppm	72.00 m^3	1.53E+03 ppm	1.08E+03 ppm

Figure 6: Airflow into main bedroom, tracer gas concentrations in the house and carbon dioxide concentrations in the bedroom and the hall.

The equation used to calculate the source strength of a pollutant in the room is:

$$F_{1P} = V_1 \times dC_{1P}/dt + q_{01}(C_{1P}-400) + q_{21} \times (C_{1P}-C_{2P})$$

F_{1P} is the source strength of pollution in room 1.

V_1 is the volume of the room.

dC_{1P}/dt is change in pollution concentration with respect to time.

q_{01} is flow into room 1 from outdoor.

q_{21} is flow into room 1 from adjoining room.

C_{1P} is pollution concentration in room.

C_{2P} is pollution concentration in adjoining room.

A somewhat easier way to calculate the carbon dioxide production is to use the following simplified equation:

$$F_{1P} = V_1 \times n_B \times (C_{1P} - 400)$$

n_B is the total measured air-exchange in the room (the graph C 10).

However, this equation has its limitations, especially because it assumes that the carbon dioxide concentrations and the R-22 tracer gas are equally spread all over the house. Especially at the beginning of the night this is not true. The result of the calculations using these two equations can be seen in figure 7. Calculation of the production using the first-mentioned equation is shown as "User index 2", and calculation using the second equation is shown as "User index 3".

From figure 7 it appears that the calculated production is varying during the night from 25 l/h to 30 l/h. The expected production from 2 adults is 38 l/h in the first hour of the night and 26 l/h the rest of the night (ref. 3).

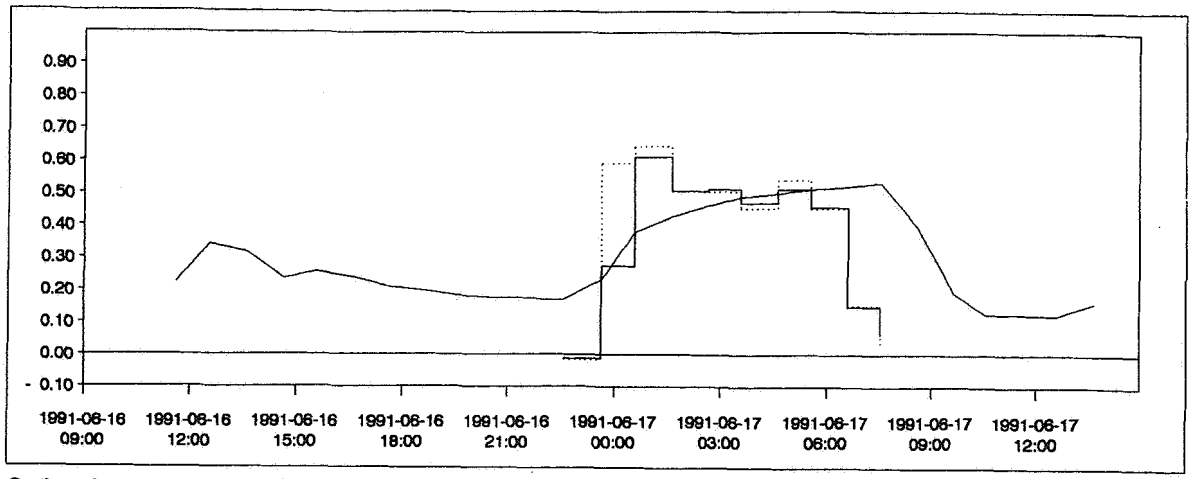

C	Location:	Measurement	Line	Scale	Unit	Room Vol.	Max.val.	Mean val. of c.p.
4	Main bedroom	Carbon Dioxide	——	5E+03	ppm	34.00 m^3	2.66E+03 ppm	1.46E+03 ppm
2	User index 2	Calculated	_┌┐_	5E+04			3.06E+04	1.78E+04
3	User index 3	Calculated	·····	5E+04			3.23E+04	1.93E+04

Figure 7: Carbondioxide concentration in main bedroom and the calculated production in the main bedroom. "User index 2" and "User index 3" show production of Carbondioxide in ml/h. "User index 3" shows calculation using the simplified equation.

In figures 8 and 9 the data are shown for a 24-hours period with a constant concentration of the tracer gas R-22 in the livingroom/kitchen. As in figure 6 you will also here see the low air-exchange between livingroom/ kitchen and the rest of the house. Only twice during the day you find the door between the two rooms open for a longer period.

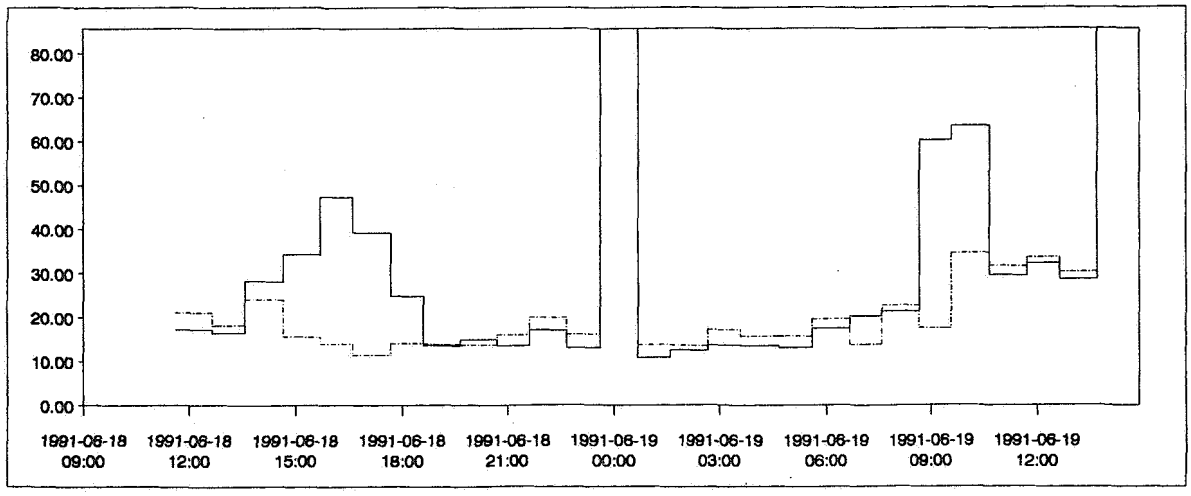

C	Location:	Measurement	Line	Scale	Unit	Room Vol.	Mean val. of c.p.
6	Livingroom-Kitc	Air-change	_┌┐_	1E+00	m^3/h	127.00 m^3	27.68 m3/h
12	Livingroom-Kitc	Air-change	_┌┐_	1E+00	m^3/h	127.00 m^3	34.28 m3/h

Figure 8: Airflow into the livingroom/kitchen.

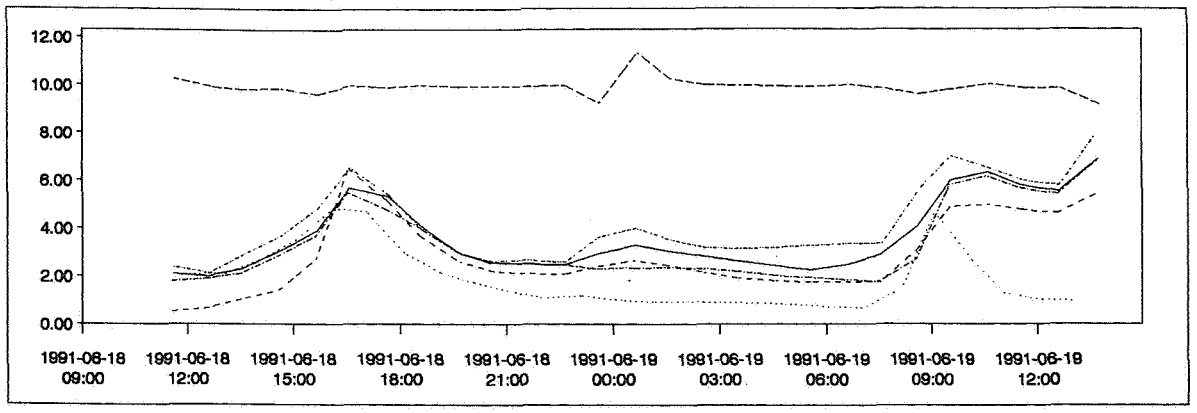

C	Location:	Measurement	Line	Scale	Unit	Room Vol.	Mean val. of c.p.
1	Scullery	R22	·····	1E+00	ppm	14.00 m^3	1.90 ppm
2	Bedroom	R22	——	1E+00	ppm	23.00 m^3	3.29 ppm
3	Bathroom	R22	- - - -	1E+00	ppm	8.10 m^3	2.86 ppm
4	Main bedroom	R22	——	1E+00	ppm	34.00 m^3	3.65 ppm
5	Hall	R22	·····	1E+00	ppm	72.00 m^3	4.15 ppm
6	Livingroom-Kitc	R22	- - - -	1E+00	ppm	127.00 m^3	9.91 ppm

Figure 9: Tracer gas concentrations in the house.

5. Conclusion.

The most exiting results from the performed measurements are the capability of the measurement method to determine the source strength of a pollutant placed in a certain room. The possible applications for this type of measurements are many, a.o. determination of the strength of a humidity source in houses or to calculate production rate of pollution in the industry.

The measurements carried out also prove that the measurement method gives reliable results of interzonal airflow, although we have not adduced any real proof of the accuracy of the measurement method. In order to evaluate the accuracy of the measurement method we have to compare this with a more precise reference than the test-house. Therefore, we are not able to decide whether it is a good idea to correct the measured tracer gas concentrations before they are used to calculate the interzonal airflow.

When calculating the production of carbon dioxide in the main bedroom the accuracy was surprisingly high, in fact much better than could be expected, as the calculated strength of the source deviated less than 10% from the expected values.

6. References.

1. B. Kvisgaard, P.F. Collet, J. Kure, "Research on Fresh-air Change Rate: 1", Technological Institute, Copenhagen, 1985

2. Bjørn Kvisgaard and P.F. Collet, "The User's Influence on Air Change", pp67-76 in "Air Change Rate and Airtightness in Buildings" by M.H. Shermann, STP 1067, ASTM, March 1990.

3. J. Pejtersen, G. Clausen, J. Sørensen, D. Quistgaard, G. Iwashita, Y. Zhang, T. Ouishi and P.O. Fanger, Laboratory of Heating and Air Conditioning, Technical University of Denmark. "Air Pollution Sources in Kindergartens", Healthy Buildings, IAQ 1991, Washington, September 1991 (submitted).

4. Bjørn Kvisgaard, P.F. Collet "Constant Concentration Measurement with 2 Tracers", Paper 10 of Proceedings of the 9th AIVC Conference, vol. 1, 1988.